THEORETICAL STUDIES IN HETEROGENEOUS COMBUSTION

Thesis by

Forman A. Williams

In Partial Fulfillment of the Requirements

For the Degree of

Doctor of Philosophy

California Institute of Technology

Pasadena, California

1958

To My Wife

ACKNOWLEDGMENT

The author wishes especially to thank Dr. S. S. Penner for suggesting the topics investigated in this thesis and for many very helpful discussions relating to the problems encountered in the work.

Financial assistance for the academic years during which this work was carried out was provided by a Daniel and Florence Guggenheim Jet Propulsion Fellowship for the year 1955-56, and National Science Foundation Fellowships for the years 1956-57 and 1957-58. Portions of the work in this thesis were supported by the Office of Ordnance Research, U. S. Army under contract No. DA 04-495-Ord-446.

ABSTRACT

The theory of the steady-state burning of a single spherically-symmetric liquid monopropellant droplet in an infinite inert atmosphere is formulated. Numerical solutions for the temperature and composition profiles and burning rate are obtained in the case of a one-step chemical reaction of the second order. It is shown that the size and location of the reaction zone depend strongly upon the activation energy. Approximate analytical solutions for the burning rate which are valid for large activation energies are obtained for arbitrary chemical reactions. The results indicate that the mass burning rate is proportional to the droplet radius raised to a power which varies from two at small activation energies to unity at large activation energies.

The Shvab-Zeldovich formulation of the problem of burning of initially unmixed systems is developed and applied to the case of a single fuel droplet burning in an infinite oxidizing atmosphere. Some simplification over other methods for treating this problem is obtained, and the burning rate is shown to be unaffected by a distributed reaction zone when the Lewis number is unity.

A general statistical formalism for describing the behavior of sprays is presented, which includes the effects of droplet growth, the formation of new droplets, collisions and aerodynamic forces. The method is applied to the problem of the determination of the size distribution of a spray formed by the impingement of two streams of droplets of known properties. It is shown that if the two incident jets

have a size distribution of a generalized Rosin-Rammler type, then the resulting spray belongs to the same class of distributions. The size history of evaporating sprays is also obtained from the theory. A spray combustion analysis given by Probert is extended to include more general size distributions and the effects of droplet interactions and relative motion of the droplets and the fluid. It is shown that sprays of a uniform size yield the highest combustion efficiency.

TABLE OF CONTENTS

LIST OF FIGURES

PREFACE

This manuscript is composed of three separate theoretical problems in heterogeneous combustion. We begin by considering in detail the steady-state burning of a single liquid monopropellant droplet. Numerical results for the temperature and composition profiles and for the mass burning rate for second-order reactions, as well as approximate analytical expressions for the burning rate for arbitrary reactions, are obtained.

In Chapter II we turn our attention to the opposite problem of initially unmixed reacting systems and develop the general formalism of Shvab and Zeldovich for treating such systems. This formalism is applied to the burning of a single fuel droplet in an infinite oxidizing medium and is found to yield the droplet burning rate with a minimum number of assumptions regarding the chemical reaction rate.

The last topic treated (Chapter III) is that of sprays, for which a general statistical formulation is developed, which is capable of describing a large number of spray properties and processes. In order to illustrate the use of the theory, the problems of spray combustion and impinging jet atomization are considered. The results of Chapters I and II are needed in the spray combustion problem in order to determine the burning rate of sprays.

Each chapter is divided into parts (denoted by capital letters), sections (denoted by Arabic numbers), and sometimes sub-sections (denoted by small letters). In order to avoid confusion in notation

we present a list of symbols at the beginning of each chapter. In addition, a complete introduction is given for each chapter. The equations are numbered consecutively in each chapter, and when an equation of another chapter is referred to the chapter number is indicated by Roman numerals; e.g., Eq. (II-17) is Eq. (17) of Chapter II. Superscript numbers in parentheses refer to references listed at the end of this thesis.

Chapter I

THEORY OF THE BURNING OF MONOPROPELLANT DROPLETS

List of Symbols

a_i Constant determining flux fraction [see Eq. (58)].

B Frequency factor for chemical reaction rate.

b_i Constant determining flux fraction [see Eq. (58)].

$\bar{c}_p$ Average specific heat at constant pressure.

c_i Constant determining mass fraction [see Eq. (59)].

D Diffusion coefficient.

d Droplet diameter.

f Functions of ε_p defined in Eqs. (38), (81), and (107).

g Integrals defined in Eqs. (39), (82), and (108).

H Dimensionless enthalpy of formation.

h An integral defined in Eq. (48).

h_j Enthalpy per unit mass of species j.

K Droplet evaporation constant [see Eq. (44)].

ℓ Effective Lewis number.

M Molecular weight.

$\bar{M}$ Average molecular weight.

$\dot{m}$ Mass flow rate (gm/sec).

n An integer characterizing the type of first-order reaction.

σ Order of the reaction.

p Hydrostatic pressure.

q Heat of reaction.

R Universal gas constant.

r Distance from the center of the droplet.

s	Total number of chemical species.
T	Temperature.
T_a	Activation temperature.
T_r	Activation temperature for r'th reaction.
t	Time.
ℓ	Total number of chemical reactions.
V	Diffusion velocity.
V^*	A dimensionless parameter (see pages 24, 57 and 69).
v	Mass average velocity.
X	Mole fraction.
Y	Weight fraction.
α	Dimensionless heat of vaporization, $\Delta\ell/\bar{c}_p T_f$.
β	Dimensionless reaction rate frequency factor.
γ_{ij}	Ratio of the binary diffusion coefficient for species i-P to that for species i-j.
$\Delta\ell$	Heat of vaporization.
δ	Fuel-oxidizer ratio $\epsilon_{F,\ell}/\epsilon_{0,\ell}$.
ϵ	Flux fraction.
η	Dimensionless distance r_ℓ/r.
θ	Dimensionless temperature T/T_f.
θ_a	Dimensionless activation temperature T_a/T_f.
θ_r	Dimensionless activation temperature for r'th reaction T_r/T_f.
$\mathcal{M}_{ij}$	Ratio of the molecular weight of species i to that of species j.
Λ^*	Dimensionless eigenvalue for mass flow rate (see pages 24, 58 and 68).

λ Thermal conductivity.

ν' Stoichiometric coefficient for a reactant.

ν'' Stoichiometric coefficient for a product.

ρ Density.

σ Dimensionless distance r/r_ℓ.

ϕ Equivalence ratio.

$\dot{\omega}$ Rate of production of chemical species per unit volume.

Subscripts

c Position at which 50% of the reaction has been completed.

F Fuel.

f Final conditions after combustion has been completed, at $r=\infty$.

i A chemical species.

j A chemical species.

ℓ Conditions at the surface of the liquid droplet.

N An inert component.

O Oxidizer.

o Initial condition.

P Products.

r An elementary reaction step.

A. INTRODUCTION

We begin this dissertation by treating in detail the steady-state burning of single liquid droplets of monopropellant in an infinite inert atmosphere. This problem is similar to the one-dimensional premixed laminar flame problem, but the spherical symmetry introduces some additional complications. The solution is necessary for a basic understanding of the combustion mechanism in liquid monopropellant rocket motors.

While the diffusion flame burning of single fuel droplets has been exhaustively studied in the literature,* it appears that virtually no consideration has been given to the monopropellant counterpart of this problem with the same geometry. The only theoretical investigation that has been published appears to be that of Lorell and Wise[1] in which they solved numerically the governing equations for a monopropellant droplet with a first-order chemical reaction. In addition to carrying out numerical solutions for second-order reactions similar to those of Lorell and Wise, we obtain approximate analytical expressions for the steady-state mass burning rate in limiting cases.

Although Kiley[2] was unable to produce the steady-state burning of monopropellant droplets in an inert atmosphere, fortunately some experimental results have been given by Barrère and Moutet[3] and by Rosser.[4] Rosser measured the burning rate of nitromethane, hydrazine and ethyl nitrate droplets by use of a porous sphere apparatus.

---

* See, for example, reference 20.

In the experiments of Barrère and Moutet droplets of ethyl nitrate, propyl nitrate, hydrogen peroxide, and some fuel-nitric acid mixtures were suspended on quartz fibers and the rate of change of droplet diameter with time was measured during burning. It is these results with which we compare our theoretical predictions.

Since the details of solution of the problem are found to depend to a certain extent upon the order of the rate-controlling step of the chemical reaction, the analysis here is divided according to whether the reaction is of second order (Part B), first order (Part C), or higher order (Part D). After deriving from basic principles the governing equations for the second-order process, we put the equations in a dimensionless form which is most suitable for the analysis. Solutions for the mole fraction distribution of the chemical species as a function of temperature alone are obtained for the special case of adiabatic burning when the Lewis number is unity. The method of complete numerical solution and the approximate solution for the burning rate are then given in Section B-11.

After discussing the nature of the solutions and comparing them with experiments, we proceed to consider ways in which the analysis and results can be extended to more general cases. Thus in Section B-15 we indicate that the restriction of Lewis number equal to unity is not essential for the results to be valid. The necessary modifications in the analysis to account for the effects of conductive heat transfer to the surroundings and the presence of an inert component are also pointed out.

The conditions under which the analysis may be extended to systems which obey first-order chemical kinetic equations are derived in Part C. It is shown that there are no essential modifications of the results. In Part D we present a general formulation of the monopropellant droplet burning problem which is valid for reaction kinetics of any order and an arbitrary number of chemical reactions. Necessary conditions for the applicability of the previous results are stated. The wide range of considerations presented in this chapter should indicate useful methods for attacking problems of combustion in premixed spherically-symmetric systems.

B. SECOND-ORDER KINETICS

1. Definition of the Problem

We shall investigate the problem of a single liquid droplet of monopropellant burning steadily in a still atmosphere. The case considered is that in which the arrangement is spherically symmetric and the only coordinate of importance is r, the distance from the center of the drop. An attempt will be made to construct a complete theory, including both diffusion and chemical kinetic effects, for predicting the burning rate of the droplet and other physical properties of the system. The conservation equations for mass, momentum, and energy, as well as the chemical reaction rate equations, must be satisfied. In the course of the development it will be found necessary to introduce a number of simplifying assumptions which are summarized in detail in Appendix A.

Let us consider a reaction involving three components, fuel

symbolically denoted by F, oxidizer denoted by O, and products identified by the subscript P. The system is illustrated schematically in Fig. 1. Fuel and oxidizer evaporate from the monopropellant droplet surface at its boiling point T_ℓ. The subscript ℓ refers to the conditions at the surface of the droplet while f will denote final conditions after burning is completed, which will be obtained at an infinite distance from the droplet, $r = \infty$. The fuel and oxidizer diffuse radially outward from the droplet surface, are continuously heated, and reach a temperature at which they begin to react rapidly. Energy liberated by the reaction is conducted to the droplet surface and causes more reactants to evaporate. We shall treat stoichiometric and oxidizer-rich systems in which case after completion of the reaction either product or product plus some oxidizer will flow toward infinity. In view of the symmetry between fuel and oxidizer in the chemical reaction it is clear that results for an oxidizer-rich system will apply equally well to a fuel-rich system provided all quantities referring to fuel and oxidizer are interchanged.

Throughout the analysis the assumption of steady-state conditions will be made which implies that all partial derivatives with respect to time are zero. This is rigorously true only if the droplet is continually supplied with monopropellant from an internal source in order to maintain a constant diameter. It is reasonable to postulate* that for droplets which do not burn extremely rapidly the solution thus obtained would

---

* See, however, El Wakil et al, reference 21.

apply even when no mass is being added to the droplet. This has been a basic assumption of nearly all theories of droplet combustion.

2. Mass Conservation

If $\dot{\omega}_j(r)$ is the rate of production (mass per unit volume per second) of chemical species j at the position r, and $\varepsilon_j(r) \equiv \rho_j v_j / \rho v$ is the flux fraction of component j at r, then the conservation of mass of this species is expressed by the relation

$$\dot{\omega}_j = \nabla \cdot (\rho v \varepsilon_j) = \frac{1}{r^2} \frac{d}{dr} (r^2 \rho v \varepsilon_j) \tag{1}$$

where $\rho(r)$ is the mass density and v(r) is the velocity of the fluid at r. The subscript j may refer to either fuel, oxidizer, or product. Summing Eq. (1) over all components j, we obtain the overall continuity equation

$$\frac{d}{dr} (\rho v r^2) = 0$$

the integral of which is

$$\dot{m} \equiv 4\pi r^2 \rho v = \text{constant}. \tag{2}$$

Here use has been made of the conservation of mass in chemical reactions,

$$\sum_j \dot{\omega}_j = 0,$$

and the fact that

$$\sum_j \varepsilon_j = \varepsilon_F + \varepsilon_O + \varepsilon_P = 1 \tag{3}$$

which follows from the definition of the flux fraction ε_j. It is seen that $\dot{m}$ is the total mass flow rate and therefore must be constant in a steady-

state situation. The burning rate $\dot{m}$ is the most important quantity that is to be determined.

Since mass of a chemical component can be transported by convection or diffusion, the flux fraction of species j is given by the relation

$$\rho v \varepsilon_j = \rho v Y_j + \rho V_j Y_j$$

or

$$\varepsilon_j = Y_j\left(1 + \frac{V_j}{v}\right) \tag{4}$$

where $Y_j(r) \equiv \rho_j/\rho$ is the mass fraction of species j and $V_j(r) \equiv v_j - v$ is the diffusion velocity of species j. It is clear from the definitions that

$$\sum_j Y_j V_j = 0$$

and

$$\sum_j Y_j = Y_F + Y_O + Y_P = 1. \tag{5}$$

3. Momentum Conservation

While the general momentum conservation equation written in vector notation is somewhat complicated even in orthogonal curvilinear coordinates, this equation can be written quite compactly in tensor notation in a form which holds in non-orthogonal coordinate systems as well. In order to illustrate the relationship between these two notations, the form of the momentum equation applicable to this spherically symmetric problem is deduced from the general tensor form of the equation in Appendix D. The resulting steady-state equation in the absence of external forces and viscosity is

$$\frac{dp}{dr} = -\rho v \frac{dv}{dr} \qquad (B\text{-}12)$$

where p is the hydrostatic pressure. Equation (B-12) can be written in the equivalent form

$$\frac{d\ell np}{dr} = -\frac{\rho v^2}{p} \frac{d\ell nv}{dr} \qquad (6)$$

which shows that if the hydrostatic pressure is very much greater than the momentum of ordered motion transported per unit area per second then

$$\left|\frac{d\ell np}{dr}\right| \ll \left|\frac{d\ell nv}{dr}\right| . \qquad (7)$$

It can easily be seen from the continuity and energy equations of our problem that the fractional change in velocity is of an order of magnitude comparable to that of the other variables. Therefore, in comparison to all other gradients in the problem, the relation

$$\frac{d\ell np}{dr} = 0$$

is valid, whence

$$p = \text{constant} \qquad (8)$$

is the solution of the momentum equation.

Since the shear stresses are proportional to velocity gradients, the viscous forces will be very small even in a viscous fluid provided the velocity gradients are sufficiently small. The kinetic theory of gases shows that $p \sim \rho c^2$ where c is the average velocity of a molecule. This implies that assuming $p >> \rho v^2$ is equivalent to assuming that the energy involved in the ordered motion of the gas is much less than its thermal energy, i.e., the Mach number is low. Thus, for the high

temperatures encountered in droplet burning and for the low velocities and velocity gradients involved, constant pressure is an acceptable approximate solution to the momentum equation. (This argument is much the same for all geometries and the conclusion holds for any deflagration.)

4. Chemical Reaction Rate

The second-order chemical reaction that we shall investigate in this part is written symbolically as $F + O \longrightarrow 2P$. It follows that the rates of production of the three species by chemical reaction obey the relations

$$\frac{1}{M_F}\,\dot{\omega}_F = \frac{1}{M_O}\,\dot{\omega}_O = -\frac{1}{2M_P}\,\dot{\omega}_P$$

where M_j is the gram molecular weight of species j. From Eqs. (1) and (2) it then follows that

$$\frac{1}{M_F}\,\frac{d\varepsilon_F}{dr} = \frac{1}{M_O}\,\frac{d\varepsilon_O}{dr} = -\frac{1}{2M_P}\,\frac{d\varepsilon_P}{dr} \tag{9}$$

the integral of which is

$$\frac{1}{M_F}(\varepsilon_F - \varepsilon_{F,\ell}) = \frac{1}{M_O}(\varepsilon_O - \varepsilon_{O,\ell}) = -\frac{1}{2M_P}(\varepsilon_P - \varepsilon_{P,\ell}). \tag{10}$$

The general kinetic expression for the reaction rate is in this case*

$$\dot{\omega}_P = 2B \exp(-T_a/T)\, M_P \rho^2 \frac{Y_F}{M_F}\,\frac{Y_O}{M_O}$$

where $B(T)$ is the frequency factor (in sec^{-1} volume/mole) and T_a is the

---

* See, for example, Section I E of reference 5 for a discussion of the general rate equations.

activation temperature for the reaction. It will later be assumed for convenience that B is constant, but this is not essential for the applicability of the method of solution to be used. If use is made of Eqs. (1) and (2), then the above relation becomes

$$\frac{d\varepsilon_P}{dr} = \frac{4\pi r^2}{\dot{m}} \, 2B \, M_P \rho^2 \exp(-T_a/T) \, \frac{Y_F}{M_F} \frac{Y_O}{M_O} \, . \qquad (11)$$

5. Energy Conservation

As with the momentum equation, the equation of conservation of energy can be deduced from the general energy equation derived from kinetic theory. However, it is more convenient to use an elementary derivation here. Energy may be transported across a surface by macroscopic motion of the gas across the surface (diffusion and convection) and by conduction (thermal motion of particles) across the surface. If λ is the thermal conductivity of the mixture, then the total energy flowing through any spherical shell of radius r about the droplet is

$$\dot{m}(\varepsilon_F h_F + \varepsilon_O h_O + \varepsilon_P h_P) - 4\pi r^2 \lambda \frac{dT}{dr}$$

where h_F, h_O, and h_P are the total enthalpies per unit mass for fuel, oxidizer and product, respectively.

Since the net energy flowing into any region must be zero in order for a steady state to exist, the energy flux must be a constant. At the surface of the droplet, the energy entering the droplet by conduction must be equal to that required to vaporize the monopropellant. If $\Delta\ell$ is the heat of vaporization per unit mass then this energy is $\dot{m}\Delta\ell$. The equation of conservation of energy can therefore be written in the form

$$\dot{m}(\varepsilon_F h_F + \varepsilon_O h_O + \varepsilon_P h_P) - 4\pi r^2 \lambda \frac{dT}{dr}$$

$$= \dot{m}(\varepsilon_{F,\ell} h_{F,\ell} + \varepsilon_{O,\ell} h_{O,\ell} + \varepsilon_{P,\ell} h_{P,\ell}) - \dot{m}\Delta\ell \qquad (12)$$

where the constant energy flux has been equated to its value at the surface of the droplet.

We define the mean specific heat of the mixture by the relation

$$\bar{c}_p \equiv \frac{1}{T-T_\ell}\left[\varepsilon_F(h_F - h^o_F) + \varepsilon_O(h_O - h^o_O) + \varepsilon_P(h_P - h^o_P)\right.$$

$$\left. - \varepsilon_{F,\ell}(h_{F,\ell} - h^o_F) - \varepsilon_{O,\ell}(h_{O,\ell} - h^o_O) - \varepsilon_{P,\ell}(h_{P,\ell} - h^o_P)\right] \qquad (13)$$

where the superscript o refers to a standard reference temperature. Equation (12) then becomes

$$4\pi r^2 \lambda \frac{dT}{dr} = \dot{m}\left[\Delta\ell + (\varepsilon_F - \varepsilon_{F,\ell})h^o_F + (\varepsilon_O - \varepsilon_{O,\ell})h^o_O\right.$$

$$\left. + (\varepsilon_P - \varepsilon_{P,\ell})h^o_P + \bar{c}_p(T - T_\ell)\right]. \qquad (14)$$

We notice that, for the particular case in which the specific heats of all three components are equal, $\bar{c}_p$ as defined in Eq. (13) reduces to this common specific heat by virtue of Eq. (3).

By using Eq. (10) to replace $\varepsilon_F - \varepsilon_{F,\ell}$ and $\varepsilon_O - \varepsilon_{O,\ell}$ in terms of $\varepsilon_P - \varepsilon_{P,\ell}$ in Eq. (14), we obtain the relation

$$4\pi r^2 \lambda \frac{dT}{dr} = \dot{m}\left[\Delta\ell - q(\varepsilon_P - \varepsilon_{P,\ell}) + \bar{c}_p(T - T_\ell)\right] \qquad (15)$$

where q is the standard heat of reaction per gram of products and is given by

$$q = \frac{1}{2}\frac{M_F}{M_P} h^o_F + \frac{1}{2}\frac{M_O}{M_P} h^o_O - h^o_P \,. \tag{16}$$

In order to be definite we shall assume that the mean specific heat varies so slightly that it may be taken as constant and equal to

$$\bar{c}_p = \frac{1}{T_f - T_\ell}\left[\varepsilon_{F,f}(h_{F,f} - h^o_F) + \varepsilon_{O,f}(h_{O,f} - h^o_O) + \varepsilon_{P,f}(h_{P,f} - h^o_P)\right.$$

$$\left. - \varepsilon_{F,\ell}(h_{F,\ell} - h^o_F) - \varepsilon_{O,\ell}(h_{O,\ell} - h^o_O) - \varepsilon_{P,\ell}(h_{P,\ell} - h^o_P)\right]. \tag{17}$$

This equation is rigorously valid only when the specific heats of all components are constant and equal, but usually the heat capacity varies so slowly that Eq. (17) will be an excellent approximation.* Also in order to be specific, the thermal conductivity will be assumed to be proportional to temperature, as predicted in a first approximation for Maxwellian molecules from kinetic theory;** i.e.,

$$\lambda = \lambda_f \frac{T}{T_f} \,. \tag{18}$$

6. Diffusion

In order to make use of Eq. (4) it is necessary to obtain expressions for the diffusion velocities, V_j. It is a good approximation to neglect thermal diffusion effects which are much smaller than the

---

* Any other temperature dependence of $\bar{c}_p$ could be assumed if a particular problem merited it, and this dependence could be rechecked a posteriori. This would not affect the method of solution to be used.

** See, for example, reference 6, Sections 9.82 and 10.32.

ordinary concentration gradient diffusion.* Then, to first order in a Sonine polynomial expansion for the diffusion coefficients, the following relation holds:**

$$\sum_j \frac{X_i X_j}{D_{ij}} (V_j - V_i) = \frac{dX_i}{dr} \tag{19}$$

where $X_j(r)$ is the mole fraction of species j and D_{ij} is the binary diffusion coefficient for species i and j. A derivation of Eq. (19) from the point of view of elementary kinetic theory is presented in Appendix C.

The mole fractions are related to the weight fractions through the equation

$$Y_i = \frac{M_i X_i}{\sum_j M_j X_j} = \frac{M_i X_i}{\bar{M}} \tag{20}$$

where $\bar{M} \equiv \sum_j M_j X_j$ is the mean molecular weight of the mixture. By substituting Eqs. (4) and (20) into Eq. (19) one obtains the relation

$$\frac{dX_i}{dr} = \sum_j \frac{1}{D_{ij}} \left(\frac{X_i \epsilon_j}{M_j} - \frac{X_j \epsilon_i}{M_i} \right) v\bar{M}. \tag{21}$$

In order to avoid numerical integration we find it necessary here to introduce two simplifying assumptions. The molecular weights of all three components are taken to be equal,

$$M_F = M_O = M_P \equiv M,$$

and all three binary diffusion coefficients are assumed equal,

---

* The thermal diffusion coefficient is identically zero for Maxwellian molecules.

** See reference 7, Section 7.4 c i.

$$D_{FO} = D_{OP} = D_{PF} \equiv D.$$

The first of these assumptions will often be nearly correct in hydrocarbon-oxygen flames for example. The second assumption is perhaps the most drastic one made in the analysis; however we expect it to hold in some cases, particularly when the molecular weights are nearly equal.

With these two assumptions the mole fraction becomes equal to the weight fraction,

$$X_j = Y_j,$$

and in view of Eq. (2), Eq. (21) becomes

$$\frac{dX_i}{dr} = \frac{\dot{m}}{4\pi r^2} \frac{1}{\rho D} \sum_j (X_i \varepsilon_j - X_j \varepsilon_i). \tag{22}$$

By use of Eqs. (3) and (5) this equation can be written in the form

$$\frac{dX_i}{dr} = \frac{\dot{m}}{4\pi r^2} \frac{1}{\rho D} (X_i - \varepsilon_i) \tag{23}$$

where i may refer to fuel, oxidizer, or product.

We shall assume that the binary diffusion coefficient divided by the thermal conductivity is proportional to temperature as is predicted by first-order kinetic theory for central force molecular models.* By using Eq. (18) we then obtain the relation

$$D = D_f \left(\frac{T}{T_f}\right)^2. \tag{24}$$

---

* See, for example, reference 6, Sections 9.81 and 10.3.

It will also be assumed that the ideal gas law holds;

$$\rho = \frac{p\bar{M}}{RT} \quad . \tag{25}$$

Since pressure is constant, Eq. (25) can be written in the alternate form

$$\rho = \rho_f \frac{T_f}{T} \quad . \tag{25a}$$

7. Dimensionless Form of the Governing Equations

Equations (10), (11), (15), and (23) provide seven relations for the seven unknowns, X_j, ε_j, and T as functions of r. The mass flow rate $\dot{m}$ is an eigenvalue of these equations. The fact that all of the equations are of the first order will enable us to obtain an approximate analytical solution.

Before proceeding with the solution of these equations, it is convenient to introduce dimensionless variables. We define the dimensionless temperature and radial coordinate as $\theta \equiv T/T_f$ and $\sigma \equiv r/r_\ell$ respectively. Then, because of the equality of the molecular weights, the fact that $X = Y$, and Eq. (25a), Eq. (11) becomes

$$\frac{d\varepsilon_P}{d\sigma} = \frac{4\pi r_\ell^3}{\dot{m}} \frac{2B}{M} \rho_f^2 \frac{\sigma^2}{\theta^2} \exp(-\theta_a/\theta) X_F X_O . \tag{26}$$

If the dimensionless heat of vaporization of the liquid in the droplet is defined as $\alpha \equiv \Delta\ell/\bar{c}_p T_f$, then in view of Eq. (18), Eq. (15) reduces to

$$\frac{4\pi r_\ell}{\dot{m}} \frac{\lambda_f}{\bar{c}_p} \sigma^2 \theta \frac{d\theta}{d\sigma} = \alpha - \frac{q}{\bar{c}_p T_f} (\varepsilon_P - \varepsilon_{P,\ell}) + \theta - \theta_\ell \quad . \tag{27}$$

By using Eqs. (24) and (25a), the dimensionless form of Eq. (23) is

found to be

$$\frac{dX_i}{d\sigma} = \frac{\dot{m}}{4\pi r_\ell} \frac{1}{\rho_f D_f} \frac{X_i - \epsilon_i}{\sigma^2 \theta} \quad . \tag{28}$$

The dependence on temperature of all physical parameters entering into the problem has been specified. It will therefore be convenient to treat temperature as the independent variable instead of the distance, r. After discussing the boundary conditions, a particular solution for the mole fractions X_j as functions of the temperature T will be determined by the method of von Kármán and Penner.[5] The energy and reaction rate equations will then be combined and integrated approximately to obtain a relation for the mass flow rate, $\dot{m}$.

8. Boundary Conditions

The solution of Eqs. (26), (27) and (28) will depend upon the boundary conditions imposed at the droplet surface and at $r = \infty$. It is quite obvious that at the droplet surface the relations $\sigma = 1$ and $\theta = \theta_\ell$ hold, while at $r = \infty$ we find by definition that $\sigma = \infty$ and $\theta = 1$. The boiling point T_ℓ is known and the final temperature T_f must also be given to determine θ_ℓ. We shall consider only the case of adiabatic burning in which there is no heat conduction at $r = \infty$.* The left-hand

* This is expected to be very nearly true for droplets burning in a combustion chamber in which the surrounding temperature is near the adiabatic flame temperature. However, for a droplet burning in an atmosphere at room temperature the energy transferred to the surroundings may be of the same order of magnitude as that transferred to the liquid drop. The modifications which arise in the non-adiabatic case are discussed in section B-16b.

side of Eq. (27) then goes to zero as θ approaches unity and we find

$$\frac{q}{\bar{c}_p T_f} = \frac{1 - \theta_\ell + \alpha}{\varepsilon_{P,f} - \varepsilon_{P,\ell}} . \tag{29}$$

This equation determines T_f and hence θ_ℓ in terms of $\varepsilon_{P,f}$, $\varepsilon_{P,\ell}$, and physical constants. Since the heat of vaporization $\Delta\ell$ is usually much less than the heat of reaction $q(\varepsilon_{P,f} - \varepsilon_{P,\ell})$, it is seen that T_f is nearly the ordinary adiabatic flame temperature, $T_\ell + (\varepsilon_{P,f} - \varepsilon_{P,\ell})q/\bar{c}_p$.

We assume that the mixture is uniform at infinity which implies that as $r \longrightarrow \infty$ the concentration gradients will go to zero more rapidly than $1/r^2$. This indicates that the diffusion velocities will approach zero and also [see Eq. (28)] $\varepsilon_{j,f} = X_{j,f}$ for all components at $r=\infty$. Furthermore, assuming for convenience an oxidizer-rich or stoichiometric mixture, we find that $\varepsilon_{F,f}=0$ because all of the fuel will eventually be burned.

It will also be assumed that no liquid-phase reaction occurs and that there is no product present in the droplet.* In this case no product

---

* The case in which liquid-phase reaction does occur can be treated by the same method provided the following information is available: (a) The extent of liquid-phase reaction must be given in order to determine $\varepsilon_{P,\ell}$. (b) The effect of heat liberation within the droplet upon the energy flux across the droplet surface must be obtained. (This will usually be possible by a simple energy balance.) Since little is known about the mechanism of liquid-phase monopropellant reactions it is difficult to provide the information required in (a). For many monopropellants virtually no reaction occurs at temperatures below the boiling point; therefore $\varepsilon_{P,\ell}=0$ is an excellent approximation in these cases.

can flow out of the droplet, i.e., $\varepsilon_{P,\ell}=0$. The concentration gradients do not necessarily go to zero at the droplet surface, hence $X_{j,\ell} \neq \varepsilon_{j,\ell}$ in general.

The values of $\varepsilon_{F,\ell}$ and $\varepsilon_{O,\ell}$ will depend upon the fuel-oxidizer ratio in the droplet and upon the mechanism of evaporation. We may define δ as the ratio of fuel to oxidizer evaporating from the droplet, $\delta \equiv \varepsilon_{F,\ell}/\varepsilon_{O,\ell}$, and note that this is the fuel-oxidizer ratio within the droplet only when fuel and oxidizer evaporate in the same ratio in which they are present in the droplet, which need not be the case even for components of equal volatility. The relation $\delta \leq 1$ will hold for a non-fuel-rich system. Equation (3) implies that $\varepsilon_{F,\ell} = \delta/(\delta+1)$ and $\varepsilon_{O,\ell} = 1/(\delta+1)$. Since $\varepsilon_{F,f}=0$, Eq. (10) yields the relations $\varepsilon_{O,f} = (1-\delta)/(\delta+1)$ and $\varepsilon_{P,f} = 2\delta/(\delta+1)$. The chemical reaction, the absence of conduction and diffusion at infinity, and the physics of evaporation of the droplet thus determine all the boundary values except $X_{j,\ell}$. The quantities $X_{j,\ell}$ are obtained from the solution of Eq. (28) and cannot be determined before solving the problem.

Equation (5) determines X_O in terms of X_F and X_P while Eqs. (3) and (10) give ε_O and ε_F as functions of ε_P. The problem therefore essentially consists of four first-order differential equations in the four unknowns, X_F, X_P, ε_P, and θ. It has been seen that the boundary conditions, $X_{F,f}$, $X_{P,f}$, $\varepsilon_{P,\ell}$, $\varepsilon_{P,f}$, θ_ℓ, and $\theta_f \equiv 1$ are determined. Thus there are four first-order equations and six boundary conditions. This implies that the problem may contain two eigenvalues, one of which is $\dot{m}$. We shall obtain a consistent solution by

adjusting only $\dot{m}$ which shows that only one eigenvalue exists for the boundary conditions chosen here. This arises from the fact that all integral curves pass through the point $\sigma = \infty$.

9. Solution for $X_j(\theta)$ with $\mathcal{L} = 1$

In the special case in which the dimensionless ratio $\lambda_f/\rho_f D_f \bar{c}_p$ is unity, an explicit solution for the mole fractions $X_j(\theta)$ can be found. This has already been pointed out for one-dimensional flame problems by Semenov[8] and von Kármán and Penner,* and is readily extended to spherically symmetric cases.[1]

By multiplying Eq. (28) for the product, X_p, by $(4\pi r_\ell/\dot{m})\rho_f D_f (q/\bar{c}_p T_f)\sigma^2\theta$ and subtracting the result from Eq. (27) we find for the case $\epsilon_{p,j} = 0$ that

$$\frac{4\pi r_\ell}{\dot{m}} \frac{\lambda_f}{\bar{c}_p} \sigma^2\theta \left(\frac{d\theta}{d\sigma} - \frac{1}{\mathcal{L}} \frac{q}{\bar{c}_p T_f} \frac{dX_p}{d\sigma} \right)$$

$$= \alpha - \theta_\ell + \theta - \frac{q}{\bar{c}_p T_f} X_p \qquad (30)$$

where $\mathcal{L} \equiv \lambda_f/\rho_f D_f \bar{c}_p$ is an effective Lewis number for the problem. When the Lewis number is unity ($\mathcal{L} = 1$) Eq. (30) can be integrated explicitly and has a particular solution

$$X_p = \frac{\bar{c}_p T_f}{q} (\theta - \theta_\ell + \alpha). \qquad (31)$$

This differs from the result of von Kármán and Penner only in the

---

* See Section IG(b) of reference 5.

presence of the term α which is due to heat conduction across the cold boundary, an effect that is absent in the one-dimensional case.

Similarly, in Eq. (28) for the fuel (i=F), one can multiply by $2(4\pi r_\ell / \dot{m})\rho_f D_f (q/\bar{c}_p T_f)\sigma^2\theta$ and use Eq. (10) to express ϵ_F in terms of ϵ_P and $\epsilon_{F,\ell}$. If the result is added to Eq. (27) then the expression

$$\frac{4\pi r_\ell}{\dot{m}} \frac{\lambda_f}{\bar{c}_p} \sigma^2\theta \left(\frac{d\theta}{d\sigma} + \frac{2}{\mathcal{L}} \frac{q}{\bar{c}_p T_f} \frac{dX_F}{d\sigma} \right)$$

$$= \alpha - \theta_\ell + \theta + 2 \frac{q}{\bar{c}_p T_f} (X_F - \epsilon_{F,\ell}) \tag{32}$$

is obtained which, when $\mathcal{L} = 1$, has the particular solution

$$X_F = \epsilon_{F,\ell} - \frac{1}{2} \frac{\bar{c}_p T_f}{q} (\theta - \theta_\ell + \alpha) . \tag{33}$$

If use is made of the boundary condition expressed by Eq. (29), then Eqs. (31) and (33) become

$$X_P = \epsilon_{P,f} \frac{\theta - \theta_\ell + \alpha}{1 - \theta_\ell + \alpha} \tag{31a}$$

and

$$X_F = \epsilon_{F,\ell} - \frac{1}{2} \epsilon_{P,f} \frac{\theta - \theta_\ell + \alpha}{1 - \theta_\ell + \alpha} = \frac{1}{2} \epsilon_{P,f} \frac{1 - \theta}{1 - \theta_\ell + \alpha} \tag{33a}$$

where use has been made of Eq. (10) and the fact that $\epsilon_{F,f} = \epsilon_{P,\ell} = 0$. In this form it is obvious that these solutions satisfy the proper boundary conditions at $\theta = 1$. In addition, they provide the remaining boundary values for the mole fractions at the droplet surface.

$$X_{F,l} = \varepsilon_{F,l}(1-\theta_l)/(1-\theta_l+\alpha)$$

and

$$X_{P,l} = \frac{\varepsilon_{P,f}\alpha}{1-\theta_l+\alpha} = \frac{\Delta l}{q} .$$

The mole fraction of oxidizer X_O is obtained from Eq. (5);

$$X_O = 1 - \varepsilon_{P,f} + \frac{1}{2}\varepsilon_{P,f}\frac{1-\theta}{1-\theta_l+\alpha} . \qquad (34)$$

It is seen that when $\mathcal{L}=1$ all mole fractions are linear functions of temperature. We will proceed to give the solution for the case in which the Lewis number is equal to unity and later indicate the method to be used when $\mathcal{L} \neq 1$.

10. Methods for Obtaining Complete Solution

With the exact solution for $X_j(\theta)$ given in the previous section, only Eqs. (26) and (27) remain to be solved for $\varepsilon_p(\sigma)$, $\theta(\sigma)$, and $\dot{m}$. Because of the non-linearity of these equations the exact solution cannot be obtained analytically. In this section we describe a method for obtaining an approximate analytical solution for the mass burning rate $\dot{m}$. While yielding good values for $\dot{m}$, the method fails to provide accurate representations of the functions $\varepsilon_p(\sigma)$ and $\theta(\sigma)$ except in the neighborhood of the end points, $\sigma=1$ and $\sigma=\infty$. For this reason and also in order to check the accuracy of the approximate expression for the mass flow rate $\dot{m}$ an exact numerical solution has been performed. Equations (26) and (27) are well-suited to numerical integration techniques. The method of integration, which was carried out on a high-speed electronic

digital computer, is described in Appendix E.

In order to obtain approximate expressions for the burning rate $\dot{m}$ it is convenient to write Eqs. (26) and (27) in a different form. Multiplying Eq. (26) by Eq. (27) one obtains

$$\left(\frac{d\theta}{d\sigma}\right)^2 = V^* \frac{1}{\theta^3} \exp(-\theta_a/\theta) X_F X_O (1-\theta) \left[-1 + \left(\frac{\epsilon_{P,f} - \epsilon_P}{1-\theta}\right)\left(\frac{1-\theta_\ell + \alpha}{\epsilon_{P,f}}\right)\right] \frac{d\theta}{d\epsilon_P} \quad (35)$$

where the dimensionless constant

$$V^* \equiv \frac{2B}{M} \frac{\rho_f^2 \bar{c}_p}{\lambda_f} r_\ell^2$$

is independent of $\dot{m}$. In this expression we have used the relation

$$\alpha - \frac{q}{\bar{c}_p T_f} \epsilon_P + \theta - \theta_\ell = (1-\theta)\left[-1 + \left(\frac{\epsilon_{P,f} - \epsilon_P}{1-\theta}\right)\left(\frac{1-\theta_\ell + \alpha}{\epsilon_{P,f}}\right)\right]$$

which may easily be derived from Eq. (29). By dividing Eq. (26) by Eq. (27) we similarly find

$$\frac{1}{\sigma^4}\left[-1 + \left(\frac{\epsilon_{P,f} - \epsilon_P}{1-\theta}\right)\left(\frac{1-\theta_\ell + \alpha}{\epsilon_{P,f}}\right)\right] \frac{d\epsilon_P}{d\theta} = \Lambda^* \exp(-\theta_a/\theta) \frac{X_F X_O}{\theta(1-\theta)} \quad (36)$$

where

$$\Lambda^* \equiv \frac{2B}{M} \frac{\rho_f^2 \lambda_f}{\bar{c}_p} 16\pi^2 \frac{r_\ell^4}{\dot{m}^2}$$

is the dimensionless eigenvalue which determines the mass flow rate.

If the expressions for the mole fractions X_F and X_O given in Eqs. (33a) and (34) are substituted into Eq. (36), then by integrating the resulting equation from $\sigma = 1$ to $\sigma = \infty$ we obtain the relation

$$\int_0^{\varepsilon_{P,f}} \frac{1}{\sigma^4}\left[-1+\left(\frac{\varepsilon_{P,f}-\varepsilon_P}{1-\theta}\right)\left(\frac{1-\theta_l+\alpha}{\varepsilon_{P,f}}\right)\right] d\varepsilon_P$$

$$= \Lambda^* \frac{\varepsilon_{P,f}}{2(1-\theta_l+\alpha)} \int_{\theta_l}^{1} \frac{1}{\theta}\exp(-\theta_a/\theta)\left[(1-\varepsilon_{P,f})+(1-\theta)\frac{\varepsilon_{P,f}}{2(1-\theta_l+\alpha)}\right] d\theta . \quad (37)$$

If we define the function $f(\varepsilon_P)$ by the equation

$$f(\varepsilon_P) \equiv \frac{1}{\sigma^4}\left[-1+\left(\frac{\varepsilon_{P,f}-\varepsilon_P}{1-\theta}\right)\left(\frac{1-\theta_l+\alpha}{\varepsilon_{P,f}}\right)\right] \quad (38)$$

and the integral g is given by the relation

$$g \equiv \int_{\theta_l}^{1} \frac{1}{\theta}\exp(-\theta_a/\theta)\left[(1-\varepsilon_{P,f})+(1-\theta)\frac{\varepsilon_{P,f}}{2(1-\theta_l+\alpha)}\right] d\theta . \quad (39)$$

then Eq. (37) may be written in the form

$$\int_0^{\varepsilon_{P,f}} f(\varepsilon_P) d\varepsilon_P = \Lambda^* \frac{\varepsilon_{P,f} g}{2(1-\theta_l+\alpha)} . \quad (37a)$$

The quantity g is a constant which depends only upon θ_l, θ_a, $\varepsilon_{P,f}$, and α and can be determined exactly. The function $f(\varepsilon_P)$ can be approximated by expansion about the end points $\varepsilon_P=0$ and $\varepsilon_P=\varepsilon_{P,f}$. It is then possible to perform the integration in Eq. (37a) in order to obtain the eigenvalue, Λ^*.

There is a good reason for performing the integration in the manner described above. It is seen by the reasoning illustrated in Fig. 2 that for intermediate and large values of the activation temperature θ_a the major contribution to the integral of $f(\varepsilon_P)$ is from the neighborhood of the cold boundary, $\varepsilon_P=0$. A smaller error in the integral is

then made by approximating $f(\varepsilon_p)$ by expansion about the cold boundary point than would be made if a different function were approximated in this manner.

By evaluating the integral in Eq. (39) we obtain the relation

$$g = \left(1-\varepsilon_{P,f}+\frac{\varepsilon_{P,f}}{2(1-\theta_\ell+\alpha)}\right)\left[\mathrm{Ei}(-\theta_a/\theta_\ell)-\mathrm{Ei}(-\theta_a)\right]$$

$$+\frac{\varepsilon_{P,f}}{2(1-\theta_\ell+\alpha)}\left[\theta_\ell\exp(-\theta_a/\theta_\ell)-\exp(-\theta_a)+\theta_a\mathrm{Ei}(-\theta_a/\theta_\ell)-\theta_a\mathrm{Ei}(-\theta_a)\right] \quad (40)$$

where $\mathrm{Ei}(x)$ is the exponential integral which may be defined by the equation

$$-\mathrm{Ei}(-x) = \int_x^\infty \exp(-t)/t\ dt.$$

For $\theta_a \gg 1$ and $\theta_\ell \ll 1$ Eq. (40) may be closely approximated by the expression

$$g \approx (1-\varepsilon_{P,f})\left[-\mathrm{Ei}(-\theta_a)\right]+\frac{\varepsilon_{P,f}}{2(1-\theta_\ell+\alpha)}\left[-(1-\theta_a)\mathrm{Ei}(-\theta_a)-\exp(-\theta_a)\right]$$

$$\approx\left[1-\varepsilon_{P,f}+\frac{\varepsilon_{P,f}}{2\theta_a(1-\theta_\ell+\alpha)}\right]\exp(-\theta_a)/\theta_a^2. \quad (40a)^*$$

---

* In Eqs. (40a) and (40c) the first approximate relations are accurate within one percent for $\theta_a/\theta_\ell \geq 5$. The second relations are within one percent only when $\theta_a \geq 30$; more terms in the asymptotic expansion must be kept for smaller θ_a. The appropriate complete asymptotic expression is

$$(1-\varepsilon_{P,f})\left[-\mathrm{Ei}(-\theta_a)\right]+\frac{\varepsilon_{P,f}}{2(1-\theta_\ell+\alpha)}\left[-(1-\theta_a)\mathrm{Ei}(-\theta_a)-\exp(-\theta_a)\right]$$

$$\sim(1-\varepsilon_{P,f})\frac{1}{\theta_a}\exp(-\theta_a)\sum_{n=0}^{\infty} n!\left(\frac{-1}{\theta_a}\right)^n$$

$$+\frac{\varepsilon_{P,f}}{2(1-\theta_\ell+\alpha)}\frac{1}{\theta_a^2}\exp(-\theta_a)\sum_{n=0}^{\infty}(n+1)(n+1)!\left(\frac{-1}{\theta_a}\right)^n$$

which is divergent.

For stoichiometric mixtures ($\varepsilon_{p,f}=1$), Eq. (40) reduces to

$$g=\frac{1}{2(1-\theta_\ell+\alpha)}\left[\theta_\ell \exp(-\theta_a/\theta_\ell)-\exp(-\theta_a)+(1+\theta_a)\mathrm{Ei}(-\theta_a/\theta_\ell)-(1+\theta_a)\mathrm{Ei}(-\theta_a)\right] \tag{40b}$$

which becomes, for large θ_a and small θ_ℓ,

$$g\approx\frac{1}{2(1-\theta_\ell+\alpha)}\left[-(1+\theta_a)\mathrm{Ei}(-\theta_a)-\exp(-\theta_a)\right]\approx\frac{1}{2(1-\theta_\ell+\alpha)}\exp(-\theta_a)/\theta_a^{\,2}. \tag{40c}$$

With the aid of these relations and the approximation of the function $f(\varepsilon_p)$ given in Appendix D, the eigenvalue Λ^* and therefore the mass burning rate $\dot{m}$ are determined from Eq. (37a).

11. Approximate Expressions for the Burning Rate

In Appendix D it is shown for both stoichiometric and non-stoichiometric mixtures that in the neighborhood of the point $\varepsilon_p=0$, the function $f(\varepsilon_p)$ may be approximated by the relation

$$f(\varepsilon_p)=\frac{\alpha}{1-\theta_\ell}-\varepsilon_p\left\{-\frac{1}{\Lambda^*}\alpha\theta_\ell\exp(\theta_a/\theta_\ell)\frac{(1-\theta_\ell+\alpha)^2}{\frac{1}{2}\varepsilon_{p,f}(1-\theta_\ell)^3}\left[1-\varepsilon_{p,f}+\frac{\frac{1}{2}\varepsilon_{p,f}(1-\theta_\ell)}{1-\theta_\ell+\alpha}\right]^{-1}\right.$$

$$\left.+\frac{1}{\sqrt{\Lambda^* V^*}}4\alpha\theta_\ell^{\,2}\exp(\theta_a/\theta_\ell)\frac{1-\theta_\ell+\alpha}{\frac{1}{2}\varepsilon_{p,f}(1-\theta_\ell)^2}\left[1-\varepsilon_{p,f}+\frac{\frac{1}{2}\varepsilon_{p,f}(1-\theta_\ell)}{1-\theta_\ell+\alpha}\right]^{-1}+\frac{1-\theta_\ell+\alpha}{\varepsilon_{p,f}(1-\theta_\ell)}\right\}. \tag{D-5}$$

It is also shown there that $f(\varepsilon_p)$ approaches zero in the limit $\varepsilon_p\longrightarrow\varepsilon_{p,f}$. Since we expect that the mass flow rate $\dot{m}$ will decrease

and hence Λ^* will increase as the activation temperature θ_a is increased at a given value of r_ℓ, it follows that for sufficiently large values of θ_a the quantity in the curly brackets in Eq. (D-5) will be positive. Hence the function $f(\varepsilon_p)$ behaves somewhat as illustrated in Fig. 2(f), and the approximation in Eq. (D-5) corresponds to the straight line in Fig. 2(f). It is apparent that for intermediate and large values of θ_a there is little error involved in the integral in Eq. (37a) if Eq. (D-5) is assumed to hold for all ε_p. If we perform the integration in Eq. (37a) by using the approximation in Eq. (D-5), then we obtain the relation

$$\Lambda^{*2}\frac{g}{2(1-\theta_\ell+\alpha)}+\Lambda^*\frac{(1-\theta_\ell-\alpha)}{2(1-\theta_\ell)}$$

$$+\sqrt{\frac{\Lambda^*}{V^*}}\,4\alpha\theta_\ell^{\,2}\exp(\theta_a/\theta_\ell)\frac{(1-\theta_\ell+\alpha)}{(1-\theta_\ell)^2}\left[1-\varepsilon_{p,f}+\frac{\frac{1}{2}\varepsilon_{p,f}(1-\theta_\ell)}{1-\theta_\ell+\alpha}\right]^{-1}$$

$$-\alpha\theta_\ell\exp(\theta_a/\theta_\ell)\frac{(1-\theta_\ell+\alpha)^2}{(1-\theta_\ell)^3}\left[1-\varepsilon_{p,f}+\frac{\frac{1}{2}\varepsilon_{p,f}(1-\theta_\ell)}{1-\theta_\ell+\alpha}\right]^{-1}=0. \qquad (41)$$

Because of the factor $\exp(\theta_a/\theta_\ell)$ in the last two terms of Eq. (41), for all activation temperatures greater than approximately $20,000^\circ K$ the first two terms are negligible in comparison to the last two. This may be seen by substituting typical numerical values into the equation. Since in many applications the activation temperatures exceed this value, it will often be possible to neglect the first two terms in Eq. (41) and employ the approximate relation

$$\sqrt{\frac{\Lambda^*}{V^*}}\,\frac{4\theta_\ell(1-\theta_\ell)}{1-\theta_\ell+\alpha} = 1 \tag{42}$$

to obtain the mass flow rate. In view of the definitions of the parameters Λ^* and V^*, Eq. (42) can be written as

$$\dot{m} = 4\pi r_\ell \frac{\lambda_f}{\bar{c}_p} \frac{4\theta_\ell(1-\theta_\ell)}{1-\theta_\ell+\alpha}$$

$$= 16\pi r_\ell \frac{\lambda_f T_\ell}{\epsilon_{P,f}{}^q} \frac{\epsilon_{P,f}{}^{q-\Delta\ell}}{\bar{c}_p T_\ell + \epsilon_{P,f}{}^{q-\Delta\ell}} \tag{42a}$$

where we have used Eq. (29) to eliminate the final temperature T_f. A number of conclusions concerning droplet burning rates may be obtained from Eq. (42a).

If ρ_ℓ is the density of the liquid droplet, then the rate of change of droplet diameter with time is determined by the relation

$$\dot{m} = -4\pi\rho_\ell r_\ell{}^2 \frac{dr_\ell}{dt} \tag{43}$$

provided no mass is being added to the droplet.* It follows from Eqs. (43) and (42a) that $dr_\ell{}^2/dt$ = constant; the square of the droplet diameter decreases linearly with time. This is a well-known experimental fact for large activation energies.** If $d \equiv 2r_\ell$ is the droplet diameter, then the integration of Eq. (43) yields the relation

---

* This would be the case in a combustion chamber for example.

** See, for example, reference 3.

$$d_o^2 - d^2 = 32 \frac{\lambda_f}{\rho_\ell \bar{c}_p} \left[\frac{\theta_\ell (1 - \theta_\ell)}{1 - \theta_\ell + \alpha} \right] (t - t_o) \equiv K(t - t_o) \qquad (44)$$

where the subscript o refers to an initial condition of the droplet. Equation (44) determines the droplet evaporation constant K.

It is also seen from Eq. (42a) that the mass flow rate increases as the thermal conductivity and the liquid droplet temperature increase, while it decreases with increasing specific heat and heat of vaporization. These results are to be expected from physical considerations. Furthermore it is seen that, for activation temperatures greater than about $20,000^{\circ}K$ the mass burning rate is essentially independent of the reaction rate parameters B and θ_a. We shall discuss the significance of this conclusion in Section 14.

Because of the term $\exp(\theta_a/\theta_\ell)$ in Eq. (41), for small values of the dimensionless activation energy θ_a the third term in the equation becomes much smaller than the first terms. This is particularly true for large droplet radii r_ℓ in which case V^* becomes quite large. As can be verified by substituting typical values into Eq. (41), the second and third terms of the expressions are negligible when the activation temperature is less than approximately $12,000^{\circ}K$.* The resulting simplified form of Eq. (41) shows that the eigenvalue Λ^* is independent of the parameter V^*. This implies that the mass flow rate $\dot{m}$ is proportional to the square of the droplet radius r_ℓ^2. This conclusion is to

* The exact value of this limiting activation temperature will, of course, depend upon r_ℓ and T_f.

be expected in the limit of large droplet radii and low activation energies θ_a because the reaction then goes nearly to completion in a layer small compared to the droplet diameter thus causing the effect of curvature of the droplet surface to decrease. The geometry becomes effectively one-dimensional in which case the burning rate is proportional to the surface area which varies as r_ℓ^2. It follows that for small activation energies, if no mass is added internally to the liquid drop, then the droplet diameter decreases linearly with time. Equation (41) thus predicts in general that

$$(d_o^m - d^m) \sim (t - t_o), \quad 1 \le m \le 2 \tag{45}$$

where m varies from 1 at small activation energies to 2 at large activation energies. As is shown in the following section, this conclusion is also verified by the numerical calculations.

The approximate form of Eq. (41) valid for small values of the parameter θ_a shows that the eigenvalue Λ^* is roughly proportional to $\exp\left[\theta_a(1+\theta_\ell)/2\theta_\ell\right]$. This implies that the dependence of the mass flow rate upon reaction rate is given approximately by

$$\dot{m} \sim \sqrt{B}\, \exp\left[-\theta_a(1+\theta_\ell)/4\theta_\ell\right]$$

The mass flow rate therefore increases with increasing reaction rate and is largest for small activation energies. The dependence of $\dot{m}$ upon other parameters is essentially the same for all values of the activation temperature θ_a. These conclusions are physically reasonable and are verified by the numerical solution.

It must be emphasized that while these trends are correct, the

magnitude of Λ^* obtained from Eq. (41) for small values of the parameter θ_a is not expected to be very accurate. The reason for this conclusion is that, as pointed out in the beginning of this section, the coefficient of ε_p in Eq. (D-5) becomes negative at low activation energies. It is then obvious (see Fig. 3) that a much greater error arises in the approximate integration which causes a correspondingly large error in the magnitude of the burning rate for small values of θ_a.

12. Comparison and Correlation of Solutions

The numerical solutions were carried out for systems with the physical constants listed in Table I. A wide range of values of r_ℓ and θ_a were considered. The resulting variation of ε_p with temperature was found to be similar to that for an ordinary one-dimensional laminar flame (see Figs. 4 through 7). For large activation energies the temperature must rise a great deal before reaction begins, and the reaction proceeds rapidly after ignition. Thus for large θ_a the flux fraction $\varepsilon_p(\theta)$ remains practically zero until θ is near unity at which point it rises rapidly to its final value, while for smaller activation temperatures ε_p increases more uniformly.

It is seen from Figs. 4 through 7 that for small values of θ_a most of the reaction and temperature change occurs very near the droplet surface, $\eta = 1/\sigma \approx 1$, while at large activation energies the reaction occurs far from the droplet, η near zero. The location of the "flame front", $r=r_c$, may be defined as the point at which $\varepsilon_p = \varepsilon_{p,f}/2$ in which case it is found from Figs. 4 through 7 to vary from $r_c = 1.005\, r_\ell$ at

$\theta_a = 3.9$ to $r_c = 42\, r_\ell$ at $\theta_a = 23.4$ (see Table V). As is expected for premixed monopropellants, the dependence of flame position upon activation energy is much larger than that found for bipropellant droplet burning which is controlled by diffusion. This indicates that effective activation energies must lie in a relatively narrow critical range for a useful monopropellant which is safe to handle and yet burns sufficiently rapidly in a combustion chamber.

Figures 4, 7, 8 and 11 illustrate that there is little difference in results for stoichiometric and non-stoichiometric mixtures except, of course, that the burning rate is somewhat larger in the stoichiometric case. The combustion profiles and the variations of mass flow rate with droplet radius are the same for both cases.

The dependence of the burning rate upon droplet radius derived from both analytical and numerical results is shown in Figs. 8 through 11. From the slope of the numerical curves for large activation temperatures, it can be seen that for the range of values of r_ℓ considered, the mass flow rate is proportional to the droplet radius raised to a power between 1.02 and 1.40 with an average of $\dot{m} \sim r_\ell^{1.10}$ in the cases $\theta_a = 23.4$, $\delta = 0.818$ and $\theta_a = 20.6$, $\delta = 1$. This is seen to be very nearly the variation $\dot{m} \sim r_\ell$ predicted in the previous section from an approximate analytical solution. In addition, the approximate solution yields very good agreement with the numerical results for the magnitude of the burning rate $\dot{m}$. The average difference is less than 10% and the maximum difference is a factor of 1.45 for the non-stoichiometric case and 2.30 for the stoichiometric case treated. The large

discrepancies occur only at large values of r_ℓ where the second term in Eq. (41) begins to become small invalidating the approximation used to obtain Eq. (42). For droplet radii smaller than those considered, the large activation temperature approximation is expected to still yield good results; this conclusion is also indicated by an extrapolation of the curves in Figs. 8 and 11. However, for large droplets the reasoning presented in the previous section indicates that the relation $\dot{m} \sim r_\ell^2$ should be approached causing the approximation to rapidly fail.

At the smaller activation temperatures, $\theta_a = 11.7$ and $\theta_a = 3.9$, in the range of values of r_ℓ of practical interest the large activation energy approximation is no longer valid. The numerical results illustrated in Figs. 9 and 10 indicate that $\dot{m} \sim r_\ell^2$ for $\theta_a = 3.9$ and show a variation from $\dot{m} \sim r_\ell^2$ to $\dot{m} \sim r_\ell^{1.8}$ for $\theta_a = 11.7$. This dependence is in agreement with the reasoning presented in the preceding section. It is also seen that the magnitude of the mass flow rate increases rapidly as the activation temperature decreases at a given droplet radius in this range of values of θ_a.

It is interesting to note that the dependence of mass flow rate upon droplet size can be correlated quite well for θ_a less than about 15 by the following method. In Eq. (36) we assume that

$$\frac{1}{\nu^4}\left(\alpha - \frac{q}{\bar{c}_p T_f}\,\varepsilon_p + \theta - \theta_\ell\right) \approx \alpha \quad . \tag{46}$$

where α is the value of the left-hand side at the droplet surface. Equation (36) then becomes

$$\alpha \frac{d\varepsilon_p}{d\theta} = \Lambda^* \frac{X_F X_O}{\theta} \exp(-\theta_a/\theta)$$

which, by substituting for X_F and X_O from Eqs. (33a) and (34), can be integrated from $\varepsilon_p=0$, $\theta=\theta_\ell$ to $\varepsilon_p=\varepsilon_{p,f}$, $\theta=1$. The result of the integration is

$$\int_0^{\varepsilon_{p,f}} \alpha d\varepsilon_p = \alpha \varepsilon_{p,f} = \frac{\varepsilon_{p,f} \Lambda^* h}{2(1-\theta_\ell+\alpha)}$$

which implies that the eigenvalue Λ^* is determined by the relation

$$\Lambda^* = 2\alpha(1-\theta_\ell+\alpha)(h)^{-1}. \tag{47}$$

Here the function h is defined by the equation

$$h \equiv \int_{\theta_\ell}^{1} \exp(-\theta_a/\theta) \frac{1-\theta}{\theta} \left[1-\varepsilon_{p,f}+\frac{\varepsilon_{p,f}(1-\theta)}{2(1-\theta_\ell+\alpha)}\right] d\theta \tag{48}$$

and is given explicitly by the expression

$$\begin{aligned} h=&(1-\varepsilon_{p,f})\left\{(1+\theta_a)\left[-Ei(-\theta_a)\right]-\exp(-\theta_a)-(1+\theta_a)\left[-Ei(-\theta_a/\theta_\ell)\right]+\theta_\ell \exp(-\theta_a/\theta_\ell)\right\} \\ &+\frac{\varepsilon_{p,f}}{2(1-\theta_\ell+\alpha)}\left\{(1+2\theta_a+\theta_a^2/2)\left[-Ei(-\theta_a)\right]-\left[(3+\theta_a)/2\right]\exp(-\theta_a)\right. \\ &\left.-(1+2\theta_a+\theta_a^2/2)\left[-Ei(-\theta_a/\theta_\ell)\right]+\theta_\ell(2+\theta_a/2-\theta_\ell/2)\exp(-\theta_a/\theta_\ell)\right\} \\ \approx&(1-\varepsilon_{p,f})\left\{(1+\theta_a)\left[-Ei(-\theta_a)\right]-\exp(-\theta_a)\right\} \\ &+\frac{\varepsilon_{p,f}}{2(1-\theta_\ell+\alpha)}\left\{(1+2\theta_a+\theta_a^2/2)\left[-Ei(-\theta_a)\right]-\left[(3+\theta_a)/2\right]\exp(-\theta_a)\right\} \end{aligned} \tag{49}$$

where the approximate relation is valid for $\theta_a/\theta_\ell \gtrsim 5$. For values of

θ_a larger than about 12, the quantity h is most easily evaluated by means of the asymptotic expression

$$h \sim \left[(1-\varepsilon_{p,f})/\theta_a^{\,2}\right] \exp(-\theta_a) \sum_{n=0}^{\infty} (n+1)(n+1)!\,(-1/\theta_a)^n$$

$$+ \left[\varepsilon_{p,f}/4(1-\theta_f+\alpha)\theta_a^{\,3}\right] \exp(-\theta_a) \sum_{n=0}^{\infty} (n^2+3n+2)(n+2)!\,(-1/\theta_a)^n. \qquad (50)$$

Equation (47) for the eigenvalue Λ^* is consistent with the relation $\dot{m} \sim r_f^{\,2}$. The values for the burning rate predicted by Eq. (47) are shown in Tables III and IV and Figs. 9 and 10 which indicate very good agreement with the numerical solution. The maximum difference is less than 20% and the average discrepancy is about 8%. This agreement must be treated as a fortuitous correlation* since the approximation expressed by Eq. (46) is quite poor. Figure 3 indicates that the function in Eq. (46) increases rapidly at small values of the flux fraction and then decreases to zero as $\varepsilon_p \longrightarrow \varepsilon_{p,f}$. Hence a cancellation of the error in the integral at small and large values of ε_p leads to a useful correlation for small activation energies.

13. Comparison with Experiment

Experimental verification of the theory presented here cannot be obtained from combustion chamber experiments since many other effects

---

* Equations (46) and (47) may be considered to be a first approximation to an iterative solution; however the second approximation involves integrals which must be evaluated numerically.

(non-radial heat conduction, droplet interaction, convective flow, etc.) cause it to be almost impossible to extricate the desired process. The only accurate test is obtained from measurements performed upon single droplets burning under controlled conditions. Very few such experiments have been carried out for monopropellants. The most complete work in this field appears to be that of Barrère and Moutet[3] who tested ethyl nitrate, propyl nitrate, hydrogen peroxide, and some composite propellants. The monopropellant droplets were suspended upon quartz fibers and the rate of decrease of droplet diameter was measured. Rosser[4] has also carried out some recent experiments using ethyl nitrate, nitromethane, and hydrazine.

The theory predicts that the functional dependence of the burning rate upon the droplet diameter is determined by the activation temperature, θ_a. Overall activation energies for ethyl nitrate and many similar compounds (ethyl nitrite, n-butyl nitrite, amyl nitrite, amyl nitrate, etc.) have been measured by B. P. Mullins[11] using ignition delay techniques. By an interpolation procedure a reasonably accurate value for the overall activation energy of propyl nitrate can be induced from this data. In view of the calculated values of θ_a (see Table VI) the numerical results presented in Figs. 8 through 11 indicate that the square (or perhaps 1.7 power) of the droplet diameter d should decrease linearly with time for propyl nitrate, while the relation $d_o - d \sim t - t_o$ should be observed for ethyl nitrate. Barrère and Moutet find that $d_o^2 - d^2 \sim t - t_o$ for both cases, a result which agrees reasonably well with

the theory for propyl nitrate but is contradictory to the theory for ethyl nitrate. This last discrepancy may imply that in ignition time lag measurements the effective overall activation energies are different than for droplet burning experiments. The experimental results discussed in the following paragraph seem to indicate, however, that the discrepancy possibly arises from the failure of the quasi-steady-state hypothesis.

Recently W. A. Rosser[4] has reported experiments performed with a porous sphere apparatus. The droplet radius was held constant and the rate of flow of propellant into the sphere was measured. The results indicate that the relation $\dot{m} \sim r_\ell^2$ is valid for ethyl nitrate as predicted from the present theory. If the quasi-steady-state hypothesis is valid for ethyl nitrate then these results are in contradiction to those of Barrère and Moutet unless the relatively low ambient temperature of the experiments reported in reference 3 invalidates the adiabatic assumption.

Rosser also observed that the mass flow rate is proportional to the square of the droplet radius for the hydrazine decomposition flame. This result is in agreement with the theory provided use is made of the presently accepted overall activation energy[12,13] of 36 kcal per mole which leads to a dimensionless activation temperature of $\theta_a \approx 12$. Rosser's experimental results seem to indicate that for any given fuel the relation $\dot{m} \sim r_\ell$ is observed for sufficiently small spheres, while the burning rate is proportional to the square of the droplet radius for large droplets. This conclusion is also in agreement with the theory (see

Section 12).

The overall activation energy for hydrogen peroxide decomposition is observed to be about 45 kcal per mole for the homogeneous gas phase reaction,* and the calculated value of the dimensionless activation temperature is 47.7 (see Table VI). For activation temperatures of this order of magnitude the relation $d_o^2 - d^2 \sim t - t_o$ is unambiguously predicted by the analysis for the case in which no mass is added to the droplet. This relation is in agreement with the hydrogen peroxide experiments of Barrère and Moutet.[3]

The burning rate constant, K, has been calculated for these propellants by using Eq. (44) which is in close agreement with the numerical results for large activation energies ($\theta_a \gtrsim 15$). It is seen from Table VI that the theoretical values differ from the experimental values for K by factors of 1.2, 1.9, and 16 for H_2O_2, $C_3H_7NO_3$, and $C_2H_5NO_3$, respectively. Care was taken to interpolate or extrapolate the experimental curves of K as a function of T_f to the adiabatic value of the final temperature which was treated in the theory.

The largest sources of error in the theoretical calculations are the uncertainties in the values of the thermal conductivity λ_f and the average specific heat $\bar{c}_p$. These uncertainties are sufficiently large to cause the observed differences for hydrogen peroxide and propyl nitrate. Equation (44) is really not expected to apply for ethyl nitrate because of the low activation temperature. Although the departure from spherical

---

* See, for example, reference 17 or 18.

symmetry is much less for monopropellant than for bipropellant droplets,* the fact that the calculated value of K is always less than the observed value may be traceable to non-spherically-symmetric natural convection effects which were neglected in the analysis and are found to be important at atmospheric pressures for bi-propellants.[14,15,16,19] Free convection tends to increase the burning rate and therefore may account for the discrepancies.

The burning rate as a function of equivalence ratio, ϕ, has been measured experimentally for monopropellant droplets consisting of a mixture of amyl acetate as fuel and nitric acid as oxidizer.[3] The experimental results presented in Fig. 12 are to be compared with the theoretical curve (Fig. 12) which was calculated from the data given in Table VII. The theoretical results are much less accurate here than in the previous cases because the density, heat of vaporization, and boiling point of liquid propellant mixtures are not accurately known. In this case we assumed for these properties average values which are between those of the pure constituents. It is also difficult to experimentally ascertain the mixture ratio because of the possibility of preferential evaporation of one component of the mixture. The theoretical and experimental curves of K as a function of ϕ are found to have similar shapes. In both cases there are maxima for slightly rich mixtures ($\phi \sim 1.05$ theoretically and $\phi \sim 1.15$ experimentally). Small

---

* See M. Barrère and H. Moutet, reference 3.

differences in the shape of the curves may be attributed to heat losses arising from the fact that the experiments were carried out at a constant ambient temperature of 896°K whereas the theory applies to problems in which the final temperature varies with the adiabatic flame temperature. Here again the magnitude of the theoretical burning rate is 20 to 30% lower than the experimental value. In order to obtain a better comparison experiments which eliminate convective effects are needed.*

14. On the Nature of the Large Activation Energy Limit

It was stated in Section 11 that the mass burning rate becomes independent of the chemical reaction rate for large values of the dimensionless activation energy θ_a. This result can be arrived at by the following physical reasoning. For large values of θ_a the reaction rate is strongly dependent upon temperature. The flux fraction of products ε_p will therefore remain virtually equal to its value at the droplet surface $\varepsilon_{p,l}$ until the temperature rise is nearly completed, $\theta \approx 1$. At this point ε_p increases rapidly to its final value $\varepsilon_{p,f}$. Clearly as θ_a goes to infinity the function $\varepsilon_p(\theta)$ approaches the constant value $\varepsilon_{p,l}$ except for a discontinuity at the end point $\theta=1$. This tendency is also well borne out by the numerical solutions (see Figs. 4 through 6). Furthermore, as $\theta_a \longrightarrow \infty$ the flame front σ_c moves toward infinity and virtually no reaction occurs at the finite values of σ over which θ increases from θ_l to 1. Hence we may assume in the limiting case that

* Some such experiments with diffusion flames are reported in reference 19.

$d\varepsilon_p/d\theta = d\varepsilon_p/d\sigma = 0$ and $\varepsilon_p = \varepsilon_{p,l}$. Equation (26) then becomes superfluous and only Eq. (27) remains to be solved in the case $\mathcal{L} = 1$.

By substituting into Eq. (27) the relation $\varepsilon_p = \varepsilon_{p,l}$ and using the definition of the parameters V^* and Λ^* we obtain the expression

$$\frac{d\theta}{d\sigma} = \sqrt{\frac{V^*}{\Lambda^*}}\ \frac{1}{\sigma^2}\ \frac{\theta - \theta_l + \alpha}{\theta}$$

which is separable and can be solved with the boundary condition $\theta = \theta_l$ at $\sigma = 1$. The result is

$$\frac{1}{\sigma} = \eta = 1 - \sqrt{\frac{\Lambda^*}{V^*}}\ \left[\theta - \theta_l - (\alpha - \theta_l)\ln\left(1 + \frac{\theta - \theta_l}{\alpha}\right)\right]. \qquad (51)$$

In view of Eq. (51) the requirement that $\theta = 1$ at $\sigma = \infty$ determines the eigenvalue Λ^* through the relation

$$\sqrt{\frac{V^*}{\Lambda^*}} = 1 - \theta_l - (\alpha - \theta_l)\ln\left(\frac{1 - \theta_l + \alpha}{\alpha}\right). \qquad (52)$$

A complete solution for $\sigma(\theta)$ and the burning rate is thus obtained quite simply in this idealized limiting case $\theta_a = \infty$.

Equation (52) is very similar to Eq. (42) of Section II. The dependence of mass flow rate upon the basic physical properties is nearly the same in both cases including the lack of dependence upon reaction rate. It follows that in the above sense there exists a solution even for infinite activation energy. Although some functions may become discontinuous, the mass flow rate remains well-defined and approaches a finite limiting value.

Since the reaction rate for the above physical picture is zero

except at the surface $\theta=1$, the limiting case $\theta_a \longrightarrow \infty$ is similar to the flame surface approximation of diffusion flames. In both of these problems the reaction rate $\dot{\omega}$ exhibits a strong spacial dependence, but $\dot{\omega} \sim \delta(T-T_f)$ in the present case while $\dot{\omega} \sim \delta(X_F)\delta(X_O)$ for diffusion flames. Here δ is the Dirac delta function. From this point of view a diffusion flame may be thought of as the limiting case of large activation energies.

15. Method for Arbitrary Lewis Numbers ($\mathcal{L} \neq 1$)

If the Lewis number is not equal to unity then the particular solutions for the mole fractions $X_i(\theta)$ obtained in Section 9 are no longer valid. Since the one-step reaction rate expression provides relations between the flux fractions ε_i [see Eq. (10)], the assumption of equal binary diffusion coefficients enables us to express all of the X_i in terms of a single mole fraction. By subtracting the form of Eq. (28) for which i=O from that for which i=F we obtain the relation

$$\frac{dX_F}{d\sigma} - \frac{dX_O}{d\sigma} = \frac{\dot{m}}{4\pi r_f} \frac{1}{\rho_f D_f} \frac{1}{\sigma^2 \theta} (X_F - X_O + \varepsilon_{O,f} - \varepsilon_{F,f})$$

where use has been made of Eq. (10). A solution of this equation is

$$X_O = X_F + \varepsilon_{O,f} - \varepsilon_{F,f} = X_F + \frac{1-\delta}{1+\delta} = X_F + 1 - \varepsilon_{P,f}. \qquad (53)$$

Since $X_{F,f} = 0$ this solution obviously obeys the correct boundary condition at $\sigma = \infty$. In view of Eqs. (5) and (53), the mole fraction of products is given by

$$X_P = 1 - X_F - X_O = \frac{2\delta}{1+\delta} - 2X_F = \varepsilon_{P,f} - 2X_F. \qquad (54)$$

Equations (53) and (54) express the mole fractions X_O and X_P in terms

of the single concentration variable X_F.

It is now clear that in order to carry out the numerical solution in this case the three equations (26), (27), and (28) with i=F must be integrated simultaneously. The change from two to three equations is trivial for a high-speed computing machine. An essential modification arises, however, in obtaining an approximate solution valid for large values of θ_a as was done in Section 10 for the case $\mathcal{L}=1$.

In order to obtain the approximate solution it is still convenient to use Eqs. (35) and (36). These equations must be supplemented by an equation for X_F, the most useful of which can be obtained by dividing Eq. (28) for i=F by Eq. (27). If use is made of Eq. (10) to eliminate $\mathcal{E}_F$ in terms of $\mathcal{E}_P$ then we obtain the result

$$\frac{dX_F}{d\theta} = \mathcal{L}\,\frac{X_F + \frac{1}{2}\mathcal{E}_P - \frac{1}{2}\mathcal{E}_{P,f}}{(1-\theta)\left[-1+\left(\frac{\mathcal{E}_{P,f}-\mathcal{E}_P}{1-\theta}\right)\left(\frac{1-\theta_\ell+\alpha}{\mathcal{E}_{P,f}}\right)\right]} \tag{55}$$

where Eq. (29) has been employed in the denominator.

The approximate expression for the burning rate valid for large values of θ_a is then obtained in a manner analogous to that used in Section 10; namely, Eq. (36) is integrated and yields Eq. (37a). In this case, however, in Eq. (37a) the function g is given by

$$g \equiv \frac{2(1-\theta_\ell+\alpha)}{\mathcal{E}_{P,f}} \int_{\theta_\ell}^{1} \exp(-\theta_a/\theta)\,\frac{X_F X_O}{\theta(1-\theta)}\,d\theta \tag{39a}$$

where $X_F(\theta)$ and $X_O(\theta)$ are determined by Eqs. (55) and (53). Since the exponential $\exp(-\theta_a/\theta)$ decreases very rapidly as θ decreases, only the behavior of the functions $X_i(\theta)$ near $\theta=1$ is important in the integral.

Hence little error is introduced if $X_F(\theta)$ is determined by expanding Eq. (55) about $\theta=1$. By performing the expansion we find

$$X_F \approx \mathcal{L}\,\frac{\frac{1}{2}\,\varepsilon_{P,f}(1-\theta)}{1-\theta_\ell+\alpha}$$

and

$$X_O \approx 1-\varepsilon_{P,f}+\mathcal{L}\,\frac{\frac{1}{2}\,\varepsilon_{P,f}(1-\theta)}{1-\theta_\ell+\alpha}$$

which upon substitution into Eq. (39a) yields

$$g \approx \mathcal{L}\int_{\theta_\ell}^{1} \exp(-\theta_a/\theta)\,\frac{1}{\theta}\left[1-\varepsilon_{P,f}+\mathcal{L}\,\frac{\frac{1}{2}\,\varepsilon_{P,f}(1-\theta)}{1-\theta_\ell+\alpha}\right] d\theta\,. \qquad (56)$$

This determines the right-hand side of Eq. (37a).

In the case $\mathcal{L}\neq 1$ the expansion of the function $f(\varepsilon_p)$ can be carried out by the method used in Appendix D. The only modification of the previous result is that

$$\frac{\frac{1}{2}\,\varepsilon_{P,f}(1-\theta_\ell)}{1-\theta_\ell+\alpha}\left(1-\varepsilon_{P,f}+\frac{\frac{1}{2}\,\varepsilon_{P,f}(1-\theta_\ell)}{1-\theta_\ell+\alpha}\right)$$

is replaced by the unknown quantity $X_{F,\ell}X_{O,\ell}$ in Eqs. (D-2), (D-4), and (D-5). For $\mathcal{L}$ near unity (as is always the case) the accuracy involved in approximating $f(\varepsilon_p)$ by expansion about the end point $\varepsilon_p=0$ is the same as described in Sections 10 and 11. By evaluating the integral $\int_0^{\varepsilon_{P,f}} f(\varepsilon_p)\,d\varepsilon_p$ with this approximation, we obtain the relation [compare Eq. (41)]

$$\Lambda^{*2}\,\frac{g}{2(1-\theta_\ell+\alpha)}+\Lambda^{*}\,\frac{(1-\theta_\ell+\alpha)}{2(1-\theta_\ell)}+\sqrt{\frac{\Lambda^{*}}{V^{*}}}\,4\alpha\theta_\ell^{2}\exp(\theta_a/\theta_\ell)\,\frac{\varepsilon_{P,f}}{2(1-\theta_\ell)X_{F,\ell}X_{O,\ell}}$$

$$-\alpha\theta_\ell\exp(\theta_a/\theta_\ell)\,\frac{(1-\theta_\ell+\alpha)\varepsilon_{P,f}}{2(1-\theta_\ell)^{2}X_{F,\ell}X_{O,\ell}}=0 \qquad (57)$$

where g is given by Eq. (56).

Because of the exponentials in the last two terms of Eq. (57), for values of θ_a larger than about 15 the first two terms are negligible and Eq. (42) is obtained. It follows that for large activation energies the approximate expression for the burning rate obtained for $\mathcal{L}=1$ applies with the same accuracy even when $\mathcal{L}\neq 1$. Specifically, Eqs. (42a) and (44) are independent of the assumption that the Lewis number is unity. It appears likely that for large activation energies the strong temperature dependence of the reaction rate determines the mass flow rate; the competition of thermal conduction and diffusion serves only to establish the concentration distributions.

16. Inert Atmosphere, Heat Loss to Surroundings, and Other Effects

a. General Considerations

In many practical cases the assumptions of no diffusion or thermal conduction at $r=\infty$ (see Section 8) will not be valid. Experiments are often carried out in an inert surrounding atmosphere which is at a temperature below the value of T_f given by Eq. (29). A modification of the procedures described in Section 9 f.f. is necessary in these cases. We shall demonstrate that these problems also involve the simultaneous solution of two first-order differential equations.

If we consider a single one-step chemical reaction, then relations similar to those given in Eq. (10) for the flux fractions ϵ_i will be valid. Hence we may write symbolically

$$\epsilon_i = a_i \epsilon_p + b_i \tag{58}$$

where the quantities a_i and b_i are constants determined only by the

chemical reaction and the relative evaporation rates of the components in the droplet.

Equations (27) and (28) are valid in the more general cases considered here. By substituting Eq. (58) into Eq. (28), multiplying Eq. (27) by $(-a_i \bar{c}_p T_f / q\sigma^2\theta)\sqrt{V^*/\Lambda^*}$, and adding the two resulting relations, we find

$$\frac{d}{d\sigma}\left(X_i - a_i \frac{\bar{c}_p T_f}{q}\theta - a_i\alpha\frac{\bar{c}_p T_f}{q} - a_i\epsilon_{P,l} + a_i\theta_l\frac{\bar{c}_p T_f}{q} - b_i\right)$$

$$= \frac{1}{\sigma^2\theta}\sqrt{\frac{V^*}{\Lambda^*}}\left(X_i - a_i\frac{\bar{c}_p T_f}{q}\theta - a_i\alpha\frac{\bar{c}_p T_f}{q} - a_i\epsilon_{P,l} + a_i\theta_l\frac{\bar{c}_p T_f}{q} - b_i\right).$$

Here use has been made of the definitions of the dimensionless parameters V^* and Λ^*. The solution to this equation is

$$X_i = b_i - a_i\theta_l\frac{\bar{c}_p T_f}{q} + a_i\epsilon_{P,l} + a_i\alpha\frac{\bar{c}_p T_f}{q} + a_i\frac{\bar{c}_p T_f}{q}\theta + c_i\exp\left(-\sqrt{\frac{V^*}{\Lambda^*}}\int_\sigma^\infty \frac{d\sigma}{\theta\sigma^2}\right). \quad (59)$$

where c_i is a constant of integration which is determined by the boundary conditions at $\sigma = \infty$.

Equation (59) provides little simplification since the function $\theta(\sigma)$ must be known in order to evaluate the integral appearing in the exponential. If we replace Eqs. (18) and (24) by the somewhat less realistic assumptions that the thermal conductivity λ is constant and the product ρD is constant (i.e., the diffusion coefficient $D \sim \theta$), then the factor θ disappears from Eqs. (27) and (28). This leads to the deletion of the factor $1/\theta$ from the integrand in Eq. (59), and the integration may then be explicitly carried out yielding the relation*

* This has been pointed out by J. Lorell and H. Wise, reference 1.

$$X_i = b_i - a_i \theta_\ell \frac{\bar{c}_p T_f}{q} + a_i \varepsilon_{p,\ell} + a_i \alpha \frac{\bar{c}_p T_f}{q} + a_i \frac{\bar{c}_p T_f}{q} \theta + c_i \exp\left(-\frac{1}{\sigma}\sqrt{\frac{V^*}{\lambda^*}}\right). \qquad (59a)$$

It is thus seen that for this alternate temperature dependence of the transport coefficients, the mole fractions $X_i(\theta,\sigma)$ are obtained explicitly and only Eqs. (26) and (27) remain to be solved simultaneously.

With the simplification expressed by Eq. (59a), numerical solutions to this more general class of problems may be carried out as described in Section 10 and Appendix E. After the boundary conditions are specified, no additional difficulties are encountered. It is expected that approximate analytical solutions valid for large activation energies may be obtained by expansion about the cold boundary as described in Section 11. If the expansion is carried out then the relation $\dot{m} \sim r_\ell$ is obtained for large values of θ_a. The constant of proportionality between the burning rate and the droplet radius is found to depend upon the boundary conditions. This is in agreement with the experimental results of Barrère and Moutet[3] who observe that the evaporation constant K depends upon the boundary temperature T_f.

b. Heat Transfer to Surroundings

It is of interest to consider some special cases in greater detail. When only fuel, oxidizer and products are present and the relative diffusion velocities of all chemical species vanish at $\sigma = \infty$, then heat may be added or withdrawn by the surrounding atmosphere. In this case the requirement that

$$\lim_{\sigma \to \infty} \left(\sigma^2 \frac{dX_F}{d\sigma}\right) = \lim_{\sigma \to \infty} \left(\sigma^2 \frac{dX_O}{d\sigma}\right) = \lim_{\sigma \to \infty} \left(\sigma^2 \frac{dX_P}{d\sigma}\right) = 0$$

may be applied to Eq. (59) to yield Eqs. (53) and (54) for the mole fractions X_O and X_P in terms of X_F. A modified relation for the function $X_F(\theta)$ is obtained because of the fact that $\lim_{\sigma\to\infty} (\sigma^2 d\theta/d\sigma) \neq 0$ when T_f is not given by Eq. (29). By substituting for a_F and b_F from Eq. (10), we find

$$X_F = \frac{\varepsilon_{P,f}}{2} - \frac{\alpha \bar{c}_p T_f}{2q} + \frac{\theta_l \bar{c}_p T_f}{2q} - \frac{\theta \bar{c}_p T_f}{2q} + c_F \exp\left(-\sqrt{\frac{V^*}{\Lambda^*}} \int_\sigma^\infty \frac{d\sigma}{\theta\sigma^2}\right)$$

in which the constant c_F may be evaluated from the condition that $X_{F,f} = 0$ for fuel-rich systems. The resulting expression for the mole fraction of fuel is

$$X_F = \frac{\varepsilon_{P,f}}{2} - \frac{\alpha \bar{c}_p T_f}{2q} + \frac{\theta_l \bar{c}_p T_f}{2q} - \frac{\theta \bar{c}_p T_f}{2q}$$

$$+\left(\frac{\bar{c}_p T_f}{2q} - \frac{\theta_l \bar{c}_p T_f}{2q} + \frac{\alpha \bar{c}_p T_f}{2q} - \frac{\varepsilon_{P,f}}{2}\right) \exp\left(-\sqrt{\frac{V^*}{\Lambda^*}} \int_\sigma^\infty \frac{d\sigma}{\theta\sigma^2}\right). \qquad (60)$$

For the transport property behavior leading to Eq. (59a) this relation is replaced by

$$X_F = \frac{\varepsilon_{P,f}}{2q} - \frac{\alpha \bar{c}_p T_f}{2q} + \frac{\theta_l \bar{c}_p T_f}{2q} - \frac{\theta \bar{c}_p T_f}{2q}$$

$$+\left(\frac{\bar{c}_p T_f}{2q} - \frac{\theta_l \bar{c}_p T_f}{2q} + \frac{\alpha \bar{c}_p T_f}{2q} - \frac{\varepsilon_{P,f}}{2}\right) \exp\left(-\frac{1}{\sigma}\sqrt{\frac{V^*}{\Lambda^*}}\right). \qquad (60a)$$

By substituting Eqs. (53), (54), and (60) into Eqs. (26) and (27) and expanding the result about the end points, it may easily be deduced that the temperature profile behaves as illustrated in Fig. 13. When T_f is greater than the value given by Eq. (29), then the profile remains

monotonic, heat is added at $\sigma = \infty$, and the burning rate is increased. If T_f is less than its adiabatic value, then a temperature maximum develops in the flow field, heat is conducted out of the fluid at $\sigma = \infty$, and the burning rate is decreased.

The above conclusion concerning the burning rate is also supported by an approximate analytical solution for $\dot{m}$ valid for large activation energies. By proceeding as in Section II and Appendix D, but not using Eq. (29) for T_f, we obtain Eq. (42) for the burning rate. Since the quantity $(1 - \theta_\ell + \alpha)$ is no longer related to the heat of reaction q, it follows that Eq. (42a) is replaced by the relation

$$\dot{m} = 16\pi r_\ell \frac{\lambda_\ell}{\bar{c}_p} \frac{T_f - T_\ell}{T_f - T_\ell + \frac{\Delta_\ell}{\bar{c}_p}} . \qquad (42b)$$

Equation (42b) shows that the mass flow rate increases as the temperature of the surroundings is increased.

c. Effect of Inert Component

The case in which an inert species, N, is present requires similar modification. For brevity we assume here that the adiabatic condition expressed by Eq. (29) is valid and that no liquid phase reaction occurs. Imposing other boundary conditions for the temperature and flux fraction of products causes no additional difficulty. For a fuel-rich system ($X_{F,f} = 0$) with $\varepsilon_{P,\ell} = 0$, the constants a_F and b_F are found from Eq. (10) and may be substituted into Eq. (59). The resulting expression for the mole fraction of fuel is

$$X_F = \varepsilon_{F,\ell} + \frac{\bar{c}_p T_f}{2q}(\theta_\ell - \alpha - \theta) \tag{33}$$

which, by use of Eq. (29), reduces to Eq. (33a). The concentration profile of the less-abundant reactant is therefore unaffected by the presence of a neutral component.

Since $a_N = 0$ and ε_N is constant, for the inert component Eq. (59) reduces to

$$X_N = \varepsilon_N + c_N \exp\left(-\sqrt{\frac{\nu^*}{\Lambda^*}} \int_\sigma^\infty \frac{d\sigma}{\theta\sigma^2}\right) . \tag{61}$$

The flux fraction ε_N is determined by the rate of evaporation of neutral species present in the droplet, and the constant c_N is fixed by the concentration of the neutral component at $\sigma = \infty$.

By subtracting the form of Eq. (59) for fuel from the form corresponding to oxidizer we find

$$X_O = X_F + \varepsilon_{O,\ell} - \varepsilon_{F,\ell} + c_O \exp\left(-\sqrt{\frac{\nu^*}{\Lambda^*}} \int_\sigma^\infty \frac{d\sigma}{\theta\sigma^2}\right)$$

$$= X_F + 1 - \varepsilon_{P,f} - \varepsilon_N + c_O \exp\left(-\sqrt{\frac{\nu^*}{\Lambda^*}} \int_\sigma^\infty \frac{d\sigma}{\theta\sigma^2}\right) . \tag{62}$$

The requirement that

$$X_O + X_F + X_P + X_N = 1$$

then leads to the relation

$$X_P = \varepsilon_{P,f} - 2X_F - (c_O + c_N) \exp\left(-\sqrt{\frac{\nu^*}{\Lambda^*}} \int_\sigma^\infty \frac{d\sigma}{\theta\sigma^2}\right) \tag{63}$$

which determines the constant c_P in terms of c_O and c_N. The final flux fraction $\varepsilon_{P,f}$ is determined by the relative evaporation rates of fuel

and oxidizer as described in Section 8, while c_O depends upon the boundary conditions imposed on the oxidizer diffusion at $\sigma = \infty$.

If all of the inert component present in the gaseous phase was originally contained within the droplet, then it is possible to arrange for the diffusion velocities to vanish at $\sigma = \infty$ by letting $c_N = c_O = 0$. In this case $\varepsilon_N \neq 0$, the mole fraction X_N is constant, and the inert species acts only as a diluent which reduces $\varepsilon_{P,f}$ and the heat added per unit mass of mixture. With this modification the solutions obtained in Sections 10 and 11 remain valid.

A case of greater practical interest is that in which the droplet contains no inert component, but burning occurs in a partially inert atmosphere. Here the flux fraction $\varepsilon_N = 0$, the constant $c_N \neq 0$, and the concentration profile of the neutral species is seen from Eq. (61) to be approximately an exponential function of $1/\sigma$. In this case either the oxidizer or product concentration profiles must differ from the linear temperature dependence by an exponential term involving σ [see Eqs. (62) and (63)]. We may assume that no oxidizer diffusion occurs at $\sigma = \infty$, (i.e., $c_O = 0$), or no product diffusion occurs at infinity, (i.e., $c_O = -c_N$). The boundary condition at $\sigma = \infty$ which corresponds to most experiments is that there can be no relative diffusion of oxidizer and products. According to Eq. (63) this requires that $c_O = -(c_O + c_N)$, which implies that $c_O = -c_N/2$. If the surrounding atmosphere is completely inert then $c_N = 1$.

It is seen that concentration profiles may be significantly affected

by the presence of a neutral species. The mass burning rate is, however, changed very little in the case of large activation energies. This conclusion follows from the fact that the approximate derivation of Eq. (42) remains valid for large values of θ_a even when an inert gas is present. The burning rate is affected much less by the relative diffusion of chemical species than by thermal conduction across the boundaries of the system.

C. FIRST-ORDER KINETICS

1. Definition of the Problem

Another class of reactions often encountered in monopropellant droplet combustion is represented symbolically by $F \longrightarrow nP$ where n may be any positive number. These reactions are of the first order and require no oxidizer. An approximate solution will be found by a method very similar to that used in Part B of this chapter.

We include in Appendix A a complete list of assumptions which will serve to define the problem as well as state the approximations that will be introduced in obtaining the solution. It is seen from Appendix A that the most restrictive assumptions of Part B, namely the equality of diffusion coefficients, the equality of molecular weights, and a Lewis number of unity, are not made here. It is therefore expected that the results obtained here will represent more closely the corresponding physical system than do those obtained in Part B.

2. Basic Equations and Boundary Conditions

Many of the basic equations used in Part B are also valid in this case. For example, the equations of conservation of mass [Eqs. (1)

through (5)] are quite general and apply for any type of kinetics. For the present two-component system Eqs. (3) and (5) become, respectively,

$$\varepsilon_F = 1 - \varepsilon_P, \tag{64}$$

and

$$Y_F = 1 - Y_P. \tag{65}$$

For the reaction $F \longrightarrow nP$ the conservation of mass implies that the rates of production of the chemical species (mass per unit volume per second) are related by the equation $\dot{\omega}_F = -\dot{\omega}_P$. Equations (1) and (2) then imply that

$$\frac{d\varepsilon_F}{dr} = -\frac{d\varepsilon_P}{dr} \tag{66}$$

which may be integrated to obtain

$$\varepsilon_F - \varepsilon_{F,\ell} = -(\varepsilon_P - \varepsilon_{P,\ell}). \tag{67}$$

The first-order reaction rate expression for $\dot{\omega}_P$ is*

$$\dot{\omega}_P = B\rho \exp(-T_a/T)\, Y_F$$

which implies that

$$\frac{d\varepsilon_P}{dr} = \frac{4\pi r^2}{\dot{m}}\, B\rho \exp(-T_a/T)\, Y_F. \tag{68}$$

Here use has been made of Eqs. (1) and (2) and B represents the reaction rate frequency factor in sec^{-1}. By using the ideal gas law [Eq. (25)] and the relation between the functions Y_i and X_i given in Eq. (20), we can put Eq. (68) into the form

---

* This is again a special case of the general rate equations given by von Kármán and Penner, reference 5.

$$\frac{d\varepsilon_P}{dr} = \frac{4\pi r^2}{\dot{m}} \frac{pM_F B}{RT} \exp(-T_a/T) X_F. \tag{68a}$$

The derivation of the energy equation is given in Section B-5. By setting $\varepsilon_O = 0$ we obtain the result

$$4\pi r^2 \lambda \frac{dT}{dr} = \dot{m}\left[\Delta\ell - q(\varepsilon_P - \varepsilon_{P,\ell}) + \bar{c}_p(T - T_\ell)\right] \tag{69}$$

where the heat of reaction and enthalpies of formation per unit mass are related by the equation

$$q \equiv h_F^\circ - h_P^\circ. \tag{70}$$

Here the average specific heat has been defined by the relation

$$\begin{aligned}\bar{c}_p \equiv \frac{1}{T - T_\ell} &\left[\varepsilon_F(h_F - h_F^\circ) + \varepsilon_P(h_P - h_P^\circ)\right. \\ &\left. - \varepsilon_{F,\ell}(h_{F,\ell} - h_F^\circ) - \varepsilon_{P,\ell}(h_{P,\ell} - h_P^\circ)\right] \\ = \frac{1}{T_f - T_\ell} &\left[\varepsilon_{F,f}(h_{F,f} - h_F^\circ) + \varepsilon_{P,f}(h_{P,f} - h_P^\circ)\right. \\ &\left. - \varepsilon_{F,\ell}(h_{F,\ell} - h_F^\circ) - \varepsilon_{P,\ell}(h_{P,\ell} - h_P^\circ)\right].\end{aligned} \tag{71}$$

In Eq. (71) the last equality involves the assumption that the mean specific heat is independent of temperature.

The general diffusion equation [Eq. (21)] reduces to the relation

$$\frac{dX_P}{dr} = \frac{v\bar{M}}{DM_F}(X_P \varepsilon_F - nX_F \varepsilon_P) \tag{72}$$

where D is the binary diffusion coefficient for the fuel-product mixture. In view of Eq. (2) and the ideal gas law [Eq. (25)], Eq. (72) can be written in the form

$$\frac{dX_P}{dr} = \frac{\dot{m}}{4\pi r^2}\,\frac{RT}{pDM_F}\left[X_P(1-\varepsilon_P)-n\varepsilon_P(1-X_P)\right]. \qquad (72a)$$

Equation (64) and the relation $X_F + X_P = 1$ have been used here.

Equations (68a), (69), and (72a) consist of three first-order differential equations in the three unknowns, T, X_P, and ε_P. The three boundary conditions T_ℓ, $\varepsilon_{P,f}$, and $X_{P,f}$ are physically determined. The temperature T_ℓ is the boiling point of the liquid droplet. It is necessary that $\varepsilon_{F,f}=0$ for the reaction to be completed as $r\longrightarrow\infty$. In view of Eq. (64) this implies that $\varepsilon_{P,f}=1$. We assume that the concentration gradients approach zero as $r\longrightarrow\infty$. Therefore the diffusion velocities go to zero at infinity and $Y_{P,f}=\varepsilon_{P,f}=1$. It then follows from Eq. (20) that $X_{P,f}=1$.

The boundary value $\varepsilon_{P,\ell}$ will be determined by the composition of the droplet and its evaporation characteristics. We shall treat the important case in which $\varepsilon_{P,\ell}=0$. This implies that there is no liquid phase reaction and no product present in the droplet. A fourth boundary condition is thereby provided insuring the existence of an eigenvalue which will be the mass burning rate $\dot{m}$. We shall consider the case of adiabatic burning for which, according to Eq. (69), the relation

$$T_f = T_\ell + \frac{q-\Delta\ell}{\bar{c}_p} \qquad (78)$$

is valid [compare Eq. (29)].

3. Method of Solution

If we introduce the dimensionless distance and temperature variables σ and θ defined in Section B-7, then Eqs. (68a), (69), and

(72a) become, respectively,

$$\frac{d\varepsilon_p}{d\sigma} = \frac{4\pi r_\ell^3}{\dot{m}} \frac{p M_F B}{R T_F} \frac{\sigma^2}{\theta} \exp(-\theta_a/\theta)(1-X_p). \tag{74}$$

$$\frac{4\pi r_\ell}{\dot{m}} \frac{\lambda_f}{\bar{c}_p} \sigma^2 \theta \frac{d\theta}{d\sigma} = \alpha - \frac{q}{\bar{c}_p T_f} \varepsilon_p + \vartheta - \vartheta_\ell . \tag{75}$$

and

$$\frac{dX_p}{d\sigma} = \frac{\dot{m}}{4\pi r_\ell} \frac{R T_f}{p D_f M_F} \frac{\left[X_p(1-\varepsilon_p) - n\varepsilon_p(1-X_p)\right]}{\sigma^2 \theta} . \tag{76}$$

In the last two equations use has been made of the assumptions that $\lambda \sim T$ and $D \sim T^2$ as given in Eqs. (18) and (24).

It is convenient to replace the distance variable σ by the dimensionless temperature θ as the independent variable in Eqs. (74), (75), and (76). In order to accomplish this we may first multiply Eq. (74) by Eq. (75) obtaining the expression

$$\frac{d\sigma}{d\theta} = \left\{ \frac{\exp(\theta_a/\theta)\, \theta^2 \frac{d\varepsilon_p}{d\theta}}{V^*(1-X_p)(1-\theta)\left[-1 + \frac{1-\varepsilon_p}{1-\theta}(1-\vartheta_\ell+\alpha)\right]} \right\}^{1/2} \tag{77}$$

where the quantity V^* has been defined by the relation

$$V^* \equiv \frac{p M_F B \bar{c}_p}{R T_f \lambda_f} r_\ell^2 .$$

Here use has been made of Eq. (73). Dividing Eq. (74) by Eq. (75) one finds that

$$\frac{d\varepsilon_p}{d\theta} = \frac{\Lambda^* \sigma^4 \exp(-\theta_a/\theta)(1-X_p)}{\left[-1 + \frac{1-\varepsilon_p}{1-\theta}(1-\vartheta_\ell+\alpha)\right](1-\theta)} \tag{78}$$

where the dimensionless eigenvalue Λ^* is given by

$$\Lambda^* \equiv \frac{pM_F B \lambda_f}{RT_f \bar{c}_p} \, 16\pi^2 \frac{r_\ell^4}{\dot{m}^2} \, .$$

It is seen that Λ^* and V^* are dimensionless parameters similar to those defined in Section B-10. If Eq. (76) is divided by Eq. (75) then the variable τ does not appear in the resulting equation which is

$$\frac{dX_p}{d\theta} = \mathcal{L} \frac{X_p(1-\varepsilon_p) - n\varepsilon_p(1-X_p)}{(1-\theta)\left[-1 + \frac{1-\varepsilon_p}{1-\theta}(1-\theta_\ell + \alpha)\right]} \, . \tag{79}$$

Here the quantity

$$\mathcal{L} \equiv \frac{RT_f \lambda_f}{pM_F D_f \bar{c}_p}$$

is the effective Lewis number for this problem. Equations (74), (75), and (76) are well suited for an exact solution of the problem by numerical integration. It will now be shown that an accurate approximation to Λ^* may be obtained from Eqs. (77), (78), and (79) by a method quite similar to that used in Part B.

By integrating Eq. (78) from the end point $\theta = \theta_\ell$ to $\theta = 1$, we obtain the relation

$$\int_0^1 f(\varepsilon_p) d\varepsilon_p = \Lambda^* g \tag{80}$$

where the function $f(\varepsilon_p)$ has been defined as

$$f(\varepsilon_p) \equiv \frac{1}{\sigma - 4} \left[-1 + \frac{1-\varepsilon_p}{1-\theta}(1-\theta_\ell + \alpha)\right] \tag{81}$$

and the quantity g is given by

$$g \equiv \int_{\theta_l}^{1} \exp(-\theta_a/\theta)\, \frac{1-X_p}{1-\theta}\, d\theta \quad . \tag{82}$$

Because of the presence of the exponential factor $\exp(-\theta_a/\theta)$ in the integrand of Eq. (82), the largest contribution to the integral will come from the range of values of θ near unity. Equation (79) may be expanded about the boundary point $\theta = 1$ in order to obtain an approximate expression for the mole fraction X_p. Since

$$\lim_{\theta \to 1} \left(\frac{1-\varepsilon_p}{1-\theta} \right) = \left. \frac{d\varepsilon_p}{d\theta} \right|_{\theta=1}$$

and

$$\lim_{\theta \to 1} \left(\frac{1-X_p}{1-\theta} \right) = \left. \frac{dX_p}{d\theta} \right|_{\theta=1} ,$$

the expansion shows that

$$\frac{dX_p}{d\theta} = \mathcal{L}\, \frac{\dfrac{d\varepsilon_p}{d\theta} - n \dfrac{dX_p}{d\theta}}{-1 + \dfrac{d\varepsilon_p}{d\theta}\,(1-\theta_l+\alpha)} \tag{83}$$

near $\theta = 1$. It will be proven in the following section that $d\varepsilon_p/d\theta$ approaches infinity as $\theta \longrightarrow 1$. Therefore a solution of the above equation is

$$\left. \frac{dX_p}{d\theta} \right|_{\theta=1} = \frac{\mathcal{L}}{1-\theta_l+\alpha}$$

which may be integrated to show that

$$X_p = 1 - \frac{\mathcal{L}}{1-\theta_l+\alpha}\,(1-\theta) \tag{84}$$

near the end point $\theta=1$. The results of Section B-10 indicate* that for all reasonable values of the Lewis numbers the mole fraction X_p will be nearly a linear function of the dimensionless temperature θ. This implies that using Eq. (84) in Eq. (82) will provide an accurate expression for the quantity g.

The substitution of Eq. (84) into Eq. (82) yields the relation

$$g = \frac{\mathcal{L}}{1-\theta_\ell+\alpha} \int_{\theta_\ell}^{1} \exp(-\theta_a/\theta)\,d\theta$$

$$= \frac{\mathcal{L}}{1-\theta_\ell+\alpha} \left[\exp(-\theta_a) - \theta_\ell \exp(-\theta_a/\theta_\ell) + \theta_a \mathrm{Ei}(-\theta_a) \right.$$

$$\left. - \theta_a \mathrm{Ei}(-\theta_a/\theta_\ell) \right]. \qquad (85)$$

For a large activation energy θ_a and small values of θ_ℓ this equation is closely approximated by the expression

$$g \approx \frac{\mathcal{L}}{1-\theta_\ell+\alpha} \left[\exp(-\theta_a) + \theta_a \mathrm{Ei}(-\theta_a) \right] \approx \frac{\mathcal{L}}{1-\theta_\ell+\alpha} \frac{\exp(-\theta_a)}{\theta_a}. \qquad (85a)$$

It follows from Eq. (80) that, having found a good approximation for the quantity g, we must finally obtain an appropriate expression for the function $f(\varepsilon_p)$ in order to evaluate the eigenvalue Λ^*.

4. The Approximation of $f(\varepsilon_p)$

Let us first investigate the behavior of the function $f(\varepsilon_p)$ near the hot boundary ($\varepsilon_p=1$). Setting $\theta=1$ in Eq. (78) leads to the relation

---

* See Section IIB of reference 5.

$$\lim_{\varepsilon_p \to 1} \left\{ \frac{\dfrac{d\varepsilon_p}{d\theta}\left[-1 + (1-\theta_\ell+\alpha)\dfrac{d\varepsilon_p}{d\theta}\right]}{\dfrac{dX_p}{d\theta}\ \sigma^4} \right\} = \Lambda^* \exp(-\theta_a).$$

By eliminating the derivative $dX_p/d\theta$ from this equation by means of Eq. (33), we obtain the expression

$$\lim_{\varepsilon_p \to 1} \left\{ \frac{1}{\sigma^4}\left[\mathcal{L}n-1+(1-\theta_\ell+\alpha)\frac{d\varepsilon_p}{d\theta}\right]\left[-1+(1-\theta_\ell+\alpha)\frac{d\varepsilon_p}{d\theta}\right] \right\}$$

$$= \mathcal{L}\Lambda^* \exp(-\theta_a). \tag{86}$$

Since $\sigma \longrightarrow \infty$ as $\theta \longrightarrow 1$ this equation implies that $d\varepsilon_p/d\theta$ must approach infinity as $\varepsilon_p \longrightarrow 1$. Equation (86) may therefore be written in the form

$$\lim_{\varepsilon_p \to 1}\left(\frac{1}{\sigma^2}\frac{d\varepsilon_p}{d\theta}\right) = \sqrt{\frac{\mathcal{L}\Lambda^* \exp(-\theta_a)}{(1-\theta_\ell+\alpha)^2}}\ . \tag{86a}$$

In the neighborhood of the point $\theta=1$ Eq. (81) becomes

$$\lim_{\varepsilon_p \to 1}\left[\sigma^2 f(\varepsilon_p)\right] = \sqrt{\mathcal{L}\Lambda^* \exp(-\theta_a)} \tag{87}$$

where use has been made of Eq. (86a). Since $\sigma \longrightarrow \infty$ as $\theta \longrightarrow 1$ it follows from Eq. (87) that $f(1) = 0$. Furthermore, by expanding Eq. (77) about $\theta=1$ and using Eq. (84), we find that

$$\frac{d\sigma}{d\theta} = \frac{1}{(1-\vartheta)\sqrt{\mathcal{L}V^* \exp(-\theta_a)}}$$

near the hot boundary which implies that in the neighborhood of the point $\theta=1$, the relation

$$\sigma = \frac{-\log(1-\theta)}{\sqrt{\mathcal{L}\nu^* \exp(-\theta_a)}} \tag{88}$$

is valid. It follows from Eq. (88) that

$$\frac{d\left(\frac{1}{\sigma^2}\right)}{d\varepsilon_p} = \frac{2\mathcal{L}\nu^* \exp(-\theta_a)}{\left[\log(1-\theta)\right]^3 (1-\theta)\frac{d\varepsilon_p}{d\theta}}$$

near the hot boundary. By using this relation and the continuity of all functions involved, we find from Eq. (87) that

$$\frac{df}{d\varepsilon_p} = \sqrt{\mathcal{L}\Lambda^* \exp(-\theta_a)}\,\frac{d\left(\frac{1}{\sigma^2}\right)}{d\varepsilon_p} = \frac{2\left[\mathcal{L}\nu^* \exp(-\theta_a)\right]^2 (1-\theta_\ell+\alpha)}{(1-\delta)\left[\log(1-\theta)\right]^5} \tag{89}$$

in the limit $\varepsilon_p \longrightarrow 1$. In this last relation use has been made of Eq. (86a). Equation (89) shows that $df/d\varepsilon_p$ becomes negatively infinite as $\varepsilon_p \longrightarrow 1$.

It can be seen by comparing the equations obtained in the previous paragraph with those of Appendix D that the behavior of the function $f(\varepsilon_p)$ here is very similar to that of the corresponding function for non-stoichiometric mixtures with a second-order chemical reaction. The functional form of the result is identical in both cases; the only differences are multiplicative constants. It follows that Fig. 2(f) also represents the function $f(\varepsilon_p)$ for a first-order reaction. Employing the linear approximation illustrated in Fig. 2(f) leads to little error in the integral in Eq. (80) for large activation energies.

In order to expand $f(\varepsilon_p)$ about the cold boundary ($\varepsilon_p=0$) we note from Eq. (81) that $f(0)=\alpha/(1-\theta_\ell)$. By differentiating Eq. (81) we obtain Eq. (D-1a) which implies that

$$\left.\frac{df}{d\varepsilon_p}\right|_{\varepsilon_p=0} = -\frac{4\alpha}{1-\theta_\ell}\left.\frac{d\sigma}{d\theta}\right|_{\theta=\theta_\ell}\left.\frac{d\theta}{d\varepsilon_p}\right|_{\theta=\theta_\ell} - \frac{1-\theta_\ell+\alpha}{1-\theta_\ell} + \frac{1-\theta_\ell+\alpha}{(1-\theta_\ell)^2}\left.\frac{d\theta}{d\varepsilon_p}\right|_{\theta=\theta_\ell}. \tag{90}$$

Equations (77) and (78) show that

$$\left.\frac{d\varepsilon_p}{d\theta}\right|_{\theta=\theta_\ell} = \frac{1}{\alpha}\Lambda^* \exp(-\theta_a/\theta_\ell)(1-X_{p,\ell}) \tag{91}$$

and

$$\left.\frac{d\sigma}{d\theta}\right|_{\theta=\theta_\ell} = \frac{\theta_\ell}{\alpha}\sqrt{\frac{\Lambda^*}{V^*}}. \tag{92}$$

The substitution of these values into Eq. (90) yields the relation

$$\left.\frac{df}{d\varepsilon_p}\right|_{\varepsilon_p=0} = -\frac{4\theta_\ell\alpha}{1-\theta_\ell}\,\frac{1}{\sqrt{V^*\Lambda^*}}\,\frac{\exp(\theta_a/\theta_\ell)}{(1-X_{p,\ell})}$$

$$+\frac{\alpha(1-\theta_\ell+\alpha)}{(1-\theta_\ell)^2}\,\frac{1}{\Lambda^*}\,\frac{\exp(\theta_a/\theta_\ell)}{(1-X_{p,\ell})} - \frac{1-\theta_\ell+\alpha}{1-\theta_\ell}. \tag{93}$$

Hence near the point $\varepsilon_p=0$ the function $f(\varepsilon_p)$ may be approximated by the equation

$$f(\varepsilon_p) = \frac{\alpha}{1-\theta_\ell} - \varepsilon_p \left\{ -\frac{1}{\Lambda^*}\frac{\alpha(1-\theta_\ell+\alpha)}{(1-\theta_\ell)^2}\,\frac{\exp(\theta_a/\theta_\ell)}{(1-X_{p,\ell})} + \frac{1}{\sqrt{\Lambda^* V^*}}\,\frac{4\theta_\ell\alpha}{1-\theta_\ell}\,\frac{\exp(\theta_a/\theta_\ell)}{(1-X_{p,\ell})} + \frac{1-\theta_\ell+\alpha}{1-\theta_\ell} \right\}. \tag{94}$$

In accordance with the discussion in the previous paragraph we shall assume that Eq. (94) is valid for all values of ϵ_p.

5. The Determination of the Burning Rate for Large Values of θ_a

If we perform the integration in Eq. (80) by using the approximation of Eq. (94) then we obtain the relation

$$\Lambda^{*2}\, g + \Lambda^* \frac{(1-\theta_\ell-\alpha)}{2(1-\theta_\ell)} + \sqrt{\frac{\Lambda^*}{V^*}}\, \frac{2\theta_\ell\alpha}{(1-\theta_\ell)}\, \frac{\exp(\theta_a/\theta_\ell)}{(1-\chi_{p,\ell})}$$

$$- \frac{\alpha(1-\theta_\ell+\alpha)}{2(1-\theta_\ell)^2}\, \frac{\exp(\theta_a/\theta_\ell)}{(1-\chi_{p,\ell})} = 0 . \qquad (95)$$

This equation determining the eigenvalue Λ^* is very similar to Eq. (41). As in the case of Eq. (41), unless the activation temperature is less than about 15,000°K the last two terms are much larger than the first two because of the exponential factor. Equation (95) then reduces approximately to the relation

$$\sqrt{\frac{\Lambda^*}{V^*}} = \frac{1-\theta_\ell+\alpha}{4\theta_\ell(1-\theta_\ell)} . \qquad (96)$$

which is identical to Eq. (42) of Section B-11. It can be seen from the definitions of the parameters V^* and Λ^* used in this part that Eqs. (42a), (43), and (44) are valid in the present case as well as for the second-order reaction treated in Part B. All of the discussion of Section B-11 therefore applies also for the first-order reactions investigated here.

The fact that Eqs. (96) and (42) are identical indicates that they may be relatively general relations and may hold for a great variety of reactions of different orders. The necessary conditions required for Eq. (96) to be valid are investigated in the next part of this chapter. The equality of Eqs. (96) and (42) also shows that it will be necessary to use higher-order approximations for the function $f(\varepsilon_p)$ to find the effect of the order of the chemical reaction upon the mass burning rate of monopropellant droplets at large activation energies.

D. EXTENSION TO ARBITRARY ORDER KINETICS

1. Basic Equations

In this part we shall discuss the general requirements which must be satisfied in order that the methods used in Parts B and C can be employed. Let us consider a droplet that contains an arbitrary number s of different chemical constituents. The conservation of mass in chemical reactions is expressed by the equation

$$\omega_j = \frac{\dot{m}}{4\pi r^2} \frac{d\varepsilon_j}{dr} \qquad j=1,2,\ldots,s \tag{97}$$

which can easily be deduced from Eqs. (1) and (2). As was pointed out by von Kármán and Penner,* if t chemical reactions may occur in the gaseous phase then the rate of production of species j is given by the relation

$$\omega_j = M_j \sum_{r=1}^{t} \left(\nu''_{j,r} - \nu'_{j,r}\right) B_r \exp(-T_r/T) \prod_{i=1}^{s} \left(\frac{pX_i}{RT}\right)^{\nu'_{i,r}} \qquad j=1,2,\ldots,s \tag{98}$$

---

* Section I E of reference 5.

where T_r is the activation temperature for the r'th chemical reaction and the quantities $\nu''_{j,r}$ and $\nu'_{j,r}$ are the stoichiometric coefficients of species j appearing as product and reactant respectively in the r'th reaction.

The general equation for conservation of energy is

$$4\pi r^2 \lambda \frac{dT}{dr} = \dot{m}\left[\Delta l + \bar{c}_p(T-T_l) + \sum_{j=1}^{s} (\varepsilon_j - \varepsilon_{j,l})h^o_j\right], \qquad (99)$$

where

$$\bar{c}_p \equiv \frac{1}{T-T_l}\sum_{j=1}^{s}\left[\varepsilon_j(h_j - h^o_j) - \varepsilon_{j,l}(h_{j,l} - h^o_j)\right]. \qquad (100)$$

This may be derived by the method that was used in Section B-5.

The values of the mole fractions X_j appearing in Eq. (98) are determined by the diffusion equation, Eq. (21), which is valid when there are an arbitrary number of chemical species present. By using Eqs. (2) and (25) to eliminate the velocity v and the ratio $\bar{M}/\rho$ from Eq. (21), we obtain the expression

$$\frac{dX_j}{dr} = \frac{\dot{m}}{4\pi r^2}\frac{RT}{p}\sum_{i=1}^{s}\frac{1}{D_{ij}}\left(\frac{X_j\varepsilon_i}{M_i} - \frac{X_i\varepsilon_j}{M_j}\right) \quad j=1,2,\ldots,s. \qquad (101)$$

Equations (97), (99), and (101) provide 2s+1 equations in the 2s+1 unknowns X_j, ε_j, and T. Presumably the composition and evaporation characteristics of the droplet determine the boundary values $\varepsilon_{j,l}$ and T_l, while the nature of the surrounding atmosphere determines the final temperature T_f and concentrations $X_{j,f}$. A relation between the values of the flux fractions $\varepsilon_{j,f}$ is determined by the requirement that

chemical equilibrium at the temperature T_f is obtained as $r \longrightarrow \infty$. This last condition insures that we have an eigenvalue problem of the type that was treated in the previous sections.

2. Dimensionless Form of the Governing Equations

If the quantity $h^o_j / \bar{c}_p T_f \equiv H_j$ is the dimensionless enthalpy of formation, then by introducing the previously-defined dimensionless variables we may put Eq. (99) into the form

$$\frac{d\theta}{d\sigma} = \frac{\rho \bar{c}_p}{4\pi r_\ell \lambda \sigma^2} \left[\alpha + \theta - \theta_\ell + \sum_{j=1}^{s} H_j (\varepsilon_j - \varepsilon_{j,\ell}) \right] . \tag{102}$$

It is possible to select a characteristic species (perhaps a principal product) and to denote it by the subscript P. A Lewis number for species j may then be defined as

$$\mathcal{L}_j \equiv \frac{\lambda R T}{\bar{c}_p \, p M_j D_{jP}} \qquad j=1, 2, \ldots, s,$$

and a dimensionless diffusivity will be denoted by $\gamma_{ij} \equiv D_{iP} / D_{ij}$. These quantities may be functions of the temperature. In view of these definitions, the division of Eq. (101) by Eq. (102) leads to the relation

$$\frac{dX_j}{d\theta} = \mathcal{L}_j \frac{\sum_{i=1}^{s} \gamma_{ji} (\mathcal{M}_{ji} X_j \varepsilon_i - X_i \varepsilon_j)}{\alpha + \theta - \theta_\ell + \sum_{i=1}^{s} H_i (\varepsilon_i - \varepsilon_{i,\ell})} \qquad j=1, 2, \ldots, s \tag{103}$$

where the molecular weight ratio has been defined as $\mathcal{M}_{ij} \equiv M_i / M_j$.

By letting the first reaction (r=1) be an important reaction in which species P is formed, we may define a dimensionless reaction

rate frequency factor for the j'th species and r'th reaction by the relation

$$\beta_{j,r} \equiv \frac{(\nu''_{j,r}-\nu'_{j,r})B_r\left(\frac{p}{RT}\right)^{\sigma_r} M_j \lambda \bar{c}_{p,f}}{(\nu''_{p,1}-\nu'_{p,1})B_{1,f}\left(\frac{p}{RT_f}\right)^{\sigma_1} M_p \lambda_f \bar{c}_p} \qquad j=1,2,\ldots,s;\ r=1,2,\ldots,t,$$

where $\sigma_r \equiv \sum_{i=1}^{s} \nu'_{i,r}$ is the order of the r'th chemical reaction. Since the frequency factor is approximately proportional to a simple power of the temperature, the temperature dependence of the quantities λ and $\bar{c}_p$ is for convenience also included in $\beta_{j,r}$. We define the constant dimensionless mass burning rate eigenvalue by the expression

$$\Lambda^* \equiv \left(\frac{4\pi r_\ell^2}{\dot{m}}\right)^2 \frac{\lambda_f}{\bar{c}_{p,f}} M_p^{(\nu''_{p,1}-\nu'_{p,1})} B_{1,f}\left(\frac{p}{RT_f}\right)^{\sigma_1}.$$

In view of these definitions, by substituting Eq. (98) into Eq. (97) and dividing the resulting relation by Eq. (102) we find that

$$\frac{d\mathcal{E}_j}{d\theta} = \Lambda^* \frac{\theta^4 \sum_{r=1}^{t} \beta_{j,r} \exp(-\theta_r/\theta) \prod_{i=1}^{s} X_i^{\nu'_{i,r}}}{\alpha+\theta-\theta_\ell+\sum_{i=1}^{s} H_i(\epsilon_i-\epsilon_{i,\ell})} \qquad j=1,2,\ldots,s \qquad (104)$$

where $\theta_r = T_r/T_f$ is the dimensionless activation energy for the r'th reaction.

If we define the parameter $V^*(\theta)$ by the equation

$$\nu^* \equiv r_\ell^2 \frac{\bar{c}_p^{\,2}}{\lambda^2} \frac{\lambda_f}{\bar{c}_{p,f}} M_p(\nu''_{p,1} - \nu'_{p,1}) B_{1,f} \left(\frac{p}{RT_f}\right)^{\sigma_1}$$

then Eq. (102) may be rewritten in the form

$$\frac{d\sigma}{d\theta} = \sigma^2 \sqrt{\frac{\Lambda^*}{\nu^*}} \left[\alpha + \theta - \theta_\ell + \sum_{j=1}^{s} M_j(\varepsilon_j - \varepsilon_{j,\ell}) \right]^{-1} . \qquad (105)$$

Equations (103) through (105) compose the desired dimensionless formulation.

3. General Methods of Solution

The 2s+1 first-order relations given in Eqs. (103) through (105) may be solved by stepwise numerical integration techniques. The eigenvalue Λ^* is determined by the trial and error procedure described in Appendix E. In general all the equations must be solved simultaneously; however in most cases physical considerations will enable many equations to be eliminated. For example, the assumption of a one-step reaction, the steady-state assumption for reaction intermediaries,* or the assumption of consecutive spacially-separated reactions (e.g., burning to CO first and then to CO_2) may be used to obtain all of the functions ε_j algebraically in terms of a single flux fraction ε_p. Since all of the coefficients appearing in Eqs. (103) through (105) are simple functions of the temperature, the numerical procedure is straightforward.

Since the approximation methods discussed earlier did not yield accurate functions $\theta(\sigma)$ and $\varepsilon_j(\theta)$, it is expected that similar analytical

---

* T. von Kármán and S. S. Penner, Section III B of reference 5.

approximations to these functions in the present case will be poor. Analytical procedures are therefore expected to be useful only in obtaining approximate relations for the eigenvalue Λ^*. We shall attempt to obtain an expression for Λ^* valid for large values of the activation energies by methods similar to those used in the previous parts of this chapter.

4. An Approximate Expression for Λ^* and its Validity

The form of Eq. (104) for which j=P is taken to be the basic equation for determining Λ^*. By integrating this equation from the droplet surface to the hot boundary ($\sigma = \infty$) we find that

$$\int_{\varepsilon_{P,\ell}}^{\varepsilon_{P,f}} f(\varepsilon_P)\,d\varepsilon_P = \Lambda^* g \tag{106}$$

where the function $f(\varepsilon_P)$ has been defined by the equation

$$f(\varepsilon_P) \equiv \frac{\alpha+\theta-\theta_\ell+\sum_{j=1}^{s} B_j(\varepsilon_j-\varepsilon_{j,\ell})}{\sigma^4(1-\theta)} \tag{107}$$

and the quantity g is given by the expression

$$g \equiv \sum_{r=1}^{t} \int_{\theta_\ell}^{1} \frac{\beta_{P,r}\exp(-\theta_r/\theta)}{1-\theta} \prod_{j=1}^{s} X_j^{\nu'_{j,r}}\,d\theta \,. \tag{108}$$

If the activation energies, θ_r, of all reactions which have rates large enough to contribute appreciably to the summation in Eq. (108) are sufficiently large, then nearly all of the contributions to the integrals in Eq. (108) will come from the range $\theta \approx 1$. In this case we may

expand Eqs. (103) about $\theta=1$ in order to obtain approximate expressions for the mole fractions $X_j(\theta)$ which are valid near $\theta=1$. By substituting these results into Eq. (108) we obtain for the quantity g an accurate approximation which is given by the equation

$$g \approx \sum_{r=1}^{t} \int_{\theta_\ell}^{1} \frac{\beta_{P,r} \exp(-\theta_r/\theta)}{1-\theta} \prod_{j=1}^{s} \left[X_{j,f} - (1-\theta) \mathcal{L}_{j,f} \frac{\sum_{i=1}^{s} \gamma_{ji} (\varkappa_{ji} \varepsilon_{i,f} X_{j,f} - X_{i,f} \varepsilon_{j,f})}{\alpha + 1 - \theta_\ell + \sum_{i=1}^{s} H_i (\varepsilon_{i,f} - \varepsilon_{i,\ell})} \right]^{\nu'_{j,r}} d\theta . \qquad (108a)$$

Here it is understood that limiting procedures are to be used if necessary. All integrals involved in Eq. (108a) may be evaluated in terms of sums of exponential or error integrals.

It is necessary to obtain a reasonable approximation for the function $f(\varepsilon_P)$ in order to complete the solution. Although an approximation may be obtained by an expansion about the cold boundary ($\varepsilon_P = \varepsilon_{P,\ell}$) as in the previous simpler cases, it is more difficult to justify this procedure here.

It is apparent from Eq. (107) that

$$f(\varepsilon_{P,\ell}) = \frac{\alpha}{1-\theta_\ell} . \qquad (109)$$

For non-adiabatic systems the quantity $\left[\alpha + \theta - \theta_\ell + \sum_{j=1}^{s} H_j (\varepsilon_j - \varepsilon_{j,\ell})\right]$ remains non-zero as $\theta \longrightarrow 1$ and Eq. (105) shows that $(1-\theta) \sim 1/\sigma$ near

$\theta=1$. By substituting this result into Eq. (107) we find that $f(\varepsilon_p)\sim 1/\sigma^3$ which approaches zero as $\varepsilon_p \longrightarrow \varepsilon_{p,f}$. In the adiabatic cases the asymptotic behavior is governed by the nature of the reaction through Eq. (104) and must be determined separately for each chemical system. For non-adiabatic systems and also for the adiabatic cases in which $f(\varepsilon_{p,f})=0$, it is expected that the largest contribution to the integral in Eq. (106) will usually come from the neighborhood of the cold boundary. In these cases the integral can be evaluated by a linear expansion about the end point $\varepsilon_p=\varepsilon_{p,l}$. If a series of chain reactions occur, however, then the function $f(\varepsilon_p)$ may pass through a number of maxima and minima which tend to reduce the accuracy of the expansion. The method will always be applicable to systems with one-step chemical reactions.

Having discussed the limits of validity of the procedure, we shall now expand and integrate the function $f(\varepsilon_p)$. By differentiating Eq. (107) we obtain the equation

$$\frac{df}{d\varepsilon_p} = -\frac{4}{\sigma^5(1-\sigma)}\left[\alpha+\varphi-\varphi_l+\sum_{j=1}^{s} H_j(\varepsilon_j-\varepsilon_{j,l})\right]\frac{d\sigma}{d\theta}\,\frac{d\theta}{d\varepsilon_p}$$

$$+\frac{1}{\sigma^4(1-\sigma)^2}\left[1-\varphi_l+\alpha+\sum_{j=1}^{s} H_j(\varepsilon_j-\varepsilon_{j,l})\right]\frac{d\theta}{d\varepsilon_p}+\frac{1}{\sigma^4(1-\theta)}\sum_{j=1}^{s} H_j\frac{d\varepsilon_j}{d\theta}\,\frac{d\varphi}{d\varepsilon_p} \tag{110}$$

which, in view of Eqs. (104) and (105), may be evaluated at the droplet surface with the result

$$\left.\frac{df}{d\varepsilon_p}\right|_{\varepsilon_p=\varepsilon_{p,\ell}} = \left\{ \frac{1-\theta_\ell+\alpha}{(1-\theta_\ell)^2} - \frac{4}{1-\theta_\ell}\sqrt{\frac{\Lambda^*}{V_\ell^*}} \right.$$

$$\left. + \frac{\Lambda^*}{\alpha(1-\theta_\ell)} \sum_{r=1}^{t} \left[\left(\sum_{j=1}^{s} H_j \beta_{j,r,\ell} \right) \exp(-\theta_r/\theta_\ell) \prod_{i=1}^{s} X_{i,\ell}^{\nu'_{i,r}} \right] \right\}$$

$$\left[\frac{\Lambda^*}{\alpha} \sum_{r=1}^{t} \beta_{p,r,\ell} \exp(-\theta_r/\theta_\ell) \prod_{i=1}^{s} X_{i,\ell}^{\nu'_{i,r}} \right]^{-1} . \qquad (111)$$

A two-term expansion for $f(\varepsilon_p)$ may be used to obtain the relation

$$f(\varepsilon_p) \approx f(\varepsilon_{p,\ell}) + \left.\frac{df}{d\varepsilon_p}\right|_{\varepsilon_p=\varepsilon_{p,\ell}} (\varepsilon_p - \varepsilon_{p,\ell}),$$

the integral of which is

$$\int_{\varepsilon_{p,\ell}}^{\varepsilon_{p,f}} f(\varepsilon_p) d\varepsilon_p = f(\varepsilon_{p,\ell})(\varepsilon_{p,f} - \varepsilon_{p,\ell}) + \frac{1}{2} \left.\frac{df}{d\varepsilon_p}\right|_{\varepsilon_p=\varepsilon_{p,\ell}} (\varepsilon_{p,f} - \varepsilon_{p,\ell})^2 . \qquad (112)$$

By substituting Eqs. (109) and (111) into Eq. (112) and equating the result to the right-hand side of Eq. (106), we obtain the relation

$$\left[\frac{\Lambda^*}{\alpha} \sum_{r=1}^{t} \beta_{p,r,\ell} \exp(-\theta_r/\theta_\ell) \prod_{i=1}^{s} X_{i,\ell}^{\nu'_{i,r}} \right] \left[\frac{\alpha(\varepsilon_{p,f} - \varepsilon_{p,\ell})}{(1-\theta_\ell)} \right.$$

$$\left. - \Lambda^* g \right] + \frac{(\varepsilon_{p,f} - \varepsilon_{p,\ell})^2}{2(1-\theta_\ell)} \left\{ \frac{(1-\theta_\ell+\alpha)}{(1-\theta_\ell)} - 4\sqrt{\frac{\Lambda^*}{V_\ell^*}} \right.$$

$$+\frac{\Lambda^*}{\alpha}\sum_{r=1}^{t}\left[\left(\sum_{j=1}^{s} M_j \beta_{j,r,\ell}\right)\exp(-\theta_r/\theta_\ell)\prod_{i=1}^{s} X_{i,\ell}^{\nu'_{i,r}}\right]\Bigg\} = 0. \qquad (113)$$

Equation (113) with the quantity g given approximately by Eq. (108a) determines the burning rate eigenvalue Λ^* in terms of the other physical properties of the system.

5. Properties of the Burning Rate

In the derivation of Eq. (113) the assumption was made that the activation energies θ_r for the important reactions were large. From this it follows that if the value of θ_ℓ is somewhat less than unity, then the terms involving the exponential factors in Eq. (113) are negligibly small. With this approximation the simplified form of Eq. (113) is

$$\sqrt{\frac{\Lambda^*}{\nu_\ell^*}} = \frac{(1-\theta_\ell+\alpha)}{4(1-\theta_\ell)} . \qquad (114)$$

Equation (114) will be valid in most cases for which Eq. (113) is applicable.

It is seen that Eq. (114) is similar to Eq. (42); if $\nu^* \sim \theta^{-2}$ here then the two equations are identical. In particular, it follows from Eq. (114) that the mass burning rate is proportional to the droplet radius. This result may be clearly seen by writing this equation in the physical form

$$\dot{m} = 4\pi r_\ell \frac{\lambda_\ell}{\bar{c}_{p,\ell}} \frac{4(1-\theta_\ell)}{(1-\theta_\ell+\alpha)} . \qquad (115)$$

Most of the discussion of the characteristics of the burning rate given in Section B-11 will also be true in the present case. This analysis implies

that when some heat is exchanged with the surrounding atmosphere and there are no rapid spacial variations in the total enthalpy flux in regions far from the hot or cold boundaries, then the equation for the mass burning rate is unaffected by the type of reaction or the number of chemical species. This may help to explain why the results of simplified treatments agree with experiments performed with real systems in which a large number of chemical reactions occur. It is believed that any steady-state spherically-symmetric gaseous deflagration problem can be treated within the framework of the basic formulation presented here in Part D.

Chapter II

THE THEORY OF FLAMES FORMED FROM INITIALLY SEPARATED REACTANTS AND THE BURNING OF FUEL DROPLETS IN AN OXIDIZING MEDIUM*

List of Symbols

$\bar{c}_p$	Average specific heat at constant pressure.
D	Binary diffusion coefficient.
h	Enthalpy per unit mass.
L	An operator defined in Eq. (12).
Le	Lewis number.
$\dot{m}$	Mass flow rate.
p	A compound variable [see Eq. (27)].
q	Heat of combustion.
r	Radial coordinate.
T	Temperature.
t	Time.
V	Diffusion velocity.
v	Velocity.
w	Mass rate of chemical reaction per unit volume.
x	Coordinate.
Y	Mass fraction.
Y_X	Abbreviation for mass fraction of products or temperature difference.
Δl	Specific heat of vaporization of the fuel.
η	Coupling function defined in Eq. (45).
λ	Thermal conductivity.

* This discussion follows closely the analysis given in Technical Report No. 19 of the Office of Ordnance Research, U.S. Army, Contract DA-04-495-Ord-446 with the California Institute of Technology, Pasadena.

ξ Coupling function defined in Eq. (46).

ρ Density.

Subscripts

c Conditions at the flame surface.

F Fuel.

K A chemical species.

ℓ Component in the ℓ direction.

ℓ Conditions at the droplet surface.

O Oxidizer.

o An initial condition.

P A product.

P' A product.

∞ Conditions at $r=\infty$.

Superscripts

o A standard condition.

* Values corresponding to a hypothetical stoichiometric reaction step.

A. INTRODUCTION

In the previous chapter we have treated a problem which is exemplary of an initially premixed system. For monopropellant burning as well as for premixed laminar flames both fuel and oxidizer are present at the same boundary of the flow regime. Another important class of problems is that in which the reactants are initially unmixed. In this case fuel and oxidizer are not simultaneously present at the same boundary. A practical example of such a system which arises in ramjet combustion is the problem of burning of a fuel droplet in an oxidizing atmosphere. Under suitable simplifying assumptions a fairly concise analytical description of this last class of problems can be obtained.

The treatment of laminar, inviscid, constant-pressure, diffusion flames formed from initially unmixed gases by a single rate-controlling reaction step is greatly simplified in the special case in which the Lewis number is unity and all of the (binary) diffusion coefficients are equal provided the product of density and diffusion coefficient, the average specific heat at constant pressure and the thermal conductivity are assumed to be independent of temperature. We present a general formulation for the solution of problems of this type following the earlier work of Shvab[22] and Zeldovich[23] (Part B). Also a detailed discussion is presented on the burning of a single fuel droplet in an infinite oxidizing medium. Both the diffusion flame approximation (Part C) and a treatment allowing a distributed reaction zone (Part D) are considered. For a Lewis number of unity the mass

burning rate and fuel weight fraction at the droplet surface are independent of the form of the reaction rate and identical results are obtained in the two cases. These results concerning bipropellant droplet burning will be found useful in the following chapter on spray combustion.

B. THE SHVAB-ZELDOVICH APPROXIMATION FOR INITIALLY SEPARATED REACTANTS[22, 23]

An instructive treatment for the partial solution of steady, constant-pressure flames for gases with Lewis number of unity has been described in several recent Russian publications.[22, 23] We shall survey these studies and emphasize the approximations involved in the reduction of the general equations to the equations actually used in the solution.

1. Conservation Equations*

The general equations for conservation of mass of individual chemical species may be written in the form

$$\frac{D\ell nY_K}{Dt} = \frac{w_K}{\rho Y_K} - \frac{1}{\rho Y_K}\frac{\partial}{\partial x_\ell}\left(\rho Y_K V_{K,\ell}\right) \qquad (1)$$

where D/Dt is the Euler derivative, Y_K denotes the mass fraction of species K, ρ is the density of the fluid mixture, w_K equals the mass rate of production of species K per unit volume, V_K is the diffusion velocity of species K, the subscript ℓ (ℓ=1, 2, 3) denotes the ℓ'th

---

* See, for example, reference 7 for a kinetic theory approach or reference 24 for a continuum theory approach.

component of a vector, x_ℓ is the ℓ'th component of the cartesian coordinate vector, and the repeated index ℓ identifies summation according to conventional cartesian tensor notation. We shall use for $V_{K,\ell}$ a binary mixture approximation, viz.,

$$V_{K,\ell} = -\frac{D_K}{Y_K}\frac{\partial Y_K}{\partial x_\ell} . \tag{2}$$

For steady flow Eqs. (1) and (2) may be combined with the result

$$\rho v_\ell \frac{\partial Y_K}{\partial x_\ell} - \frac{\partial}{\partial x_\ell}\left(\rho D_K \frac{\partial Y_K}{\partial x_\ell}\right) = w_K .$$

The overall continuity equation is

$$\frac{\partial}{\partial x_\ell}(\rho v_\ell) = 0 \tag{3}$$

for steady flow. Hence

$$\frac{\partial}{\partial x_\ell}(\rho v_\ell Y_K) - \frac{\partial}{\partial x_\ell}\left(\rho D_K \frac{\partial Y_K}{\partial x_\ell}\right) = w_K . \tag{4}$$

For inviscid, constant-pressure, flow with negligible translational energy and without external forces the energy equation becomes approximately[24]

$$\rho v_\ell \frac{dh}{dx_\ell} + \frac{\partial}{\partial x_\ell}\left(\rho \sum_K Y_K h_K V_{K,\ell}\right) = \frac{\partial}{\partial x_\ell}\left(\lambda \frac{\partial T}{\partial x_\ell}\right) \tag{5}$$

where h is the enthalpy of the fluid mixture per unit mass, h_K is the specific enthalpy of species K, λ represents the thermal conductivity of the fluid mixture, T denotes the absolute temperature, and the other symbols have their previous meaning. In view of Eq. (3) and the relation

$$h = \sum_K Y_K h_K \tag{6}$$

it follows that Eq. (5) may be rewritten as

$$\frac{\partial}{\partial x_\ell}\left[\rho v_\ell \sum_K Y_K h_K \left(1 + \frac{V_{K,\ell}}{v_\ell}\right)\right] = \frac{\partial}{\partial x_\ell}\left(\lambda \frac{\partial T}{\partial x_\ell}\right).$$

Utilizing the approximation

$$h_K = h_K^{\circ} + \bar{c}_p (T - T^{\circ})$$

and remembering that

$$\sum_K Y_K V_{K,\ell} = 0, \qquad \sum_K Y_K = 1, \tag{7}$$

it is apparent that

$$\sum_K Y_K h_K \left(1 + \frac{V_{K,\ell}}{v_\ell}\right) = \sum_K Y_K h_K^{\circ}\left(1 + \frac{V_{K,\ell}}{v_\ell}\right) + \bar{c}_p (T - T^{\circ}).$$

Here $\bar{c}_p$ is an average specific heat at constant pressure. The energy equation becomes now

$$\frac{\partial}{\partial x_\ell}(\rho v_\ell \bar{c}_p T) - \frac{\partial}{\partial x_\ell}\left(\lambda \frac{\partial T}{\partial x_\ell}\right) = -\frac{\partial}{\partial x_\ell}\left[\rho v_\ell \sum_K Y_K h_K^{\circ}\left(1 + \frac{V_{K,\ell}}{v_\ell}\right)\right]$$

or, for constant $\bar{c}_p$,

$$\frac{\partial}{\partial x_\ell}(\rho v_\ell T) - \frac{\partial}{\partial x_\ell}\left(\frac{\lambda}{\bar{c}_p}\frac{\partial T}{\partial x_\ell}\right) = \frac{1}{\bar{c}_p}\sum_K h_K^{\circ}\left[\rho v_\ell \frac{\partial Y_K}{\partial x_\ell} + \frac{\partial}{\partial x_\ell}(\rho Y_K V_{K,\ell})\right]. \tag{8}$$

We now note that, in view of Eqs. (2) and (4),

$$\frac{1}{\bar{c}_p} \sum_K h_K^{\circ} \left[\rho v_\ell \frac{\partial Y_K}{\partial x_\ell} + \frac{\partial}{\partial x_\ell} \left(\rho Y_K V_{K,\ell} \right) \right] = \frac{1}{\bar{c}_p} \sum_K h_K^{\circ} w_K . \tag{9}$$

Furthermore, for a Lewis number of unity,

$$Le = \frac{\lambda}{\rho \bar{c}_p D} = 1, \tag{10}$$

Equations (8) to (10) may now be combined with the result

$$\frac{\partial}{\partial x_\ell} \left(\rho v_\ell T \right) - \frac{\partial}{\partial x_\ell} \left(\rho D_K \frac{\partial T}{\partial x_\ell} \right) = \frac{1}{\bar{c}_p} \sum_K h_K^{\circ} w_K . \tag{11}$$

The momentum equation does not appear explicitly in the present formulation since its integral is already accounted for through the statement p = constant.

2. Uniform Representation of the Conservation and Energy Equations for One-Step Chemical Reactions

Let

$$L(\alpha) = \frac{\partial}{\partial x_\ell} \left(\rho v_\ell \alpha \right) - \frac{\partial}{\partial x_\ell} \left(\rho D_K \frac{\partial \alpha}{\partial x_\ell} \right) . \tag{12}$$

It is then apparent that the continuity and energy equations may be represented by the relations

$$L(Y_K) = w_K, \qquad K = 1, 2, \ldots, n, \tag{13}$$

and

$$L(T) = - \frac{1}{\bar{c}_p} \sum_K h_K^{\circ} w_K . \tag{14}$$

If the assumption is introduced that chemical changes occur only by a single rate-controlling reaction step, then we find that the w_K and

$-(1/\bar{c}_p) \sum_K h_K^{\circ} w_K$ are related. Thus consider, for example, the schematic bimolecular reaction

$$F + O \longrightarrow P + P' \tag{15}$$

and let w represent the production rate of grams of mixture per unit volume. In this case

$$\begin{aligned} w_F &= - Y_F^* w, \\ w_O &= - Y_O^* w, \\ w_P &= + Y_P^* w, \end{aligned} \tag{16}$$

and

$$w_{P'} = + Y_{P'}^* w,$$

where Y_F^*, Y_O^*, Y_P^*, and $Y_{P'}^*$ denote, respectively, the mass fractions of fuel, oxidizer, and reaction products entering into the hypothetical rate-controlling reaction step. For example, if the hypothetical rate-controlling reaction controls the overall chemical change

$$\underset{F}{CH_4} + \underset{O}{2O_2} \longrightarrow \underset{P}{CO_2} + \underset{P'}{2H_2O}$$

then we find that $Y_F^* = 16/(16 + 64) = 1/5$, $Y_O^* = 64/80 = 1/1.25$, $Y_P^* = 44/80 = 1/1.82$, and $Y_{P'}^* = 36/80 = 1/2.22$. Finally

$$-\frac{1}{\bar{c}_p} \sum_K h_K^{\circ} w_K = \frac{w}{\bar{c}_p} (h_F^{\circ} Y_F^* + h_O^{\circ} Y_O^* - h_P^{\circ} Y_P^* - h_{P'}^{\circ} Y_{P'}^*) \equiv w T^* \tag{17}$$

where T^* denotes the temperature rise in $^{\circ}K$ per unit mass of reacting mixture under standard conditions, i.e., T^* equals the ratio of the heat release per unit mass under standard conditions to the average specific

heat at constant pressure $\bar{c}_p$. In the methane-oxygen mixture

$$T^* \simeq \frac{192,000\ (\text{cal})}{80(\text{g}) \times \frac{1}{2}\ (\text{cal/g} - {}^\circ\text{K})} = 4800^\circ\text{K}.$$

It is apparent that combination of Eqs. (13) to (17) leads to the conclusions

$$L(Y_K/Y_K^*) = \pm w \tag{18}$$

and

$$L(T/T^*) = w \tag{19}$$

where the positive sign in Eq. (18) must be used with reaction products and the negative sign with reactants.

It is now possible to relate, in general, Y_P, $Y_{P'}$, and T to the local mass fractions of fuel and oxidizer, viz., Y_F and Y_O. Thus let

$$Y_K = Y_P,\ Y_{P'},\ \text{or}\ (T-T_o);\quad Y_K^* = Y_P^*,\ Y_{P'}^*\ \text{or}\ T^*. \tag{20}$$

where T_o is the temperature at a boundary. The complete set of differential equations is then represented by

$$L\left(\frac{Y_F}{Y_F^*}\right) = -w, \tag{21}$$

$$L\left(\frac{Y_O}{Y_O^*}\right) = -w, \tag{22}$$

and

$$L\left(\frac{Y_X}{Y_X^*}\right) = w,\ Y_K = Y_P,\ Y_{P'},\ \text{or}\ (T-T_o),\ Y_K^* = Y_P^*,\ Y_{P'}^*\ \text{or}\ T^*. \tag{23}$$

3. Classical Solution of Diffusion-Flame Problems[25]

For diffusion flames of the Burke-Schumann type[25] the boundary conditions at the exit of the fuel (I) and oxidizer (II) pipes are, respectively,

$$\left.\begin{aligned} Y_F &= Y_{F,o} \text{ for I} \\ \text{and} \\ Y_O &= Y_{O,o} \text{ for II.} \end{aligned}\right\} \tag{24}$$

Following Shvab and Zeldovich,[23] we now look for a new independent variable p such that

$$L(p) = 0 \tag{25}$$

with the boundary conditions

$$p = 1 \text{ in I and in II.} \tag{26}$$

In view of Eqs. (21) to (23), Eq. (25) is satisfied for

$$p = n\left[\frac{Y_X}{Y_X}_* + m\frac{Y_F}{Y_F}_* + (1-m)\frac{Y_O}{Y_O}_*\right]$$

where m and n are arbitrary constants. However, the boundary conditions specified by Eq. (26) are satisfied only if

$$nm\frac{Y_{F,o}}{Y_F}_* = n(1-m)\frac{Y_{O,o}}{Y_O}_* = 1$$

since $Y_X = 0$ at both I and II provided we assume fuel and oxidizer are both at the same initial temperature, T_o. Solving the preceding relation for m and n we find that

$$m = \frac{Y_{O,o}/Y_O^*}{(Y_{F,o}/Y_F^*) + (Y_{O,o}/Y_O^*)} ,$$

$$n = \frac{(Y_{F,o}/Y_F^*) + (Y_{O,o}/Y_O^*)}{(Y_{F,o}/Y_F^*)(Y_{O,o}/Y_O^*)}$$

whence

$$p = \frac{Y_X}{Y_X^*}\left[\frac{1}{(Y_{F,o}/Y_F^*)} + \frac{1}{(Y_{O,o}/Y_O^*)}\right] + \frac{Y_F}{Y_{F,o}} + \frac{Y_O}{Y_{O,o}} . \qquad (27)$$

The function p defined in Eq. (27) satisfies the differential equation $L(p) = 0$ everywhere. The particular value

$$p = 1 \qquad (28)$$

satisfies both the differential equation and the boundary conditions. Hence p=1 is a solution of the general combustion problem in which the chemical reaction can be approximated by a one-step process. From Eqs. (27) and (28) it follows then that

$$Y_X = \frac{Y_X^*}{Y_O^* Y_F^*}\,\frac{Y_{F,o}Y_{O,o} - Y_F Y_{O,o} - Y_{F,o}Y_O}{(Y_{F,o}/Y_F^*) + (Y_{O,o}/Y_O^*)} \quad \text{for } Y_X = Y_p,\ Y_p, \text{ and } (T - T_o). \qquad (29)$$

Following Burke and Schumann,[25] the flame front is identified by the condition

$$Y_F = Y_O = 0 \qquad (30)$$

which applies only for an infinitely thin reaction zone. It now follows from Eq. (29) that, at the flame front,

$$Y_{X,c} = Y_X^* \frac{(Y_{F,o}/Y_F^*)(Y_{O,o}/Y_O^*)}{(Y_{F,o}/Y_F^*)+(Y_{O,o}/Y_O^*)} \quad \text{for } Y_{X,c} = Y_{P,c}, Y_{P',c} \text{ or } (T_c - T_o). \tag{31}$$

For a given chemical system, Eq. (31) provides an immediate solution to the steady-state gas composition and temperature at the flame front.

4. Complete Solution for Initially Unmixed Gases with Finite Reaction Rates

For a three-dimensional flow problem in the general case where $Y_{X,o} \neq 0$ we may first integrate the differential equation

$$L(p) = 0$$

and find

$$p = p(x, y, z).$$

Next we use Eq. (27) to obtain (Y_X/Y_X^*) as a function of x, y, z, $Y_F/Y_{F,o}$, and $Y_O/Y_{O,o}$. Utilization of the equation of state and of the continuity equation now gives ρ and v_l in terms of x, y, z, $Y_F/Y_{F,o}$ and $Y_O/Y_{O,o}$. A relation between Y_F/Y_F^* and Y_O/Y_O^* is obtained conveniently by solving the differential equation

$$L(Y_F/Y_F^*) - L(Y_O/Y_O^*) = 0;$$

hence we may replace, for example, Y_O in terms of Y_F. Finally, we must solve the single differential equation

$$L(Y_F/Y_F^*) = -w,$$

which is, in general, a partial differential equation of the second order in three variables, two of which (e.g., Y_O and T) may be expressed in terms of the third (e.g., Y_F). In this manner a unified method of solution is obtained for the treatment of initially unmixed gases.

5. Critique of the Shvab-Zeldovich Procedure

There is, of course, no doubt that the solution of combustion problems is greatly simplified through the introduction of the approximations made in the Shvab-Zeldovich procedure. Thus it is well known that the use of Le = 1, as well as of constant coefficients λ, $\bar{c}_p$ and ρD leads to considerable simplification of flow problems with chemical reactions,* as does also the introduction of a single rate-controlling reaction step.** In defense of the formulation presented in Sections B-1 and B-2 we may note that we generally do not know transport parameters and detailed reaction steps sufficiently well to justify any more than the crudest approximations in the solution of problems in aerothermochemistry. Thus Eqs. (21) to (23) should be useful for the solution of complicated constant-pressure, low velocity, combustion problems where we are primarily interested in deriving the functional form of the results.

The elegant analysis given in Section B-3 corresponds to a straight-forward transcription of the usual approximations introduced into the conventional treatment of diffusion flames, which was first used by Burke and Schumann.[25] The deceptively simple general results derived in Eqs. (29) and (30) are actually of very limited practical significance. In particular, they afford little or no simplification in the actual derivation of flame shapes for the Burke-Schumann model.[25]

---

* See, for example, reference 5 or Chapter I of this thesis.

** See, for example, reference 26 or Chapter I of this thesis.

The use of a Lewis number equal to unity implies that energy transport by thermal conduction and by diffusion are balanced. Under these conditions we expect, for example, that the burning rate of a single fuel droplet in an infinite oxidizing medium becomes completely independent of the absolute value of the reaction rate. Hence identical results are obtained for a diffusion-flame approximation and for a distributed reaction zone. We shall demonstrate this conclusion in a rather laborious but instructive manner by presenting first (in Part C) a treatment analogous to that given earlier by Goldsmith and Penner[20] for the more general case of arbitrary Lewis number and variable transport coefficients. In Part D we use the Shvab-Zeldovich formulation which permits a very simple and direct derivation of the equation for the mass burning rate of a fuel droplet.

C. DIFFUSION-FLAME APPROXIMATION TO THE BURNING OF A FUEL DROPLET IN AN INFINITE OXIDIZING MEDIUM

1. Definition of the Problem

The diffusion-flame approximation to the burning of a single fuel droplet in an infinite oxidizing medium[20] corresponds to the boundary conditions

$w = 0$ for $r_\ell < r < r_c$ and for $r_c < r < \infty$; $w = \infty$ at $r = r_c$;

$Y_F = Y_{F,\ell}$ at $r = r_\ell$, $T = T_\ell$;

$Y_P + Y_F = 1$ for $r_\ell < r < r_c$, $Y_O = 0$ for $r_\ell < r < r_c$;

$Y_F = Y_O = 0$ at $r = r_c$, $T = T_c$;

$Y_P + Y_O = 1$ for $r_c < r < \infty$, $Y_F = 0$ for $r_c < r < \infty$;

$$
\left.
\begin{aligned}
&Y_O = Y_{O,\infty} \text{ at } r = \infty,\ T = T_\infty; \\
&-(4\pi r^2 \rho D \frac{dY_F}{dr})_{r_c} = \dot{m}_F \\
&(4\pi r^2 \rho D \frac{dY_O}{dr})_{r_c} = \dot{m}_F (Y_O^*/Y_F^*).
\end{aligned}
\right\} \qquad (32)
$$

Here Y_P is the total mass fraction of reaction product(s); $\dot{m}_F$ denotes the mass flow rate of fuel vapor to the flame surface at $r=r_c$, $T=T_c$, where the chemical reactions occur instantaneously in such a way that Y_O^* grams of oxidizer are consumed for Y_F^* grams of fuel with the production of $\left[1 + (Y_O^*/Y_F^*)\right] \dot{m}_F$ grams of reaction product. For specified values of r_ℓ, T_ℓ, T_∞, and heat release per unit mass at the flame front we seek the eigenvalue $\dot{m}_F$ for steady burning. The conservation of mass equation may be written[20] in the form

$$
\dot{m}_K = \dot{m}_F Y_K - 4\pi r^2 \rho D \frac{dY_K}{dr} \qquad (33)
$$

where $\dot{m}_F Y_K$ denotes the transport of species K associated with the average mass flow rate $\dot{m}_F$ and $-4\pi r^2 \rho D \frac{dY_K}{dr}$ is the diffusion contribution. The boundary condition

$$
\dot{m}_F = (4\pi r^2 \rho D \frac{dY_F}{dr})_{r=r_c}
$$

follows directly from Eq. (33) by noting that $Y_F=0$ at $r=r_c$. Also for $r_c < r < \infty$, $\dot{m}_O = -\dot{m}_F(Y_O^*/Y_F^*)$ whence we obtain from Eq. (33) the last of the boundary conditions listed in (32).

2. An Expression for $\dot{m}_F$ in Terms of T_c and r_c

An expression may be obtained for $\dot{m}_F$ in terms of T_c and r_c by applying Eq. (23) with $Y_X/Y_X^* = (T-T_o)/T^*$ to the region $r_\ell < r < r_c$ with $w=0$. Thus

$$\frac{d}{dr}(r^2 \rho v T) = \frac{d}{dr}\left(r^2 \rho D \frac{dT}{dr}\right). \tag{34}$$

But

$$r^2 \rho v = \frac{\dot{m}_F}{4\pi}, \quad \rho D = \frac{\lambda}{\bar{c}_p};$$

whence Eq. (34) becomes, after integration between r_ℓ, T_ℓ, and r, T,

$$\frac{\dot{m}_F}{4\pi}(T-T_\ell) = r^2 \frac{\lambda}{\bar{c}_p}\frac{dT}{dr} - \frac{1}{\bar{c}_p}\left(\lambda r^2 \frac{dT}{dr}\right)_{r_\ell}.$$

But

$$\left(\lambda r^2 \frac{dT}{dr}\right)_{r_\ell} = \frac{\dot{m}_F}{4\pi}\Delta\ell \tag{35}$$

where $\Delta\ell$ denotes the specific heat of evaporation of the fuel vapor. Hence

$$\frac{\dot{m}_F}{4\pi}\left(T-T_\ell + \frac{\Delta\ell}{\bar{c}_p}\right) = \frac{\lambda}{\bar{c}_p} r^2 \frac{dT}{dr}$$

which may now be integrated from r_ℓ, T_ℓ to r_c, T_c. In this manner we find

$$\dot{m}_F = \frac{4\pi\lambda}{\bar{c}_p} \frac{\ell n\left[1 + \dfrac{\bar{c}_p(T_c - T_\ell)}{\Delta\ell}\right]}{\left(\dfrac{1}{r_\ell} - \dfrac{1}{r_c}\right)}. \tag{36}$$

Equation (36) is Godsave's equation[20] but cannot be used for calculations of $\dot{m}_F$ because neither T_c nor r_c are known.

3. A Relation Between the Temperature T_c and Flame Surface Radius r_c

A relation between the flame radius r_c and the temperature T_c can be obtained by applying Eq. (34) also to the region between r_c and ∞. Thus, integrating Eq. (34) between r_c, T_c, and r, T, leads to the result

$$\frac{\dot{m}_F}{4\pi}(T-T_c) = \frac{\lambda}{\bar{c}_p} r^2 \frac{dT}{dr} - \frac{1}{\bar{c}_p}\left(\lambda r^2 \frac{dT}{dr}\right)_{r_c}.$$

But

$$-(4\pi\lambda r^2 \frac{dT}{dr})_{r_c} = \dot{m}_F\left[q - \bar{c}_p(T_c - T_\ell) - \Delta\ell\right]$$

where q is the heat released at the flame surface for unit mass of fuel (g) reacting with Y_O^*/Y_F^* g of oxidizer to produce $\left[1+(Y_O^*/Y_F^*)\right]$ g of reaction products. Thus

$$q = \left[1+(Y_O^*/Y_F^*)\right] h_{P,T_c} - h_{F,T_c} - (Y_O^*/Y_F^*) h_{O,T_c}$$

where the subscript T_c identifies absolute enthalpies evaluated at the temperature of the flame surface. Furthermore, since all of the specific heats involved are constant and equal, it follows that

$$q = \left[1+(Y_O^*/Y_F^*)\right] h_P^\circ - h_F^\circ - (Y_O^*/Y_F^*) h_O^*$$

or

$$q = \bar{c}_p T^* \left[1+(Y_O^*/Y_F^*)\right],$$

where the same definition has been used for T^* as in Eq. (17). Hence

$$-(4\pi\lambda r^2 \frac{dT}{dr})_{r_c} = \dot{m}_F\left\{\bar{c}_p\left[T^*\left(1+\frac{Y_O^*}{Y_F^*}\right) - (T_c - T_\ell)\right] - \Delta\ell\right\}. \qquad (37)$$

Using Eq. (37) the differential equation now becomes

$$\frac{\dot{m}_F}{4\pi}\left[(T-T_\ell) + \frac{\Delta\ell}{\bar{c}_p} - T^*\left(1+\frac{Y_O^*}{Y_F^*}\right)\right] = \frac{\lambda}{\bar{c}_p} r^2 \frac{dT}{dr}$$

which may be integrated from r_c, T_c, to ∞, T_∞, with the result

$$\dot{m}_F = \frac{4\pi\lambda r_c}{\bar{c}_p} \ln\left\{1 + \frac{(T_c-T_\infty)}{\left[T^*\left(1-\frac{Y_O^*}{Y_F^*}\right) - (T_c-T_\ell) - \frac{\Delta\ell}{\bar{c}_p}\right]}\right\} . \qquad (38)$$

It is apparent that by eliminating $\dot{m}_F$ between Eqs. (36) and (38), a relation is obtained for r_c in terms of T_c. The result is

$$\frac{r_c}{r_\ell} = 1 + \frac{\ln\left[1 + \frac{\bar{c}_p(T_c - T_\ell)}{\Delta\ell}\right]}{\ln\left\{1 + \frac{(T_c-T_\infty)}{\left[T^*\left(1+\frac{Y_O^*}{Y_F^*}\right) - (T_c-T_\ell) - \frac{\Delta\ell}{\bar{c}_p}\right]}\right\}} . \qquad (39)$$

4. Determination of r_c in Terms of $\dot{m}_F$

The use of Eq. (22) with w=0 for $r_c < r < \infty$ yields the relation

$$\frac{d}{dr}\left(r^2\rho v Y_O\right) = \frac{d}{dr}\left(r^2\rho D \frac{dY_O}{dr}\right)$$

which may be integrated from r_c, 0 to r, Y_O with the result

$$\frac{\dot{m}_F}{4\pi} Y_O = r^2\rho D \frac{dY_O}{dr} - \left(r^2\rho D \frac{dY_O}{dr}\right)_{r_c}$$

or, in view of the last boundary condition listed in (32),

$$\frac{\dot{m}_F}{4\pi}\left(Y_O + \frac{Y_O^*}{Y_F^*}\right) = r^2 \rho D \frac{dY_O}{dr} .$$

Integration of the preceding relation between r_c, 0 and ∞, $Y_{O,\infty}$ leads to the desired expression, viz.,

$$\frac{\dot{m}_F}{4\pi r_c} = \frac{\lambda}{\bar{c}_p} \ln\left(1 + \frac{Y_F^*}{Y_O^*} Y_{O,\infty}\right) . \tag{40}$$

Introduction of Eq. (40) into Eq. (36) leads to an explicit relation for $\dot{m}_F$ in terms of T_c and known parameters, viz.,

$$\dot{m}_F = \frac{4\pi\lambda r_\ell}{\bar{c}_p} \ln\left\{\left(1 + \frac{Y_F^*}{Y_O^*} Y_{O,\infty}\right)\left[1 + \frac{\bar{c}_p(T_c - T_\ell)}{\Delta\ell}\right]\right\} . \tag{36a}$$

5. Theoretical Calculation of $\dot{m}_F$

We may now obtain a simple explicit procedure for the theoretical calculation of $\dot{m}_F$. First we combine Eqs. (38) and (40) and solve for T_c with the result

$$T_c = \frac{T_\infty + \frac{Y_F^*}{Y_O^*} Y_{O,\infty}\left[T^*\left(1 + \frac{Y_O^*}{Y_F^*}\right) + T_\ell - \frac{\Delta\ell}{\bar{c}_p}\right]}{1 + \frac{Y_F^*}{Y_O^*} Y_{O,\infty}} . \tag{41}$$

The quantity r_c/r_ℓ may then be obtained from Eq. (39) and, finally, $\dot{m}_F$ is evaluated either from Eq. (36) or Eq. (36a). An explicit relation for $\dot{m}_F$ is obtained by replacing T_c in Eq. (36a). The result is

$$\dot{m}_F = \frac{4\pi\lambda r_\ell}{\bar{c}_p} \ln\left\{1 + \frac{\bar{c}_p T^*}{\Delta\ell}\left[\frac{(T_\infty - T_\ell)}{T^*} + \frac{Y_{O,\infty}}{Y_O^*}\right]\right\} \tag{36b}$$

where use has been made of the relation $Y_O^* + Y_F^* = 1$.

6. The Fuel Mass Fraction at the Droplet Surface $Y_{F,\ell}$

The fuel mass fraction at the droplet surface, $Y_{F,\ell}$, is readily obtained by integrating Eq. (21) with w=0 first between r_ℓ, $Y_{F,\ell}$, and r, Y_F, and, after collecting terms, between r_ℓ, $Y_{F,\ell}$, and r_c, 0. The results are

$$\frac{\dot{m}_F}{4\pi}(Y_F - Y_{F,\ell}) = \left(r^2\rho D\frac{dY_F}{dr}\right) - \left(r^2\rho D\frac{dY_F}{dr}\right)_{r_\ell}$$

or, since according to Eq. (33)

$$-\left(r^2\rho D\frac{dY_F}{dr}\right)_{r_\ell} = \frac{\dot{m}_F}{4\pi}(1 - Y_{F,\ell}),$$

$$-\frac{\dot{m}_F}{4\pi}(1 - Y_F) = \rho D r^2\frac{dY_F}{dr}$$

whence, finally,

$$Y_{F,\ell} = 1 - \exp\left[-\frac{\dot{m}_F\bar{c}_p}{4\pi\lambda}\left(\frac{1}{r_\ell} - \frac{1}{r_c}\right)\right]$$

$$= 1 - \left(1 + \frac{Y_F^*}{Y_O^*}Y_{O,\infty}\right)\exp\left(-\frac{\dot{m}_F\bar{c}_p}{4\pi r_\ell\lambda}\right) \tag{42}$$

where in the last relation we have used Eq. (40).

7. Composition and Temperature Profiles

Composition and temperature profiles may be constructed without difficulty by integrating the differential relations leading to Eqs. (36),

(38), (40) and (42) to arbitrary values of r and T, Y_O or Y_F. Thus

$$\left.\begin{aligned} T &= T_\ell + \frac{\Delta\ell}{\bar{c}_p}\left[\exp\left\{\frac{\dot{m}_F \bar{c}_p}{4\pi\lambda}\left(\frac{1}{r_\ell}-\frac{1}{r}\right)\right\}-1\right], \\ Y_F &= 1 - Y_P = 1-(1-Y_{F,\ell})\exp\left[\frac{\dot{m}_F \bar{c}_p}{4\pi\lambda}\left(\frac{1}{r}-\frac{1}{r}\right)\right] \end{aligned}\right\} \quad (43)$$

for $r_\ell < r < r_c$ and

$$\left.\begin{aligned} T &= T_c - \left[T^*\left(1+\frac{Y_O^*}{Y_F^*}\right)-(T_c-T_\ell)-\frac{\Delta\ell}{\bar{c}_p}\right]\left[\exp\left\{\frac{\dot{m}_F \bar{c}_p}{4\pi\lambda}\left(\frac{1}{r_c}-\frac{1}{r}\right)\right\}-1\right], \\ Y_O &= 1-Y_P = \frac{Y_O^*}{Y_F^*}\left[\exp\left\{\frac{\dot{m}_F}{4\pi}\frac{c_p}{\lambda}\left(\frac{1}{r_c}-\frac{1}{r}\right)\right\}-1\right] \end{aligned}\right\} \quad (44)$$

for $r_c < r < \infty$.

8. Concluding Remarks

The analysis presented in this Section C actually parallels closely the treatment of Goldsmith and Penner.[20] Since we have not utilized the special form of Eqs. (21) to (23), the analytical labor is only a little less involved than in the original treatment of the problem.

D. BURNING OF A FUEL DROPLET IN AN INFINITE OXIDIZING MEDIUM WITH A DISTRIBUTED REACTION ZONE

1. Definitions

For the treatment of the burning of a single fuel droplet in an infinite oxidizing medium with a distributed reaction zone it is convenient to start from Eqs. (21) to (23) and to introduce new variables. Thus let

$$\eta = \frac{T}{T^*} + \frac{Y_O}{Y_O^*} \tag{45}$$

and

$$\xi = \frac{Y_F}{Y_F^*} - \frac{Y_O}{Y_O^*} \, . \tag{46}$$

Then

$$L(\eta) = L(\xi) = 0 \tag{47}$$

and we expect that the differential equation in η will ultimately relate the temperature profile to the oxidizer mass fraction whereas the equation $L(\xi) = 0$ will provide a relation between Y_F and Y_O.

Appropriate boundary conditions for the composition variables in the case of a distributed reaction zone are the following:

$$Y_O = 0 \text{ at } r = r_l \, , \; T = T_l \, , \tag{48}$$

and

$$Y_F = 0 \text{ at } r = \infty, \; T = T_\infty \, . \tag{49}$$

Other obvious boundary conditions will be introduced as the need arises.

2. The Mass Burning Rate $\dot{m}_F$

From $L(\eta) = 0$ we have

$$\frac{d}{dr}(r^2 \rho v \eta) = \frac{d}{dr}(r^2 \rho D \frac{d\eta}{dr})$$

which, after integration between r_l, T_l, and r, T, leads to the expression

$$\frac{\dot{m}_F}{4\pi}(\eta - \eta_l) = r^2 \rho D \frac{d\eta}{dr} - (r^2 \rho D \frac{d\eta}{dr})_{r_l} \, . \tag{50}$$

But

$$\eta_l = \frac{T_l}{T^*} \tag{51}$$

and

$$\left(r^2 \rho D \frac{d\eta}{dr}\right)_{r_\ell} = \frac{1}{4\pi \bar{c}_p T^*} \left(4\pi r^2 \lambda \frac{dT}{dr}\right)_{r_\ell} = \frac{\dot{m}_F \Delta_\ell}{4\pi \bar{c}_p T^*} \quad . \tag{52}$$

From Eqs. (50) to (52) it follows now that

$$\frac{\dot{m}_F}{4\pi} \int_{r_\ell}^{\infty} \frac{dr}{r^2} = \frac{\lambda}{\bar{c}_p} \int_{\eta_\ell}^{\eta_\infty} \frac{d\eta}{\left(\eta - \frac{T_\ell}{T^*} + \frac{\Delta_\ell}{\bar{c}_p T^*}\right)}$$

whence

$$\dot{m}_F = \frac{4\pi \lambda r_\ell}{\bar{c}_p} \ln \left\{ 1 + \frac{\bar{c}_p T^*}{\Delta_\ell} \left[\frac{(T_\infty - T_\ell)}{T^*} + \frac{Y_{O,\infty}}{Y_O^*} \right] \right\} \quad . \tag{53}$$

Equation (53) is seen to be identical with Eq. (36b) in accord with our earlier prediction that, for a Lewis number of unity, the mass burning rate cannot depend on the chemical reaction rate or the heat release profile.

3. The Fuel Mass Fraction $Y_{F,\ell}$ at the Droplet Surface

From $L(\xi) = 0$ we find, after integration between $\xi = \xi_\ell = Y_{F,\ell} / Y_F^*$, $r = r_\ell$, and ξ, r, the result

$$\frac{\dot{m}_F}{4\pi} \left(\xi - \frac{Y_{F,\ell}}{Y_F^*} \right) = r^2 \rho D \frac{d\xi}{dr} - \left(r^2 \rho D \frac{d\xi}{dr} \right)_{r_\ell} \quad . \tag{54}$$

But

$$-\left(r^2 \rho D \frac{d\xi}{dr}\right)_{r_\ell} = -\left(\frac{r^2 \rho D}{Y_F^*} \frac{dY_F}{dr} \right)_{r_\ell} = \frac{\dot{m}_F}{4\pi} \frac{(1 - Y_{F,\ell})}{Y_F^*}$$

whence

$$\frac{\dot{m}_F}{4\pi}\left(\xi - \frac{1}{Y_F^*}\right) = r^2 \rho D \frac{d\xi}{dr} \quad . \tag{55}$$

After integration between r_ℓ , ξ_ℓ , and $r = \infty$, ξ_∞ we find now

$$\frac{\dot{m}_F}{4\pi r_\ell} = \frac{\lambda}{\bar{c}_p} \ln \frac{\left(\xi_\infty - \frac{1}{Y_F^*}\right)}{\left(\xi_\ell - \frac{1}{Y_F^*}\right)}$$

and, since

$$\xi_\infty = - Y_{O,\infty}/Y_O^* , \quad \xi_\ell = Y_{F,\ell}/Y_F^* , \tag{56}$$

$$\frac{\dot{m}_F}{4\pi r_\ell}\frac{\bar{c}_p}{\lambda} = \ln \frac{Y_{O,\infty} Y_F^* + Y_O^*}{Y_O^*(1 - Y_{F,\ell})} \tag{57}$$

or, after introducing Eq. (53) for $\dot{m}_F$,

$$Y_{F,\ell} = 1 - \frac{1 + Y_{O,\infty}(Y_F^*/Y_O^*)}{1 + \frac{\bar{c}_p T^*}{\Delta h}\left[\frac{(T_\infty - T_\ell)}{T^*} + \frac{Y_{O,\infty}}{Y_O^*}\right]} \quad . \tag{58}$$

Equation (57) is identical with the result obtained from Eq. (42) by replacing $\dot{m}_F \bar{c}_p / 4\pi r_c \lambda$ according to Eq. (40), i.e., the fuel mass fraction at the droplet surface is also completely independent of the rate of the overall chemical reaction.

4. The Coupling Function $\xi(r)$

The function $\xi(r)$ shows how the oxidiser and fuel mass fractions are coupled throughout space. It may be obtained convenient-

ly from Eq. (55) by replacing the upper limits of integration by r and $\xi(r)$, respectively. In this manner it is found that

$$\frac{\dot{m}_F}{4\pi}\left(\frac{1}{r_\ell}-\frac{1}{r}\right) = \rho D \ell n \frac{\left(\xi - \frac{1}{Y_F^*}\right)}{\left(\frac{Y_{F,\ell}}{Y_F^*} - \frac{1}{Y_F^*}\right)} \tag{59}$$

or

$$\frac{\dot{m}_F}{4\pi}\left(\frac{1}{r_\ell}-\frac{1}{r}\right) = \frac{\lambda}{\bar{c}_p} \ell n \frac{(1-Y_F^*\xi)}{(1-Y_{F,\ell})} . \tag{60}$$

Explicit solution of Eq. (60) for ξ shows that

$$\xi(r) = \frac{Y_F(r)}{Y_F^*} - \frac{Y_O(r)}{Y_O^*} = \frac{1}{Y_F^*}\left[1-(1-Y_{F,\ell})\exp\left\{\frac{\dot{m}_F \bar{c}_p}{4\pi\lambda}\left(\frac{1}{r_\ell}-\frac{1}{r}\right)\right\}\right] . \tag{61}$$

Comparison of Eqs. (43), (44), and (61) shows that $\xi(r)$ for the distributed reaction zone is identical with $Y_F(r)/Y_F^*$ for the diffusion-flame approximation in the region $r_\ell < r < r_c$; also $\xi(r)$ is identical with $-Y_O(r)/Y_O^*$ for the diffusion-flame approximation in the region $r_c < r < \infty$. In other words, the diffusion flame approximation represents a special solution to the general problem which has the feature of yielding a mass burning rate $\dot{m}_F$ and a fuel mass fraction $Y_{F,\ell}$ which is independent of w.

An alternate coupling relation between fuel and oxidizer mass fraction may be obtained by replacing the lower limits in the integration of $L(\xi)$ by r and ξ. In this manner it is found that

$$\xi(r) = \frac{Y_F(r)}{Y_F^*} - \frac{Y_O(r)}{Y_O^*} = \frac{1}{Y_F^*}\left[1 - \frac{Y_{O,\infty} Y_F^* + Y_O^*}{Y_O^*} \exp\left(-\frac{\dot{m}_F \bar{c}_p}{4\pi\lambda}\frac{1}{r}\right)\right] . \quad (62)$$

Equations (61) and (62) are, of course, consistent as is easily demonstrated by showing that use of the equality of the right-hand sides of Eqs. (61) and (62) leads directly to Eq. (53) for $\dot{m}_F$.

5. The Coupling Function $\eta(r)$

The function $\eta(r)$ shows how the temperature and fuel mass fractions are coupled throughout space. It may be obtained conveniently by replacing the upper limits of integration in Eq. (50) by r and η, respectively. In this manner it is found that

$$\frac{\dot{m}_F}{4\pi}\left(\frac{1}{r_\ell} - \frac{1}{r}\right) = \frac{\lambda}{\bar{c}_p} \ln \frac{\left(\eta - \frac{T_\ell}{T^*} + \frac{\Delta\ell}{\bar{c}_p T^*}\right)}{\left(\frac{\Delta\ell}{\bar{c}_p T^*}\right)}$$

or

$$\eta(r) = \frac{T(r)}{T^*} + \frac{Y_O(r)}{Y_O^*} = \frac{1}{T^*}\left\{T_\ell + \frac{\Delta\ell}{\bar{c}_p}\left[\exp\left\{\frac{\dot{m}_F \bar{c}_p}{4\pi\lambda}\left(\frac{1}{r_\ell} - \frac{1}{r}\right)\right\} - 1\right]\right\} . \quad (63)$$

Comparison of Eqs. (43) and (63) shows that $\eta(r)$ and $T(r)/T^*$ for the diffusion-flame approximation are identical in the region $r_\ell < r < r_c$. Similarly, it may be shown that $\xi(r)+\eta(r) = \frac{T(r)}{T^*} + \frac{Y_F(r)}{Y_F^*}$ and $T(r)/T^*$ for the diffusion-flame approximation are identical for $r_c < r < \infty$.

6. Absolute Composition and Temperature Profiles for a Distributed Reaction Zone

Absolute composition and temperature profiles for the diffusion

flame approximation have been summarized in Eqs. (43) and (44). Corresponding results for a distributed reaction zone depend, of course, on the exact form of the reaction-rate function w.

Equation (22) becomes explicitly

$$\frac{d}{dr}\left(r^2 \rho v \frac{Y_O}{Y_O^*}\right) - \frac{d}{dr}\left(\frac{r^2 \rho D}{Y_O^*}\frac{dY_O}{dr}\right) = w(Y_F, Y_O, \rho, T)\, r^2 \qquad (64)$$

where Y_F, T and ρ (for constant-pressure processes) are known functions of Y_O and r. Thus Eq. (64) represents a single second order total differential equation the integration of which, after imposition of suitable boundary conditions, will yield $Y_O(r)$. Use of the coupling relations given previously will then allow the computation of $Y_F(r)$ and T(r), thus giving a complete solution to the problem under discussion.

7. Concluding Remarks

The analysis presented in Parts C and D and the detailed comparison of the derived theoretical relations serve to emphasize the obvious fact that all results calculated from a differential equation which was derived by eliminating w between Eqs. (21) to (23) are of general applicability and are independent of the exact form of w. Thus there exists a class of combustion problems for which the assumption that the Lewis number is unity simplifies the problem to such an extent that useful observable parameters can be obtained without regard to the form of the reaction rate. We have illustrated this conclusion for a special combustion problem. The Shvab-Zeldovich formalism is useful for categorizing the method of solution.

Chapter III

A GENERAL THEORY OF SPRAYS

List of Symbols

A	Spacial dependence of the droplet growth rate [see Eq. (64)].
a	Radius of impinging jets.
B	Reaction rate frequency factor.
b	Impact parameter.
C_D	Drag coefficient.
c	Mass flow rate correction factor for droplet interaction [see Eq. (34)].
$\bar{c}_p$	Average specific heat at constant pressure.
D	Binary diffusion coefficient.
$\vec{F}$	Force per unit droplet mass.
$\bar{\vec{F}}$	Average acceleration of droplets with velocity $\vec{v}$.
f	Droplet number density distribution function.
$f^{(N)}$	N'th order probability density function for droplets.
G	Droplet size distribution function.
g	Droplet velocity distribution function.
h	A function defined in Eq. (I-48) of Chapter I.
I	Energy dissipated in a collision.
J_n	Functions defined in Eq. (66).
k	Exponent of r in the droplet growth rate expression.
$\mathcal{L}$	Effective Lewis number.
ℓ	Path length within the collision zone.
M	Average molecular weight.
m	Mass of a droplet.

$\dot{m}$	Droplet evaporation rate (mass per second).
N	Number of droplets produced in a collision.
n	Number density of droplets.
Pr	Prandtl number.
p	Pressure.
Q	Droplet source term.
Q'	Total rate of formation of new droplets (number per unit volume).
q	Heat of reaction.
R	Droplet growth rate (cm/sec).
R'	Gas constant per gram.
$\bar{R}$	Average growth rate of droplets of size r.
Re	Reynolds number.
r	Droplet radius.
$\hat{r}$	Dimensionless droplet radius defined in Eq. (75).
$\bar{r}$	Average droplet radius.
$\overline{(\pi r^2)}$	Average droplet cross-sectional area.
S	Surface tension.
Sc	Schmidt number.
s	Parameter characterizing droplet size distribution. [see Eq. (59)].
T	Temperature.
t	Time.
t	Parameter characterizing droplet size distribution. [see Eq. (59)].
$\vec{U}$	Diffusion velocity of a component of the fluid.

$\vec{u}$ Fluid velocity.

V Average volume of a droplet.

$\dot{V}$ Average rate of change of droplet volume caused by droplet growth.

v_k k'th component of the droplet velocity.

v_o Magnitude of $\vec{v}_o$.

$\vec{v}$ Droplet velocity vector.

$\vec{v}_o$ Particle velocity within incident jets.

$\bar{\vec{v}}$ Average droplet velocity (averaged over r and $\vec{v}$).

$\bar{\vec{v}}_r$ Droplet velocity averaged over r.

$\bar{\vec{v}}_v$ Droplet velocity averaged over $\vec{v}$.

$\dot{\vec{v}}_m$ Average rate of change of velocity caused by droplet growth. [see Eq. (46)].

$(\vec{v}\,\vec{v})$ Velocity dyadic product tensor.

W Weber number.

W_{cr} Critical Weber number.

X Mole fraction.

x Spacial coordinate.

$\hat{x}$ Dimensionless distance defined in Eq. (76).

Y Mass fraction.

y Spacial coordinate.

$\hat{y}$ A dimensionless variable defined in Eq. (78).

Z A dimensionless distance defined in Eq. (79).

z Spacial coordinate.

$\hat{z}$ A dimensionless variable defined in Section E-4-d.

α Droplet collision function defined in Section B-2-a.

β Droplet interaction constant [see Eq. (64) f.f.].

Γ Collisional rate of change of the droplet distribution function.

$\Gamma^{(+)}$ Rate of scattering of particles into a range of phase space by collisions.

$\Gamma^{(-)}$ Rate of scatterings of particles out of a range of phase space by collisions.

γ Evaporation rate correction caused by fluid motion [see Eq. (64) f.f.].

$\Delta\ell$ Specific heat of vaporization of a liquid droplet.

Δn $n-n^{[0]}$.

$\Delta(n\bar{r})$ $n\bar{r}-n^{[0]}\bar{r}^{[0]}$.

$\Delta(nV)$ $nV-n^{[0]}V^{[0]}$.

δ Dirac delta function.

ϵ The step function.

η A variable defined in Eq. (68).

θ Jet impingement angle.

λ Thermal conductivity.

μ Viscosity.

ν Ratio of the volume occupied by droplets to the volume occupied by gas.

ξ A variable defined in Eq. (67).

ρ Density.

σ Differential collision cross-section for production of new particles.

Φ Spacial dependence of the aerodynamic force [see Eq. (63)].

ϕ Azimuthal droplet collision angle.

$\varphi^{[n]}$ A modified n'th order distribution function defined in Eq. (69).

Ω Droplet potential energy caused by surface tension.

Subscripts

ae	Asymptotic.
D	Drag.
f	Final or free stream.
G	Gravitational.
i	A particular droplet.
j	An incident jet (j = 1 or 2).
ℓ	Liquid.
m	Mass-weighted average.
[n]	n'th order iteration
O	Oxidizer.
o	A known initial condition.
p	Pressure gradient.
R	Rotation.
x	Component in the x direction.
y	Component in the y direction.
z	Component in the z direction.

Superscripts

[n]	n'th order perturbation.
o	Ideal quantity neglecting droplet interaction and relative motion of droplet and fluid.
*	Stoichiometric value.

A. INTRODUCTION

The knowledge of the burning mechanism of single droplets does not enable us to determine the mechanism of heterogeneous combustion in rocket motors. A large number of interacting droplets are present in practical combustion chambers, and a reasonable description of these sprays must be developed in order to evaluate the performance. It is our purpose in this chapter to develop a formalism by means of which the results of Chapters I and II may be extended to predict the properties of sprays.

In view of the complex disorder encountered in most sprays, it appears that a statistical approach to the problem is required. Previous descriptions of sprays[27] and spray combustion[28, 29] have been essentially one-dimensional and to a large extent phenomenological. An effort is made here to reduce the phenomenological aspects of the analysis to a minimum and to state explicitly the assumptions introduced. We develop the three-dimensional equations which apply to a larger class of problems.

After deriving the governing differential equation for sprays, we explain the form of the collision term by describing the mechanics of droplet collisions. The aerodynamic force expressions are quoted from known single-particle results. We next review the growth rate equations for single evaporating or burning particles and indicate the corrections to the ideal relations caused by fluid motion and droplet interactions. This completes the explicit definition of all terms appearing in the basic governing equation. In Part C we

derive differential expressions for the total droplet number density and other integrated quantities. By use of the collision conservation relations, differential equations which eliminate the collision term are derived for use in problems in which droplet collisions are important.

In order to illustrate the use of this general theory for describing sprays, we consider two examples in Parts D and E. We first apply the basic equation to the problem of atomization by means of impinging jets. If it is assumed that droplets of known size and velocity distribution compose the incident streams, then it is possible to obtain expressions for the droplet number density distribution downstream from the interaction region. For the case of cylindrical jets with sharp edges we evaluate explicitly the droplet size and velocity distributions far downstream. It is shown that if the incident size distribution is of a generalized Rosin-Rammler type, then the downstream size distribution belongs to the same class. A table of the number-weighted average diameter is given, and a criterion for efficient impingement atomization is obtained. Although many of the specific assumptions concerning droplet interaction mechanism, geometry, or size distribution may be found to be inaccurate, these results are expected to agree approximately with experiments. More important is the fact that the analysis can easily be modified to include jets with different characteristics.

A second problem to which we apply the basic equations (Part E) is the evaporation and combustion of sprays of a known initial size distribution. Expressions for the fraction of the evaporation completed and the size distribution as functions of the distance downstream from an injector are derived. An iterative perturbation technique is described for including accurately the interaction of the fluid and the spray. The analysis given by Probert[28] is extended to include more general droplet evaporation rate expressions and initial size distributions. The modifications of the statistical spray characteristics, caused by the aerodynamic forces and the droplet interaction and fluid motion corrections to the burning rate, are obtained from a perturbation analysis. We compute average spray properties which are directly related to the heterogeneous combustion efficiency of motors. It is thus demonstrated that the formulation of the problem of describing sprays presented in this chapter has a wide range of applicability and may be used to obtain combustion chamber performance results.

B. THE GOVERNING EQUATION FOR SPRAYS

1. Formulation of the Spray Problem

a. General Formulation

Let us suppose that, throughout a region of space containing a gaseous fluid of varying composition in arbitrary motion, a large number N of particles is dispersed. These particles may be evaporating, condensing, burning, and undergoing mutual collisions. We

have insufficient information to state explicitly the position and behavior of each droplet and therefore must develop a statistical description of the system. This approach is expected to be useful when we are interested in the properties of volumes large enough to contain a great number of particles.

A complete statistical description of the system involves the specification of the function

$$f^{(N)}(s^1, \vec{x}^1, \vec{v}^1; \ldots; s^N, \vec{x}^N, \vec{v}^N; t)\, ds^1\, d\vec{x}^1\, d\vec{v}^1 \ldots ds^N\, d\vec{x}^N\, d\vec{v}^N,$$

which is the probability of finding one drop at a position in a small range $d\vec{x}^1$ about $\vec{x}^1$ with velocity in a small range $d\vec{v}^1$ about $\vec{v}^1$ and size and shape in a small range ds^1 about s^1, while at the same time t the other N-1 particles are found in ranges $(d\vec{x}^2, d\vec{v}^2, ds^2), (d\vec{x}^3, d\vec{v}^3, ds^3)$, etc. Here $\vec{x}$ involves the three coordinates (x, y, z), $d\vec{x}$ is an abbreviation for the volume element dx dy dz, and the velocities $\vec{v}$ and $d\vec{v}$ have meanings similar to $\vec{x}$ and $d\vec{x}$. The variable s which specifies size and shape actually represents an infinite number of variables which may, for example, be the droplet volume, the coefficients of the surface-harmonic expansion of the equation of the surface, and the rate of change of these coefficients with time. If the flow field of the gas and all of the variables defined above are specified at one instant of time, then the equations of motion of the droplets combined with the fluid dynamical equations for the flow will, in principle, determine the entire subsequent behavior of the system. Since the equations of motion of the droplet

are of the second order, the velocity and position must both be specified in order to determine completely the motion.

By means of an ergodic hypothesis the time-average behavior of the system may be equated to a statistical ensemble average. The Liouville theorem may then be applied to the phase space* of the system in order to provide an equation governing the behavior of $f^{(N)}$. By integration over the phase-space coordinates of N-1 particles, it is then possible to obtain a relation for the probability of finding a single droplet in the range $(d\vec{x}, d\vec{v}, ds)$. Unfortunately this procedure is impractical because of the complexity of the system under consideration. These general considerations can therefore serve only to provide a basis for determining the approximations which are implicit in spray theories.

b. Physical Assumptions

In view of the above difficulties, we shall treat a simplified problem in which we omit some of the variables which produce negligible effects in many practical cases. It will then be necessary to give a physical derivation of the equation governing the behavior of the simplified distribution function.

We shall assume that all droplets are spherical or, more generally, that a single parameter r (the radius in the case of spherical droplets) is sufficient to characterize the size and shape of the particles. This assumption will be most nearly valid for

* In this case, the phase space is of a multiply infinite number of dimensions.

small droplets with low velocity relative to the gas and for small ratios of the inter-droplet collision duration time to the time between collisions. A large relative velocity between the fluid and the droplet induces deformation and oscillation which may eventually lead to the break-up of large droplets. When the time between collisions is sufficiently long, the internal droplet viscosity can damp out oscillations induced by collisions and cause the drops to become more nearly spherical.

Dimensional considerations lead to the conclusion* that important parameters determining the degree of oscillation and deformation of droplets are the Weber number $W = 2r\rho|\vec{v} - \vec{u}|^2/S$ and the ratio of the volume occupied by droplets to that occupied by gas ν. Here ρ is the gas density, $\vec{v}$ and $\vec{u}$ are the droplet and fluid velocities respectively, S represents the surface tension of the droplet, and 2r is the droplet diameter. Experiments show that there is a critical Weber number, $W_{cr} \simeq 20$,[35] such that aerodynamic forces will cause the droplet to break up for $W > W_{cr}$. Droplets will therefore be nearly spherical only when $W << W_{cr}$. The volume ratio ν determines the average magnitude of the droplet collision-induced oscillations. Maximum values for ν are discussed in Section 5.

c. Derivation of the Governing Equation

We shall neglect the multiple distribution functions, $f^{(2)}$, ..., $f^{(N)}$, and investigate the probable number of droplets with

* See, for example, references 30, 31, 32, 33, or 34.

radius between r and r + dr located in the position range $d\vec{x}$ about $\vec{x}$ with a velocity in the range $d\vec{v}$ about $\vec{v}$. This probability will be denoted by

$$f(r, \vec{x}, \vec{v}, t)\, dr\, d\vec{x}\, d\vec{v},$$

and we shall tabulate the ways in which f can change with time.

The flow of droplets with velocity $\vec{v}$ out of the special range $d\vec{x}$ contributes a term $-\vec{v} \cdot \nabla_x f$ to the rate of change of the function f with time. Here the subscript x on the gradient operator distinguishes it from derivatives with respect to velocity.

The radius of a given droplet may change with time because of evaporation or condensation. The rate of growth $R \equiv dr/dt$ is determined by physical laws and the properties of the surrounding fluid. This leads to the transfer of particles into the range dr and contributes a term $-\partial(Rf)/\partial r$ to the rate of change of f with time.

As a result of the relative motion of a droplet and the gaseous fluid surrounding it, aerodynamic forces can be exerted on the drop. Particles may also experience body forces (gravity for example). If $\vec{F}$ is the resulting force per unit droplet mass (i.e. the droplet acceleration), then droplets are added to the velocity range $d\vec{v}$ at a rate given by $-\nabla_v \cdot (\vec{F} f)$. The subscript v on the gradient operator implies that the derivatives are taken with respect to the velocity.

New droplets may be added to the fluid by spray injection, the breaking up of large droplets, or condensation. Particles may also be taken out of the fluid by impinging on a solid surface and

adhering to it. It will often be possible to account for these effects by including them as boundary conditions of the problem. This procedure is successful in most spray combustion problems, for example. However, in some cases (e.g. when condensation or droplet break-up occur) it may be convenient to introduce a source term Q giving the rate of change of the number density f resulting from droplet formation.

The final mechanism by which the number of particles in the range $(dr, d\vec{x}, d\vec{v})$ can change is by collisions between two or more droplets. These are expected to be relatively more important with impinging jet atomization, for example, than with droplet injection by means of a swirl atomizer. Collisions cause changes in the size and velocity of droplets but not in their position. The collision forces can be separated from the previously-mentioned aerodynamic forces when the collision time is much shorter than the time between collisions. We shall let Γ represent the rate of increase of the function f caused by collisions.

By summing all of these contributions to the change of f with time, we obtain the equation governing the behavior of the distribution function, viz.,

$$\frac{\partial f}{\partial t} = -\frac{\partial}{\partial r}(Rf) - \nabla_x \cdot (\vec{v} f) - \nabla_v \cdot (\vec{F} f) + Q + \Gamma . \qquad (1)$$

The equations of motion of the gaseous fluid are coupled to this equation through the variables R and $\vec{F}$. Equation (1) and the hydrodynamical equations therefore determine the statistical behavior of the spray.

2. Droplet Collisions

a. Collision Mechanics

In order to use Eq. (1), expressions for R, $\vec{F}$, Q, and Γ must be obtained. The first three of these variables may often depend upon the characteristics of the gaseous flow field around the particles; the collision term has been assumed to depend only on the nature of the droplet interactions. The quantity Γ may therefore be evaluated without knowledge of the macroscopic fluid flow. We use a formalism analogous to that employed in the study of transport properties in the kinetic theory of gases. Our methodology leads to precise definitions of the collision parameters which must be measured before our analysis can be reduced to practically useful predictions of the change in droplet distribution function associated with collisions.

In view of the previous assumption that the droplet volume is small compared to the gaseous volume, we shall assume that collisions between more than two droplets seldom occur and have a negligible effect upon the distribution functions. The discussion will therefore be restricted to binary collisions.

Let us consider in detail a collision between a droplet of mass m and one of mass m'. Except in the case of weak interactions (glancing collisions), the two incident droplets will not retain their identities. Instead they will coalesce to form an excited compound droplet which may in turn break up into a number N of smaller droplets. If m_i (i = 1, 2, ..., N) are the masses of each

of the particles produced in the collision, then the conservation of mass in the collision is given by the relation

$$m + m' = \sum_{i=1}^{N} m_i \, . \qquad (2)$$

Let $\vec{v}$ and $\vec{v}'$ be the velocities of the incident particles and let $\vec{v}_i$ $(i = 1, 2, \ldots, N)$ represent the velocities of the collision products. The conservation of momentum and energy in collisions may then be written, respectively, as

$$m \vec{v} + m' \vec{v}' = \sum_{i=1}^{N} m_i \vec{v}_i \, . \qquad (3)$$

and

$$\Omega + \Omega' + \tfrac{1}{2} m v^2 + \tfrac{1}{2} m' v'^2 = \sum_{i=1}^{N} \tfrac{1}{2} m_i v_i^2 + \sum_{i=1}^{N} \Omega_i + I. \qquad (4)$$

In Eq. (4) the symbol Ω represents the potential energy resulting from surface tension ($-4\pi r^2 S$) and other internal excitations, while I denotes energy dissipated in the collision by viscosity and other effects.

It is apparent that Eqs. (2) through (4) do not completely determine the masses and velocities of the outgoing particles in terms of those of the incident droplets. It is necessary to investigate the forces acting during the collision in order to determine m_i and $\vec{v}_i$ uniquely. Although it is, in principle, possible to determine theoretically the dependence of N, m_i, and $\vec{v}_i$ upon the important collision parameters, the task is hopelessly complicated

except in over-simplified cases. Unfortunately experiments have not yet been carried out in sufficient detail to provide this dependence. We shall therefore present a formalism valid for arbitrary interactions.

If we use a coordinate system in which the particle of mass m is at rest, then it is apparent from the symmetry of the system (see Fig. 14) that the number, masses, and composition of the product droplets can depend only upon the composition of the incident drops, the masses m and m', the radii r and r', the magnitude of the relative velocity $|\vec{v}' - \vec{v}|$ and the impact parameter b which determines the strength of the collision. Since the droplet composition determines its density ρ_ℓ, it follows that the masses are related to the radii by the equation

$$m = \frac{4}{3} \pi r^3 \rho_\ell .$$

Hence r, r', $|\vec{v}' - \vec{v}|$ and b are the only variables which can affect the number and size of the outgoing droplets. The velocity vectors of the resulting droplets will depend upon $\vec{v}$, $\vec{v}'$, and the angle ϕ which the plane determined by the line of impact at collision and the relative velocity vector makes with a reference plane through the center of droplet r parallel to the relative velocity (see Fig. 14). For incident droplets of known composition, all properties of the products of a collision are therefore determined by the six variables r, r', $\vec{v}$, $\vec{v}'$, b, and ϕ. Hence we can define a function

$$\alpha(r, \vec{v}\ ; b, \phi\ ; r', \vec{v}'; r'', \vec{v}'')\ dr\ d\vec{v}$$

as the number of droplets of radius in a range dr about r with velocity in a range $d\vec{v}$ about $\vec{v}$ produced by the collision of two droplets of radii r' and r'' with velocities $\vec{v}'$ and $\vec{v}''$ and with collision parameters b and ϕ. For deterministic interactions α may be represented as a sum of products of Dirac delta functions of $(r - r_i)$ and $(\vec{v} - \vec{v}_i)$, where the values of r_i and $\vec{v}_i$ are determined by the quantities r', r'', $\vec{v}'$, $\vec{v}''$, b, and ϕ which characterize the collision. It is obvious that α must always be symmetric upon the interchange of $(r', \vec{v}')$ and $(r'', \vec{v}'')$.

b. Evaluation of the Collision Term

From the definition of the function α it is possible to derive an expression for the collision term which appears in Eq. (1). We shall define $\Gamma^{(-)}\ dr\ d\vec{x}\ d\vec{v}\ dt$ as the number of droplets scattered out of the range $(dr, d\vec{x}, d\vec{v})$ in the time dt by collisions. Since all collisions will cause the incident droplets to change their range $(dr, d\vec{x}, d\vec{v})$, the quantity $\Gamma^{(-)}\ dr\ d\vec{x}\ d\vec{v}\ dt$ must be equal to the number of droplets in this range, $f(r, \vec{x}, \vec{v}, t)\ dr\ d\vec{x}\ d\vec{v}$, multiplied by the total number of collisions which these droplets experience in time dt. The total number of these collisions is the sum over all values of b, ϕ, r', $\vec{x}'$, and $\vec{v}'$ of the quantity

$$f(r', \vec{x}', \vec{v}', t)\ \delta(\vec{x} - \vec{x}')\ dr'\ d\vec{x}'\ d\vec{v}'\ b\ d\phi\ db\ |\vec{v}' - \vec{v}|\,dt.$$

Here the factor $\delta(\vec{x} - \vec{x}')\ dx'$ involving the Dirac delta function signifies that collisions can occur only when the two droplets are

in the same small region of space. The quantity $b\, d\phi\, db\, |\vec{v}' - \vec{v}|\, dt$ is the volume of the column in which the colliding droplet must lie for a collision to occur in time dt. We therefore find that

$$\Gamma^{(-)}\, dr\, d\vec{x}\, d\vec{v}\, dt = \int dr' \int d\vec{x}' \int d\vec{v}' \int db \int d\phi \; f(r, \vec{x}, \vec{v}, t)\, dr\, d\vec{x}\, d\vec{v}\, f(r', \vec{x}', \vec{v}', t)\, \delta(\vec{x} - \vec{x}')\, b\, |\vec{v}' - \vec{v}|\, dt. \tag{5}$$

By using the identity

$$\int d\vec{x}'\, f(r', \vec{x}', \vec{v}', t)\, \delta(\vec{x} - \vec{x}') = f(r', \vec{x}, \vec{v}', t)$$

we may reduce Eq. (5) to the form

$$\Gamma^{(-)} = \int dr' \int d\vec{v}' \int b\, db \int_0^{2\pi} d\phi\, |\vec{v}' - \vec{v}|\, f(r', \vec{x}, \vec{v}', t)\, f(r, \vec{x}, \vec{v}, t). \tag{6}$$

The integrand is independent of ϕ and b, and these integrations can be carried out immediately. It is seen from Fig. 14 that the range of integration over b is from zero to $r + r'$ because no collision will occur if the distance between the centers of the two droplets remains larger than $r + r'$.* If we perform these two integrations then Eq. (6) becomes

$$\Gamma^{(-)} = \iint f(r, \vec{x}, \vec{v}, t)\, f(r', \vec{x}, \vec{v}', t)\, \pi (r + r')^2\, |\vec{v}' - \vec{v}|\, dr'\, d\vec{v}'. \tag{7}$$

Since the term $\pi (r + r')^2$ is the collision cross section for droplets of radii r and r', Eq. (7) has the following obvious

---

* The upper limit may actually be slightly larger than this because of aerodynamic effects.

physical interpretation: The collision rate is the product of the volume swept out per second and the number per unit volume.

By similar reasoning it is possible to evaluate $\Gamma^{(+)}\, dr\, d\vec{x}\, d\vec{v}\, dt$, the number of droplets scattered into the range $(dr, d\vec{x}, d\vec{v})$ by collisions in time dt. Here the unprimed coordinates are those of a product of a collision and the incident particles will be denoted by primes and double primes. By the reasoning presented above, the quantity

$$\left[f(r', \vec{x}', \vec{v}', t)\, dr'\, d\vec{x}'\, d\vec{v}'\right]\left[f(r'', \vec{x}'', \vec{v}'', t)\, \delta(\vec{x}'' - \vec{x}')\, dr''\, d\vec{x}''\, d\vec{v}''\, b\, d\phi\, db\, |\vec{v}' - \vec{v}''|\, dt\right]$$

is seen to be the number of collisions with collision parameters b and ϕ between particles in the ranges $(dr', d\vec{x}', d\vec{v}')$ and $(dr'', d\vec{x}'', d\vec{v}'')$ in time dt. In order to obtain $\Gamma^{(+)}\, dr\, d\vec{x}\, d\vec{v}\, dt$, this quantity must be multiplied by the fraction of such collisions which yield an outgoing droplet in the range $(dr, d\vec{x}, d\vec{v})$ and then summed over all values of b, ϕ, r', r'', $\vec{x}'$, $\vec{x}''$, $\vec{v}'$, and $\vec{v}''$. From the definition of α it follows that the fraction of these collisions producing an outgoing droplet in the desired range is

$$\alpha(r, \vec{v}; b, \phi; r', \vec{v}'; r'', \vec{v}'')\, dr\, d\vec{v}\, \delta(\vec{x}' - \vec{x})\, d\vec{x},$$

which implies that

$$\Gamma^{(+)}\, dr\, d\vec{x}\, d\vec{v}\, dt = \int dr' \int d\vec{x}' \int d\vec{v}' \int dr'' \int d\vec{x}'' \int d\vec{v}'' \int db \int d\phi\, f(r', \vec{x}', \vec{v}', t)\, f(r'', \vec{x}'', \vec{v}'', t)\, \delta(\vec{x}'' - \vec{x}')\, b\, |\vec{v}' - \vec{v}''|\, dt$$

$$\frac{1}{2}\, \alpha(r, \vec{v}; b, \phi; r', \vec{v}'; r'', \vec{v}'')\, dr\, d\vec{v}\, \delta(\vec{x}' - \vec{x})\, d\vec{x}. \qquad (8)$$

The factor $\frac{1}{2}$ appears in Eq. (8) because the integration over $(r'', \vec{x}'', \vec{v}'')$ and $(r', \vec{x}', \vec{v}')$ accounts for each collision twice, once as a collision of a particle with primed coordinates and once as a collision of a particle with double-primed coordinates.

By performing the integrations over $\vec{x}'$ and $\vec{x}''$ in Eq. (8), we obtain the relation

$$\Gamma^{(+)} = \int dr' \int d\vec{v}' \int dr'' \int d\vec{v}'' \int bdb \int d\phi \; f(r', \vec{x}, \vec{v}', t) \; f(r'', \vec{x}, \vec{v}'', t) \; |\vec{v}' - \vec{v}''| \; \frac{1}{2} \alpha(r, \vec{v}; b, \phi; r', \vec{v}'; r'', \vec{v}''). \quad (9)$$

The differential cross-section for the production of droplets in the range $(dr, d\vec{v})$ can be defined as

$$\sigma(r, \vec{v}; r', \vec{v}'; r'', \vec{v}'') \; \frac{1}{2} \int_0^{2\pi} \int_0^{\infty} \alpha(r, \vec{v}; b, \phi; r', \vec{v}'; r'', \vec{v}'') \; bdbd\phi. \quad (10)$$

Equation (9) then becomes

$$\Gamma^{(+)} = \iiiint f(r', \vec{x}, \vec{v}', t) \; f(r'', \vec{x}, \vec{v}'', t) \; |\vec{v}' - \vec{v}''| \; \sigma(r, \vec{v}; r', \vec{v}'; r'', \vec{v}'') \; dr' \, dr'' \, d\vec{v}' \, d\vec{v}''. \quad (11)$$

Equation (11) cannot be simplified further without knowing the collision mechanics which determine the differential cross-section σ.

Equations (7) and (11) may be combined to provide an expression for the collision terms appearing in Eq. (1). We thus obtain the relation

$$\Gamma \equiv \Gamma^{(+)} - \Gamma^{(-)} = \iiiint f(r', \vec{x}, \vec{v}', t)\, f(r'', \vec{x}, \vec{v}'', t)\, |\vec{v}' - \vec{v}''|$$
$$\sigma(r, \vec{v}; r', \vec{v}'; r'', \vec{v}'')\, dr'\, dr''\, d\vec{v}'\, d\vec{v}'' - \iint f(r, \vec{x}, \vec{v}, t)$$
$$f(r', \vec{x}, \vec{v}', t)\, \pi (r + r')^2\, |\vec{v}' - \vec{v}|\, dr'\, d\vec{v}', \qquad (12)$$

which may be expressed more concisely in the form

$$\Gamma = \iiiint f(r', \vec{x}, \vec{v}', t)\, f(r'', \vec{x}, \vec{v}'', t)\, |\vec{v}' - \vec{v}''|$$
$$\left[\sigma(r, \vec{v}; r', \vec{v}'; r'', \vec{v}'') - \pi (r' + r'')^2\, \delta(r - r'')\right.$$
$$\left.\delta(\vec{v} - \vec{v}'')\right] dr'\, dr''\, d\vec{v}'\, d\vec{v}''. \qquad (13)$$

Equation (13) is the collision integral needed to determine the statistical behavior of the cloud of particles. Substituting Eq. (13) into Eq. (1) yields a somewhat complicated governing non-linear integro-differential equation.

3. Aerodynamic Forces

The force term $\vec{F}$ appearing in Eq. (1) depends upon the fluid flow field about the droplets. Although the particles do not affect the form of the hydrodynamical equations, the gas flow will nevertheless depend upon the droplet variables through the boundary conditions which must be applied at the surfaces of the droplets. This dependence provides a coupling of the hydrodynamical field with the droplet distribution and also causes the flow variables to assume a statistical character. For small ratios ν of droplet volume to fluid volume, these statistical variations in the flow field are confined to relatively small regions about the droplets.

We can then define accurate average flow quantities which may be used as the approach flow variables at infinity in computing the forces upon individual droplets.

There are a number of different possible causes of external forces. Velocity gradients in the average flow field must be supported by gradients in the pressure p. An approximate application of Newton's law indicates that a droplet located in a non-uniform pressure field will experience a force per unit mass

$$\vec{F}_p \approx \frac{\nabla p}{\rho_\ell} \tag{14}$$

where ρ_ℓ is the density of the droplet. Furthermore, if the droplet rotates relative to the fluid, then a lift force is produced by the well-known Magnus effect. Experiments show that the resulting lift per unit droplet mass $\vec{F}_R$ may approach 2/3 of the drag per unit mass of the droplet* when the equatorial rotational velocity of the sphere becomes equal to twice the relative translational velocity of the droplet and the fluid, $|\vec{v} - \vec{u}|$. For sufficiently large droplets the gravitational acceleration $\vec{F}_G = 32.2$ ft./sec^2 will also play an important role.

In addition to the above effects which are present even for ideal fluids, there is a drag force resulting from flow seperation and skin friction. In most practical cases this provides the largest contribution to $\vec{F}$. The drag force per unit mass is given by

$$\vec{F}_D = \frac{1}{m}\frac{1}{2}\rho\,\pi r^2 |\vec{u} - \vec{v}|\,(\vec{u} - \vec{v})\,C_D = \frac{3}{8}\frac{\rho}{\rho_\ell}\frac{1}{r}\,|\vec{u} - \vec{v}|\,(\vec{u} - \vec{v})\,C_D \tag{15}$$

---

* See, for example, reference 36.

where ρ and ρ_ℓ are the fluid and droplet densities, $\vec{u}$ and $\vec{v}$ represent the fluid and droplet velocities, and C_D is the drag coefficient of the droplet.

The order of magnitude of C_D is unity, and the fluid momentum equation shows that ∇p is of the same order of magnitude as $\rho\, \vec{u} \cdot \nabla \vec{u}$. An estimate of the relative importance of pressure gradient forces and drag can therefore easily be obtained. Equations (14) and (15) show that

$$\frac{|\vec{F}_p|}{|\vec{F}_D|} \approx \frac{|\nabla p|}{\rho} \frac{r}{|\vec{u} - \vec{v}|^2} \sim \frac{r\,|\vec{u} \cdot \nabla \vec{u}|}{|\vec{u} - \vec{v}|^2} \sim \frac{r}{\ell} \frac{|\vec{u}|^2}{|\vec{u} - \vec{v}|^2} \qquad (16)$$

where ℓ is a characteristic length over which the average flow velocity changes by an appreciable fraction of its magnitude. It is seen from Eq. (16) that, for the small droplets encountered in many sprays, it is an excellent approximation to neglect pressure gradient forces in comparison to drag, provided the relative velocity of the droplet and the fluid does not approach zero. In our applications pressure gradients are small, and we shall neglect $\vec{F}_p$.

Since the force resulting from droplet rotation is always less than the drag, and high rotational velocities are rapidly damped out by viscous dissipation, we will neglect $\vec{F}_R$ in our analysis. In treating sprays with droplets of radii less than about a millimeter in diameter, it is also possible to neglect gravitational effects, $\vec{F}_G$. We shall consider only cases in which $\vec{F} = \vec{F}_D$.

The drag coefficient C_D must be known in order to evaluate $\vec{F}$ from Eq. (15). Theoretical and experimental determination of C_D have been made for solid and liquid spheres. It is easily predicted and generally observed that for low speed flows the drag coefficient depends mainly upon the Reynolds number,

$$Re \equiv \frac{\rho |\vec{v} - \vec{u}| 2r}{\mu} \tag{17}$$

Here μ is the fluid viscosity and 2r appears in the numerator since Re is based on droplet diameter. The drag coefficient exhibits irregular behavior at large Reynolds numbers where turbulence becomes important.[36] Droplets, however, become unstable, oscillate and break up long before these large values of Re are reached. Hence we need only consider the low Reynolds number range $Re < 1000$ for which comparatively accurate theories and experiments exist.

The simplest small Reynolds number theory for the drag coefficient is that of Stokes* which yields

$$C_D = \frac{24}{Re} \frac{2\mu + 3\mu_\ell}{3\mu + 3\mu_\ell} , \tag{18}$$

where μ and μ_ℓ are the viscosities of the gas and droplet, respectively. An improvement over the Stokes theory by Oseen[36] leads to the expression

$$C_D = \frac{24}{Re} \left(1 + \frac{3}{16} Re + \ldots\right) \tag{19}$$

for solid spheres ($\mu_\ell \to \infty$). Experiments on both solid and liquid

---

* See, for example, reference 37.

spheres in sprays[38] are correlated very well by the expression

$$C_D = 27/Re^{0.84} \qquad (20)$$

for Reynolds numbers between 6 and 400. This result lies between those predicted by Stokes and Oseen and is relatively accurate for practical application. However, the drag coefficient for a rapidly evaporating or burning droplet may be very different from the results computed from Eqs. (18) to (20).

4. The Droplet Source Term

In addition to depending to a large extent upon the particular problem under consideration, the source term Q appearing in Eq. (1) can be modified by changing the formulation of the problem. For example, in problems involving the condensation of liquid or solid particles from super-saturated vapors (e.g. carbon formation), it is possible to set Q equal to zero and to include the formation of small ($r = 0$) particles by suitably adjusting the growth rate R at $r = 0$. Since the mechanism of formation of new particles is different from the growth mechanism in these cases, it may be more convenient to let $(Rf)\big|_{r=0} = 0$ and include particle formation in the term Q. From this last viewpoint, since the newly-formed particles will initially be traveling at the same velocity as the component of the fluid from which they were formed, we conclude that the relation

$$Q = Q' \, \delta(r) \, \delta(\vec{u} + \vec{U} - \vec{v}) \qquad (21)$$

will be valid. Here $\vec{U}$ is the diffusion velocity (relative to $\vec{u}$) of the gaseous material forming the particles and Q' represents the total number of new particles per unit volume being formed in unit time. For the disappearance of particles by evaporation it will be convenient to let Q = 0 and account for the sink through the term $(Rf)\big|_{r=0}$, because the mechanism of disappearance of droplets is in this case the same as their shrinkage mechanism.

The source term Q may be used to account in an approximate phenomenological manner for the break-up of droplets traveling at a high velocity relative to the fluid. Since the size and shape of the particles are characterized by a single parameter in the present theory, it is impossible to consider the oscillations of the liquid droplet before it disintegrates. We pointed out in Section 1 that there is a critical Weber number W_{cr} which divides the regime in which oscillations damp out from the regime where deformations tend to grow leading to droplet break-up. A rough approximate treatment of droplet break-up may be obtained by assuming that droplets retain their spherical shape until they arrive at this critical flow condition, at which time they break up instantly into a number of smaller droplets. The source term Q describes this instantaneous disappearance and creation of particles.

5. The Droplet Growth Rate

The term in Eq. (1) involving R, the rate of growth of the droplet, depends to a large extent upon the flow conditions about

the droplet and the kinds of physical processes occurring. We shall consider only evaporation and combustion. In the simple case in which there is no relative motion between the droplet and the surrounding flow field, the mass transfer rate is controlled by molecular transport processes. If changes in the droplet size and flow conditions occur sufficiently slowly, then quasi-steady-state equations may be used to determine R. By this we mean that time derivatives in the equations governing the evaporation rate may be neglected. In this case any time dependence of R is caused by changes in ambient flow conditions and droplet diameter. If the droplets are, on the average, sufficiently far apart to justify neglect of interactions between droplets, then it may justifiably be assumed that there is a spherically symmetric transport field around each droplet. Under these three restrictive conditions, the analyses given in the two preceding chapters determine the growth rate with combustion. The growth rate with pure evaporation is obtained by setting the heat of reaction equal to zero in the results of either of the two preceding chapters. We shall first discuss these ideal rates of growth and then indicate practical methods for removing the above assumptions.

a. Evaporation

Let us first investigate the case of evaporation without chemical reaction. For the sake of simplicity we shall consider a binary mixture composed of the evaporating substance and the atmosphere into which it is evaporating. The essential features of the

derivation of Eqs. (I-27) and (I-28) of Chapter I are unmodified in the absence of chemical reaction, except for the simplifications that the heat of reaction q is zero and the flux fraction ϵ_i of any species i is constant. If we let X represent the mole fraction of the evaporating component, then the corresponding constant mass flux fraction must be equal to its value at the surface of the liquid droplet, which is unity. Equations (I-27) and (I-28) may then be written as

$$\frac{4\pi r}{\dot{m}^o}\,\frac{\lambda}{\bar{c}_p}\,\sigma^2\,\frac{dT}{d\sigma} = \frac{\Delta\ell}{\bar{c}_p} + T - T_\ell \qquad (22)$$

and

$$\frac{4\pi r}{\dot{m}^o}\,\rho\, D\,\sigma^2\,\frac{dX}{d\sigma} = X - 1 \qquad (23)$$

respectively, where $\dot{m}^o$ is the evaporation rate (gm/sec) of the droplet, D represents the binary diffusion coefficient, and σ is the distance from the center of the droplet measured in units of the droplet radius, r. In Eq. (22) T is the temperature, λ is the thermal conductivity, $\bar{c}_p$ represents the average specific heat at constant pressure per unit mass of the mixture, and $\Delta\ell$ denotes the heat of vaporization per gram.

We shall assume for simplicity that the Lewis number $\mathcal{L} = \lambda / \bar{c}_p \rho D$, and the product ρD are constant. By integrating Eqs. (22) and (23) from the surface of the droplet we then obtain explicitly the temperature and concentration profiles, viz.

$$\frac{T - T_\ell}{\Delta\ell/\bar{c}_p} + 1 = \exp\left[\frac{\dot{m}^\circ}{4\pi r}\frac{\bar{c}_p}{\lambda}\left(\frac{\sigma - 1}{\sigma}\right)\right] \qquad (24)$$

and

$$\frac{1 - X}{1 - X_\ell} = \exp\left[\mathcal{L}\frac{\dot{m}^\circ}{4\pi}\frac{\bar{c}_p}{\lambda}\left(\frac{\sigma - 1}{\sigma}\right)\right] . \qquad (25)$$

Evaluating these equations at the free-stream conditions f (corresponding to $\sigma = \infty$) determines the evaporation rate*,

$$\dot{m}^\circ = 4\pi r\frac{\lambda}{\bar{c}_p}\ln\left(1 + \frac{T_f - T_\ell}{\Delta\ell/\bar{c}_p}\right) = \frac{4\pi r}{\mathcal{L}}\frac{\lambda}{\bar{c}_p}\ln\left(\frac{1 - X_f}{1 - X_\ell}\right) . \qquad (26)$$

Since Eq. (I-43) implies that

$$R = \frac{-\dot{m}^\circ}{4\pi r^2\rho_\ell} , \qquad (27)$$

Eq. (26) determines the growth rate for evaporating droplets.

b. Combustion

For the burning of fuel droplets in an oxidizing atmosphere Eq. (26) is replaced by Eq. (II-36b) which may be written as

$$\dot{m}^\circ = 4\pi r\frac{\lambda}{\bar{c}_p}\ln\left(1 + \frac{T_f - T_\ell}{\Delta\ell/\bar{c}_p} + \frac{\alpha}{\Delta\ell}\frac{Y_{O,f}}{Y_O}\right) \qquad (28)$$

where Y_O is the mass fraction of oxidizer, the subscript f identifies

---

* When the Lewis number $\mathcal{L}$ is unity, Eq. (26) may also be obtained directly from Eqs. (II-36b) and (II-42) of Chapter II by setting the heat of reaction (T^*) equal to zero. The simplicity of this reduction indicates that bipropellant diffusion-flame droplet combustion has more in common with pure evaporation than does monopropellant droplet burning. The reason for this is that reaction kinetics play an essential role in the combustion of premixed systems, while they may be neglected in comparison to the rate-controlling diffusion process in the other cases.

the free-stream value, and the superscript * signifies the stoichiometric value in a mixture of pure fuel and oxidiser. The assumptions required for the derivation of Eq. (28) are stated in Parts B and C of Chapter II.

The burning rate of monopropellant droplets with reactions of arbitrary order but with large activation energies is given by Eq. (I-42b), viz.

$$\dot{m}^{\circ} = 16\pi r \frac{\lambda_\ell}{\bar{c}_p} \frac{T_f - T_\ell}{T_f - T_\ell + (\Delta\ell/\bar{c}_p)} . \qquad (29)$$

For second-order monopropellant reactions of low activation energies, an empirical correlation Eq. (I-47) yields

$$\dot{m}^{\circ} = 4\pi r^2 \frac{p}{R' T_\ell} \sqrt{\frac{B}{M} \frac{\lambda_\ell T_\ell}{\Delta\ell}} \sqrt{\frac{h T_f}{T_f - T_\ell + (\Delta\ell/\bar{c}_p)}} \qquad (30)$$

where B is the frequency factor of the reaction rate, M is the average molecular weight, and R' represents the gas constant per gram. Here h depends on the stoichiometry, activation energy, and the free-stream temperature; it is defined in Eq. (I-48). Equation (30) should be used only for activation energies less than about 15 k cal and under the assumptions listed in Appendix A.

Equations (26), (28), (29), and (30) determine the ideal rate of growth of the droplets for the problems that will be treated in Section E. It is seen that the dependence of the mass flow rate upon droplet radius may be expressed as $\dot{m}^{\circ} \sim r^2$ for Eq. (30) and

$\dot{m}_o \sim r$ in the other cases. It has also been pointed out* that $\dot{m}_o \sim r^2$ when radiative heat transfer to the droplet is the controlling process. Hence in all practical spray combustion problems the ideal droplet growth rate will obey the relation $R \sim r^{-k}$ where $0 \leq k \leq 1$. It will be seen that corrections to the ideal mass flow rate do not alter this conclusion concerning the growth rate.

c. Convection Correction

We shall now estimate the effects of relative motion of the droplet and fluid, the variation of external conditions with time, and droplet interaction. Few attempts have been made to describe theoretically the flow field around an evaporating or burning droplet which is not stationary with respect to the surrounding fluid. For the case of evaporation without combustion, Frössling[39] has given the boundary layer equations describing the flow, but it has been found to be impossible to obtain explicit solutions in closed form. Kumagai[41]** treated the case of a burning droplet (diffusion flame) by means of a highly simplified model. In view of the lack of rigorous theoretical results, it is best to use empirical correlations which are based upon dimensional analysis.

For evaporation without combustion the effect of fluid motion upon the evaporation rate has been accounted for by the relation[39,40,43]

---

* See, for example, reference 27. The result follows directly from the fact that the rate of evaporation is proportional to the rate at which energy is received by the droplet, which is in turn proportional to the surface area of the droplet for radiative transfer.

** See also reference 42.

$$\frac{\dot{m} - \dot{m}^{\circ}}{\dot{m}^{\circ}} = 0.276\ Re^{1/2}\ Sc^{1/3}, \qquad (31)$$

where $\dot{m}^{\circ}$ is the ideal mass flow rate given previously and $\dot{m}$ is the evaporation rate in the presence of relative motion. Here the Schmidt number Sc represents the ratio of viscous to diffusional energy transfer and is defined as $Sc = \mu/\rho D$. By combining Eqs. (26) and (31), we obtain for the droplet growth rate with forced convection the expression

$$R = -\frac{1}{r}\frac{\lambda}{\bar{c}_p\ \rho_\ell} \ln\left(1 + \frac{T_f - T_\ell}{\Delta\ell/\bar{c}_p}\right)(1 + 0.276\ Re^{1/2}\ Sc^{1/3}) \quad . \qquad (32)$$

It appears likely[15] that for a burning fuel droplet the motion of the fluid increases the mass burning rate by a mechanism similar to that for pure evaporation. It has been suggested[43] that in Eq. (31) the Schmidt number should be replaced by the Prandtl number $Pr \equiv \mu\,\bar{c}_p/\lambda$ for a burning droplet, because in this case thermal conduction is more important than diffusion. This hypothesis is in reasonable agreement with some experiments.[43] The corresponding rate of growth is found from Eq. (28) to be

$$R = -\frac{1}{r}\frac{\lambda}{\bar{c}_p\ \rho_\ell} \ln\left(1 + \frac{T_f - T_\ell}{\Delta\ell/\bar{c}_p} + \frac{q}{\Delta\ell}\frac{Y_{O,f}}{Y_O^*}\right)(1 + 0.276\ Re^{1/2}\ Pr^{1/3}). \qquad (33)$$

Since the chemical reaction rate is the controlling step in monopropellant droplet burning, we do not expect a simple correction of the type expressed by Eq. (31) to be valid for premixed systems.

No observations of the effect of forced convection on the burning rate of monopropellant droplets appear to have been published to date.

d. Droplet Interactions

The effect of droplet interactions upon the diffusion flame burning of droplets has been investigated by Rex, Fuhs, and Penner.[42] They find that, as two droplets are brought closer together, the burning rate first increases (presumably because of a reduction in heat loss to the surrounding atmosphere), and then decreases (because of a resulting oxidizer deficiency). An extrapolation of the results indicates that when the distance between the droplets is greater than about 10 droplet diameters, then no appreciable effect upon the burning rate is observed. We therefore expect that when the volume ratio $\nu \leq 10^{-3}$, droplet interactions can be neglected for diffusion flames. For values of ν somewhat greater than this limiting value the experimental results can be roughly approximated by

$$\dot{m} = \dot{m}^{o} \left(1 + \frac{c\,\nu}{\nu + 1}\right) , \qquad (34)$$

where the experimentally determined constant c is found by analysis of the results of Rex, Fuhs, and Penner[42] to be 10 for methyl and ethyl alcohol droplets and 150 for n-heptane droplets.

We expect that similar physical effects of the proximity of two droplets will be observed for monopropellant sprays. By comparing the flame radii computed in Chapter I to typical flame radii

for droplet diffusion flames, one may infer that the limiting ratio will depend strongly upon the reaction rate for monopropellant burning, and may vary from 1/3 for rapid reaction rates to 10^{-5} for slow reactions with large activation energies.

For an evaporating droplet the thickness of the surrounding layer in which the composition varies is approximately equal to the droplet radius, while the diffusion flame about a burning droplet is located between 2 and 10 radii from the droplet surface. Hence the limiting value of ν above which interactions are important is about 500 times larger for pure evaporation than for bipropellant droplet burning. Since ν will nearly always be less than 1/2, it appears that the interaction effects of evaporating droplets which are not burning will almost always be negligible.

e. Quasi-Steady-State Hypothesis

It is difficult to determine theoretically the importance of the assumption that time-dependent terms in the equations governing the evaporation rate are negligible. It appears that no estimates have been made of the range of validity of this assumption for the case of droplet burning. An investigation of the initial unsteady period of droplet evaporation without combustion has been carried out by El Wakil and collaborators.[21] The results indicate that for droplets of the size and kind ordinarily encountered in sprays, the unsteady state often composes the greater part of the evaporation time. The quasi-steady-state hypothesis was found to be valid only

for droplets of low volatility in an atmosphere at a temperature not greatly in excess of the droplet temperature. Although the quasi-steady-state hypothesis is probably inaccurate for spray problems, the complexity of the unsteady growth-rate differential equations prohibits the solution of spray equations in which they are included.

C DERIVATION OF GENERAL RELATIONS

1. Number Density and Other Integrated Quantities

For many applications it may be unnecessary to obtain the distribution function f because less complete information about the spray is required. Before considering particular examples, we shall therefore derive some general relations applicable to all sprays of the type considered in Part B. These relations will involve various integrated and averaged quantities which may be of practical interest.

Three integrated number densities may be defined in the following manner. The number of droplets per unit volume at $\vec{x}$ in a unit velocity range about $\vec{v}$ at time t, irrespective of their radii, is

$$\mathcal{E}(\vec{x}, \vec{v}, t) \equiv \int_0^\infty f(r, \vec{x}, \vec{v}, t)\, dr;$$

the number per unit volume at x in a unit radius range about r is given by

$$\mathcal{G}(r, \vec{x}, t) \equiv \int f(r, \vec{x}, \vec{v}, t)\, d\vec{v},$$

where the integration is to be carried over all values of $\vec{v}$. The

functions g and G may be called the velocity and size distribution functions, respectively. The total number density of particles at $\vec{x}$ and t is now defined as

$$n(\vec{x}, t) \equiv \int_0^\infty \int f(r, \vec{x}, \vec{v}, t)\, d\vec{v}\, dr = \int_0^\infty G(r, \vec{x}, t)\, dr = \int g(\vec{x}, \vec{v}, t) d\vec{v}. \quad (35)$$

We can obtain differential equations for these number densities by performing suitable integrations of Eq. (1). The quantities r, $\vec{x}$, $\vec{v}$, and t are all independent variables, and the function f vanishes when $|\vec{v}| = \infty$. By integrating Eq. (1) over all velocities we therefore obtain the expression

$$\frac{\partial G}{\partial t} = -\frac{\partial}{\partial r}(\bar{R}\, G) - \nabla_x \cdot (\vec{\bar{v}}_v\, G) + \int (Q + \Gamma)\, d\vec{v}. \quad (36)$$

In this relation the average droplet growth rate has been defined as

$$\bar{R} \equiv \int R\, f\, d\vec{v}/G,$$

and the quantity

$$\vec{\bar{v}}_v \equiv \int \vec{v}\, f\, d\vec{v}/G$$

represents the mean velocity averaged over $\vec{v}$ but dependent upon r, $\vec{x}$, and t. The last term in Eq. (36) is zero when the source term Q is zero and only weak droplet interactions occur (i.e. when each drop retains its size and identity in collisions). In this case the integro-differential equation reduces to a partial differential equation.

If we integrate Eq. (1) over r and use the fact that there are no particles of infinite size ($f = 0$ at $r = \infty$), then we obtain

the equation for $\mathcal{G}$, viz.

$$\frac{\partial \mathcal{G}}{\partial t} = (Rf)\Big|_{r=0} - \nabla_x \cdot (\mathcal{G}\,\vec{\bar{v}}_r) - \nabla_v \cdot (\mathcal{G}\,\vec{\bar{F}}) + \int_0^\infty (Q + \Gamma)\, dr. \quad (37)$$

Here the average acceleration of droplets at $(\vec{x}, t)$ with velocity $\vec{v}$ has been defined as

$$\vec{\bar{F}} \equiv \int_0^\infty \vec{F}\, f\, dr/\mathcal{G},$$

and the quantity

$$\vec{\bar{v}}_r \equiv \int_0^\infty \vec{v}\, f\, dr/\mathcal{G}$$

is the velocity averaged over r.

The differential equation for the number density n is obtained by integrating Eq. (1) over r and $\vec{v}$. If use is made of Eqs. (35) and (36), then it is found that

$$\frac{\partial n}{\partial t} = (\bar{R}\, G)\Big|_{r=0} - \nabla_x \cdot (n\,\vec{\bar{v}}) + \int_0^\infty \int (Q + \Gamma)\, d\vec{v}\, dr. \quad (38)$$

Here the number-average velocity $\vec{\bar{v}}$ has been defined as

$$\vec{\bar{v}} \equiv \int_0^\infty \int \vec{v}\, f\, d\vec{v}\, dr/n = \int_0^\infty \vec{\bar{v}}_v\, G dr/n = \int \vec{\bar{v}}_r\, g\, d\vec{v}/n, \quad (39)$$

and use has been made of the fact that G vanishes at $r = \infty$.

Equation (38) states that, in addition to the usual divergence term, the total number of droplets per unit volume may be increased by three different effects. The first term on the right-hand side of Eq. (38) accounts for the number increase because of the growth of particles of zero radius. The contribution of sources to the increase in the total number of droplets is given by

$$\int_0^\infty \int Q \, d\vec{v} \, dr = Q' \, .$$

The third effect is the collision term which is zero when for any collision the number of incident particles is the same as the number of particles produced. Since it may often be easier to solve Eqs. (36), (37), or (38) than to obtain the complete solution to Eq. (1), the equations derived in this section may be of value in problems in which the density function f is not required.*

2. Expressions Which Eliminate the Collision Term

In spray problems in which collisions are of importance and the collision mechanism is not well known, it may be useful to employ expressions from which the collision term has been eliminated. These expressions are analogous to the equations of change for summational invariants of the kinetic theory of gases. They are obtained by averaging Eq. (1) over r and $\vec{v}$ with suitable weighting factors which are determined by the conservation equations that govern collisions.

Equation (2) expresses the fact that mass is conserved in collisions. If it is assumed that all droplets have the same density ρ_ℓ, then Eq. (2) implies that the total volume of the droplets is unchanged by collisions. By multiplying Eq. (1) by the droplet volume $\frac{4}{3}\pi r^3$ and differentiating by parts, we obtain the relation

*Previous treatments of sprays have usually used expressions similar to these integrated relations [e.g., Eq. (36) is used in references 27 and 28].

$$\frac{\partial}{\partial t}\left(\frac{4}{3}\pi r^3 f\right) = -\frac{\partial}{\partial r}\left(\frac{4}{3}\pi r^3 f R\right) + 4\pi r^2 f R - \nabla_x \cdot \left(\frac{4}{3}\pi r^3 f \vec{v}\right)$$
$$-\nabla_v \cdot \left(\frac{4}{3}\pi r^3 f \vec{F}\right) + \frac{4}{3}\pi r^3 (Q + \Gamma).$$

If it is assumed for simplicity that the only contributions to the source term come from droplet break-up, then by integrating the preceding equation over r and $\vec{v}$ we obtain the droplet continuity equation

$$\frac{\partial}{\partial t}(n V) = n \dot{V} - \nabla_x \cdot (n V \vec{v}_m) \qquad (40)$$

in which the collision and source terms do not appear. Here we have used the fact that f vanishes at the limits of the integration over velocity, while $f = 0$ at $r = \infty$ and fR remains finite as $r \to 0$. The definition and meaning of the factors appearing in Eq. (40) are described in the following paragraph.

In Eq. (40) the average droplet volume, V, has been defined as

$$V \equiv \int_0^\infty \int \frac{4}{3}\pi r^3 f \, d\vec{v} \, dr/n = \int_0^\infty \frac{4}{3}\pi r^3 G \, dr/n = \int \mathcal{G}_m \, d\vec{v}/n \qquad (41)$$

where the volume density function $\mathcal{G}_m(\vec{x}, \vec{v}, t)$ is given by

$$\mathcal{G}_m \equiv \int_0^\infty \frac{4}{3}\pi r^3 f \, dr \, .$$

It follows from the previous definition of ν, the ratio of the total droplet volume to the volume occupied by the gas, that the total volume of the droplets per unit volume of space is given by

$$n V = \frac{\nu}{\nu + 1} \, . \qquad (42)$$

In Eq. (40) the average rate of change of volume of a droplet produced by growth is defined as

$$\dot{V} \equiv \int_0^\infty \int 4\pi r^2 \, f \, R \, d\vec{v} \, dr/n = \int_0^\infty 4\pi r^2 \, \bar{R} \, G \, dr/n, \tag{43}$$

and the mass (or volume) - weighted average velocity of the droplets is

$$\vec{v}_m \equiv \int_0^\infty \int \frac{4}{3}\pi r^3 \, f \, \vec{v} \, d\vec{v} \, dr/n \, V = \int_0^\infty \frac{4}{3}\pi r^3 \, G \, \vec{\bar{v}}_v \, dr/n \, V =$$

$$\int \mathcal{G}_m \, \vec{v} \, d\vec{v}/n \, V \, . \tag{44}$$

Since Eq. (3) states that momentum is conserved in droplet collisions, a spray momentum conservation equation may be obtained by multiplying Eq. (1) by $\frac{4}{3}\pi r^3 \vec{v}$. Proceeding as before, we find

$$\frac{\partial}{\partial t}\left(\frac{4}{3}\pi r^3 f \vec{v}\right) = -\frac{\partial}{\partial r}\left(\frac{4}{3}\pi r^3 f R \vec{v}\right) + 4\pi r^2 f R \vec{v} - \nabla_x \cdot \left[\frac{4}{3}\pi r^3 f(\vec{v}\,\vec{v})\right]$$

$$- \nabla_v \cdot \left[\frac{4}{3}\pi r^3 f(\vec{F}\,\vec{v})\right] + \frac{4}{3}\pi r^3 f \vec{F} + \frac{4}{3}\pi r^3 \vec{v}(Q + \Gamma) \, ,$$

where the tensors $(\vec{v}\,\vec{v})$ and $(\vec{F}\,\vec{v})$ are the dyadic products of the corresponding vectors and use has been made of the identity $\vec{F} \cdot \nabla_v \vec{v} = \vec{F}$. If this equation is integrated over all values of r and $\vec{v}$, then the momentum conservation equation

$$\frac{\partial}{\partial t}(n \, V \, \vec{v}_m) = n \, V \, \dot{\vec{v}}_m + n \, V \, \vec{F}_m - \nabla_x \cdot \left[n \, V \, (\vec{v}\,\vec{v})_m\right] \tag{45}$$

is obtained. Here the contribution of the droplet growth to the

average rate of change of momentum of a droplet is given by

$$\rho_\ell V \dot{\vec{v}}_m \equiv \rho_\ell \int_0^\infty \int 4\pi r^2 f R \vec{v} \, d\vec{v} \, dr/n \quad , \tag{46}$$

and the mass-weighted average acceleration acting on a particle is defined as

$$\vec{F}_m \equiv \int_0^\infty \int \frac{4}{3}\pi r^3 f \vec{F} \, d\vec{v} \, dr/nV \quad . \tag{47}$$

In Eq. (45) the quantity $(\vec{v}\,\vec{v})_m$ represents the mass-weighted average value of the dyadic $(\vec{v}\,\vec{v})$, which is given by the equation

$$(\vec{v}\,\vec{v})_m \equiv \int_0^\infty \int \frac{4}{3}\pi r^3 f (\vec{v}\,\vec{v}) \, d\vec{v} \, dr/n V = \int g_m (\vec{v}\,\vec{v}) \, d\vec{v}/n V \quad . \tag{48}$$

By using Eq. (40), the momentum conservation equation may be written in the alternate form

$$\frac{\partial \vec{v}_m}{\partial t} + \vec{v}_m \cdot \nabla_x \vec{v}_m = \dot{\vec{v}}_m - \frac{\dot{V}}{V} \vec{v}_m + \vec{F}_m - \frac{1}{nV} \nabla_x \cdot \left\{ n V \left[(\vec{v}\,\vec{v})_m - (\vec{v}_m \vec{v}_m) \right] \right\} . \tag{45a}$$

This equation states that as one follows the average motion of the droplets, the velocity may be changed by three different effects. The first two terms on the right-hand side of Eq. (45a) account for the contribution of droplet growth to the average rate of change of velocity. It is easily seen that

$$\dot{\vec{v}}_m - \frac{\dot{V}}{V} \vec{v}_m = \int_0^\infty \int_0^\infty \iint \frac{16}{3}\pi^2 r^2 r'^3 f f' R (\vec{v}-\vec{v}') \, d\vec{v}' d\vec{v} \, dr' \, dr/(nV)^2$$

where the prime on the second f indicates that it is a function of

r' and $\vec{v}'$. The acceleration term $\vec{F}_m$ determines the change in velocity caused by external and aerodynamic forces. The last term in Eq. (45a) is analogous to the divergence of the hydrodynamic total stress tensor. The spray stress tensor may be defined as $\rho_\ell n V \left[(\vec{v}\,\vec{v})_m - (\vec{v}_m \vec{v}_m)\right]$, in which case the usual fluid dynamical interpretation can be given to Eq. (45a). More "external forces" appear in Eq. (45a) than in the ordinary momentum equation of fluid dynamics because of the greater complexity of sprays.

It is obvious that Eqs. (40) and (45) involve far more variables than the number of equations. We therefore expect that only in special cases will it be possible to obtain a complete solution to the problem without including equations involving the collision terms. The usefulness of the results obtained in this section is therefore limited. Equations (40) and (45) are, however, only slightly more complicated than the ordinary hydrodynamical equations for density ($\rho_\ell n V$) and velocity ($\vec{v}_m$) when suitable approximations* can be made for the other terms appearing in these equations.

D APPLICATION TO IMPINGING JET ATOMIZATION

In order to illustrate the use of the preceding formalism for the description of sprays, we shall consider impinging jet

*The assumptions that $(\vec{v}\,\vec{v})_m = (\vec{v}_m \vec{v}_m)$ and $\vec{v}_m = \vec{v}\,\overline{V}/\overline{V}$ are examples of the kinds of approximations which may often be valid. These two approximations are applicable when the velocity distribution exhibits little dispersion about its mean. From an estimation of the size distribution G, an approximation for $\overline{V}$ can be obtained by use of Eq. (43). After a similar estimation of $\vec{F}_m$, the only two unknowns in Eqs. (40) and (45a) are nV and $\vec{v}_m$, and the solution is therefore determined.

atomisation and the problem of evaporation and combustion of droplets in sprays. For impinging jets collisions play a dominant role, while they are of secondary interest in spray combustion. Both of these problems are encountered in conventional rocket motors.

1. Statement of the Problem

In order to treat impinging jet atomization within the framework of the present theory, we assume that upstream from the region in which the jets intersect the streams may be treated as being composed of a number of liquid particles. This assumption is expected to be valid when the fraction of the volume occupied by liquid is sufficiently small to avoid the formation of continuous streams or sheets. It will also be assumed that oscillations of these liquid particles are small and have a negligible effect upon the droplet interactions. Therefore, in this model of impingement atomization, clouds of relatively large droplets collide and form new clouds of smaller particles traveling in a somewhat different direction.

We shall consider the commonly encountered problem of steady-state atomization. In this case the droplet distribution function f is independent of time in all regions of the flow. In order to isolate the impingement process from other aspects of the practical problem, it may be assumed that the number distribution of particles is known in all jets upstream from the collision zone.

The theory then determines the steady-state value of δ throughout the region of interaction. Although the droplets in the clouds may actually be evaporating during the atomization process, it will be possible to neglect evaporation in treating impingement atomization provided the fractional change in droplet radius during the time required for the droplet to traverse the interaction zone is sufficiently small. This evaporation rate parameter is easily estimated in specific cases from a knowledge of the droplet growth rate law, the average particle velocity, and the approximate size of the interaction region. By similar order-of-magnitude estimates, it may be ascertained that for sufficiently small collision regions the external forces can be neglected during the interaction. In view of the preceding discussion, it is then apparent that the simplified form of Eq. (1) which governs the case under consideration may be written as

$$\vec{v} \cdot \nabla_x f = \Gamma \, . \tag{49}$$

Because the collision term is of dominant importance in this problem, it is expected that the results of Section C-2 will provide a significant simplification. Since these results apply only to various mean quantities and the size distribution function is of particular interest here, only Eq. (49) will be used in the following analysis. The appropriate integrations may be performed a posteriori to obtain desired mean values.

2. Specification of the Interaction Mechanism

By substituting Eq. (13) into Eq. (49), we obtain the expression

$$\vec{v} \cdot \nabla_x f(r, \vec{x}, \vec{v}) = \iiiint f(r', \vec{x}, \vec{v}') f(r'', \vec{x}, \vec{v}'') \left| \vec{v}' - \vec{v}'' \right| \left[\sigma(r, \vec{v}; r', \vec{v}'; r'', \vec{v}'') - \pi (r' + r'')^2 \delta(r - r'') \delta(\vec{v} - \vec{v}'') \right] dr' \, dr'' \, d\vec{v}' \, d\vec{v}'' \quad , \tag{49a}$$

where the dependence of the function f upon the independent variables has been explicitly indicated. In order to determine the cross section σ, the mechanics of droplet collisions must be given. Since the partition of energy and other collision parameters are unknown at present, we shall make a hypothesis for the interaction mechanism which is consistent with the conservation of mass and momentum [Eqs. (2) and (3)]. It will be assumed that when two droplets collide they produce N new droplets of equal size. We shall consider the case in which the resulting N particles all travel in the same direction with the same velocity.

Since the mass of a droplet is proportional to the cube of its radius, Eq. (2) implies that when droplets of radii r' and r'' collide the radii of the resulting droplets will be

$$\left[(r'^3 + r''^3)/N \right]^{1/3} .$$

The conservation of momentum [Eq. (3)] requires that the velocity of the new droplets is given by

$$\vec{v} = \frac{r'^3 \vec{v}'}{r'^3 + r''^3} + \frac{r''^3 \vec{v}''}{r'^3 + r''^3} .$$

The expression for the collision cross section is therefore

$$\sigma(r, \vec{v}; r', \vec{v}'; r'', \vec{v}'') = \frac{1}{2} N \pi (r' + r'')^2 \delta\left[r - \left(\frac{r'^3 + r''^3}{N}\right)^{1/3}\right]$$

$$\delta\left(\vec{v} - \frac{r'^3 \vec{v}'}{r'^3 + r''^3} - \frac{r''^3 \vec{v}''}{r'^3 + r''^3}\right) . \qquad (50)$$

The above expression is proportional to the product of the geometrical cross section and the number of particles produced in the range $(dr, d\vec{v})$ per collision.

By substituting Eq. (50) into Eq. (49a) we find

$$\vec{v} \cdot \nabla_x f(r, \vec{x}, \vec{v}) = \int\int\int\int_0^\infty f(r', \vec{x}, \vec{v}') f(r'', \vec{x}, \vec{v}'') \left|\vec{v}' - \vec{v}''\right|$$

$$\pi (r' + r'')^2 \left\{\frac{1}{2} N \delta\left[r - \left(\frac{r'^3 + r''^3}{N}\right)^{1/3}\right] \delta\left(\vec{v} - \frac{r'^3 \vec{v}'}{r'^3 + r''^3}\right.\right.$$

$$\left.\left. - \frac{r''^3 \vec{v}''}{r'^3 + r''^3}\right) - \delta(r - r'') \delta(\vec{v} - \vec{v}'')\right\} dr' \, dr'' \, d\vec{v}' \, d\vec{v}'' . \qquad (49b)$$

The integration over $\vec{v}''$ and r'' may now be explicitly carried out. The resulting relation is

$$\vec{v} \cdot \nabla_x f(r, \vec{x}, \vec{v}) = \int\int\int_0^\infty f(r', \vec{x}, \vec{v}') \left|\vec{v}' - \vec{v}\right| \pi (r' + r'')^2$$

$$\left\{ f\left(r'', \vec{x}, \frac{r'^3 + r''^3}{r''^3} \vec{v} - \frac{r'^3}{r''^3} \vec{v}'\right) \frac{1}{2} N \left(\frac{r'^3 + r''^3}{r''^3}\right)^4 \right.$$

$$\left. \delta\left[r - \left(\frac{r'^3 + r''^3}{N}\right)^{1/3}\right] - f(r'', \vec{x}, \vec{v}) \, \delta(r - r'')\right\} dr' \, dr'' \, d\vec{v}'$$

$$= \int\int_0^\infty f(r', \vec{x}, \vec{v}') \left|\vec{v}' - \vec{v}\right| \left\{ \varepsilon(Nr^3 - r'^3) \, f\left[(Nr^3 - r'^3)^{1/3}, \right.\right.$$

$$\left.\vec{x}, \frac{Nr^3}{Nr^3 - r'^3} \vec{v} - \frac{r'^3}{Nr^3 - r'^3} \vec{v}'\right] \frac{N^{4/3} \pi}{2} \left(\frac{Nr^3}{Nr^3 - r'^3}\right)^{14/3}$$

$$\left.\left[r' + (Nr^3 - r'^3)^{1/3}\right]^2 - f(r, \vec{x}, \vec{v}) \pi (r + r')^2\right\} dr' \, d\vec{v}' , \qquad (51)$$

where the step function $\varepsilon(x)$ has been defined by the equation

$$\varepsilon(x) = \begin{cases} 0 \text{ for } x < 0 \\ 1 \text{ for } x \geq 0 \end{cases} .$$

The use of $\varepsilon(x)$ enables us to extend the r' integral over the usual range, zero to infinity.

3. Boundary Conditions

We shall consider the case in which there are only two incident streams of particles. The number densities in each of these streams, f_1 and f_2, must be specified in order to determine the solution completely. We shall assume for simplicity that there is no correlation between r, $\vec{x}$, and $\vec{v}$ in the distribution functions for the incident jets*. The function f_j for each value of j (j = 1,2) may then be expressed as the product of a function of $\vec{x}$, a function of r, and a function of $\vec{v}$.

In order to investigate the effect of jet interaction it is desirable to choose an ideal incident velocity distribution which allows no collisions between particles within the same stream. If we also require that in each incident jet all the particles travel in the same direction, then the velocity dependence of f_j must be given by a factor $\delta(\vec{v} - \vec{v}_{o,j})$ where $\vec{v}_{o,j}$ is the constant characteristic velocity of the j'th stream. We let $n_j(\vec{x})$ signify the spacial number distribution of the j'th incident jet and $G_j(r)$ represent the corresponding normalized particle size distribution. The resulting incident distribution functions are then

*More detailed investigations of the type carried out by Lee(44) are needed to determine the form of f_j more accurately.

given by the expression

$$f_j(r,\vec{x},\vec{v}) = n_j(\vec{x})\, G_j(r)\, \delta(\vec{v} - \vec{v}_{o,j}),\ j = 1,2. \qquad (52)$$

The choice of $n_j(\vec{x})$ is limited by the requirement that f_j is constant along lines parallel to $\vec{v}_{o,j}$. The function $G_j(r)$ is arbitrary and may be determined by experimental or theoretical considerations of single jet atomization.

4. Method of Solution

The exact solution to Eq. (51) with the boundary conditions expressed by Eq. (52) is unfortunately not easily obtained. Equation (51) is a non-linear integro-differential equation of a somewhat complicated type. It is, however, possible to use the following iterative technique based upon the known boundary conditions [Eq. (52)]. The first approximation to the function f in the collision region is

$$f^{[1]} = f_1 + f_2 \ .$$

By substituting this relation into the integral in Eq. (51), we obtain an expression for $\vec{v} \cdot \nabla_x f$. This equation can be solved for the function f in order to obtain the second approximation $f^{[2]}$, which is valid in the collision region and downstream. The repetition of this process produces higher approximations. We shall actually carry out only the first iteration. This is equivalent to assuming that each droplet undergoes at most one collision in the interaction region. The results are therefore expected to be most accurate for dilute impinging jets (i.e., small values of ν).

By substituting the approximation $f^{[1]}$ for f into the right-hand side of Eq. (51), we obtain the relation

$$\vec{v}\cdot\nabla_x f(x,\vec{x},\vec{v}) = \int_0^\infty\int\Big[n_1(\vec{x})\,a_1(x')\;\delta(\vec{v}'-\vec{v}_{o,1}) + n_2(\vec{x})\,a_2(x')\;\delta(\vec{v}'-\vec{v}_{o,2})\Big]\left|\vec{v}'-\vec{v}\right|\Big\{\varepsilon(Nr^3-x'^3)\Big\{n_1(\vec{x})\,a_1\Big[(Nr^3-x'^3)^{1/3}\Big]\,\delta\Big(\frac{Nr^3\vec{v}}{Nr^3-x'^3}-\frac{x'^3\vec{v}'}{Nr^3-x'^3}-\vec{v}_{o,1}\Big)+n_2(\vec{x})\,a_2\Big[(Nr^3-x'^3)^{1/3}\Big]\,\delta\Big(\frac{Nr^3\vec{v}}{Nr^3-x'^3}-\frac{x'^3\vec{v}'}{Nr^3-x'^3}-\vec{v}_{o,2}\Big)\Big\}\frac{N^{4/3}\pi}{2}\Big(\frac{Nr^3}{Nr^3-x'^3}\Big)^{14/3}\Big[x'+(Nr^3-x'^3)^{1/3}\Big]^2-\Big[n_1(\vec{x})\,a_1(x)\;\delta(\vec{v}-\vec{v}_{o,1})+n_2(\vec{x})\,a_2(x)\;\delta(\vec{v}-\vec{v}_{o,2})\Big]\pi(x+x')^2\Big\}\,dx'\,d\vec{v}'\,. \tag{51a}$$

Performing the integration over $\vec{v}'$ in Eq. (51a) leads to the equation

$$\vec{v}\cdot\nabla_x f(x,\vec{x},\vec{v}) = n_1(\vec{x})\,n_2(\vec{x})\Big\{-\left|\vec{v}-\vec{v}_{o,1}\right|\delta(\vec{v}-\vec{v}_{o,2})\,a_2(x)\int_0^\infty a_1(x')\,\pi(x+x')^2\,dx' - \left|\vec{v}-\vec{v}_{o,2}\right|\delta(\vec{v}-\vec{v}_{o,1})\,a_1(x)\int_0^\infty a_2(x')\pi(x+x')^2\,dx' + \left|\vec{v}-\vec{v}_{o,1}\right|\int_0^\infty a_1(x')\;a_2\Big[(Nr^3-x'^3)^{1/3}\Big]\;\varepsilon(Nr^3-x'^3)\,\delta\Big[\vec{v}-\frac{x'^3}{Nr^3}\vec{v}_{o,1}-\Big(1-\frac{x'^3}{Nr^3}\Big)\vec{v}_{o,2}\Big]\;\frac{N^{4/3}\pi}{2}\Big(\frac{Nr^3}{Nr^3-x'^3}\Big)^{5/3}\Big[x'+(Nr^3-x'^3)^{1/3}\Big]^2\,dx' + \left|\vec{v}-\vec{v}_{o,2}\right|\int_0^\infty a_2(x')\;a_1\Big[(Nr^3-x'^3)^{1/3}\Big]\;\varepsilon(Nr^3-x'^3)\,\delta\Big[\vec{v}-\Big(1-\frac{x'^3}{Nr^3}\Big)\vec{v}_{o,1}-\frac{x'^3}{Nr^3}\vec{v}_{o,2}\Big]\;\frac{N^{4/3}\pi}{2}\Big(\frac{Nr^3}{Nr^3-x'^3}\Big)^{5/3}\Big[x'+(Nr^3-x'^3)^{1/3}\Big]^2\,dx'\Big\}\,. \tag{53}$$

Terms involving $\left[n_j(\vec{x})\right]^2$ do not appear in Eq. (53) because they all contain factors of the form $\left|\vec{v} - \vec{v}_{o,j}\right| \delta(\vec{v} - \vec{v}_{o,j})$ which are identically zero. This is consistent with the previously imposed requirement that particles in the same jet do not collide with each other. Equation (53) indicates also that f changes only in regions of space in which both n_1 and n_2 are non-zero (i.e., in the interaction region of the jets).

The four terms appearing in Eq. (53) have a direct physical interpretation. Since the factor $\delta(\vec{v} - \vec{v}_{o,2})$ in the first term is zero unless $\vec{v} = \vec{v}_{o,2}$, this term represents the scattering of particles out of beam number 2 because of collisions with jet number 1. The second term similarly represents the scattering out of incident beam 1. The last two terms in Eq. (53) are non-zero for a range of values of $\vec{v}$ and account for the new particles formed by collisions.

If one is given the functions $G_j(r)$ and the geometry of the incident jets, then Eq. (53) determines explicitly the directional derivatives of f in any direction at any point in space. Since the value of f is known upstream from the collision zone, by evaluating a definite integral along a line in space we can obtain the function $f(r, \vec{x}, \vec{v})$ for any values of r, $\vec{x}$, and $\vec{v}$. This process will be demonstrated for particular simple jet geometries.

5. Jets with Sharp Boundaries

a. Solution

The important properties of the solution may be found by

considering uniform jets with sharp boundaries. In these cases the functions $n_j(\vec{x})$ are constant within the jet boundaries and zero elsewhere. It is possible to set up a cartesian coordinate system as illustrated in Fig. 15. The x-y plane is parallel to the vectors $\vec{v}_{o,1}$ and $\vec{v}_{o,2}$, the direction of the x axis bisects the angle between $\vec{v}_{o,1}$ and $\vec{v}_{o,2}$, and the origin is taken to be the first point at which the two incident streams intersect. The angle θ between each incident jet and the x axis is one half of the angle between the directions of the vectors $\vec{v}_{o,1}$ and $\vec{v}_{o,2}$.

If we assume that the magnitude of the velocity of each incident jet is the same, i.e.,

$$\left|\vec{v}_{o,1}\right| = \left|\vec{v}_{o,2}\right| \equiv v_o,$$

then the velocities of the incident streams may be written in the form

$$\vec{v}_{o,j} = v_o \vec{e}_j \qquad j = 1,2 \quad .$$

Here the x component of the unit vectors $\vec{e}_j$ is $\cos\theta$, and the y components are $\sin\theta$ and $-\sin\theta$ for $\vec{e}_1$ and $\vec{e}_2$, respectively. The simplified form of Eq. (53) in this coordinate system can be obtained by using the fact that

$$\int_0^\infty a_{1,2}(r')\, a_{2,1} \left[(R^3 - r'^3)^{1/3}\right] E(R^3 - r'^3)\, \delta\left[\vec{v} - \frac{r'^3}{R^3}\vec{v}_{o;1,2} - \left(1 - \frac{r'^3}{R^3}\right)\vec{v}_{o;2,1}\right] \frac{R^{4/3}\pi}{2} \left(\frac{R^3}{R^3 - r'^3}\right)^{5/3} \left[r' + (R^3 - r'^3)^{1/3}\right]^2 dr'$$

$$= \delta(v_z)\ \delta(v_x - v_o \cos\theta\ ) \int_0^{r} N^{1/3} \; G_{1,2}(r')$$

$$G_{2,1}\left[(Nr^3 - r'^3)^{1/3}\right] \frac{N^{4/3}\pi}{2} \left(\frac{Nr^3}{Nr^3 - r'^3}\right)^{5/3} \left[r' + (Nr^3 - r'^3)^{1/3}\right]^2$$

$$\delta\left[v_y \pm \left(1 - \frac{2r'^3}{Nr^3}\right) v_o \sin\theta\right] dr' = \left[\mathcal{E}(v_y + v_o \sin\theta\ ) - \mathcal{E}(v_y - v_o \sin\theta)\right]$$

$$\delta(v_z)\ \delta(v_x - v_o \cos\theta\ )\ G_1\left[r\left(\frac{N}{2}\right)^{1/3} \left(1 + \frac{v_y}{v_o \sin\theta}\right)^{1/3}\right]$$

$$G_2\left[r\left(\frac{N}{2}\right)^{1/3} \left(1 - \frac{v_y}{v_o \sin\theta}\right)^{1/3}\right] \frac{\pi}{3} N^2 r^3 \left(\frac{N}{2}\right)^{1/3} (v_o \sin\theta \mp v_y)^{-1}$$

$$\left[\left(1 + \frac{v_y}{v_o \sin\theta}\right)^{-1/3} + \left(1 - \frac{v_y}{v_o \sin\theta}\right)^{-1/3}\right]^2 .$$

Here the upper signs correspond to the first subscript on the functions G_j, the lower signs correspond to the second subscript, and the quantities v_x, v_y, and v_z represent the component of the vector $\vec{v}$ in the corresponding directions. By substituting the preceding relations into Eq. (53), we obtain the result

$$\vec{v} \cdot \nabla_x f(r, \vec{x}, \vec{v}) = n_1(\vec{x})\ n_2(\vec{x})\ \delta(v_z)\ \delta(v_x - v_o \cos\theta)$$

$$\Big\{ -2v_o \sin\theta \Big[\delta(v_y + v_o \sin\theta)\ G_2(r) \int_0^{\infty} G_1(r')\, \pi(r + r')^2\ dr'$$

$$+ \delta(v_y - v_o \sin\theta)\ G_1(r) \int_0^{\infty} G_2(r')\, \pi(r + r')^2\ dr'\Big]$$

$$+ G_1\left[r\left(\frac{N}{2}\right)^{1/3} \left(1 + \frac{v_y}{v_o \sin\theta}\right)^{1/3}\right]\ G_2\left[r\left(\frac{N}{2}\right)^{1/3} \left(1 - \frac{v_y}{v_o \sin\theta}\right)^{1/3}\right]$$

$$\frac{2\pi}{3} N^2 r^3 \left(\frac{N}{2}\right)^{1/3} \left[\mathcal{E}(v_y + v_o \sin\theta) - \mathcal{E}(v_y - v_o \sin\theta)\right] \left[\left(1 + \frac{v_y}{v_o \sin\theta}\right)^{-1/3} + \left(1 - \frac{v_y}{v_o \sin\theta}\right)^{-1/3}\right]^2 , \qquad (54)$$

where use has been made of relations of the form

$$\left|\vec{v} - v_o \vec{e}_i\right| \delta(\vec{v} - v_o \vec{e}_j) = v_o \left|\vec{e}_j - \vec{e}_i\right| \delta(\vec{v} - v_o \vec{e}_j)$$

which follow from the definition of the δ function.

Since the factor $n_1(\vec{x})\, n_2(\vec{x})$ is zero except in the region of intersection of the two incident streams (see Fig. 15), Eq. (54) provides a simple geometrical method for obtaining $f(r, \vec{x}, \vec{v})$ at any point downstream. For any given point $\vec{x}$ and velocity $\vec{v}$, the line through $\vec{x}$ in the direction $\vec{v}$ may be extended upstream. We denote by ℓ the length of the segment of this line which lies within the jet intersection. Equation (54) can then be integrated in order to obtain the relation

$$f(r, \vec{x}, \vec{v}) = \delta(\vec{v} - \vec{v}_{o,1})\, G_1(r) \left[n_1(\vec{x}) - 2\ell n_1 n_2 \sin\theta \int_0^\infty G_2(r') \pi (r + r')^2 dr'\right] + \delta(\vec{v} - \vec{v}_{o,2})\, G_2(r) \left[n_2(\vec{x}) - 2\ell n_1 n_2 \sin\theta \int_0^\infty G_1(r') \pi (r + r')^2 dr'\right] + \frac{\ell}{|\vec{v}|} n_1 n_2 \delta(v_z)\, \delta(v_z - v_o \cos\theta)$$

$$G_1\left[r\left(\frac{N}{2}\right)^{1/3} \left(1 + \frac{v_y}{v_o \sin\theta}\right)^{1/3}\right] G_2\left[r\left(\frac{N}{2}\right)^{1/3} \left(1 - \frac{v_y}{v_o \sin\theta}\right)^{1/3}\right] \frac{2\pi}{3} N^2 r^3 \left(\frac{N}{2}\right)^{1/3}$$

$$\left[\mathcal{E}(v_y + v_o \sin\theta) - \mathcal{E}(v_y - v_o \sin\theta)\right] \left[\left(1 + \frac{v_y}{v_o \sin\theta}\right)^{-1/3} + \left(1 - \frac{v_y}{v_o \sin\theta}\right)^{-1/3}\right]^2 . \qquad (55)$$

Here n_1 and n_2 are the constant values of the functions $n_1(\vec{x})$ and $n_2(\vec{x})$ within their respective incident jets. The explicit expression for f given in Eq. (55) is composed of three terms; the first two give the value of f within the original beams and the third determines the distribution function in new regions.

b. Results

The factors $\delta(v_z)\ \delta(v_x - v_o \cos\theta)$ in Eq. (55) indicate that, for the chosen interaction mechanism, collisions lead to no change in the z or x components of velocity of the particles. It is evident that the y component of velocity is in the range

$$|v_y| \leq v_o \sin\theta$$

for all new droplets. The interaction therefore causes large particles to break up into smaller particles traveling in a fan of directions which are bounded by the two incident streams. The velocity and size distributions of the new droplets depend upon the size distribution of the incident particles.

6. Cylindrical Jets

An example of sharp-edge incident jets which closely approximates actual impingement atomization is the case in which both streams are circular cylinders of radius a with their axes in the x-y plane. By reference to Fig. 16a, it can be seen that any plane perpendicular to the z axis cuts the intersection region of the two jets in a rhombus, the dimensions of which are indicated in

Fig. 16b. Since the function f is zero unless $\vec{v}$ is parallel to the x-y plane, the length ℓ is the segment of the appropriate line within the rhombus.

a. Design Criteria

It is seen from Fig. 16b that for scattering out of the incident beams the length ℓ is equal to $\sqrt{a^2 - z^2} / \sin\theta\cos\theta$. The first two terms of Eq. (55) then show that for incident jets of sufficiently large diameter or number density, all incident droplets of a given size r may be scattered out of the central section of the jets. In the simplified case for which $n_1 = n_2 \equiv n$ and $G_1 = G_2 \equiv 0$, if no incident particles of size r escape collision then the relation

$$2\ell \sin\theta \geq \left[n \int_0^\infty G(r') \pi (r + r')^2 \, dr' \right]^{-1} \qquad (56)$$

must be satisfied. For circular jets this condition becomes

$$\frac{2\sqrt{a^2 - z^2}}{\cos\theta} \geq \left[n \int_0^\infty G(r') \pi (r + r')^2 \, dr' \right]^{-1} . \qquad (56a)$$

Since the quantity in square brackets in Eq. (56) is an increasing function of r, it follows that all particles larger than a critical size will be scattered by collisions. Particles of all sizes will be scattered when the relation

$$\frac{2\sqrt{a^2 - z^2}}{\cos\theta} \geq \left[n \int_0^\infty G(r') \pi r'^2 \, dr' \right]^{-1} . \qquad (56b)$$

is valid. A reasonable requirement for an efficient atomizing

system is that all particles in the central half of the incident jets are scattered at least once. This criterion is expressed by the relation

$$\frac{a\, n\overline{(\pi r^2)}}{\cos\theta} \geq 1 \qquad (56c)$$

where the average cross-sectional area of the incident droplets has been defined by the equation

$$\overline{(\pi r^2)} \equiv \int_0^\infty G(r')\, \pi\, r'^2\, dr' \quad .$$

Large incident particles and a large impingement angle θ therefore lead to more effective atomization.

Since the average cross-sectional area is approximately proportional to the two-thirds power of the average volume of a droplet, it follows that an alternate form of Eq. (56c) is

$$\frac{1}{\cos\theta}\ \frac{a}{\bar{r}}\ \frac{\nu}{\nu+1} \gtrsim 1 \qquad (56d)$$

where $\bar{r}$ is an average droplet radius in the incident jets. In view of the fact that the volume ratio ν must be small for the analysis used here to be accurate, Eq. (56d) implies that the diameter of the jets must be larger than $1/\nu$ times the average particle radius in order to obtain efficient atomization.

b. The Asymptotic Distribution Function

The distribution of newly-formed particles is determined by the last term in Eq. (55). In this case the length ℓ may be

evaluated geometrically by reference to Fig. 16b. The complete expression for ℓ is given by the equation

$$\frac{\ell}{|\vec{v}|} = \begin{cases} 0 & \text{for } v_y \geq v_o \sin\theta \left(\dfrac{y\cos\theta + \sqrt{a^2 - z^2}}{x\sin\theta - a}\right) \\[2ex] \dfrac{2v_o \tan\theta\sqrt{a^2 - z^2}}{(v_o^2 \sin^2\theta - v_y^2)}\left[1 + \dfrac{y\cos\theta}{\sqrt{a^2 - z^2}} - \dfrac{v_y}{v_o}\left(\dfrac{x}{\sqrt{a^2 - z^2}} - \dfrac{a}{\sin\theta\sqrt{a^2 - z^2}}\right)\right] & \text{for } v_o \sin\theta \left(\dfrac{y\cos\theta + \sqrt{a^2 - z^2}}{x\sin\theta - a}\right) \geq v_y \geq \dfrac{v_o \sin\theta\, y\cos\theta}{x\sin\theta - a - \dfrac{v_y}{|v_y|}\sqrt{a^2 - z^2}} \\[2ex] \dfrac{2\sqrt{a^2 - z^2}}{\cos\theta(v_o \sin\theta + |v_y|)} & \text{for } \dfrac{v_o \sin\theta\, y\cos\theta}{x\sin\theta - a - \dfrac{v_y}{|v_y|}\sqrt{a^2 - z^2}} \geq v_y \geq \dfrac{v_o \sin\theta\, y\cos\theta}{x\sin\theta - a + \dfrac{v_y}{|v_y|}\sqrt{a^2 - z^2}} \\[2ex] \dfrac{2v_o \tan\theta\sqrt{a^2 - z^2}}{(v_o^2 \sin^2\theta - v_y^2)}\left[1 - \dfrac{y\cos\theta}{\sqrt{a^2 - z^2}} + \dfrac{v_y}{v_o}\left(\dfrac{x}{\sqrt{a^2 - z^2}} - \dfrac{a}{\sin\theta\sqrt{a^2 - z^2}}\right)\right] & \text{for } \dfrac{v_o \sin\theta\, y\cos\theta}{x\sin\theta - a + \dfrac{v_y}{|v_y|}\sqrt{a^2 - z^2}} \geq v_y \geq v_o \sin\theta \left(\dfrac{y\cos\theta - \sqrt{a^2 - z^2}}{x\sin\theta - a}\right) \\[2ex] 0 & \text{for } v_o \sin\theta \left(\dfrac{y\cos\theta - \sqrt{a^2 - z^2}}{x\sin\theta - a}\right) \geq v_y \end{cases} \quad (97)$$

This determines explicitly the new distribution function f for any values of r, x, y, z, and v_y.

Of particular interest is the asymptotic value which the number density approaches far downstream from the collision region.

If v_y does not approach v_o $(\cos\Theta)$ y/x far downstream, then the line extended in the direction $\vec{v}$ does not cross the collision region and ℓ is zero. The distance ℓ must therefore become proportional to $\delta(v_y - v_o \cos\theta\, y/x)$ far downstream. The constant of proportionality may be evaluated by integrating Eq. (57) over all values of v_y for large values of x and y. The resulting relation,

$$\frac{\ell}{|\vec{v}|} \rightarrow \frac{2(e^2 - z^2)}{x \sin\theta \cos\theta}\ \delta\left(v_y - v_o \cos\theta \frac{y}{x}\right) ,$$

may be substituted into the last term of Eq. (55) to give f_{as} $(r, \vec{x}, \vec{v})$, the asymptotic distribution of new particles far downstream from the collision region. In this manner we obtain the equation

$$f_{as}(r, \vec{x}, \vec{v}) = \delta(v_z)\ \delta(v_x - v_o \cos\theta)\ \delta\left(v_y - v_o \cos\theta \frac{y}{x}\right)$$

$$\frac{4\pi N^2 n_1 n_2 (e^2 - z^2)}{3 x \sin\theta\cos\theta} \left(\frac{N}{2}\right)^{1/3} r^3 Q_1\left[r\left(\frac{N}{2}\right)^{1/3}\left(1 + \frac{y}{x \tan\theta}\right)^{1/3}\right]$$

$$Q_2\left[r\left(\frac{N}{2}\right)^{1/3}\left(1 - \frac{y}{x \tan\theta}\right)^{1/3}\right]\left[\left(1 + \frac{y}{x \tan\theta}\right)^{-1/3} + \left(1 - \frac{y}{x \tan\theta}\right)^{-1/3}\right]^2 , \quad (58)$$

which is expected to be accurate when $\sqrt{x^2 + y^2} \gtrsim 10^2$ a.

It is seen from Eq. (58) that the number density of new particles decreases approximately as the reciprocal of the distance downstream x for most initial size distributions. The total number density decreases as $|z|$ increases because of the decrease in the size of the interaction zone. The last factor in Eq. (58) tends to cause the angular distribution of scattered particles of a given

size to be a maximum on the x axis. This effect may, however, be modified by the size distribution of the incident droplets because the special distribution of the scattered particles depends upon G_1 and G_2. Since the average particle size depends upon the position (y/x), there is a tendency for droplets of different sizes to become separated in space.

c. Droplet Size Distributions and Average Asymptotic Radii

Let us consider cases in which the incident size distribution is of a generalized Rosin-Rammler type; namely $G \sim r^t \exp\left[-(r/b)^s\right]$ where b is a constant. In normalised form this is

$$G(r) = \frac{s\left[\Gamma\left(\frac{t+2}{s}\right)\right]^{t+1}}{\bar{r}\left[\Gamma\left(\frac{t+1}{s}\right)\right]^{t+2}} \left(\frac{r}{\bar{r}}\right)^t \exp\left\{-\left[\frac{r}{\bar{r}}\,\frac{\Gamma\left(\frac{t+2}{s}\right)}{\Gamma\left(\frac{t+1}{s}\right)}\right]^s\right\} \qquad (59)$$

where s and t are numbers characterizing the distribution, $\bar{r}$ is the number-weighted average radius of the incident droplets, and the Γ function is defined as

$$\Gamma(x) \equiv \int_0^\infty y^{x-1} \exp(-y)\, dy \ .$$

The two-parameter family of distribution functions given in Eq. (59) includes as special cases both the Nukiyama-Tanasawa distribution[46] and Rosin-Rammler distributions.[45]

The asymptotic size distribution of the new particles G_{as} is determined by the factor

$$r^3 \; G_1\left[r\left(\frac{N}{2}\right)^{1/3}\left(1+\frac{y}{x\tan\theta}\right)^{1/3}\right] G_2\left[r\left(\frac{N}{2}\right)^{1/3}\left(1-\frac{y}{x\tan\theta}\right)^{1/3}\right]$$

in Eq. (56). When the size distributions of both incident jets are

the same ($G_1 = G_2 \equiv G$), then in the plane y = 0 the function G_{as} is proportional to $r^3 \left\{ G\left[r\left(\frac{N}{2}\right)^{1/3} \right] \right\}^2$. If the incident distribution function G is of the form given in Eq. (59) , then the normalized asymptotic size distribution is

$$G_{as} = \frac{s}{\Gamma} \left(\frac{N}{2}\right)^{\frac{2t+4}{3}} \left[\left(1 + \frac{y}{x \tan\theta}\right)^{s/3} + \left(1 - \frac{y}{x \tan\theta}\right)^{s/3} \right]^{\frac{2t+4}{s}}$$

$$\frac{1}{\Gamma\left(\frac{2t+4}{s}\right)} \left[\frac{\Gamma\left(\frac{t+2}{s}\right)}{\Gamma\left(\frac{t+1}{s}\right)} \right]^{2t+4} \left(\frac{r}{\bar{r}}\right)^{2t+3} \exp\left\{ - \left(\frac{r}{\bar{r}}\right)^{s} \left[\frac{\Gamma\left(\frac{t+2}{s}\right)}{\Gamma\left(\frac{t+1}{s}\right)} \right]^{s} \right.$$

$$\left. \left(\frac{N}{2}\right)^{s/3} \left[\left(1 + \frac{y}{x \tan\theta}\right)^{s/3} + \left(1 - \frac{y}{x \tan\theta}\right)^{s/3} \right] \right\} \quad . \qquad (60)$$

This distribution is also of the generalized Rosin-Rammler type. The factor $(r/\bar{r})^3$ in Eq. (60) arises from the fact that larger particles are more likely to collide*.

It may be seen from Eq. (60) that the form of the distribution function is not affected by the jet interaction only when t = -3,** which corresponds to the ordinary Rosin-Rammler distribution for s = 1.

---

* Since the time required for the complete burning of a cloud of particles is determined by the size of the largest droplet, one reason for the high performance of impingement atomizers in rocket motors may be that large particles are more likely to be broken up than smaller ones.

** The case t = -3 is an example of a non-normalizable distribution for which Eq. (59) is rigorously meaningless. The difficulty arises from the fact that there are so many small droplets that the total number of droplets is mathematically infinite. In those cases the right-hand side of Eq. (59) may be interpreted as being proportional to G(r), and the ratios of Γ functions of negative integers can be evaluated by limiting procedures [i.e. $\Gamma(-n)/\Gamma(-m) = (-1)^{n-m}\Gamma(m+1)/\Gamma(n+1)$].

In all other cases the characteristic parameter s is unchanged, but the parameter corresponding to t is different in the outgoing stream. Equation (60) indicates that the collisions tend to increase the parameter t (i.e. $t \rightarrow 2t + 3$) and thereby cause the distribution to become more uniform.

The average droplet size far downstream may be computed from Eq. (60) by performing the appropriate integration. The resulting new (number-weighted) average radius $\bar{r}_{as}$ is found to be

$$\bar{r}_{as} = \bar{r} \frac{\Gamma(\frac{t+1}{s})\Gamma(\frac{2t+5}{s})}{\Gamma(\frac{t+2}{s})\Gamma(\frac{2t+4}{s})} (\frac{2}{N})^{1/3} \left[(1 + \frac{y}{x \tan\theta})^{s/3} + (1 - \frac{y}{x \tan\theta})^{s/3} \right]^{-1/s} \quad (61)$$

It may be seen from Eqs. (60) and (61) that in the case s = 3, which is often observed in practice,* both the distribution function G_{as} and the value of $\bar{r}_{as}$ are independent of the downstream position (y/x). In this case samples taken from any part of the asymptotic region will have the same size distribution. When $s \neq 3$, the dependence of G_{as} and $\bar{r}_{as}$ upon y/x is very weak. It is seen from Eq. (61) that when $s > 3$ the average asymptotic radius tends to be largest in the center of the jet (y = 0), while for $s < 3$ the mean size is larger in the wings where $y/x = \tan\theta$.

An important prediction of Eq. (61) is that the new average droplet radius varies approximately inversely as the cube root of the number of particles produced in a collision N. For example, if an average of 8 new particles is formed in each collision, then the number-weighted mean diameter of the atomized jet is reduced by only

---

* See, for example, reference 28.

a factor of 2. This estimate actually provides an upper limit for $\bar{r}_{as}$ because we have allowed a maximum of one collision for each incident particle.

Values of the quantity $\bar{r}_{as}/(\bar{r}/N^{1/3})$ on the axis of the atomized jet ($y = 0$), which were computed from Eq. (61) for various values of s and t, are listed in Table VIII and plotted in Fig. 17. In Table IX and Fig. 18 are shown the values of $\bar{r}_{as}/(\bar{r}/N^{1/3})$ on the edge of the atomized jet ($|y|/x = \tan\theta$). It can be seen by comparing Figs. 17 and 18 that the average asymptotic droplet radius on the edge of the scattered jet is a more sensitive function of the incident size distribution than is the droplet radius on the axis. If the requirement of a small asymptotic number-weighted average droplet radius is used as a criterion for atomization efficiency, then it is apparent that impingement atomization is most efficient for incident streams with large values of the parameters t and s.

E APPLICATION TO SPRAY COMBUSTION

1. Description of the Problem

In order to illustrate the use of the formulation of the theory of sprays presented in Part B for problems in spray combustion, we shall demonstrate how the analysis given by Probert[28] can be generalized to include the effects of droplet interaction and relative motion of droplets and fluid. In the system under consideration, a cloud of particles with given initial properties at $x = 0$ moves steadily in the x direction through a fluid of known

characteristics. We want to obtain a description of the statistical properties of the cloud as a function of x. Of particular interest is the ratio of the volume fraction occupied by the evaporating or burning spray at the position x to this volume fraction at the injector (x = 0). This ratio is a direct measure of the combustion efficiency of heterogeneous propellants in rocket motors of length x.[28]

For the one-dimensional (steady-state) system under investigation, the reasoning presented in Section D-3 implies that droplet collisions will be infrequent and relatively unimportant. The applicable form of Eq. (1) is therefore

$$\frac{\partial}{\partial x}(Rf) + \frac{\partial}{\partial x}(v f) + \frac{\partial}{\partial v}(Ff) = 0 , \qquad (62)$$

where the functions R and F have been given in Sections B-5 and B-3, respectively. If Stokes' relation for the drag coefficient is valid, then according to Eqs. (15) and (16)

$$F = \frac{\Phi(u - v)}{r^2} \qquad (63)$$

where the functions u and $\Phi \equiv 9\mu(2\mu + 3\mu_\ell)/2\rho_\ell(3\mu + 3\mu_\ell)$ are independent of r and v. Although we shall assume for brevity that Eq. (63) is valid, no additional complications arise in the method of solution when more accurate aerodynamic force expressions [e.g. Eq. (19) or (20)] are used. It is seen from Section B-5 that the explicit dependence of R upon r and v is determined by the equation

$$R = \frac{-A}{r^k}\left(1 + \beta + \gamma\sqrt{F}\,|u - v|^{1/2}\right) , \qquad (64)$$

which includes the effects of the droplet interactions through β [$\beta \equiv c\nu/(\nu + 1)$, see Eq. (34)] and the relative motion of droplets and fluid through γ [$\gamma \equiv 0.276\sqrt{2\rho/\mu}\,(Sc^{1/3}$ or $Pr^{1/3})$, see Eqs. (32) and (33)]. In Eq. (64) the functions A, β, and γ are independent of r and v, the exponent k lies in the range $0 \leq k \leq 1$ (see Section E-5-b), and A is determined by the type of evaporation or combustion process occuring through Eqs. (27) and (26), (28), (29), or (30) [e.g., $k = 1$ and $A = (\lambda/\bar{c}_p\,\rho_\ell)\ln\left(1 + \frac{T_f - T_\ell}{\Delta\ell/\bar{c}_p}\right)$ with pure evaporation]. Equation (62) must be solved with F and R given by Eqs. (63) and (64) in order to obtain the desired distribution function $f(r, x, v)$.

2. Method of Solution

a. Perturbation when Fluid Properties are Known

Probert[28] has given the solution to Eq. (62) for the case in which $\Phi = \beta = \gamma = 0$, A = constant, and the initial distribution (at $x = 0$) is of the Rosin-Rammler type. Often the effects on f of droplet interactions and motion of the fluid are small compared to that of the ideal evaporation rate, and a perturbation procedure may be used to account for non-zero values of Φ, β, and γ. It is then possible to assume that expansions of the form $R = R^{[0]} + R^{[1]}$, $F = F^{[1]}$, and $f = f^{[0]} + f^{[1]} + f^{[2]} + \ldots$ are valid, where $R^{[0]} = -A/r^k$, $R^{[1]} = R^{[0]}(\beta + \gamma\sqrt{F}\,|u - v|^{1/2})$, and $F^{[1]}$ is given by Eq. (63).

By substituting these relations into Eq. (62) and collecting terms of the same order of magnitude, we obtain the sequence of equations which determine the distribution function, viz.

$$\frac{\partial}{\partial r}(R^{[0]}f^{[0]}) + \frac{\partial}{\partial x}(v\, f^{[0]}) = 0$$

$$\frac{\partial}{\partial r}(R^{[0]}f^{[1]}) + \frac{\partial}{\partial x}(v\, f^{[1]}) = -\frac{\partial}{\partial r}(R^{[1]}f^{[0]}) - \frac{\partial}{\partial v}(F^{[1]}f^{[0]})$$

$$\frac{\partial}{\partial r}(R^{[0]}f^{[2]}) + \frac{\partial}{\partial x}(v\, f^{[2]}) = -\frac{\partial}{\partial r}(R^{[1]}f^{[1]}) - \frac{\partial}{\partial v}(F^{[1]}f^{[1]}) \qquad (65)$$

$$\frac{\partial}{\partial r}(R^{[0]}f^{[n]}) + \frac{\partial}{\partial x}(v\, f^{[n]}) = -\frac{\partial}{\partial r}(R^{[1]}f^{[n-1]}) - \frac{\partial}{\partial v}(F^{[1]}f^{[n-1]}),$$

When the above relations are solved in succession, the right-hand side of each equation is a known function of r, x, and v by virtue of the completion of the preceding step. The sequence of equations may therefore be abbreviated by the expression

$$\frac{\partial}{\partial x}(v\, f^{[n]}) - \frac{\partial}{\partial r}\left(\frac{A}{r^k} f^{[n]}\right) = J_n(r, x, v) \qquad n = 0, 1, \ldots \qquad (65a)$$

where

$$\left.\begin{aligned} J_0 &= 0, \\ J_n &\equiv -\frac{\partial}{\partial r}(R^{[1]}f^{[n-1]}) - \frac{\partial}{\partial v}(F^{[1]}f^{[n-1]}) \qquad n = 1, 2, \ldots \end{aligned}\right\}. \qquad (66)$$

The general solution to Eq. (65a) may be obtained by replacing x and r by new variables defined as

$$\xi = \frac{r^{k+1}}{k+1} - \frac{1}{v}\int_0^x A\, dx \qquad (67)$$

and

$$\eta = \frac{r^{k+1}}{k+1} + \frac{1}{v}\int_0^x A\,dx. \tag{68}$$

If

$$\psi^{[n]} \equiv f^{[n]}/r^k, \tag{69}$$

then in terms of ξ and η Eq. (65a) becomes

$$\frac{\partial \psi^{[n]}}{\partial \xi} = -\frac{J_n(r, x, v)}{2A\, r^k} \qquad n = 0, 1, \ldots \quad . \tag{65b}$$

The boundary conditions on the functions $f^{[n]}$ are that at the injection (i.e. at $x = 0$ or $\xi = \eta$) $f^{[0]} = f(r, 0, v)$ and $f^{[n]} = 0$ for $n > 0$, where the initial distribution function $f(r, 0, v)$ is known. Since $J_0 = 0$, the desired solution to Eq. (65b) is therefore

$$\psi^{[0]} = f(\eta, 0, v)/\eta^k \tag{70}$$

and

$$\psi^{[n]} = \int_\xi^\eta \frac{J_n(r, x, v)}{2A\, r^k}\, d\xi \qquad n = 1, 2, \ldots \quad . \tag{71}$$

In Eq. (71) the integration over ξ is to be performed with η and v held constant. The preceding expressions determine the perturbation solution to all orders of magnitude.

b. Iteration when Fluid Properties are Unknown

The procedure described above can be carried out only when the dependence of the quantities u, A, β, γ, and Φ upon the distance x is known in advance. In many practical cases (e.g. rocket motors) the fluid properties (such as temperature, velocity, etc.) which determine these quantities depend strongly upon the interaction of

the droplet cloud with the fluid. In these cases the functions u, A, β, γ, and ϕ are determined by the dynamical equations of the fluid and cannot all be specified a priori. In order to avoid the complexity of solving simultaneously the equations governing both the fluid and the droplets, an iterative technique may be utilized. By initially assuming reasonable properties for the fluid, we can compute the zeroth iterative approximation to $R^{[0]}$, $R^{[1]}$, and $F^{[1]}$, viz. $R^{[0]}_{[0]}$, $R^{[1]}_{[0]}$, and $F^{[1]}_{[0]}$. The perturbation procedure described above may then be employed to obtain the functions $f^{[0]}_{[0]}$, $f^{[1]}_{[0]}$, $f^{[2]}_{[0]}$, etc. until sufficient convergence has been obtained. The distribution function $f_{[0]} = \sum_n f^{[n]}_{[0]}$ determines the zeroth iterative approximation to the properties of the spray. Next the fluid dynamical equations are solved using these known droplet properties, and the first iterative approximations $R^{[0]}_{[1]}$, $R^{[1]}_{[1]}$, and $F^{[1]}_{[1]}$ are computed. The perturbation method then determines $f^{[n]}_{[1]}$ and the first approximation to the distribution function. By repeating this procedure accurate approximations to the properties of the spray can be obtained.

Since a treatment of the fluid dynamical equations is outside the scope of the present investigation, we shall not carry out the iterative procedure described above. Instead we shall extend Probert's zero-order solution to cases in which A is an arbitrary function of x and the initial distribution function is of the generalized Rosin-Rammler type defined in Section D-6-c.

We then perform the first perturbation for the case in which u, A, β, γ, and Φ are constants in order to determine the effect of the fluid motion and droplet interactions upon the properties of the spray.

3. Zero-Order Spray Characteristics

a. The Spray Distribution Function

Let us assume that the v and r dependences of the initial spray distribution function are separable, viz.

$$f(r, 0, v) = g_o(v)\, G_o(r) \tag{72}$$

where the velocity distribution function is normalized in such a way that $\int_{-\infty}^{\infty} g_o(v)\, dv = 1$. It then follows that the total number density of droplets at $x = 0$ is given by $n_o = \int_0^{\infty} G_o(r)\, dr$, and the average initial droplet radius is $\bar{r}_o = \int_0^{\infty} r\, G_o(r)\, dr$. Since the Nukiyama-Tanasawa distribution has recently been found to be more useful than the Rosin-Rammler distributions,[47, 48] it is advantageous to choose a form for $G_o(r)$ which includes this first case. Hence we shall use the generalized Rosin-Rammler distribution defined in Eq. (59),

$$G_o(r) = \frac{n_o\, s}{\bar{r}_o} \frac{\left[\Gamma\left(\frac{t+2}{s}\right)\right]^{t+1}}{\left[\Gamma\left(\frac{t+1}{s}\right)\right]^{t+2}} \left(\frac{r}{\bar{r}_o}\right)^t \exp\left\{-\left[\frac{r}{\bar{r}_o} \frac{\Gamma\left(\frac{t+2}{s}\right)}{\Gamma\left(\frac{t+1}{s}\right)}\right]^s\right\} \tag{73}$$

According to Eqs. (68), (69), and (70), the zero-order solution for f now becomes

$$f^{[0]}(r, x, v) = g_0(v) \frac{n_0 s \left[\Gamma\left(\frac{t+2}{s}\right)\right]^{t+1}}{\bar{r}_0 \left[\Gamma\left(\frac{t+1}{s}\right)\right]^{t+2}} \left(\frac{r}{\bar{r}_0}\right)^k \left[\left(\frac{r}{\bar{r}_0}\right)^{k+1} + \frac{(k+1)\int_0^x A\,dx}{v\,\bar{r}_0^{\,k+1}}\right]^{\frac{t-k}{k+1}} \exp\left\{-\left[\left(\frac{r}{\bar{r}_0}\right)^{k+1} + \frac{(k+1)\int_0^x A\,dx}{v\,\bar{r}_0^{\,k+1}}\right]^{\frac{s}{k+1}} \left[\frac{\Gamma\left(\frac{t+2}{s}\right)}{\Gamma\left(\frac{t+1}{s}\right)}\right]^s\right\}. \quad (74)$$

It will be found convenient to introduce the dimensionless size and distance variables $\hat{r}$ and $\hat{x}$ defined as

$$\hat{r} = r/\bar{r}_0 \quad (75)$$

and

$$\hat{x} = (k+1)\int_0^x A\,dx/v\,\bar{r}_0^{\,k+1}. \quad (76)$$

Equation (74) may then be written in the form

$$f^{[0]}(r, x, v) = g_0(v) \frac{n_0 s \left[\Gamma\left(\frac{t+2}{s}\right)\right]^{t+1}}{\bar{r}_0 \left[\Gamma\left(\frac{t+1}{s}\right)\right]^{t+2}} \hat{r}^k (\hat{r}^{k+1} + \hat{x})^{\frac{t-k}{k+1}} \exp\left\{-(\hat{r}^{k+1} + \hat{x})^{\frac{s}{k+1}} \left[\frac{\Gamma\left(\frac{t+2}{s}\right)}{\Gamma\left(\frac{t+1}{s}\right)}\right]^s\right\}, \quad (74a)$$

which determines all zero-order properties of the spray for $x \geq 0$.

b. Average Spray Properties

The droplet number density $n^{[0]}$, average radius $\bar{r}^{[0]}$, average

volume $V^{[0]}$, etc. are determined by appropriate weighted integrals of Eq. (74a) over $\hat{r}$ and v. These integrals are easily expressed in terms of the generalized form of a function defined by Probert, viz.,

$$H(a, b, c, Z) \equiv \frac{\exp(-Z)}{\Gamma(a\,b + c)} \int_0^\infty \left[(\hat{y} + Z)^a - Z^a\right]^b (\hat{y} + Z)^{c-1} \exp(-\hat{y})\, d\hat{y}. \quad (77)$$

When b is an interger, H(a, b, c, Z) is easily evaluated in terms of incomplete gamma functions.

If the substitutions

$$\hat{y} = (\hat{x}^{k+1} + \hat{x})^{\frac{s}{k+1}} \left[\frac{\Gamma(\frac{t+2}{s})}{\Gamma(\frac{t+1}{s})}\right]^s - \hat{x}^{\frac{s}{k+1}} \left[\frac{\Gamma(\frac{t+2}{s})}{\Gamma(\frac{t+1}{s})}\right]^s \quad (78)$$

and

$$Z = \hat{x}^{\frac{s}{k+1}} \left[\frac{\Gamma(\frac{t+2}{s})}{\Gamma(\frac{t+1}{s})}\right]^s \quad (79)$$

are made in Eq. (74a), then it is found from Eq. (35) that

$$n^{[0]} = n_o \int_{-\infty}^{\infty} \varepsilon_o(v)\, H(\tfrac{k+1}{s}, 0, \tfrac{t+1}{s}, Z)\, dv. \quad (80)$$

In a similar manner, Eq. (41) and the definition

$$\bar{r} = \int \int_0^\infty r\, f(r, \vec{x}, \vec{v})\, dr\, d\vec{v}/n$$

imply that

$$n^{[0]}\bar{r}^{[0]} = n_o \bar{r}_o \int_{-\infty}^{\infty} \varepsilon_o(v)\, H(\tfrac{k+1}{s}, \tfrac{1}{k+1}, \tfrac{t+1}{s}, Z)\, dv \quad (81)$$

and

$$n^{[0]}\, V^{[0]} = n_o\, V_o \int_{-\infty}^{\infty} \varepsilon_o(v)\, H(\tfrac{k+1}{s}, \tfrac{3}{k+1}, \tfrac{t+1}{s}, Z)\, dv \quad (82)$$

where the initial volume occupied by the droplets is

$$n_o V_o = n_o \frac{4}{3}\pi \bar{r}_o^{\,3} \frac{\left[\Gamma\left(\frac{t+1}{s}\right)\right]^2}{\left[\Gamma\left(\frac{t+2}{s}\right)\right]^3} \Gamma\left(\frac{t+4}{s}\right)$$

for the distribution expressed by Eq. (73). Equations (80) through (82) give important zero-order properties of the spray; in particular, Eq. (82) determines the ratio of the volume occupied by the spray at the position x to this volume at the injector (x = 0).

In order to evaluate the integrals in Eqs. (80) through (82), the function $g_o(v)$ must be specified. For cases in which the initial velocity distribution is sufficiently localized, the approximation $g_o(v) = \delta(v - v_o)$ will be valid. Equation (80) then becomes

$$n^{[0]} = n_o H\left(\frac{k+1}{s}, 0, \frac{t+1}{s}, Z\right) = n_o \left[1 - \frac{\Gamma\left(\frac{t+1}{s}, Z\right)}{\Gamma\left(\frac{t+1}{s}\right)}\right] \qquad (80a)$$

where the last equality may be verified by setting b = 0 and replacing $\hat{y}$ by $\hat{y} + Z$ as the integration variable in Eq. (77). In Eq. (80a) the incomplete gamma function has been defined as

$$\Gamma(c, Z) = \int_0^Z x^{c-1} \exp(-x)\, dx;$$

[hence $\Gamma(c) = \Gamma(c, \infty)$]. The simplified forms of Eqs. (81) and (82) are

$$n^{[0]}\bar{r}^{[0]} = n_o \bar{r}_o H\left(\frac{k+1}{s}, \frac{1}{k+1}, \frac{t+1}{s}, Z\right) \qquad (81a)$$

and

$$n^{[0]}v^{[0]} = n_o V_o H\left(\frac{k+1}{s}, \frac{3}{k+1}, \frac{t+1}{s}, Z\right), \qquad (82a)$$

respectively. For the special case in which k = 1 and t = s-4,

Probert[28] has numerically evaluated the function H appearing in Eq. (82a) in order to obtain the droplet volume fraction.

c. Behavior Near the Injector

Further information about the nature of the solutions given in Eqs. (80a) through (82a) can be obtained from expansions of the function H for large and small values of $\hat{x}$. A straightforward expansion in powers of Z of the integral in Eq. (77) shows that near the injector

$$H(a, b, c, Z) \approx 1 - b\, Z^a \frac{\Gamma(a\,b + c - a)}{\Gamma(a\,b + c)} \quad . \tag{83}$$

By substituting Eq. (83) into Eqs. (81a) and (82a) and using the definition of Z given in Eq. (79), we find that for small values of $\hat{x}$

$$n^{[0]}\bar{r}^{[0]} \approx n_o \bar{r}_o \left\{ 1 - \frac{\hat{x}}{(k+1)} \frac{\left[\Gamma\left(\frac{t+2}{s}\right)\right]^k \Gamma\left(\frac{t+1-k}{s}\right)}{\left[\Gamma\left(\frac{t+1}{s}\right)\right]^{k+1}} \right\} \tag{81b}$$

and

$$n^{[0]} v^{[0]} \approx n_o v_o \left\{ 1 - \frac{3\hat{x}}{(k+1)} \left[\frac{\Gamma\left(\frac{t+2}{s}\right)}{\Gamma\left(\frac{t+1}{s}\right)}\right]^{k+1} \frac{\Gamma\left(\frac{t+3-k}{s}\right)}{\Gamma\left(\frac{t+4}{s}\right)} \right\} . \tag{82b}$$

Equation (83) is not useful for the number density because b = 0 in that case. However, by expanding the incomplete gamma function it is easily seen from Eq. (80a) that

$$n^{[0]} \approx n_o \left\{ 1 - \frac{s\,\hat{x}^{\frac{t+1}{k+1}}}{(t+1)} \frac{\left[\Gamma\left(\frac{t+2}{s}\right)\right]^{t+1}}{\left[\Gamma\left(\frac{t+1}{s}\right)\right]^{t+2}} \right\} \tag{80b}$$

for $\hat{x}$ near zero.

In view of the definition of $\hat{x}$ [see Eq. (76)], Eqs. (80b) through (82b) illustrate the physically obvious conclusions that at a given position x, the percent of evaporation increases (i.e. $n^{[0]}/n_o$, $n^{[0]}\bar{r}^{[0]}/n_o\,\bar{r}_o$, and $n^{[0]}V^{[0]}/n_o\,V_o$ decrease) with increasing evaporation rate constant A, decreasing average droplet size $\bar{r}_o$, and decreasing velocity v. By evaluating the ratios of gamma functions in Eqs. (80b) through (82b) for typical ranges of the parameters t and s, it is found that larger values of t and s cause a more rapid initial decrease in the quantities $n^{[0]}V^{[0]}/n_o\,V_o$, $V^{[0]}/V_o$, and $\bar{r}^{[0]}/\bar{r}_o$ and a less rapid initial decrease in the quantities $n^{[0]}/n_o$ and $n^{[0]}\bar{r}^{[0]}/n_o\,\bar{r}_o$. The largest values of the initial total droplet mass-evaporation rate (i.e. smallest $n^{[0]}V^{[0]}/n_o\,V_o$) are therefore obtained when the parameters s and t are large in the injected spray. These results differ somewhat from those of Probert[28] because in this discussion we have assumed that the initial average droplet radius $\bar{r}_o$ is constant, whereas in Probert's description the quantity $\bar{r}_o\,\Gamma(\frac{t+1}{s})/\Gamma(\frac{t+2}{s})$ is constant.

d. Asymptotic Behavior

By expanding the integral in Eq. (77) asymptotically for large values of Z, we find that

$$H(a, b, c, Z) \approx a^b\, Z^{ab+c-b-1} \exp(-Z)\, \frac{\Gamma(1+b)}{\Gamma(ab+c)} \quad . \quad (84)$$

The use of Eq. (84) in Eqs. (80a) through (82a) leads to the relations

$$n^{[0]} \approx \frac{n_o}{\Gamma(\frac{t+1}{s})} \left[\frac{\Gamma(\frac{t+2}{s})}{\Gamma(\frac{t+1}{s})}\right]^{t+1-s} \hat{x}^{\frac{t+1-s}{k+1}} \exp\left\{-\hat{x}^{\frac{s}{k+1}} \left[\frac{\Gamma(\frac{t+2}{s})}{\Gamma(\frac{t+1}{s})}\right]^{s}\right\}, \tag{80c}$$

$$\dot{n}^{[0]}\bar{r}^{[0]} \approx n_o \bar{r}_o \left(\frac{k+1}{s}\right)^{\frac{1}{k+1}} \frac{\Gamma(\frac{k+2}{k+1})}{\Gamma(\frac{t+2}{s})} \left[\frac{\Gamma(\frac{t+2}{s})}{\Gamma(\frac{t+1}{s})}\right]^{t+2-\frac{s(k+2)}{k+1}} \hat{x}^{\frac{t+2}{k+1}-\frac{s(k+2)}{(k+1)^2}} \exp\left\{-\hat{x}^{\frac{s}{k+1}} \left[\frac{\Gamma(\frac{t+2}{s})}{\Gamma(\frac{t+1}{s})}\right]^{s}\right\}, \tag{81c}$$

and

$$n^{[0]}V^{[0]} \approx n_o V_o \left(\frac{k+1}{s}\right)^{\frac{1}{k+1}} \frac{\Gamma(\frac{k+4}{k+1})}{\Gamma(\frac{t+4}{s})} \left[\frac{\Gamma(\frac{t+2}{s})}{\Gamma(\frac{t+1}{s})}\right]^{t+4-\frac{s(k+4)}{k+1}} \hat{x}^{\frac{t+4}{k+1}-\frac{s(k+4)}{(k+1)^2}} \exp\left\{-\hat{x}^{\frac{s}{k+1}} \left[\frac{\Gamma(\frac{t+2}{s})}{\Gamma(\frac{t+1}{s})}\right]^{s}\right\}. \tag{82c}$$

Since the order of magnitude of the functions in Eqs. (80c) through (82c) are most strongly dependent upon the exponential factor for large values of $\hat{x}$, it is easily deduced that an increase in the parameters s or t causes a decrease in the ratios $n^{[0]}/n_o$, $n^{[0]}\bar{r}^{[0]}/n_o \bar{r}_o$, and $n^{[0]}V^{[0]}/n_o V_o$ at a given position $\hat{x}$. The parameter s, which appears as an exponent within the exponential, has the

greatest effect upon these ratios. We conclude that, in the zeroth approximation, initial droplet size distributions with small dispersion about the average radius require much less time for nearly complete evaporation than do size distributions with large dispersion (small s and t).

4. Perturbations Caused by Fluid Motion and Droplet Interactions

a. Perturbation Solution for the Distribution Function

The perturbing effect of the fluid velocity and the proximity of droplets upon the distribution function is determined by Eq. (71). In order to find $\psi^{[1]}$, the function $J_1(r, x, v)$ must be evaluated by using Eq. (66). Since $F^{[1]}$ and $R^{[1]}$ have been defined in Section 2 - a and the function $f^{[0]}$ is given by Eq. (74a), the differentiations in Eq. (66) can easily be performed to obtain J_1. In this manner it is found that

$$J_1(r, x, v) = \frac{A f^{[0]}}{\bar{r}_o^{k+1}} \left\{ \left\{ (t-k)\,(\hat{r}^{k+1} + \hat{x})^{-1} - s \left[\frac{\Gamma\left(\frac{t+2}{s}\right)}{\Gamma\left(\frac{t+1}{s}\right)} \right]^s \right\} (\hat{r}^{k+1} + \hat{x})^{\frac{s}{k+1} - 1} \left[\beta + \gamma \sqrt{\bar{r}_o} \,|u - v|^{1/2} \sqrt{\hat{r}} + \frac{\Phi \bar{r}_o^{k-1} (u - v)\,\hat{x}}{A(k+1)\, v\, \hat{r}^2} \right] \right.$$

$$\left. + \frac{\gamma \sqrt{\bar{r}_o} |u - v|^{1/2}}{2\, \hat{r}^{k+1/2}} + \frac{\Phi \bar{r}_o^{k-1}}{A\, \hat{r}^2} \left[1 - \frac{(u - v)}{g_o(v)} \frac{d\, g_o}{dv} \right] \right\}$$

By using Eqs. (67) and (68) to replace $\hat{x}$ and $\hat{r}$ by ξ and η as independent variables in this equation, we find

$$\frac{J_1(r, x, v)}{2A\, r^k} = \frac{\psi^{[0]}}{2\,\bar{r}_o^{\,k+1}}\left\{\left\{(t-k)\left[\frac{(k+1)\eta}{\bar{r}_o^{\,k+1}}\right]^{-1} - s\left[\frac{\Gamma\left(\frac{t+2}{s}\right)}{\Gamma\left(\frac{t+1}{s}\right)}\right]^{s}\right.\right.$$

$$\left.\left.\left[\frac{(k+1)\eta}{\bar{r}_o^{\,k+1}}\right]^{\frac{s}{k+1}-1}\right\}\left\{\beta + \gamma\,|u-v|^{1/2}\left[\frac{k+1}{2}\,(\xi+\eta)\right]^{\frac{1}{2(k+1)}}\right.\right.$$

$$\left.\left. + \frac{\Phi(u-v)(\eta-\xi)}{2A\,v}\left[\frac{k+1}{2}\,(\xi+\eta)\right]^{-\frac{2}{k+1}}\right\} + \frac{\gamma\,|u-v|^{1/2}\,\bar{r}_o^{\,k+1}}{2}\right.$$

$$\left.\left[\frac{k+1}{2}(\xi+\eta)\right]^{-\frac{k+1/2}{k+1}} + \frac{\Phi\,\bar{r}_o^{\,k+1}}{A}\left[\frac{k+1}{2}\,(\xi+\eta)\right]^{-\frac{2}{k+1}}\left[1 - \frac{(u-v)}{\varepsilon_o(v)}\frac{d\,\varepsilon_o}{dv}\right]\right\}.$$

If it is assumed that u, A, β, γ, and Φ are constant, then the preceding equation can be integrated easily over ξ in order to obtain $\psi^{[1]}$ according to Eq. (71). Since $\psi^{[0]}$ is independent of ξ, the result is

$$\psi^{[1]} = \frac{\psi^{[0]}}{2\,\bar{r}_o^{\,k+1}}\left\{\left\{(t-k)\left[\frac{(k+1)\eta}{\bar{r}_o^{\,k+1}}\right]^{-1} - s\left[\frac{\Gamma\left(\frac{t+2}{s}\right)}{\Gamma\left(\frac{t+1}{s}\right)}\right]\left[\frac{(k+1)\eta}{\bar{r}_o^{\,k+1}}\right]^{\frac{s}{k+1}-1}\right\}\right.$$

$$\left\{\beta(\eta-\xi) + \gamma\,|u-v|^{1/2}\,\frac{k+1}{k+3/2}\left(\frac{k+1}{2}\right)^{\frac{1}{2(k+1)}}\left[(2\eta)^{\frac{k+3/2}{k+1}}\right.\right.$$

$$\left.\left. - (\xi+\eta)^{\frac{k+3/2}{k+1}}\right] + \frac{\Phi(u-v)}{2A\,v}(k+1)\left(\frac{2}{k+1}\right)^{\frac{2}{k+1}}\left[\frac{k+1}{2k(k-1)}(2\eta)^{\frac{2k}{k+1}}\right.\right.$$

$$- \frac{2\eta}{k-1}(\xi+\eta)^{\frac{k-1}{k+1}} + \frac{1}{2k}(\xi+\eta)^{\frac{2k}{k+1}}\Bigg]\Bigg\} + \gamma|u-v|^{1/2}\,\bar{r}_o^{\,k+1}\,(k+1)$$

$$\left(\frac{k+1}{2}\right)^{-\frac{k+1/2}{k+1}}\left[(2\eta)^{\frac{1}{2(k+1)}} - (\xi+\eta)^{\frac{1}{2(k+1)}}\right] + \frac{\Phi\,\bar{r}_o^{\,k+1}}{A}$$

$$\left[1 - \frac{(u-v)}{g_o(v)}\frac{d\,g_o}{dv}\right]\left(\frac{k+1}{k-1}\right)\left(\frac{2}{k+1}\right)^{\frac{2}{k+1}}\left[(2\eta)^{\frac{k-1}{k+1}} - (\xi+\eta)^{\frac{k-1}{k+1}}\right]\Bigg\}.$$

In the preceding and in the following relations, the terms involving Φ become indeterminate for the limiting values k = 0 and k = 1. In these special cases the actual dependence of the Φ terms upon the independent variables is logarithmic in nature and may be obtained from our equations by simple limiting procedures. By using Eq. (69) to express $\psi^{[n]}$ in terms of $f^{[n]}$ and transforming from the ξ and η coordinates to $\hat{x}$ and $\hat{r}$ coordinates, the preceding equation can be written in the form

$$f^{[1]} = f^{[0]}\Bigg\{\Bigg\{(t-k)\,(\hat{r}^{k+1}+\hat{x})^{-1}\,\hat{r}^{s}\,(\hat{r}^{k+1}+\hat{x})^{\frac{s}{k+1}-1}$$

$$\left[\frac{\Gamma\left(\frac{t+2}{s}\right)}{\Gamma\left(\frac{t+1}{s}\right)}\right]^{s}\Bigg\}\Bigg\{\frac{\beta}{k+1}\,\hat{x} + \frac{\gamma\sqrt{\bar{r}_o}\,|u-v|^{1/2}}{k+3/2}\left[(\hat{r}^{k+1}+\hat{x})^{\frac{k+3/2}{k+1}} - \hat{r}^{\,k+3/2}\right]$$

$$+ \frac{\Phi\,\bar{r}_o^{\,k-1}(u-v)}{A\,v\,2k(k-1)}\left[(\hat{r}^{k+1}+\hat{x})^{\frac{2k}{k+1}} - \hat{r}^{k-1}\left(\hat{r}^{k+1} + \frac{2k}{k+1}\,\hat{x}\right)\right]\Bigg\}$$

$$+\gamma\sqrt{\bar{r}_o}\,|u-v|^{1/2}\left[(\hat{x}^{k+1}+\hat{x})^{\frac{1}{2(k+1)}}-\hat{x}^{1/2}\right]+\frac{\bar{\phi}\,\bar{r}_o^{\,k-1}}{A(k-1)}$$

$$\left[1-\frac{(u-v)}{g_o(v)}\,\frac{d\,g_o}{dv}\right]\left[(\hat{x}^{k+1}+\hat{x})^{\frac{k-1}{k+1}}-\hat{x}^{\,k-1}\right]\Bigg\}. \qquad (85)$$

All first-order properties of the spray are determined by the distribution function $f = f^{[0]} + f^{[1]}$ where $f^{[0]}$ is given by Eq. (74a) and $f^{[1]}$ is given in Eq. (85).

It is of interest to determine the properties of the spray near $x = 0$ and the asymptotic behavior as $x \to \infty$. By transforming to the variables $\hat{y}$ and Z defined in Eqs. (78) and (79), it is found that Eq. (85) assumes the approximate form

$$f^{[1]} \approx f^{[0]}\,\frac{Z^{\frac{k+1}{s}}}{k+1}\,\hat{y}^{-\frac{k+1}{s}}\Bigg\{\beta(t-k-s\hat{y})+\gamma\sqrt{\bar{r}_o}\,|u-v|^{1/2}$$

$$\left[\frac{\Gamma(\frac{t+2}{s})}{\Gamma(\frac{t+1}{s})}\right]^{-\frac{1}{2}}\hat{y}^{\frac{1}{2s}}\,(t-k+1/2-s\hat{y})+\frac{\bar{\phi}\,\bar{r}_o^{\,k-1}}{A}$$

$$\left[\frac{\Gamma(\frac{t+2}{s})}{\Gamma(\frac{t+1}{s})}\right]^{-(k-1)}\hat{y}^{\frac{k-1}{s}}\left[1-\frac{(u-v)}{g_o(v)}\,\frac{d\,g_o}{dv}\right]\Bigg\} \qquad (85a)$$

near $Z = 0$. In the limit of large values of Z we find

$$f^{[1]} \approx -f^{[0]}\,sZ\Bigg\{\frac{\beta}{k+1}+\frac{\gamma\sqrt{\bar{r}_o}\,|u-v|^{1/2}}{k+3/2}\left[\frac{\Gamma(\frac{t+2}{s})}{\Gamma(\frac{t+1}{s})}\right]^{-1/2}Z^{\frac{1}{2s}}$$

$$- \frac{\phi \bar{r}_o^{\,k-1}}{A\,v(k^2-1)} \left(\frac{k+1}{s}\right)^{\frac{k-1}{k+1}} \left[\frac{\Gamma(\frac{t+2}{s})}{\Gamma(\frac{t+1}{s})}\right]^{-(k-1)} z^{\frac{k-1}{s} - \frac{k-1}{k+1}} \hat{y}^{\frac{k-1}{k+1}} \Bigg\}. \qquad (85b)$$

b. Average Spray Properties Near the Injector

We shall let $\Delta n = n - n^{[0]}$, $\Delta(n\bar{r}) = n\bar{r} - n^{[0]}\bar{r}^{[0]}$, and $\Delta(nV) = nV - n^{[0]}V^{[0]}$ denote, respectively, the first-order deviation of the quantities n, $n\bar{r}$, and nV from the zero-order values computed in the preceding section. In view of the definitions of n, $n\bar{r}$, and nV, it can be seen by expanding Eq. (74a) about $\hat{x} = 0$ that

$$\Delta n = \frac{n_o}{\Gamma(\frac{t+1}{s})} \int_{-\infty}^{\infty} g_o(v) \int_0^{\infty} \exp(-\hat{y})\, \hat{y}^{\frac{t+1}{s}-1} \frac{f^{[1]}}{f^{[0]}}\, d\hat{y}\, dv,$$

$$\Delta(n\bar{r}) = \frac{n_o \bar{r}_o}{\Gamma(\frac{t+2}{s})} \int_{-\infty}^{\infty} g_o(v) \int_0^{\infty} \exp(-\hat{y})\, \hat{y}^{\frac{t+2}{s}-1} \frac{f^{[1]}}{f^{[0]}}\, d\hat{y}\, dv,$$

and

$$\Delta(nV) = \frac{n_o V_o}{\Gamma(\frac{t+4}{s})} \int_{-\infty}^{\infty} g_o(v) \int_0^{\infty} \exp(-\hat{y})\, \hat{y}^{\frac{t+4}{s}-1} \frac{f^{[1]}}{f^{[0]}}\, d\hat{y}\, dv$$

near $\hat{x} = 0$. By substituting Eq. (85a) into these relations and integrating, we find

$$\Delta n = n_o \frac{\phi \bar{r}_o^{\,k-1}}{A(k+1)} \left[\frac{\Gamma(\frac{t+2}{s})}{\Gamma(\frac{t+1}{s})}\right]^2 \left[\frac{\Gamma(\frac{t-1}{s})}{\Gamma(\frac{t+1}{s})}\right] \int_{-\infty}^{\infty} \hat{x} \left[g_o(v) - (u-v) \frac{d\, g_o}{dv}\right] dv, \qquad (86a)$$

$$\Delta(n\bar{r}) = -\frac{n_o \bar{r}_o}{k+1} \int_{-\infty}^{\infty} \hat{x}\, g_o(v) \left\{ \beta \left[\frac{\Gamma(\frac{t+2}{s})}{\Gamma(\frac{t+1}{s})} \right]^{k+1} \left[\frac{\Gamma(\frac{t+1-k}{s})}{\Gamma(\frac{t+2}{s})} \right] \right.$$

$$+ \gamma \sqrt{\bar{r}_o}\, |u-v|^{1/2} \left[\frac{\Gamma(\frac{t+2}{s})}{\Gamma(\frac{t+1}{s})} \right]^{k+1/2} \left[\frac{\Gamma(\frac{t+3/2-k}{s})}{\Gamma(\frac{t+2}{s})} \right] - \frac{\Phi \bar{r}_o^{\,k-1}}{A}$$

$$\left. \left[\frac{\Gamma(\frac{t+2}{s})}{\Gamma(\frac{t+1}{s})} \right]^2 \left[\frac{\Gamma(\frac{t}{s})}{\Gamma(\frac{t+2}{s})} \right] \left[1 - \frac{(u-v)}{g_o(v)} \frac{d\, g_o}{dv} \right] \right\} dv, \qquad (87a)$$

and

$$\Delta(n\bar{V}) = -\frac{n_o V_o}{k+1} \int_{-\infty}^{\infty} \hat{x}\, g_o(v) \left\{ 3\beta \left[\frac{\Gamma(\frac{t+2}{s})}{\Gamma(\frac{t+1}{s})} \right]^{k+1} \left[\frac{\Gamma(\frac{t+3-k}{s})}{\Gamma(\frac{t+4}{s})} \right] \right.$$

$$+ 3\gamma \sqrt{\bar{r}_o}\, |u-v|^{1/2} \left[\frac{\Gamma(\frac{t+2}{s})}{\Gamma(\frac{t+1}{s})} \right]^{k+1/2} \left[\frac{\Gamma(\frac{t+7/2-k}{s})}{\Gamma(\frac{t+4}{s})} \right] - \frac{\Phi \bar{r}_o^{\,k-1}}{A}$$

$$\left. \left[\frac{\Gamma(\frac{t+2}{s})}{\Gamma(\frac{t+1}{s})} \right]^2 \left[\frac{\Gamma(\frac{t+2}{s})}{\Gamma(\frac{t+4}{s})} \right] \left[1 - \frac{(u-v)}{g_o(v)} \frac{d\, g_o}{dv} \right] \right\} dv, \qquad (88a)$$

where Z has been replaced by $\hat{x}$ according to Eq. (79) after the integration.

When $g_o(v) \approx \delta(v - v_o)$ the integration over v in Eqs. (86a) through (88a) can easily be performed by use of the identity

$$\int_{-\infty}^{\infty} \varphi(v) \left[\delta(v - v_o) - (u - v) \frac{d\, \delta(v - v_o)}{dv} \right] dv = (u - v_o) \frac{d\varphi}{dv}\bigg|_{v=v_o}$$

for any function $\varphi(v)$. The resulting equations show that near the

injector the effect of the term involving ϕ (the aerodynamic force term) is to decrease n, $n\bar{r}$, and nV at a given value of x when $u < v$ and to increase the quantities when $u > v$. This result may be ascribed to the fact that when $u < v$ the retarding force of the fluid tends to slow down the droplets and thereby allows more time for evaporation in a given distance x. On the other hand, the force increases the velocity of the droplets when $u > v$. For a given value of $\bar{r}_o$ the effect of the aerodynamic forces upon n/n_o and $n\bar{r}/n_o \bar{r}_o$ is slightly larger for small values of the spray parameters t and s, while the effect upon $nV/n_o V_o$ is largest for large values of t and s. Since the acceleration of a droplet is inversely proportional to the square of its radius, it is not surprising to find that the term in ϕ increases linearly with $1/\bar{r}_o^2$.

It can be seen from Eqs. (87a) and (88a) that the terms in β and γ, which correspond to the increase in the evaporation rate caused by droplet interactions and fluid motion, respectively, both produce a decrease in $n\bar{r}/n_o \bar{r}_o$ and $nV/n_o V_o$ near $x = 0$. The effect of the parameters s and t upon this decrease is the same as described in the preceding paragraph. Equation (86a) shows that β and γ cause no linear dependence of Δn upon x; higher-order terms must be included in Eq. (85a) in order to determine the dependence of n upon β and γ. After describing the asymptotic behavior of f[1] for large values of x, we shall give an explicit first-order perturbation solution for n which is valid for all values of x when $\bar{f} = 0$. This will determine a fortiori the dependence of n upon β and γ at small values of x.

c. Asymptotic Spray Properties

By transforming to the independent variables Z and $\hat{y}$, an expansion of Eq. (74a) valid for large values of Z can be obtained. If this expansion is substituted into the definitions of n, $n\bar{r}$, and nV, then the relations

$$\Delta n = \frac{n_o}{\Gamma(\frac{t+1}{s})} \int_{-\infty}^{\infty} \varepsilon_o(v)\, Z^{\frac{t+1}{s}-1} \exp(-Z) \int_0^{\infty} \exp(-\hat{y})\, \frac{f^{[1]}}{f^{[0]}}\, d\hat{y}\, dv,$$

$$\Delta(n\bar{r}) = \frac{n_o \bar{r}_o}{\Gamma(\frac{t+2}{s})} \left(\frac{k+1}{s}\right)^{\frac{1}{k+1}} \int_{-\infty}^{\infty} \varepsilon_o(v)\, Z^{\frac{t+2}{s}-\frac{k+2}{k+1}} \exp(-Z)$$
$$\int_0^{\infty} \exp(-\hat{y})\, \hat{y}^{\frac{1}{k+1}}\, \frac{f^{[1]}}{f^{[0]}}\, d\hat{y}\, dv,$$

and

$$\Delta(nV) = \frac{n_o V_o}{\Gamma(\frac{t+4}{s})} \left(\frac{k+1}{s}\right)^{\frac{3}{k+1}} \int_{-\infty}^{\infty} \varepsilon_o(v)\, Z^{\frac{t+4}{s}-\frac{k+4}{k+1}} \exp(-Z)$$
$$\int_0^{\infty} \exp(-\hat{y})\, \hat{y}^{\frac{3}{k+1}}\, \frac{f^{[1]}}{f^{[0]}}\, d\hat{y}\, dv$$

are obtained. By substituting Eq. (85b) into these expressions and integrating, we find, for cases in which $\varepsilon_o(v) \approx \delta(v - v_o)$, that

$$\frac{\Delta n}{n^{[0]}} = -s \left[\frac{\Gamma(\frac{t+2}{s})}{\Gamma(\frac{t+1}{s})}\right]^s \hat{f}^{\frac{s}{k+1}} \left[\frac{\beta}{k+1} + \frac{\gamma\sqrt{\bar{r}_o}\,|u-v|^{1/2}}{k+3/2}\, \hat{x}^{\frac{1}{2(k+1)}}\right]$$
$$-\left(\frac{1}{1-k}\right)\left(\frac{s}{k+1}\right)^{\frac{2}{k+1}} \left[\frac{\Gamma(\frac{t+2}{s})}{\Gamma(\frac{t+1}{s})}\right]^{\frac{2s}{k+1}} \Gamma\left(\frac{2k}{k+1}\right) \frac{\phi\, \bar{r}_o^{\,k-1}(u-v)}{A\, v}$$
$$\hat{x}^{\frac{k-1}{k+1}+\frac{2s}{(k+1)^2}}, \qquad (86b)$$

$$\frac{\Delta(n\,\overline{r})}{n^{[0]}\overline{r}^{[0]}} \sim -s\left[\frac{\Gamma\left(\frac{t+2}{s}\right)}{\Gamma\left(\frac{t+1}{s}\right)}\right]^{s} \hat{x}^{\frac{s}{k+1}}\left[\frac{\beta}{k+1}+\frac{\gamma\sqrt{\overline{r}_o}\,|u-v|}{k+3/2}\,\hat{x}^{\frac{1}{2(k+1)}}\right]$$

$$-\left(\frac{1}{1-k}\right)\left(\frac{s}{k+1}\right)^{\frac{2}{k+1}}\left[\frac{\Gamma\left(\frac{t+2}{s}\right)}{\Gamma\left(\frac{t+1}{s}\right)}\right]^{\frac{2s}{k+1}}\left[\frac{\Gamma\left(\frac{2k+1}{k+1}\right)}{\Gamma\left(\frac{k+2}{k+1}\right)}\right]\frac{\Phi\,\overline{r}_o^{\,k-1}\,(u-v)}{A\,v}$$

$$\hat{x}^{\frac{k-1}{k+1}+\frac{2s}{(k+1)^2}}, \qquad (87b)$$

and

$$\frac{\Delta(n\,V)}{n^{[0]}V^{[0]}} \sim -s\left[\frac{\Gamma\left(\frac{t+2}{s}\right)}{\Gamma\left(\frac{t+1}{s}\right)}\right]^{s} \hat{x}^{\frac{s}{k+1}}\left[\frac{\beta}{k+1}+\frac{\gamma\sqrt{\overline{r}_o}\,|u-v|}{k+3/2}\,\hat{x}^{\frac{1}{2(k+1)}}\right]$$

$$-\left(\frac{1}{1-k}\right)\left(\frac{s}{k+1}\right)^{\frac{2}{k+1}}\left[\frac{\Gamma\left(\frac{t+2}{s}\right)}{\Gamma\left(\frac{t+1}{s}\right)}\right]^{\frac{2s}{k+1}}\left[\frac{\Gamma\left(\frac{2k+1}{k+1}\right)}{\Gamma\left(\frac{k+4}{k+1}\right)}\right]\frac{\Phi\,\overline{r}_o^{\,k-1}\,(u-v)}{A\,v}$$

$$\hat{x}^{\frac{k-1}{k+1}+\frac{2s}{(k+1)^2}} \qquad (88b)$$

where the appropriate asymptotic values of $n^{[0]}$, $n^{[0]}\overline{r}^{[0]}$, and $n^{[0]}V^{[0]}$ are given in Eqs. (80c) through (82c). Equations (86b) through (88b) give the first-order perturbation corrections to $n^{[0]}$, $n^{[0]}\overline{r}^{[0]}$, and $n^{[0]}V^{[0]}$ at large distances from the injector.

It is seen from Eqs. (86b) through (88b) that, contrary to the behavior near the injector, the fractional changes in n, $n\,\overline{r}$, and n V are proportional to $\hat{x}$ raised to a power which is greater than

unity for the most common initial spray distributions. The signs of Δn, $\Delta(n\,\bar{r})$ and $\Delta(n\,V)$, and the dependence upon $\bar{r}_o$, v, A, β, γ, Φ and u are, of course, the same as near x = 0. It is seen that the magnitude of the asymptotic perturbation quantities Δn, $\Delta(n\,\bar{r})$, and $\Delta(n\,V)$ depends weakly upon t but strongly upon the spray parameter s which appears as an exponent. Here large values of s and t (small dispersion) lead to large perturbation corrections, a result which was found to hold only for $\Delta(n\,V)$ near the injector.

Since the fractional perturbation corrections increase with $\hat{x}$, it is clear that for constant values of β, γ, and Φ there will be a maximum distance beyond which the perturbation corrections become larger than the zero-order values and the perturbation procedure breaks down. Nevertheless, when β, γ, and Φ are sufficiently small, Eqs. (86b) through (88b) will be valid for a wide intermediate range of values of $\hat{x}$ which will include most values of practical interest. It may be noted that $\Delta n/n^{[0]}$, $\Delta(n\,\bar{r})/n^{[0]}\bar{r}^{[0]}$, and $\Delta(n\,V)/n^{[0]}V^{[0]}$ are nearly the same asymptotically. The fractional change in any average spray property resulting from the first perturbation can therefore be estimated from Eq. (86b).

d. The Average Droplet Number Density in the Absence of Aerodynamic Forces

If the aerodynamic forces are neglected, then an explicit first-order perturbation expression for n which is valid for all values of x can be obtained. By expressing Eq. (74a) in terms of

the independent variables Z and $\hat{z} = \hat{y} + Z$, we find from the definitions of n and Δn that

$$\Delta n = \frac{n_o}{\Gamma(\frac{t+1}{s})} \int_Z^\infty \exp(-\hat{z})\, \hat{z}^{\frac{t+1}{s}-1}\, \frac{f^{[1]}}{f^{[0]}}\, d\hat{z}\,, \quad (89)$$

where $f^{[1]}$ is given by Eq. (85) with $\Phi = 0$ and it has been assumed that $g_o(v) \approx \delta(v - v_o)$. By transforming variables to Z and $\hat{z}$ in Eq. (85), it is found that when $\Phi = 0$

$$\frac{f^{[1]}}{f^{[0]}} = \frac{\beta}{k+1} \left(\frac{Z}{\hat{z}}\right)^{\frac{k+1}{s}} (t - k - s\hat{z}) + \gamma\sqrt{r_o}\, |u - v|^{1/2} \left[\frac{\Gamma(\frac{t+2}{s})}{\Gamma(\frac{t+1}{s})}\right]^{-1/2}$$

$$\left\{ \frac{\hat{z}^{-\frac{k+1}{s}}}{k+3/2} (t - k - s\hat{z}) \left[\hat{z}^{\frac{k+3/2}{s}} - \left(\hat{z}^{\frac{k+1}{s}} - Z^{\frac{k+1}{s}}\right) \frac{k+3/2}{k+1} \right] \right.$$

$$\left. + \hat{z}^{\frac{1}{2s}} - \left(\hat{z}^{\frac{k+1}{s}} - Z^{\frac{k+1}{s}}\right) \frac{1}{2(k+1)} \right\} . \quad (90)$$

When Eq. (90) is substituted into Eq. (89), a term involving γ may be integrated by parts; furthermore, we use the identity

$$(\tfrac{t-k}{s})\, \Gamma(\tfrac{t-k}{s}, \hat{z}) - \Gamma(\tfrac{t-k}{s} + 1, \hat{z}) = \hat{z}^{\frac{t-k}{s}} \exp(-\hat{z})$$

in order to show that the relation

$$\frac{\Delta n}{n_o} = -\beta \left(\frac{s}{k+1}\right) \left[\Gamma(\tfrac{t+1}{s})\right]^{-1} Z^{\frac{t+1}{s}} \exp(-Z) - \gamma\sqrt{r_o}\, |u - v|^{1/2}$$

$$\left(\frac{s}{k+3/2}\right) \left[\Gamma(\tfrac{t+1}{s})\right]^{-1/2} \left[\Gamma(\tfrac{t+2}{s})\right]^{-1/2} Z^{\frac{t+3/2}{s}} \exp(-Z) \quad (91)$$

is obtained. By combining this equation with Eq. (80a), the complete first-order expression for the number density of droplets is found to be

$$\frac{n}{n_o} = 1 - \frac{\Gamma(\frac{t+1}{s}, Z)}{\Gamma(\frac{t+1}{s})} - \beta\left(\frac{s}{k+1}\right)\frac{Z^{\frac{t+1}{s}}\exp(-Z)}{\Gamma(\frac{t+1}{s})} - \gamma\sqrt{\bar{r}_o}\left|u-v\right|^{1/2}$$

$$\left(\frac{s}{k+3/2}\right)\frac{Z^{\frac{t+3/2}{s}}\exp(-Z)}{\left[\Gamma(\frac{t+1}{s})\,\Gamma(\frac{t+2}{s})\right]^{1/2}} \quad . \tag{92}$$

Equation (91) can be used to determine the dependence of Δn upon β and γ near the injector. Since $\exp(-Z) \approx 1$ near $x = 0$, we find

$$\Delta n = -n_o\, s\,\frac{\left[\Gamma(\frac{t+2}{s})\right]^{t+1}}{\left[\Gamma(\frac{t+1}{s})\right]^{t+2}}\,\hat{x}^{\frac{t+1}{k+1}}\left[\frac{\beta}{k+1} + \frac{\gamma\sqrt{\bar{r}_o}\left|u-v\right|^{1/2}}{k+3/2}\,\hat{x}^{\frac{1}{2(k+1)}}\right]. \tag{93}$$

Hence Δn is relatively strongly dependent upon the spray parameter t. The magnitude of the number-density correction increases with decreasing s and t near the injector.

5. Concluding Remarks

The analysis presented in this section should provide a basis for further work on the effects of droplet interactions and relative motion of droplets and fluid upon the statistical properties of burning sprays.

Application of our analysis to concrete problems must await the development of further experimental information relating to the following phenomena: (a) The interaction mechanism of two colliding droplets, including the number, size, and velocity of the collision products; (b) The properties of the primary sprays formed from the break-up of liquid jets or sheets; (c) The motion and properties of the fluid near the position where sprays are initially formed in practical atomization arrangements; (d) The effects of convection and droplet interaction upon the droplet burning rate; (e) The effect of the droplet evaporation upon drag; (f) The validity of the quasi-steady-state hypothesis for single droplets.

APPENDIX A
SUMMARY OF ASSUMPTIONS

A list of all the assumptions that have been made in the analysis in Chapter I is given below. The assumptions marked (*) are those that define the problem. Those marked (**) were made for convenience or for definiteness and are not essential to the applicability of the method. The unmarked assumptions are necessary idealizations without which the procedure would be greatly complicated.

Assumptions in Part I B

* (1) The system has spherical symmetry.

* (2) There are three species present, fuel, oxidizer, and product.

* (3) Steady-state conditions hold.

** (4) The system is either stoichiometric or oxidizer rich.

* (5) Pressure is constant.

* (6) The chemical reaction is second order.

(7) Suitable mean values (averaged over all species but not over temperature) of heat capacity and thermal conductivity can be determined.

** (8) The mean specific heat is constant, independent of temperature, and the thermal conductivity is proportional to temperature.

(9) Thermal diffusion is negligible.

(10) The molecular weights of all three components are equal.

(11) The binary diffusion coefficients of all three pairs of species are equal.

** (12) The diffusion coefficient is proportional to the square of the temperature.

** (13) The frequency factor for the chemical reaction rate is independent of temperature.

* (14) The perfect gas equation of state holds.

* (15) There is no liquid phase reaction.

(16) The effective Lewis number is unity. (This is essential to the analysis presented but not to some of the results, see Section B15.)

* (17) There is no heat conduction to or from the system at infinite distance from the droplet.

* (18) The mixture is uniform at infinite distance from the droplet.

Assumptions in Part I C

The same assumptions that were made in Part I B are also made in Part I C with the following changes:

(a) Assumption (2) is changed to read

* (2) There are two species present, fuel and product.

(b) Assumptions (4), (10), (11), and (16) are omitted.

APPENDIX B

REDUCTION OF THE GENERAL MOMENTUM EQUATION TO THE FORM APPLICABLE TO THE DROPLET BURNING PROBLEM

The general equation for conservation of momentum in an arbitrary non-orthogonal coordinate system can be written in the tensor form

$$F_i - P^j_{i;j} = \rho v^j v_{i;j} + \rho \frac{\partial v_i}{\partial t} \tag{B-1}$$

where ρ is density, v_i signifies velocity, F_i is the body force vector and P_{ij} represents the stress tensor. Subscripts refer to covariant components and superscripts identify contravariant components of the tensors. The summation convention, summing over repeated indices, is used here.

The semicolon represents covariant differentiation with respect to the coordinates whose indices follow it. The covariant derivative of a tensor $A_{ij}^{\ k}$, for example, is given by

$$A_{ij}^{\ k}{}_{;\ell} = \frac{\partial}{\partial x^\ell}(A_{ij}^{\ k}) - A_{rj}^{\ k}\left\{ {r \atop i\ \ell} \right\} - A_{ir}^{\ k}\left\{ {r \atop j\ \ell} \right\} + A_{ij}^{\ r}\left\{ {k \atop r\ \ell} \right\} \tag{B-2}$$

where the Christoffel symbol of the second kind is defined by the relation

$$\left\{ {k \atop i\ j} \right\} = (1/2)g^{k\ell}\left(\frac{\partial g_{i\ell}}{\partial x^j} + \frac{\partial g_{j\ell}}{\partial x^i} - \frac{\partial g_{ij}}{\partial x^\ell} \right). \tag{B-3}$$

Here g_{ij} is the metric tensor which defines the coordinate system by means of the expression for the invariant infinitesimal distance

$$ds^2 = g_{ij}\, dx^i\, dx^j . \tag{B-4}$$

In an orthogonal curvilinear coordinate system the metric tensor is diagonal and, by use of Eq. (B-3), Eq. (B-1) can be written explicitly in terms of the diagonal components of the metric tensor. If the equation

$$g_{ij} = \begin{bmatrix} (h_1)^2 & 0 & 0 \\ 0 & (h_2)^2 & 0 \\ 0 & 0 & (h_3)^2 \end{bmatrix} \qquad \text{(B-5)}$$

is valid then it is convenient to redefine vectors and tensors in such a way that all of their components are of the same physical dimensions. This can be accomplished in general by dividing each covariant component i of the tensor by h_i and multiplying each contravariant component i by h_i. The new velocity vector u, external force vector f, and stress tensor p are thus defined by the equations

$$\left.\begin{aligned} v_i &= h_i u_i \quad \left(v^i = \frac{1}{h_i}\, u_i\right) \\ F_i &= h_i f_i \\ P_i^{\,j} &= \frac{h_i}{h_j}\, P_{ij} \end{aligned}\right\} \qquad \text{(B-6)}$$

The summation convention does not apply here nor in what follows because of the change in notation.

The new notation is equivalent to replacing g_{ij} by the unit tensor in product operations; e.g.,

$$v^i v_i = v_j g^{ij} v_i = \sum_i u_i^{\,2} .$$

This enables us to use ordinary vector notation. The distinction between covariance and contravariance disappears in the new notation and we shall use subscripts for all indices.

Equation (B-1) now becomes

$$h_i f_i - \sum_j \frac{\partial}{\partial x_j}\left(\frac{h_i}{h_j} p_{ij}\right) + \sum_{j,k} \frac{h_k}{h_j} p_{kj} \frac{1}{2} \frac{1}{h_k^2}\left[\delta_{ik} \frac{\partial(h_i^2)}{\partial x_j} + \delta_{jk} \frac{\partial(h_j^2)}{\partial x_i}\right.$$

$$\left. - \delta_{ij} \frac{\partial(h_i^2)}{\partial x_k}\right] - \sum_{j,k} \frac{h_i}{h_k} p_{ik} \frac{1}{2} \frac{1}{h_j^2} \frac{\partial(h_j^2)}{\partial x_k} = \sum_j \rho u_j \frac{1}{h_j} \frac{\partial(h_i u_i)}{\partial x_j}$$

$$- \sum_{j,k} \rho u_j u_k \frac{h_k}{h_j} \frac{1}{2} \frac{1}{h_k^2}\left[\delta_{ik} \frac{\partial(h_i^2)}{\partial x_j} + \delta_{jk} \frac{\partial(h_j^2)}{\partial x_i} - \delta_{ij} \frac{\partial(h_i^2)}{\partial x_k}\right] + \rho \frac{\partial(h_i u_i)}{\partial t} \tag{B-7}$$

where δ_{ij} is the Kronecker delta. Since the pressure tensor, p_{ij}, is always symmetric,* Eq. (B-7) reduces to the relation

$$h_i f_i - \sum_j \frac{h_i}{h_j} \frac{\partial p_{ij}}{\partial x_j} - \sum_j p_{ij} \frac{1}{h_j}\left(\frac{\partial h_i}{\partial x_j} - \frac{h_i}{h_j} \frac{\partial h_j}{\partial x_j}\right) + \sum_j p_{ij} \frac{1}{h_j} \frac{\partial h_j}{\partial x_i}$$

$$- \sum_{j,k} p_{ij} \frac{h_i}{h_j h_k} \frac{\partial h_k}{\partial x_j} = \sum_j \rho u_j\left[\frac{h_i}{h_j} \frac{\partial u_i}{\partial x_j} + \frac{1}{h_j}\left(u_i \frac{\partial h_i}{\partial x_j} - u_j \frac{\partial h_j}{\partial x_i}\right)\right] + \rho \frac{\partial(h_i u_i)}{\partial t} \tag{B-8}$$

which is a general form applicable to orthogonal curvilinear coordinate systems.

---

* The symmetry of the stress tensor is a consequence of microscopic conservation of angular momentum.

The explicit form of the momentum equation in spherical coordinates can be obtained either by direct substitution for h_i and x_i into Eq. (B-8) or by substituting the expressions for g_{ij} and x^i into Eqs. (B-3) and (B-1). It is well known that in spherical coordinates the expressions

$$x^1 = r,\ x^2 = \theta,\ x^3 = \varphi$$
$$h_1 = 1,\ h_2 = r,\ h_3 = r\sin\theta \qquad \text{(B-9)}$$

are valid. We are interested in a steady-state system with no external forces and no dependence of flow quantities upon the θ and φ coordinates. The resulting momentum equation is then

$$\left.\begin{aligned} &-\frac{dp_{rr}}{dr} - \frac{2}{r}p_{rr} + \frac{1}{r}(p_{\theta\theta} + p_{\varphi\varphi}) - \frac{1}{r\tan\theta}p_{r\theta} = \rho v\frac{dv}{dr} \\ &-\frac{dp_{r\theta}}{dr} - \frac{3}{r}p_{r\theta} + \frac{1}{r\tan\theta}(p_{\varphi\varphi} - p_{\theta\theta}) = 0 \\ &-\frac{dp_{r\varphi}}{dr} - \frac{3}{r}p_{r\varphi} - \frac{2}{r\tan\theta}p_{\theta\varphi} = 0\ . \end{aligned}\right\} \qquad \text{(B-10)}$$

The stress tensor is given in terms of the hydrostatic pressure, p, and the shear stress tensor, τ_{ij}, according to the relation

$$p_{ij} = p\delta_{ij} + \tau_{ij}.^{*} \qquad \text{(B-11)}$$

If viscous effects are negligibly small ($\tau_{ij}=0$), then Eq. (B-10) reduces to the single relation

$$-\frac{dp}{dr} = \rho v\frac{dv}{dr} \qquad \text{(B-12)}$$

---

* The shear stress tensor τ_{ij} may not have zero trace if relaxation effects cause the bulk viscosity coefficient to be non-zero.

which is the equation used in Section B-3 of Chapter I.

It is needless to say that general expressions of the type of Eq. (B-1) also exist for the continuity and energy equations. A similar reduction can be carried out in these cases. The general equations and method of reduction should be obvious from the analysis presented here.

APPENDIX C

DERIVATION OF THE DIFFUSION EQUATION FROM ELEMENTARY CONSIDERATIONS

If n_j is the number of moles of species j per unit volume, then the ideal gas law can be written in the form

$$p_j = n_j RT \tag{C-1}$$

where p_j is the partial pressure of species j in the mixture and all other quantities are defined in Chapter I. Since the total number of moles per unit volume is defined by the relation

$$n = \sum_j n_j \tag{C-2}$$

and the total pressure of the mixture is given by

$$p = \sum_j p_j, \tag{C-3}$$

the well-known ideal gas law

$$p = nRT \tag{C-4}$$

is obtained by summing Eq. (C-1) over all chemical species j.

By virtue of Eq. (C-1) concentration gradients can be interpreted as partial pressure gradients. The mole fraction of species j, X_j, is found from Eqs. (C-1) and (C-4) to obey the relation

$$X_j \equiv \frac{n_j}{n} = \frac{p_j}{p}. \tag{C-5}$$

For constant pressure processes differentiating Eq. (C-5) yields the equation

$$\nabla X_j = \nabla\left(\frac{p_j}{p}\right) = \frac{1}{p}\nabla p_j, \tag{C-6}$$

which implies that a change in mole fraction is equivalent to a change in

partial pressure.*

By elementary kinetic theory considerations** the relation

$$p_j = n_j m_j \frac{1}{3} \overline{c^2}_j$$

is obtained where m_j is the mass of molecules of species j, c_j is the velocity of a molecule of species j, and the bar signifies an average. This equation states that the partial pressure of species j is the rate of change of momentum of species j per unit area. Therefore ∇p_j is the rate of change of momentum of molecules of species j per unit volume.

A net change in momentum of molecules of a given type i can occur only through collisions with molecules of other species $j \neq i$. The average change in momentum in a collision is expected to be proportional to the reduced mass, μ_{ij}, times the average difference in velocities which is $(\vec{V}_j - \vec{V}_i)$ where $\vec{V}$ is the diffusion velocity. The average rate of change of momentum of species i due to collisions with molecules of type j is proportional to the average momentum change in a collision divided by the mean time between collisions of molecules of types i and j, t_{ij}. Hence the total rate of change of momentum of molecules of species i is given by the equation

$$\nabla p_i \simeq \sum_{j \neq i} k_{1_{ij}} \frac{\mu_{ij}}{t_{ij}} (\vec{V}_j - \vec{V}_i) = \sum_{\text{all } j} k_{1_{ij}} \frac{\mu_{ij}}{t_{ij}} (\vec{V}_j - \vec{V}_i) \qquad (C\text{-}7)$$

---

* This point of view is emphasized by Furry, reference 9.

** See, for example, Section 145 of reference 10.

where the constant factors $k_{1_{ij}}$ allow for the possibility of the averaging process resulting in different proportionality constants for different species (because of geometrical factors, etc.).

An elementary result of kinetic theory* is the obvious fact that the average time between collisions of molecules of types i and j is inversely proportional to the product of the number concentrations of molecules of the two species; i.e.,

$$t_{ij} = \frac{k_{2_{ij}}}{n_i n_j} = \frac{k_{2_{ij}}}{n^2} \frac{1}{X_i X_j} .$$

The constants $k_{2_{ij}}$ can depend only on molecular properties (cross sections, etc.) and temperature; they are independent of mole fractions. The use of this relation in Eq. (C-7) yields the expression

$$\frac{1}{p} \nabla p_i = \sum_j \frac{n^2 \mu_{ij} k_{1_{ij}}}{p k_{2_{ij}}} X_i X_j (\vec{V}_j - \vec{V}_i) = \sum_j k_{3_{ij}} X_i X_j (\vec{V}_j - \vec{V}_i). \qquad (C\text{-}8)$$

The factors $k_{3_{ij}}$ depend only upon pressure, temperature, and molecular properties; they are independent of concentrations and diffusion velocities. By substituting from Eq. (C-6) we obtain

$$\nabla X_i = \sum_j k_{3_{ij}} X_i X_j (\vec{V}_j - \vec{V}_i). \qquad (C\text{-}9)$$

Since the quantities $k_{3_{ij}}$ are independent of mole fractions we can determine them by considering the limiting case in which all except two

---

* See, for example, Section 33 of reference 10.

chemical species have zero concentrations. For species 1 and 2 in this limiting case Eq. (C-9) reduces to the relation

$$\nabla X_1 = k_{3_{12}} X_1 X_2 (\vec{V}_2 - \vec{V}_1). \tag{C-10}$$

Equation (I-20) of Chapter I gives the relation between the weight fractions, Y_j, and the mole fractions. When only two species are present Eq. (I-20) reduces to

$$Y_i = \frac{M_i X_i}{M_i X_i + M_j X_j} \tag{C-11}$$

which can be differentiated with i=1 and j=2 in order to obtain the expression

$$\nabla Y_1 = \frac{M_1 M_2 X_2 \nabla X_1 - M_1 M_2 X_1 \nabla X_2}{(M_1 X_1 + M_2 X_2)^2} .$$

In view of the binary mixture relation

$$X_2 = 1 - X_1,$$

the above expression becomes

$$\nabla Y_1 = \frac{M_1 M_2 \nabla X_1}{(X_1 M_1 + X_2 M_2)^2} . \tag{C-12}$$

By substituting this equation into Eq. (C-10) we find

$$\nabla Y_1 = k_{3_{12}} \frac{M_1 M_2 X_1 X_2}{(X_1 M_1 + X_2 M_2)^2} (\vec{V}_2 - \vec{V}_1)$$

which by virtue of Eq. (C-11) reduces to the relation

$$\nabla Y_1 = k_{3_{12}} Y_1 Y_2 (\vec{V}_2 - \vec{V}_1). \tag{C-13}$$

By using Eq. (I-5) and the equation immediately preceding it in Section B-2 of Chapter I we find that

$$\vec{V}_2 - \vec{V}_1 = -\frac{Y_1}{Y_2}\vec{V}_1 - \vec{V}_1 = -\frac{1}{Y_2}(Y_1\vec{V}_1 + Y_2\vec{V}_1) = -\frac{\vec{V}_1}{Y_2}$$

which upon substitution into Eq. (C-13) gives the expression

$$\nabla Y_1 = -k_{3_{12}} Y_1 \vec{V}_1. \tag{C-14}$$

The well-known form of Fick's law for a binary mixture is

$$D_{12}\nabla Y_1 = -Y_1\vec{V}_1. \tag{C-15}$$

Equation (C-15) can be taken to be the definition of the binary diffusion coefficient D_{12}. By comparing Eqs. (C-14) and (C-15) it becomes apparent that

$$k_{3_{12}} = \frac{1}{D_{12}}.$$

We have thus determined the factor $k_{3_{12}}$ from the limiting case of a binary mixture. It is clear that applying the same analysis to other species yields the result

$$k_{3_{ij}} = \frac{1}{D_{ij}}. \tag{C-16}$$

By substituting Eq. (C-16) into Eq. (C-9) we obtain the relation

$$\nabla X_i = \sum_j \frac{X_i X_j}{D_{ij}}(\vec{V}_j - \vec{V}_i) \tag{C-17}$$

which is the desired diffusion equation. It can be shown from the exact theory that Eq. (C-17) is valid to first order in a Sonine polynomial expansion.*

It is clear that with only a slight refinement this analysis will

---

* See Section 7.4 e.1. of reference 7.

provide explicit expressions for the binary diffusion coefficients D_{ij}. The resulting expressions are independent of concentration and agree closely with those obtained by exact methods. The usual point of view taken in treating diffusion by elementary kinetic theory does not give Eq. (C-17) and leads to relations for the coefficients D_{ij} which depend upon concentration. For these reasons the viewpoint presented here, embodied in Eq. (C-6), appears to be vastly superior.[9]

APPENDIX D

THE APPROXIMATION OF $f(\varepsilon_p)$ OF CHAPTER I

1. Non-Stoichiometric Mixtures

In order to approximate the function $f(\varepsilon_p)$ for the non-stoichiometric case we find from Eq. (I-38) of Chapter I that $\sigma=1$ and $f(\varepsilon_p) = \alpha/(1-\theta_\ell)$ at the end point $\varepsilon_p=0$. By differentiating Eq. (I-38) we obtain the relation

$$\frac{df}{d\varepsilon_p} = \frac{-4}{\sigma^5}\left[-1+\left(\frac{\varepsilon_{p,f}-\varepsilon_p}{1-\theta}\right)\left(\frac{1-\theta_\ell+\alpha}{\varepsilon_{p,f}}\right)\right]\frac{d\sigma}{d\theta}\frac{d\theta}{d\varepsilon_p}$$

$$+\frac{1}{\sigma^4}\left(\frac{1-\theta_\ell+\alpha}{\varepsilon_{p,f}}\right)\frac{d}{d\theta}\left(\frac{\varepsilon_{p,f}-\varepsilon_p}{1-\theta}\right)\frac{d\theta}{d\varepsilon_p} \qquad \text{(D-1)}$$

which may be written in the form

$$\frac{df}{d\varepsilon_p} = \frac{-4}{\sigma^5}\left[-1+\left(\frac{\varepsilon_{p,f}-\varepsilon_p}{1-\theta}\right)\left(\frac{1-\theta_\ell+\alpha}{\varepsilon_{p,f}}\right)\right]\frac{d\sigma}{d\theta}\frac{d\theta}{d\varepsilon_p}$$

$$+\frac{1}{\sigma^4}\left(\frac{1-\theta_\ell+\alpha}{\varepsilon_{p,f}}\right)\left[\frac{\varepsilon_{p,f}-\varepsilon_p}{(1-\theta)^2}\frac{d\theta}{d\varepsilon_p}-\frac{1}{1-\theta}\right]. \qquad \text{(D-1a)}$$

It is most convenient to use Eq. (D-1a) in order to find the quantity $df/d\varepsilon_p\big|_{\varepsilon_p=0}$. Equations (I-35) and (I-36) yield the relations

$$\left.\frac{d\theta}{d\varepsilon_p}\right|_{\varepsilon_p=0} = \left[\Lambda^*\frac{1}{\alpha\theta_\ell}\exp(-\theta_a/\theta_\ell)\frac{(1/2)\varepsilon_{p,f}(1-\theta_\ell)}{1-\theta_\ell+\alpha}\left(1-\varepsilon_{p,f}+\frac{(1/2)\varepsilon_{p,f}(1-\theta_\ell)}{1-\theta_\ell+\alpha}\right)\right]^{-1} \qquad \text{(D-2)}$$

and

$$\left.\frac{d\sigma}{d\theta}\right|_{\varepsilon_p=0} = \frac{\theta_\ell}{\alpha}\sqrt{\frac{\Lambda^*}{V^*}}. \qquad \text{(D-3)}$$

By substituting these results into Eq. (D-1a) we obtain the expression

$$\left.\frac{df}{d\varepsilon_p}\right|_{\varepsilon_p=0} = \frac{1}{\Lambda^*}\alpha\theta_\ell \exp(\theta_a/\theta_\ell)\frac{(1-\theta_\ell+\alpha)^2}{(1/2)\varepsilon_{p,f}(1-\theta_\ell)^3}\left[1-\varepsilon_{p,f}+\frac{(1/2)\varepsilon_{p,f}(1-\theta_\ell)}{1-\theta_\ell+\alpha}\right]^{-1}$$

$$-\frac{1}{\sqrt{V^*\Lambda^*}}\,4\alpha\theta_\ell^2 \exp(\theta_a/\theta_\ell)\frac{(1-\theta_\ell+\alpha)}{(1/2)\varepsilon_{p,f}(1-\theta_\ell)^2}\left[1-\varepsilon_{p,f}+\frac{(1/2)\varepsilon_{p,f}(1-\theta_\ell)}{1-\theta_\ell+\alpha}\right]^{-1}$$

$$-\frac{1-\theta_\ell+\alpha}{\varepsilon_{p,f}(1-\theta_\ell)}. \qquad \text{(D-4)}$$

Hence, in the neighborhood of the point $\varepsilon_p=0$, the function $f(\varepsilon_p)$ may be approximated by the equation

$$f(\varepsilon_p) = \frac{\alpha}{1-\theta_\ell}\,\varepsilon_p\left\{-\frac{1}{\Lambda^*}\alpha\theta_\ell \exp(\theta_a/\theta_\ell)\frac{(1-\theta_\ell+\alpha)^2}{(1/2)\varepsilon_{p,f}(1-\theta_\ell)^3}\right.$$

$$\left[1-\varepsilon_{p,f}+\frac{(1/2)\varepsilon_{p,f}(1-\theta_\ell)}{1-\theta_\ell+\alpha}\right]^{-1}+\frac{1}{\sqrt{\Lambda^*V^*}}\,4\alpha\theta_\ell^2 \exp(\theta_a/\theta_\ell)\frac{(1-\theta_\ell+\alpha)}{(1/2)\varepsilon_{p,f}(1-\theta_\ell)^2}$$

$$\left.\left[1-\varepsilon_{p,f}+\frac{(1/2)\varepsilon_{p,f}(1-\theta_\ell)}{1-\theta_\ell+\alpha}\right]^{-1}+\frac{1-\theta_\ell+\alpha}{\varepsilon_{p,f}(1-\theta_\ell)}\right\}. \qquad \text{(D-5)}$$

In order to determine the behavior of $f(\varepsilon_p)$ at the hot boundary ($\varepsilon_p=\varepsilon_{p,f}$) we shall use the identity

$$\varepsilon_P \xrightarrow{\lim} \varepsilon_{P,f} \left(\frac{\varepsilon_{P,f} - \varepsilon_P}{1-\theta} \right) = \left. \frac{d\varepsilon_P}{d\theta} \right|_{\varepsilon_P = \varepsilon_{P,f}} . \qquad \text{(D-6)}$$

Since σ approaches infinity in the limit $\varepsilon_P \longrightarrow \varepsilon_{P,f}$, it follows from Eqs. (D-6),(I-36), (I-33a), and (I-34) that

$$\varepsilon_P \xrightarrow{\lim} \varepsilon_{P,f} \left(\frac{1}{\sigma^2} \frac{d\varepsilon_P}{d\theta} \right) = \left[\Lambda^* \exp(-\theta_a) \frac{(1/2)\varepsilon_{P,f}^2 (1-\varepsilon_{P,f})}{(1-\theta_\ell + \alpha)^2} \right]^{1/2} . \qquad \text{(D-7)}$$

In view of Eqs. (D-6) and (D-7), Eq. (I-38) implies that the relation

$$\varepsilon_P \xrightarrow{\lim} \varepsilon_{P,f} \left[\sigma^2 f(\varepsilon_P) \right] = \left[\Lambda^* \exp(-\theta_a)(1/2)(1-\varepsilon_{P,f}) \right]^{1/2} \qquad \text{(D-8)}$$

is valid. This expression shows that the function $f(\varepsilon_P)$ approaches zero in the limit $\varepsilon_P \longrightarrow \varepsilon_{P,f}$.

It follows from Eq. (I-26) that near the hot boundary the relation

$$\frac{d\varepsilon_P}{d\sigma} \sim A\sigma^2(1-\theta)$$

is valid where A is a positive constant. This implies that

$$\frac{d\left(\frac{1}{\sigma^2}\right)}{d\varepsilon_P} \sim -\frac{1}{A\sigma^5(1-\theta)} . \qquad \text{(D-9)}$$

The expansion of Eq. (I-36) about the point $\theta = 1$ shows that near the hot boundary the relation

$$\left(\frac{d\theta}{d\sigma} \right)^2 \sim (1-\theta)^2$$

is obtained. By integrating this equation we obtain the expression

$$\sigma \sim -\log(1-\theta). \qquad \text{(D-10)}$$

Equation (D-10) shows that the quantity $1/\sigma^5(1-\theta)$ approaches infinity in

the limit $\epsilon_p \longrightarrow \epsilon_{p,f}$, and it therefore follows from Eq. (D-9) that the derivative $d(1/\sigma^2)/d\epsilon_p$ becomes negatively infinite as $\epsilon_p \longrightarrow \epsilon_{p,f}$. In view of this result, Eq. (D-8) implies that the derivative $df/d\epsilon_p$ approaches minus infinity at the hot boundary. In fact, a straightforward application of Eq. (D-1) yields the relation

$$\lim_{\epsilon_p \longrightarrow \epsilon_{p,f}} \left[\sigma^5(1-\theta)\frac{df}{d\epsilon_p}\right] = \frac{4\alpha(1-\theta_\ell+\alpha)}{\epsilon_{p,f}(1-\theta_\ell+2\alpha)} \left[V^* \exp(-\theta_a)\frac{(1-\epsilon_{p,f})}{2}\right]^{-1/2} \qquad \text{(D-11)}$$

We conclude that the function $f(\epsilon_p)$ approaches zero with a negatively infinite slope in the limit $\epsilon_p \longrightarrow \epsilon_{p,f}$.

Higher approximations to $f(\epsilon_p)$ may be obtained by differentiating Eq. (D-1) and evaluating the higher-order derivatives at the end points. In this manner the integral in Eq. (I-37a) may be found to any desired accuracy.

2. Stoichiometric Mixtures

The expansion of the function $f(\epsilon_p)$ about the cold boundary ($\epsilon_p=0$) that was given in the previous section also applies to the case of stoichiometric mixtures if the value of the flux fraction of products at the hot boundary is set equal to unity ($\epsilon_{p,f}=1$). However, the behavior of $f(\epsilon_p)$ near the end point $\epsilon_p=\epsilon_{p,f}$ is different for the stoichiometric case where the mole fractions X_F and X_O both go to zero at the hot boundary.

For stoichiometric mixtures Eq. (I-36) of Chapter I implies that the relation

$$\lim_{\varepsilon_p \to 1}\left(\frac{1}{\sqrt{1-\theta}}\ \frac{1}{\sigma^2}\ \frac{d\varepsilon_p}{d\sigma}\right) = \left[\frac{\Lambda^* \exp(-\theta_a)}{4(1-\theta_\ell+\alpha)^3}\right]^{1/2} \qquad \text{(D-12)}$$

is valid. By substituting Eqs. (D-6) and (D-12) into Eq. (I-38) which defines $f(\varepsilon_p)$ we obtain the expression

$$\lim_{\varepsilon_p \to 1}\left[\frac{\sigma^2 f(\varepsilon_p)}{\sqrt{1-\theta}}\right] = \left[\frac{\Lambda^* \exp(-\theta_a)}{4(1-\theta_\ell+\alpha)}\right]^{1/2} . \qquad \text{(D-13)}$$

Since $\sigma = \infty$ and $(1-\theta)=0$ at the end point $\varepsilon_p=1$, it follows from Eq. (D-13) that the function $f(\varepsilon_p)$ approaches zero at the hot boundary for stoichiometric ratios.

In order to obtain the slope of $f(\varepsilon_p)$ in the limit $\varepsilon_p=\varepsilon_{p,f}$, we notice that the relation

$$\frac{d\varepsilon_p}{d\sigma} \sim \sigma^2(1-\theta)^2 \qquad \text{(D-14)}$$

follows from Eq. (I-36) near the hot boundary. Equation (I-35) may be expanded about the point $\theta=1$ in order to obtain the expression

$$\left(\frac{d\theta}{d\sigma}\right)^2 \sim (1-\theta)^3 .$$

Hence

$$\sigma \sim \frac{1}{\sqrt{1-\theta}} \qquad \text{(D-15)}$$

which implies that $\sigma^2/\sqrt{1-\theta} \sim \sigma^3$ near the hot boundary. It follows from Eqs. (D-14) and (D-15) that the relation $\frac{d}{d\varepsilon_p}\left(\frac{\sqrt{1-\theta}}{\sigma^2}\right) \sim \frac{1}{\sigma^4}\frac{d\sigma}{d\varepsilon_p} \sim 1-\theta$ is valid in the neighborhood of the point $\varepsilon_p=1$. Hence the derivative $\frac{d}{d\varepsilon_p}\left(\frac{\sqrt{1-\theta}}{\sigma^2}\right)$ approaches zero in the limit $\varepsilon_p \to 1$, and it follows from Eq. (D-13) by de l'Hospital's rule that the derivative $df/d\varepsilon_p$ goes to zero. It is therefore seen that in the stoichiometric case the slope of the function

$f(\varepsilon_p)$ at the hot boundary is zero, while it is negatively infinite for the case in which $\varepsilon_{p,f} \neq 1$.

APPENDIX E

NUMERICAL CALCULATIONS FOR DROPLET BURNING PROBLEM

With one modification Eqs. (I-26) and (I-27) of Chapter I are adaptable to a numerical integration procedure for obtaining the burning rate eigenvalue $\dot{m}$ and the functions $\theta(\sigma)$ and $\varepsilon_P(\sigma)$. The change is to use $\eta = 1/\sigma$ in place of σ as the independent variable in order to make the range of integration finite. If use is made of Eq. (I-33a) for X_F, Eq. (I-34) for X_O, and Eq. (I-29) for q, then the modified equations become

$$\frac{d\varepsilon_P}{d\eta} = -\frac{4\pi r_\ell^3}{\dot{m}} \frac{2B}{M} \rho_f^2 \frac{\exp(-\theta_a/\theta)}{\eta^4 \theta^2} \frac{\varepsilon_{P,f}(1-\theta)}{2(1-\theta_\ell+\alpha)} \left[1 - \varepsilon_{P,f} + \frac{\varepsilon_{P,f}(1-\theta)}{2(1-\theta_\ell+\alpha)} \right] \quad \text{(E-1)}$$

and

$$\frac{d\theta}{d\eta} = -\frac{\dot{m}}{4\pi r_\ell} \frac{\bar{c}_p}{\lambda_f} \frac{1}{\theta} \left[\alpha - \frac{\varepsilon_P}{\varepsilon_{P,f}} (1-\theta_\ell+\alpha) + \theta - \theta_\ell \right] . \quad \text{(E-2)}$$

In these two equations all constants are known except the mass flow rate $\dot{m}$, and the integration is to be carried out from $\varepsilon_P = 0$ and $\theta = \theta_\ell$ at $\eta = 1$ to $\varepsilon_P = \varepsilon_{P,f}$ and $\theta = 1$ at $\eta = 0$. In the method of solution a trial value for $\dot{m}$ is chosen and the integration is begun at $\eta = 1$. It is determined whether the relations $\varepsilon_P = \varepsilon_{P,f}$ and $\theta = 1$ are obtained at the end point $\eta = 0$. If these conditions are not satisfied at the boundary point then the value of $\dot{m}$ is readjusted and the calculation is repeated. This process is continued until a consistent result is obtained.

The procedure described above was carried out for droplets with radii, r_ℓ, of .02 cm, .08 cm, .2 cm, .8 cm, and 2 cm for dimension-

less activation temperatures, θ_a, of 3.9, 11.7, and 23.4 in the case of non-stoichiometric mixtures with the fuel-oxidizer ratio δ=0.818 (i.e., $\varepsilon_{P,f}$=0.9). The calculation was also completed for a stoichiometric mixture with θ_a=20.6. The values which were chosen for the other physical constants appearing in Eqs. (E-1) and (E-2) are listed in Table I. For the sake of comparison we used the values which Lorell and Wise[1] assumed to be representative of the hydrazine flame.

The integration was carried out by a Runge-Kutta technique on the Electrodata "Datatron" high-speed electronic digital computer with paper tape input and automatic typewriter output at the California Institute of Technology. The program included all operations necessary for solving Eqs. (E-1) and (E-2) except the adjustment of the value of $\dot{m}$. The subroutines for evaluating the exponential function and the algebraic functions appearing on the right-hand side of Eqs. (E-1) and (E-2) were incorporated semi-automatically into the main routine for the solution of first-order differential equations. The burning rate was adjusted manually after observing the final values of the functions ε_p and θ tabulated by the computer output. The numerical integration therefore provided the functions $\varepsilon_p(\eta)$ and $\theta(\eta)$ and the mass burning rate $\dot{m}$ for each of the cases previously described.

Typical results for the functions $\varepsilon_p(\theta)$ and $\eta(\theta)$ for each of the four values of the activation temperature θ_a are given in Figs. 4 through 7. The resulting values of the burning rate $\dot{m}$ are tabulated in Table IV and illustrated in Figs. 8 through 11.

1. J. Lorell and H. Wise, J. Chem. Phys. 23, 1928-1932 (1955).

2. D. W. Kiley, "On the Burning of Single Drops of Monopropellants" Thesis, California Institute of Technology, Pasadena, (1955).

3. M. Barrère and H. Moutet, La Rech. Aéro. 9, No. 50, 31-38 (1956).

4. W. A. Rosser, "The Decomposition Burning of Monopropellant Drops; Hydrazine, Nitromethane, and Ethyl Nitrate", Progress Report No. 20-305, California Institute of Technology, JPL (1957).

5. Th. von Kármán and S. S. Penner, Selected Combustion Problems, Adv. Group Aero. Res. Dev., Butterworths Scientific Publications, London 1954, pp. 5-41.

6. S. Chapman and T. G. Cowling, The Mathematical Theory of Non-Uniform Gases, Cambridge University Press, Cambridge 1952.

7. J. O. Hirschfelder, C. F. Curtiss and R. B. Bird, Molecular Theory of Gases and Liquids, John Wiley and Sons, Inc., New York 1954.

8. N. Semenov, Adv. Phys. Sci., Moscow 24, 433-486 (1940); English translation, National Advisory Committee for Aeronautics Technical Memorandum No. 1026.

9. W. H. Furry, Am. J. of Phys. 16, 63-78 (1948).

10. J. Jeans, The Dynamical Theory of Gases, Cambridge University Press, Cambridge 1925.

11. B. P. Mullins, Fuel 32, 327-342 and 451-466 (1953).

12. P. Gray et al, Sixth Symposium (International) on Combustion, Reinhold Publishing Corp., New York 1957, pp. 255-263.

13. M. Gilbert, "The Hydrazine Flame", Progress Report No. 20-318, California Institute of Technology, JPL (1957).

14. D. B. Spalding, Fourth Symposium (International) on Combustion, Williams and Wilkins Co., Baltimore 1953, pp. 847-864.

15. G. A. Agoston, B. J. Wood, and H. Wise, "Influence of Pressure on the Combustion of Liquid Spheres", presented at American Rocket Society Semi-Annual Meeting, San Francisco, June 1957.

16. S. Kumagai, Jet Propulsion 26, 786 (1956).

17. W. C. Schumb, C. N. Satterfield and R. L. Wentworth, Hydrogen Peroxide, Reinhold Publishing Corp., New York 1955.

18. C. K. McLane, J. Chem. Phys. 17, 379-385 (1949).

19. S. Kumagai and H. Isoda, Sixth Symposium (International) on Combustion, Reinhold Publishing Corp., New York 1957, pp. 726-731.

20. M. Goldsmith and S. S. Penner, Jet Propulsion 24, 245-251 (1954).

21. M. M. El Wakil, O. A. Uyehara and P. S. Meyers, National Advisory Committee for Aeronautics Technical Note No. 3179 (1954).

22. V. A. Shvab, Gos. Energ. izd., M-L (1948).

23. Y. B. Zeldovich, Zhurnal Tech. Fiz. 19, 1199-1210 (1949); English translation, National Advisory Committee for Aeronautics Technical Memorandum No. 1296.

24. W. Nachbar, F. Williams and S. S. Penner, "The Conservation Equations for Independent Coexistent Continua and for Multi-component Reacting Gas Mixtures", Report No. LMSD 2082, Lockheed Aircraft Corp., Missile Systems Div., Palo Alto (1957), Quart. Appl. Math. (in press).

25. S. P. Burke and T. E. W. Schumann, Ind. Eng. Chem. 20, 998-1004 (1928).

26. S. S. Penner and Th. Crowe, Symposium on Aerothermochemistry, Northwestern University, Evanston 1956, pp. 113-131.

27. A. H. Shapiro and A. J. Erickson, Trans. Am. Soc. Mech. Eng. 79, 775-788 (1957).

28. R. P. Probert, Phil. Mag. 37, 94-105 (1946).

29. C. C. Miesse, "A Theory of Spray Combustion", presented at American Rocket Society Semi-Annual Meeting, San Francisco, June 1957.

30. A. E. Fuhs, "Part I Experimental and Theoretical Studies on Heterogeneous Diffusion Flames, Part II Spectroscopic Studies of Flames", Ph. D. Thesis, California Institute of Technology, Pasadena (1958).

31. J. O. Hinze, Am. Inst. Chem. Eng. J. 1, 289-295 (1955).

32. A. A. Putnam et al., "Injection and Combustion of Liquid Fuels", Wright Air Development Center Technical Report No. 56-344, Batelle Memorial Institute (1957).

33. A. R. Hanson, E. G. Domick, and H. S. Adams, "An Experimental Investigation of Impact and Shock Wave Breakup of a Liquid Drop", Report No. 125, University of Minnesota, Rosemont Aeronautics Laboratory (1956).

34. N. I. Masugi, "Theoretical and Experimental Studies of the Deformation and Atomization of a Liquid Drop in a High Velocity Gas Stream", M S Thesis, Massachusetts Institute of Technology, Cambridge (1956).

35. J. O. Hinze, Appl. Sci. Res. 1, 273-288 (1948).

36. S. Goldstein, Modern Developments in Fluid Dynamics, Oxford University Press, Oxford 1950, Vol. II Chapter XI Section 1.

37. H. Lamb, Hydrodynamics, Cambridge University Press, Cambridge 1924, Sections 337 and 338.

38. R. D. Ingebo, National Advisory Committee for Aeronautics Technical Note No. 3762 (1956).

39. N. Froessling, Gerlands Beitr. Geophys. 52, 170-216 (1938).

40. W. E. Ranz and W. R. Marshall, Chem. Eng. Progress 48, 141-146 and 173-180 (1952).

41. S. Kumagai and I. Kimura, Science of Machines 3, 431-434 (1951).

42. J. F. Rex, A. E. Fuhs and S. S. Penner, Jet Propulsion 26, 179-187 (1956).

43. G. A. Agoston, H. Wise, and W. A. Rosser, Sixth Symposium (International) on Combustion, Reinhold Publishing Corp., New York 1957, pp. 708-717.

44. D. W. Lee, National Advisory Committee for Aeronautics Report No. 425 (1932).

45. P. Rosin and E. Rammler, Zeit. des Vereins Deutscher Ing. 71, 1 (1927).

46. S. Nukiyama and Y. Tanasawa, Trans. Soc. Mech. Eng. (Japan) 5, 62-67 (1939).

47. R. D. Ingebo and H. H. Foster, National Advisory Committee for Aeronautics Technical Note No. 4087 (1957).

48. R. D. Ingebo, National Advisory Committee for Aeronautics Technical Note No. 4222 (1958).

TABLE I. Physical constants for numerical calculations

Quantity	Value for non-stoichiometric case ($\delta = 0.818$, $\varepsilon_{P,f} = 0.9$)	Value for stoichiometric case ($\delta = 1$, $\varepsilon_{P,f} = 1$)
B/M	0.834×10^{16} cm^3/gm-sec	0.834×10^{16} cm^3/gm-sec
$\bar{c}_p$	0.580 cal/gm-$^\circ$K	0.580 cal/gm-$^\circ$K
λ_f	5×10^{-4} cal/cm-sec-$^\circ$K	5×10^{-4} cal/cm-sec-$^\circ$K
ρ_f	3.12×10^{-4} gm/cm^3	3.04×10^{-4} gm/cm^3
$\Delta\ell$	380 cal/gm	380 cal/gm
q	1000 cal/gm	1000 cal/gm
T_ℓ	387 $^\circ$K	387 $^\circ$K
T_f	1283 $^\circ$K	1457 $^\circ$K
θ_ℓ	0.302	0.266
α	0.510	0.450

TABLE II. $\sqrt{V^*}$ as a function of r_ℓ for a system with physical constants given in Table I.

r_ℓ (cm)	$\sqrt{V^*}$ for non-stoichiometric case ($\delta = 0.818$)	$\sqrt{V^*}$ for stoichiometric case ($\delta = 1$)
.02	2.743×10^4	2.675×10^4
.08	1.098×10^5	1.069×10^5
.2	2.743×10^5	2.675×10^5
.8	1.098×10^6	1.069×10^6
2.0	2.743×10^6	2.675×10^6

TABLE III. $\sqrt{\Lambda^*}$ as a function of r_ℓ for the physical system described in Table I.

		r_ℓ = .02 cm	r_ℓ = .08 cm	r_ℓ = .2 cm	r_ℓ = .8 cm	r_ℓ = 2 cm
Stoichiometric case (δ =1) θ_a = 20.6	Numerical results	4.63×10^4	1.690×10^5	3.72×10^5	1.049×10^6	1.809×10^6
	Analytical approximation	4.16×10^4	1.621×10^5	4.16×10^5	1.621×10^6	4.16×10^6
Non-stoichiometric cases (δ = 0.818)						
θ_a = 23.4	Numerical results	5.12×10^4	1.930×10^5	4.46×10^5	1.420×10^6	2.70×10^6
	Analytical approximation	3.92×10^4	1.571×10^5	3.92×10^5	1.571×10^6	3.92×10^6
θ_a = 11.7	Numerical results	9.71×10^3	1.230×10^4	1.248×10^4	1.560×10^4	
	Correlation	1.345×10^4	1.345×10^4	1.345×10^4	1.345×10^4	
θ_a = 3.9	Numerical results	86.0	86.0	86.0	86.0	
	Correlation	97.0	97.0	97.0	97.0	

TABLE IV. Mass flow rate $\dot{m}$ (gm/sec) for a system with the properties given in Table I.

		r_ℓ = .02 cm	r_ℓ =.08 cm	r_ℓ = .2 cm	r_ℓ = .8 cm	r_ℓ = 2 cm
Stoichiometric case (δ=1) θ_a = 20.6	Numerical results	1.251×10^{-4}	5.48×10^{-4}	1.556×10^{-3}	8.85×10^{-3}	3.21×10^{-2}
	Analytical approximation	1.390×10^{-4}	5.71×10^{-4}	1.390×10^{-3}	5.71×10^{-3}	1.390×10^{-2}
Non-stoichiometric cases (δ = 0.818)						
θ_a = 23.4	Numerical results	1.161×10^{-4}	4.93×10^{-4}	1.332×10^{-3}	6.70×10^{-3}	2.21×10^{-2}
	Analytical approximation	1.517×10^{-4}	6.05×10^{-4}	1.517×10^{-3}	6.05×10^{-3}	1.517×10^{-2}
θ_a = 11.7	Numerical results	6.12×10^{-4}	7.73×10^{-3}	4.77×10^{-2}	6.09×10^{-1}	
	Correlation	4.42×10^{-4}	7.07×10^{-3}	4.42×10^{-2}	7.07×10^{-1}	
θ_a = 3.9	Numerical results	6.91×10^{-2}	1.109	6.91	1.109×10^{2}	
	Correlation	6.13×10^{-2}	0.981	6.13	0.981×10^{2}	

TABLE V. Position σ_c at which the reaction is half complete, $\varepsilon_p = \varepsilon_{p,f}/2$.

δ	θ_a	σ_c
1.000	20.6	27
0.818	23.4	42
0.818	11.7	1.23
0.818	3.9	1.005

TABLE VI. Comparison of theoretical and experimental burning rates for hydrogen peroxide, ethyl nitrate, and propyl nitrate

	H_2O_2	$C_2H_5ONO_2$	$C_3H_7ONO_2$
λ_f(cal/cm-sec)	1.1×10^{-4}	2×10^{-4}	3×10^{-4}
ρ_l (gm/cm^3)	1.465	1.105	1.058
Δl (cal/gm)	373	101	101
$\bar{c}_p$ (cal/gm-$^\circ$K)	0.40	0.39	0.42
T_l ($^\circ$K)	425	362	384
T_f ($^\circ$K)	472	1973	803
T_a ($^\circ$K)	22,500	12,800	11,000
θ_a	47.7	6.5	13.7
θ_l	0.900	0.183	0.478
α	1.970	0.131	0.300
theoretical K(cm^2/sec)	2.6×10^{-4}	0.24×10^{-2}	0.66×10^{-2}
experimental* K(cm^2/sec)	3×10^{-4}	4×10^{-2}	1.3×10^{-2}

* The experimental values are taken from reference 3.

TABLE VII. Data used in theoretical calculation of nitric acid-amyl acetate monopropellant burning rate

ϕ	.6	.8	1.0	1.4	2.0
λ_f (cal/cm-sec) ($\lambda_f \sim T_f$)	8.9×10^{-4}	11.0×10^{-4}	11.3×10^{-4}	9.1×10^{-4}	6.0×10^{-4}
ρ_l (gm/cm^3)	1.05 →				
Δl (cal/gm)	140 →				
$\bar{c}_p$ (cal/gm-$^\circ$K)	0.39 →				
T_l ($^\circ$K)	420 →				
T_f ($^\circ$K)	2030	2510	2590	2080	1370
K(cm^2/sec) (theory)	1.18×10^{-2}	1.23×10^{-2}	1.235×10^{-2}	1.185×10^{-2}	1.05×10^{-2}
K(cm^2/sec) (experiment)*	1.37×10^{-2}	1.60×10^{-2}	1.74×10^{-2}	1.735×10^{-2}	1.47×10^{-2}

* The experimental values are taken from reference 3.

TABLE VIII. The number-weighted average asymptotic droplet radius $\bar{r}_{as}$ on the axis of the scattered jet as a function of the size distribution parameters s and t of the incident jet.

s	$\bar{r}_{as}/(\bar{r}/N^{1/3})$ for various values of t						
	t=0	t=1	t=2	t=3	t=5	t=10	t=∞
1	2.52	1.89	1.68	1.58	1.47	1.37	1.26
2	2.10	1.67	1.53	1.46	1.39	1.33	1.26
3	2.00	1.61	1.49	1.43	1.37	1.32	1.26
4	1.97	1.59	1.47	1.41	1.36	1.31	1.26
5	1.95	1.58	1.47	1.41	1.36	1.31	1.26
10	1.95	1.57	1.46	1.40	1.35	1.30	1.26
∞	2.02	1.62	1.49	1.43	1.37	1.32	1.26

TABLE IX. The number-weighted average asymptotic droplet radius $\bar{r}_{as}$ on the edge of the scattered jet as a function of the size distribution parameters s and t of the incident jet

s	$\bar{r}_{as}/(\bar{r}/N^{1/3})$ for various values of t						
	t=0	t=1	t=2	t=3	t=5	t=10	t=∞
1	4.00	3.00	2.67	2.50	2.34	2.18	2.00
2	2.36	1.88	1.72	1.64	1.57	1.49	1.41
3	2.00	1.61	1.49	1.43	1.37	1.32	1.26
4	1.85	1.50	1.39	1.33	1.28	1.24	1.19
5	1.78	1.44	1.33	1.29	1.24	1.19	1.15
10	1.66	1.34	1.24	1.19	1.15	1.11	1.07
∞	1.60	1.29	1.19	1.14	1.09	1.05	1.00

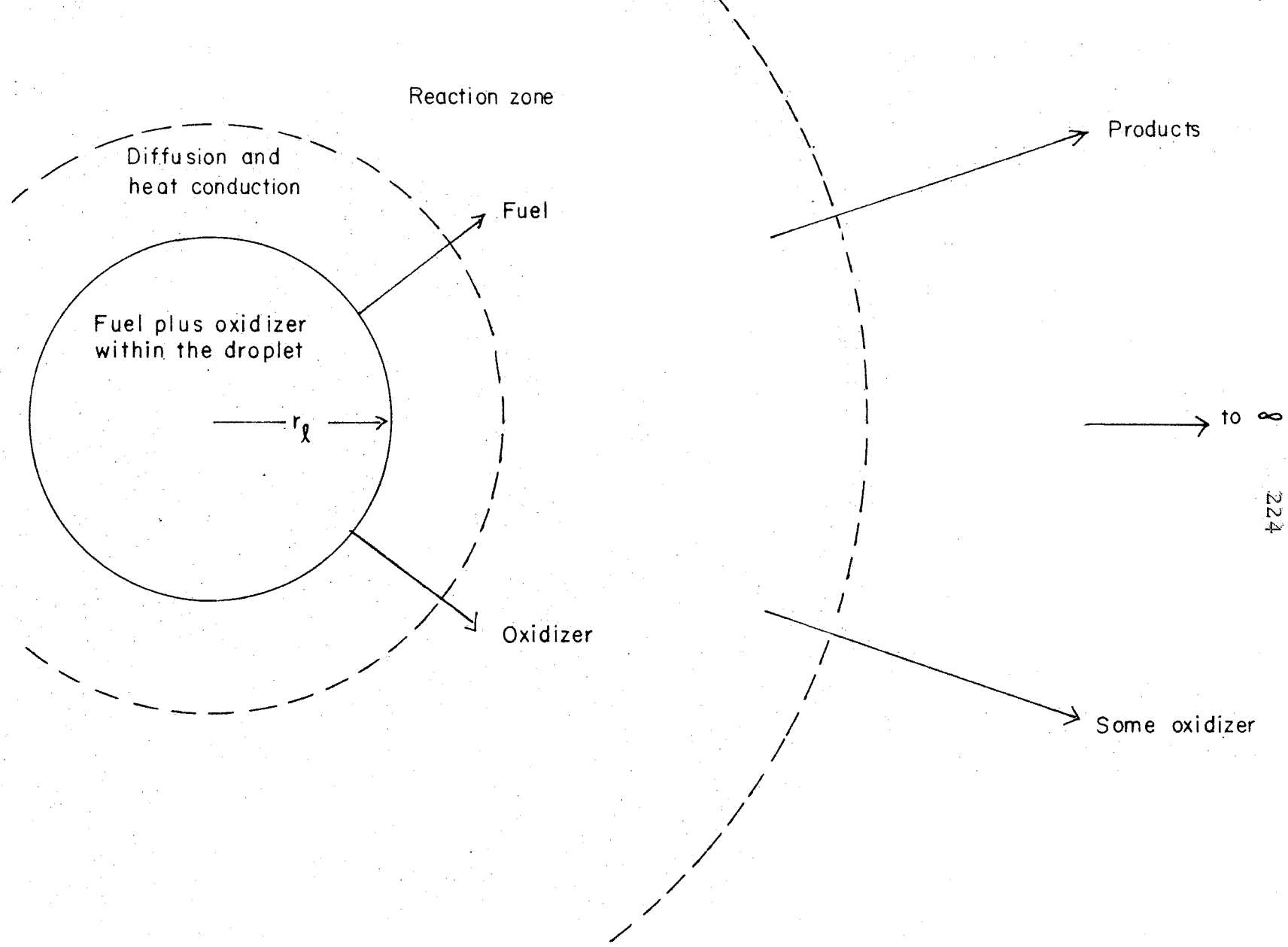

Fig 1. Schematic diagram of monopropellant droplet burning.

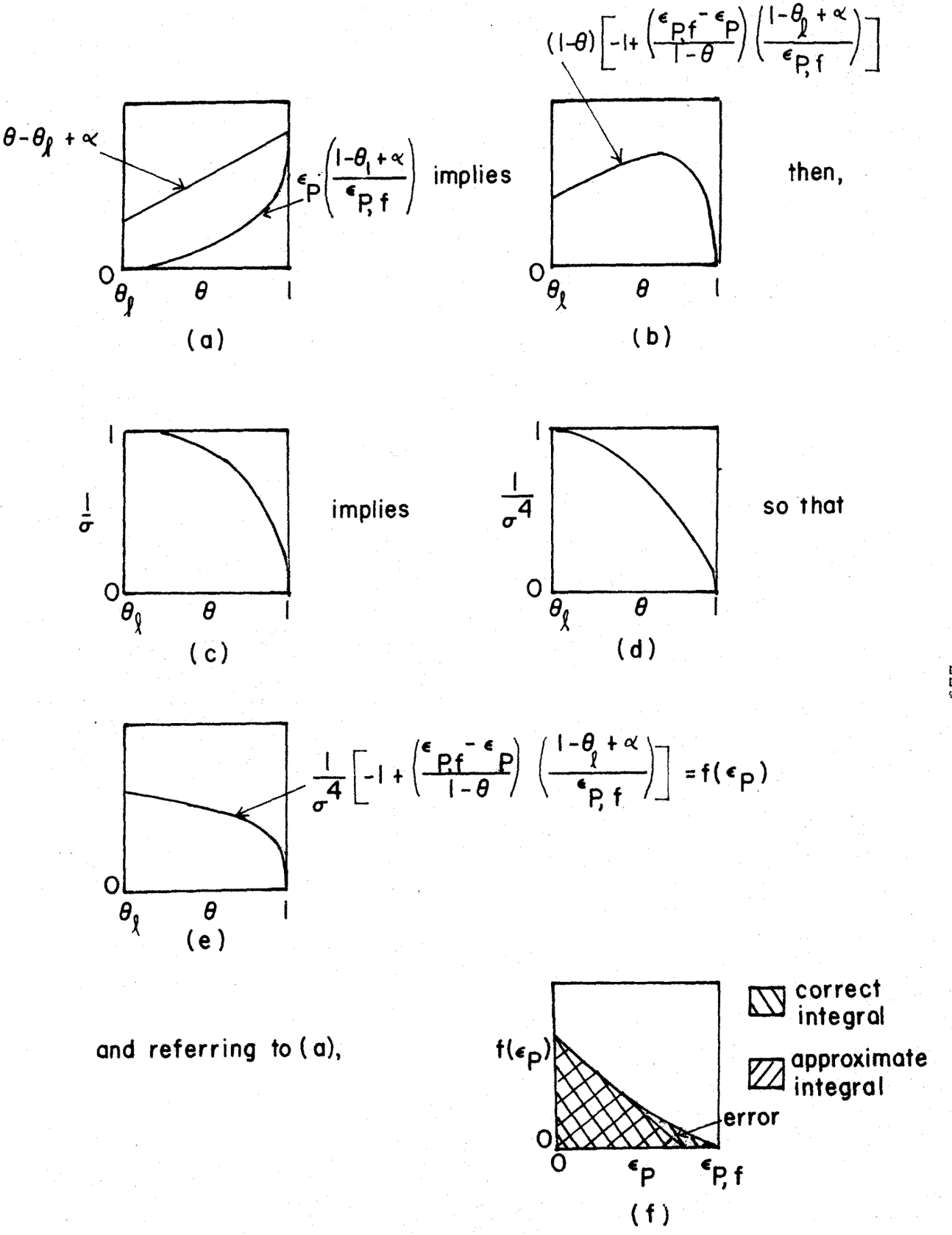

Fig. 2. Schematic representation of error in Λ^* due to approximation of $f(\epsilon_P)$ for intermediate values of θ_a.

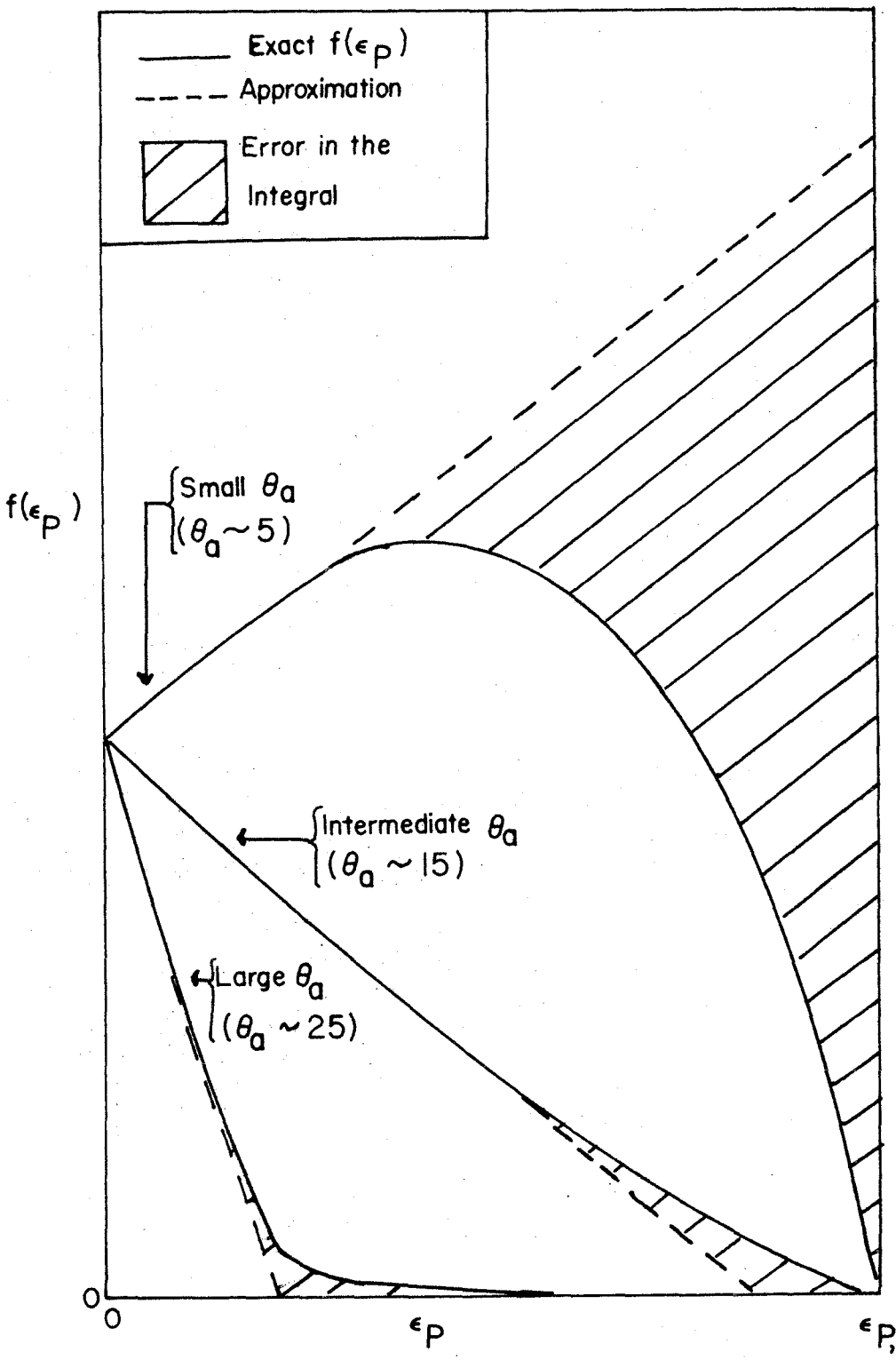

Fig.3. Schematic representation of error in Λ^* due to linear approximation of $f(\epsilon_P)$ for various values of θ_a.

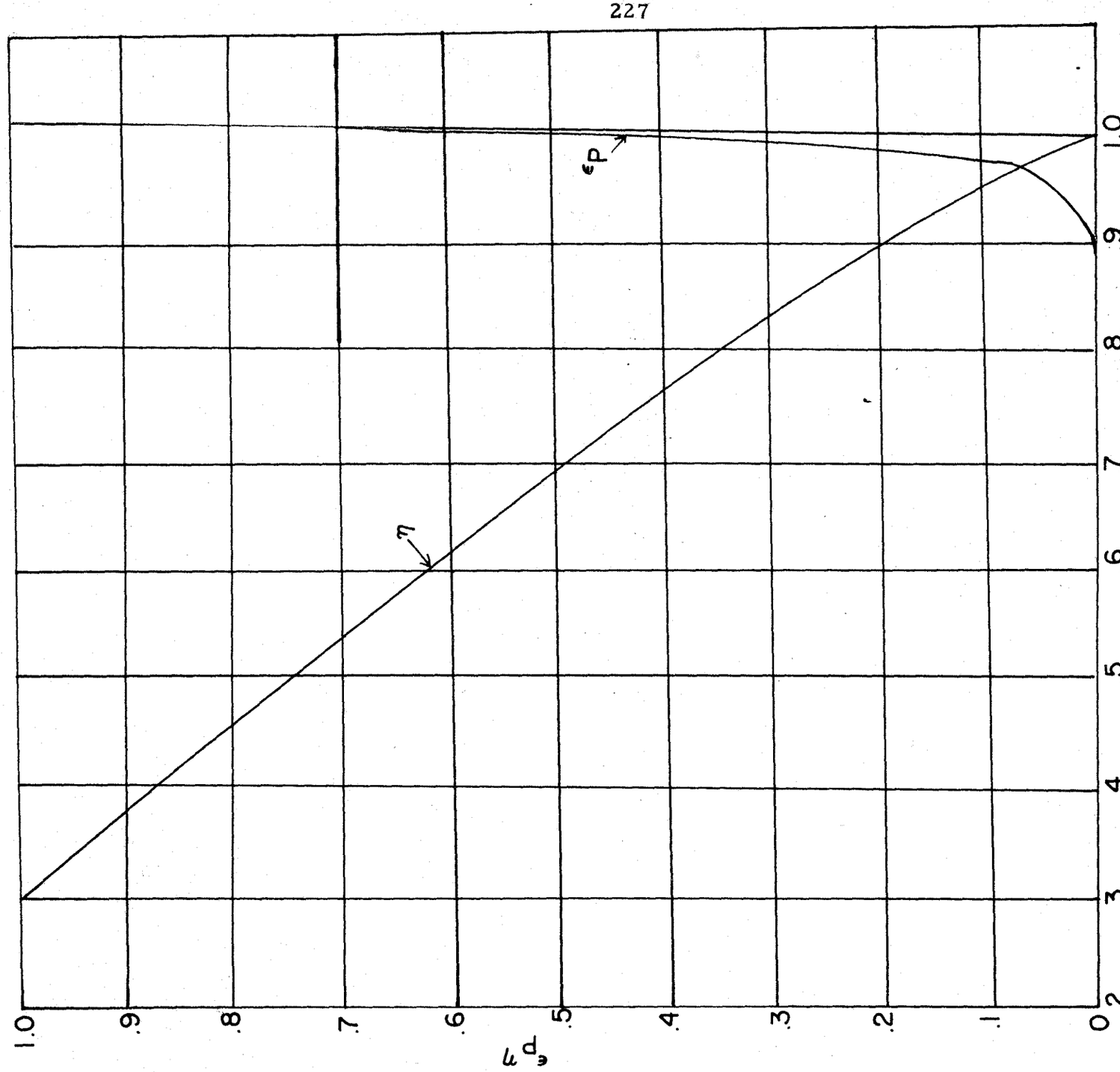

Fig. 4. The flux fraction ϵ_P and $\eta = r_\ell / r$ as a function of the dimensionless temperature θ for non-stoichiometric mixtures with fuel-oxidizer ratio $\delta = 0.818$ ($\epsilon_{P,f} = 0.9$) at a droplet radius of $r_\ell = .02$ cm and an activation temperature of $\theta_a = 23.4$.

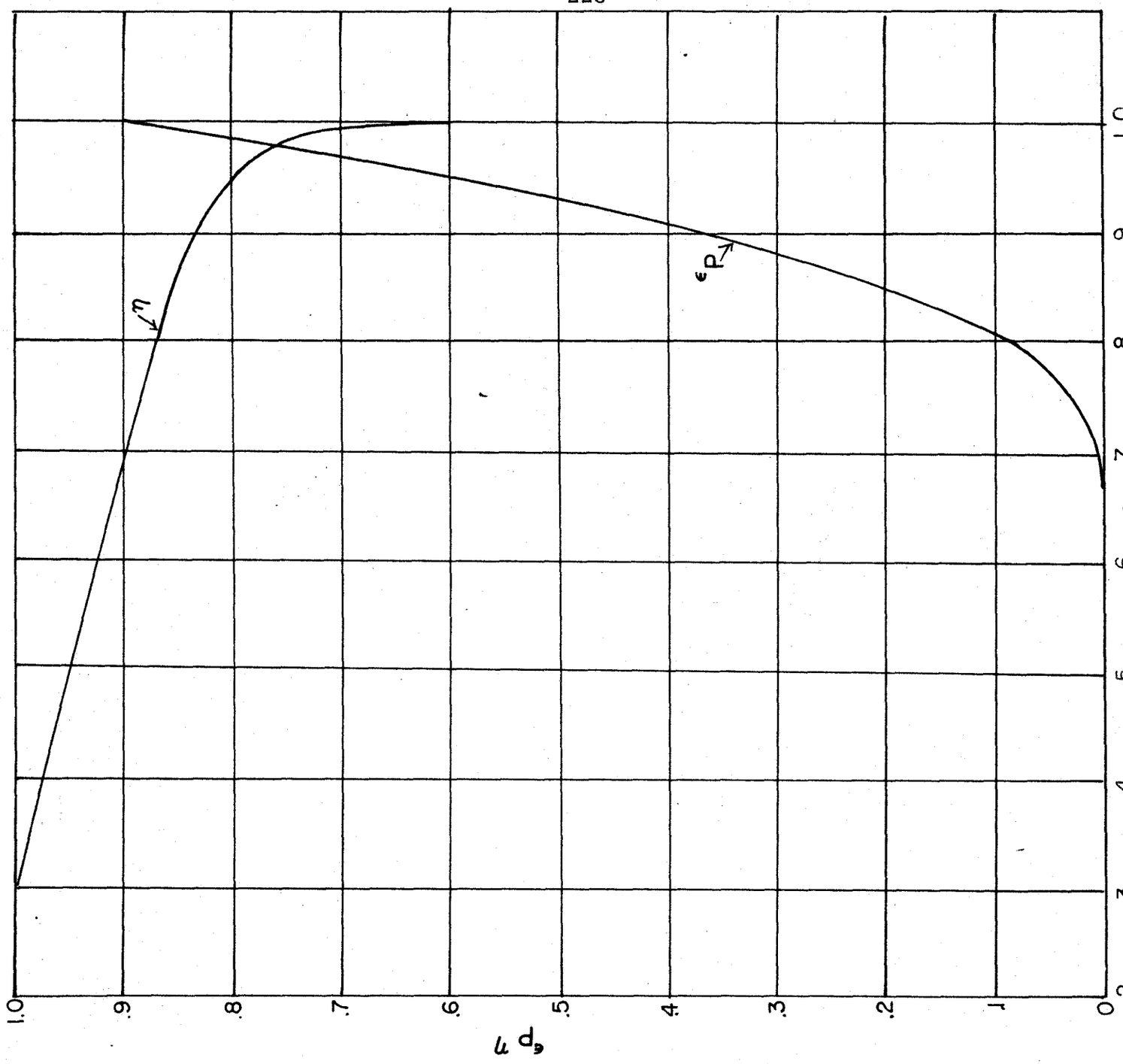

Fig. 5. The flux fraction ϵ_P and $\eta = r_\chi / r$ as a function of the dimensionless temperature θ for non-stoichiometric mixtures with fuel-oxidizer ratio $\delta = 0.818$ ($\epsilon_{P,f} = 0.9$) at a droplet radius $r_\chi = .02$ cm and an activation temperature of $\theta_a = 11.7$.

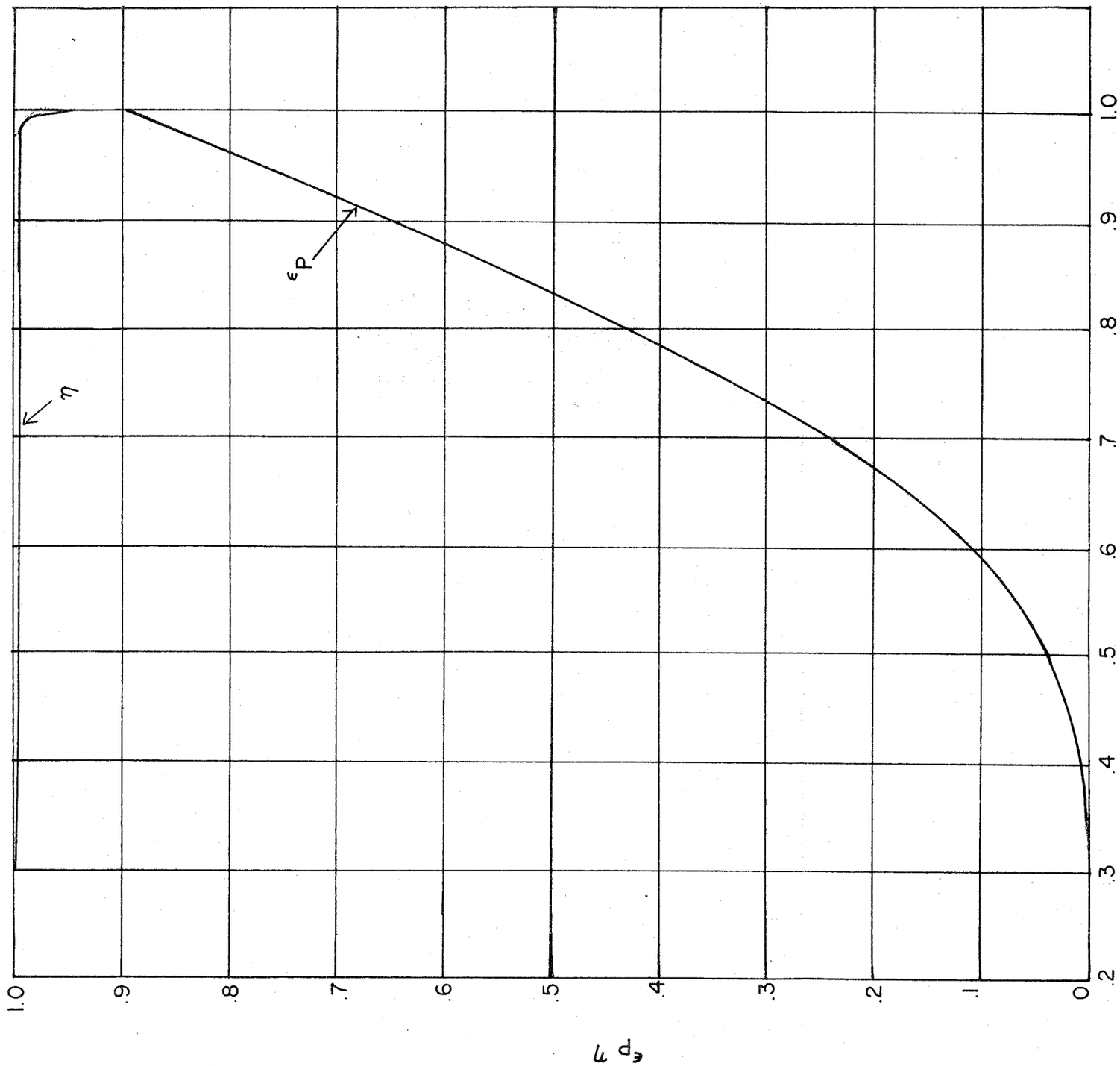

Fig. 6. The flux fraction ϵ_P and $\eta = r_\chi/r$ as a function of the dimensionless temperature θ for non-stoichiometric mixtures with fuel-oxidizer ratio δ=0.818 ($\epsilon_{P,f}$ =0.9) at a droplet radius r_χ = .02 cm and an activation temperature of θ_a = 3.9.

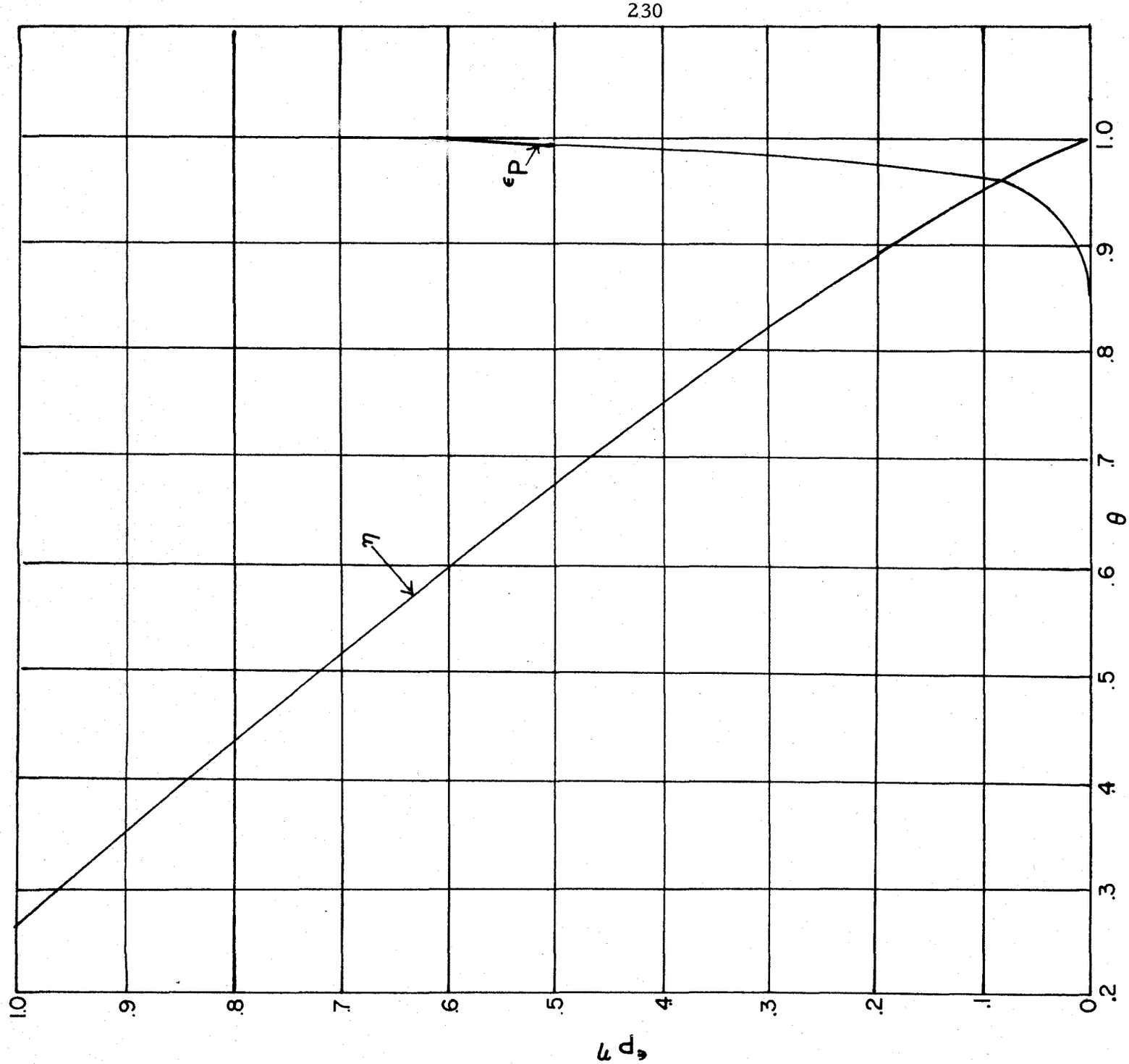

Fig. 7. The flux fraction ϵ_P and $\eta = r_\chi / r$ as a function of the dimensionless temperature θ for stoichiometric mixtures ($\delta = 1$) at a droplet radius $r_\ell = .02$ cm and an activation temperature of $\theta_a = 20.6$.

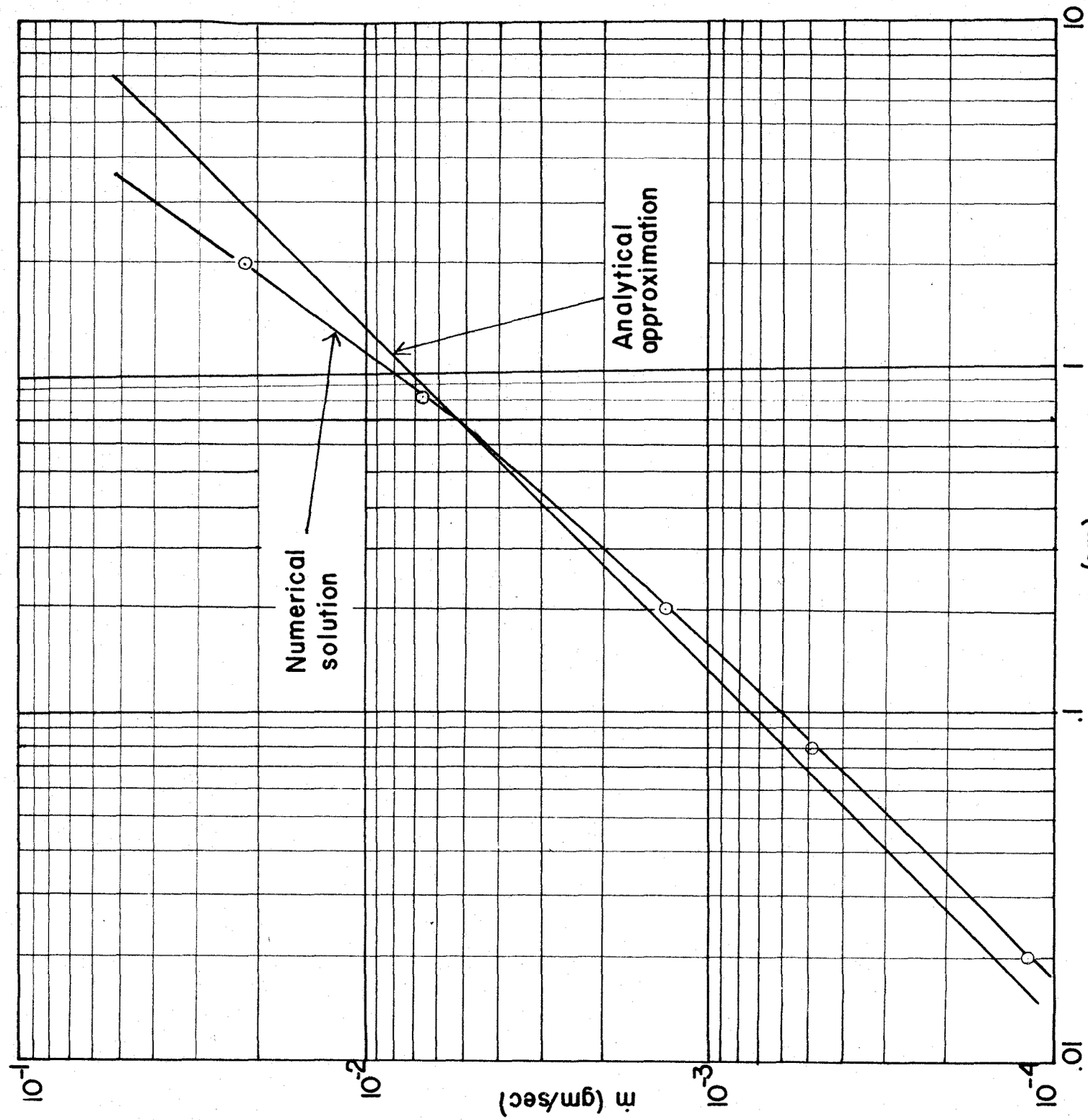

Fig. 8. Mass flow rate $\dot{m}$ as a function of droplet radius r_ℓ for non-stoichiometric mixtures with fuel-oxidizer ratio δ=0.818 ($\epsilon_{P,f}$=0.9) and an activation temperature of θ_a = 23.4.

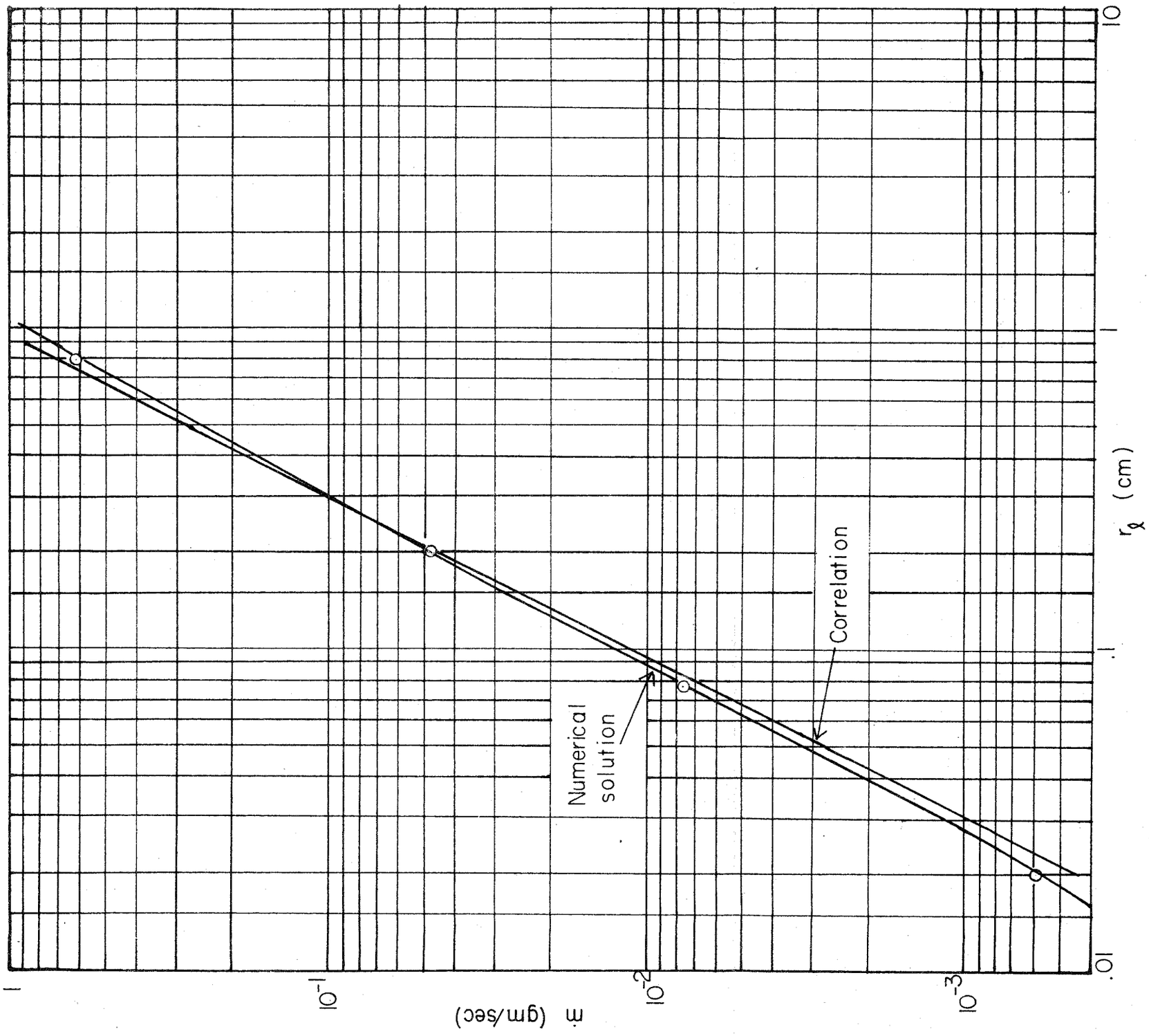

Fig. 9. Mass flow rate $\dot{m}$ as a function of droplet radius r_ℓ for non-stoichiometric mixtures with fuel-oxidizer ratio δ=0.818 ($\epsilon_{P,f}$=0.9) and an activation temperature of θ_a = 11.7.

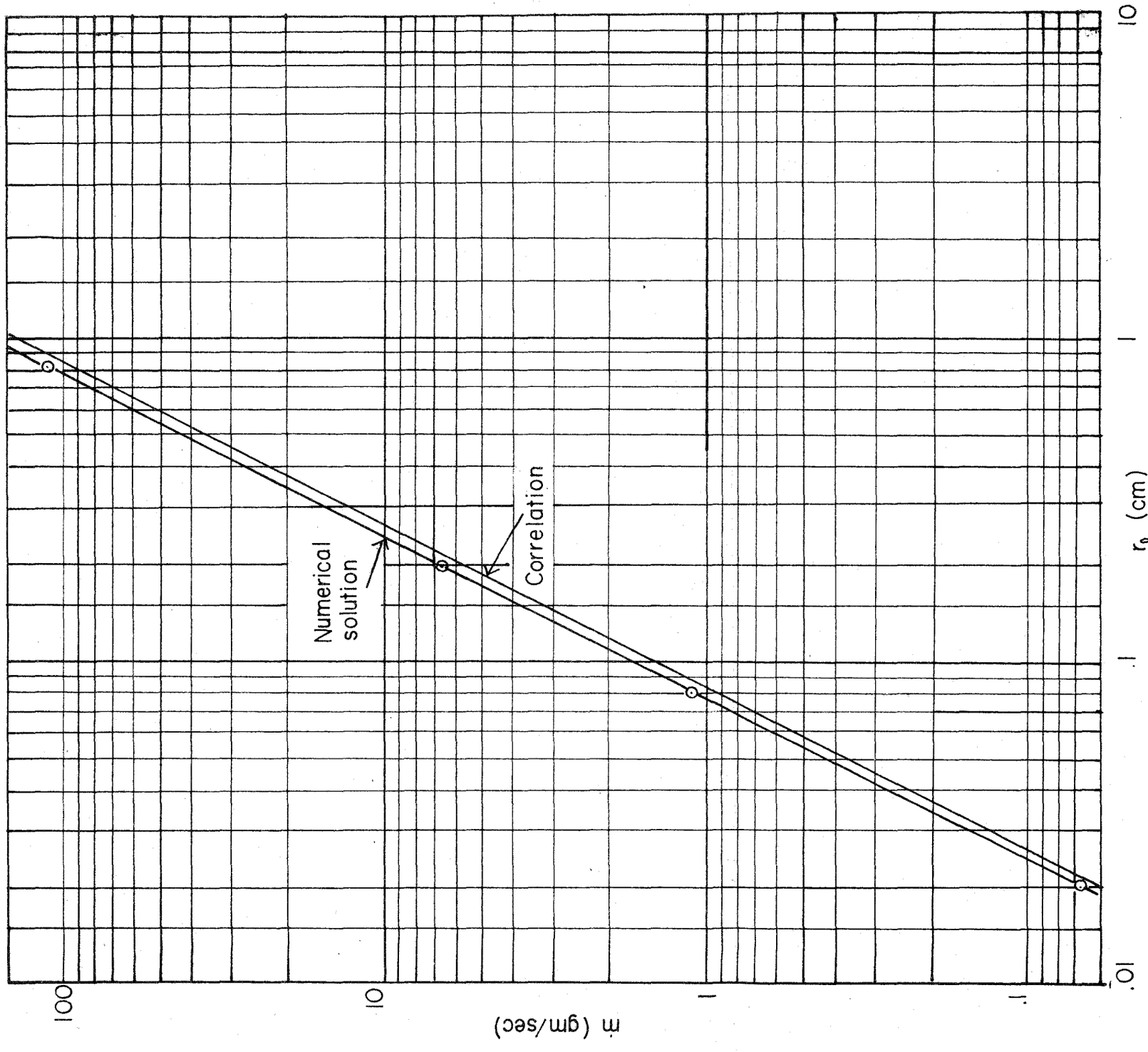

Fig. 10. Mass flow rate $\dot{m}$ as a function of droplet radius r_ℓ for non-stoichiometric mixtures with fuel-oxidizer ratio δ=0.818 ($\epsilon_{P,f}$=0.9) and an activation temperature of θ_a =3.9.

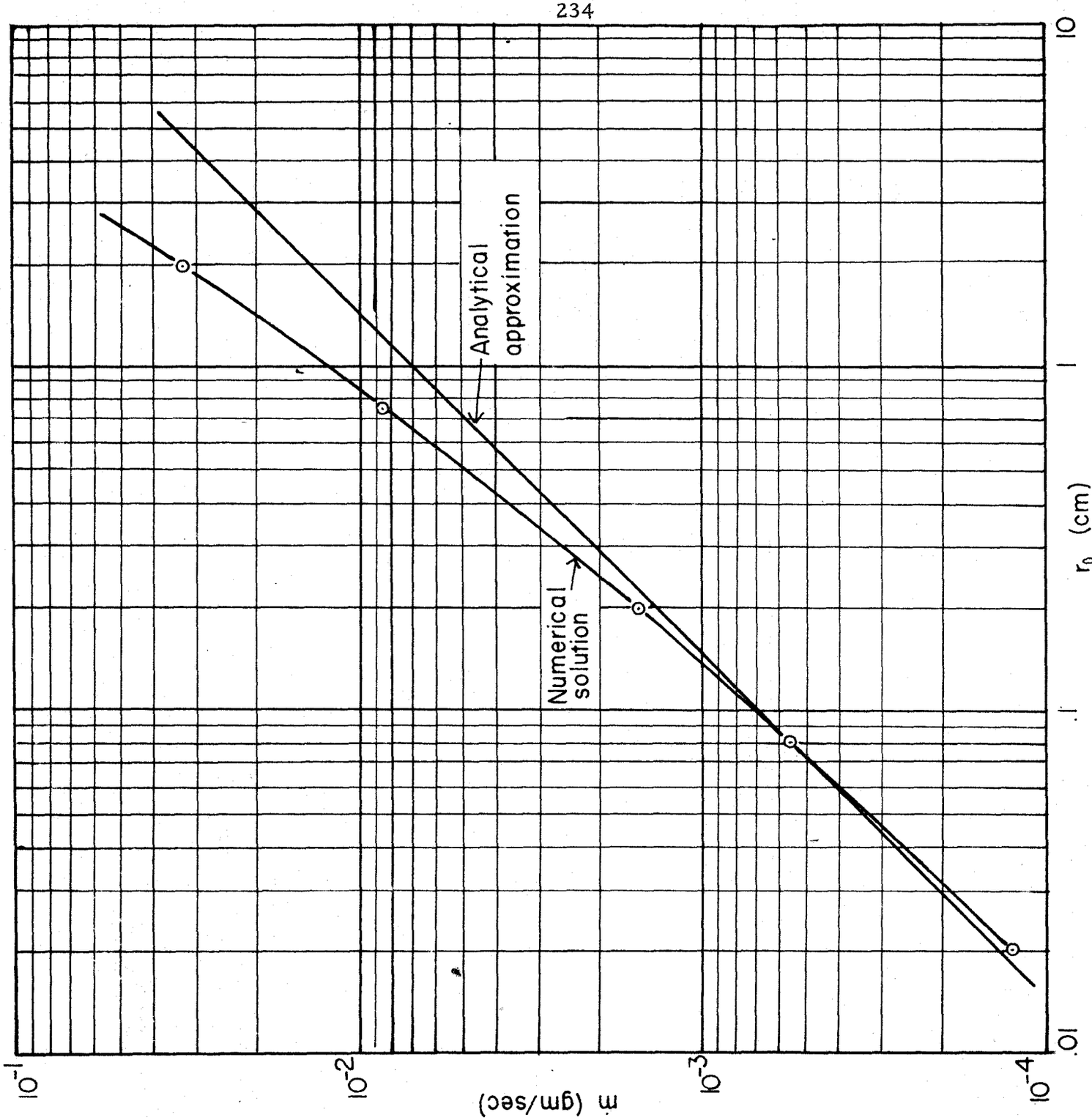

Fig.11. Mass flow rate $\dot{m}$ as a function of droplet radius r_ℓ for stoichiometric mixtures ($\delta=1$) at an activation temperature of $\theta_a = 20.6$.

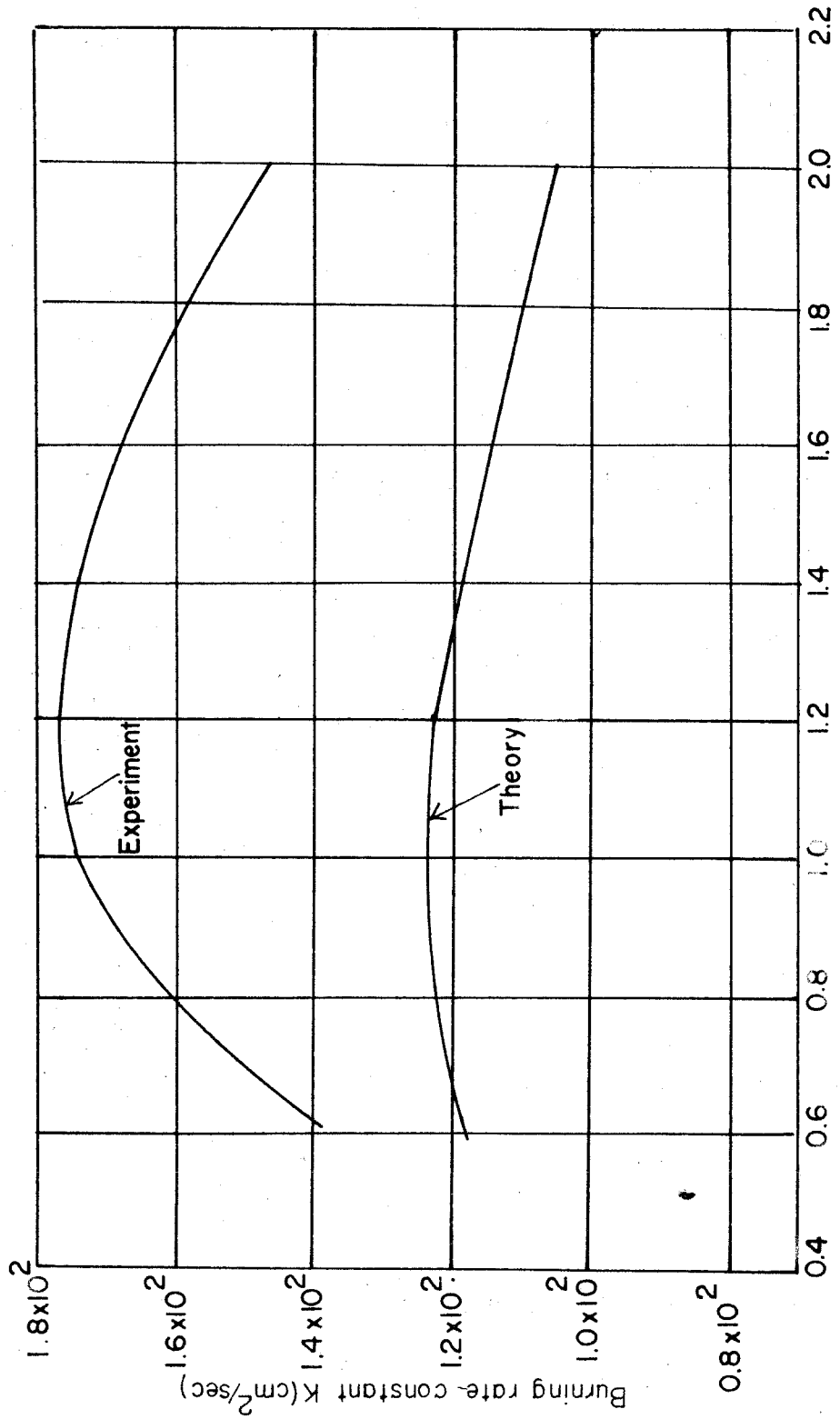

Fig. 12. Experimental and theoretical burning rate for nitric acid-amyl acetate monopropellant as a function of equivalence ratio.

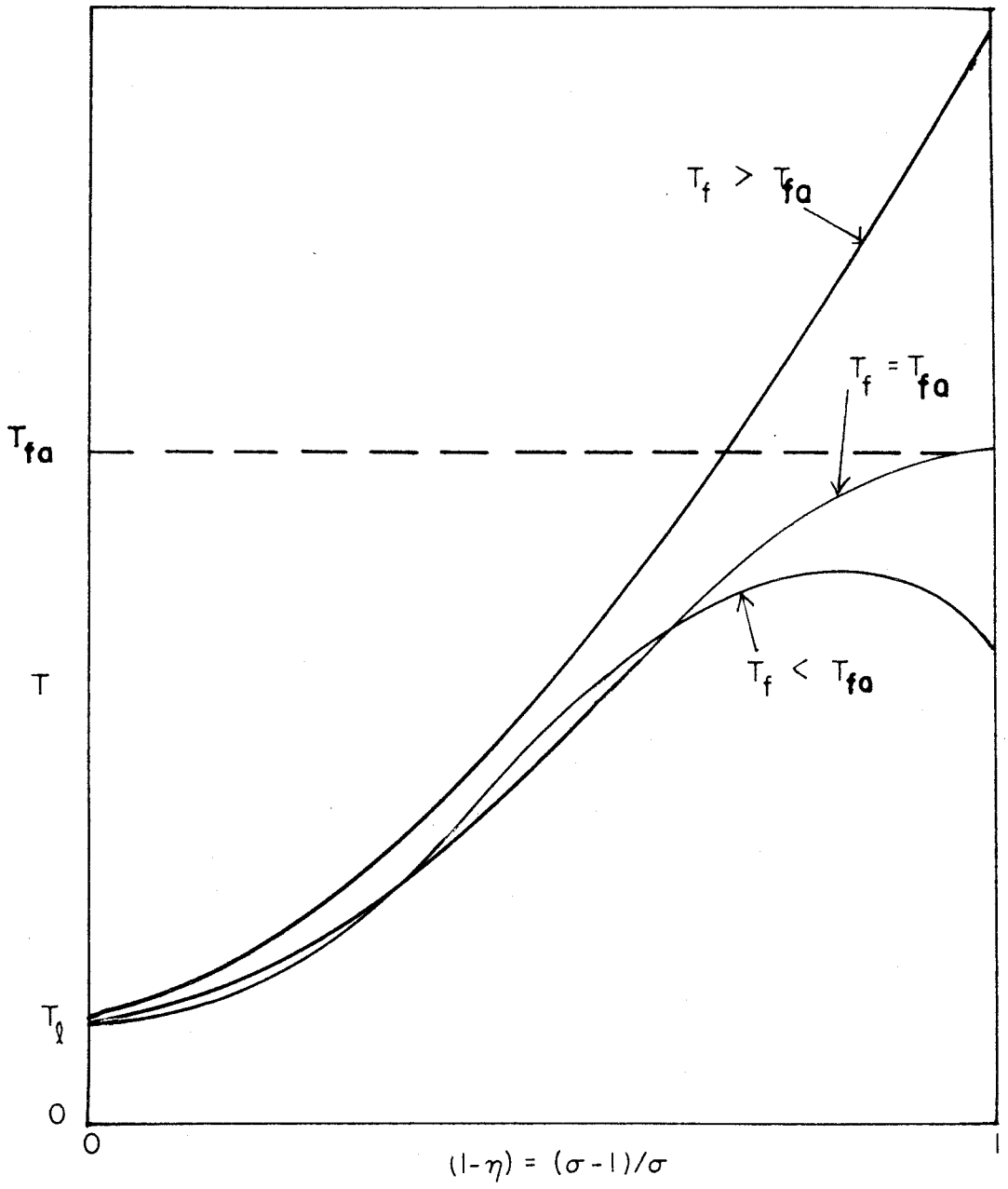

Fig. 13. Temperature profile when heat transfer to the surrounding atmosphere occurs.

(Note: T_{fa} is the adiabatic value of the final temperature as given by Eq. (29).

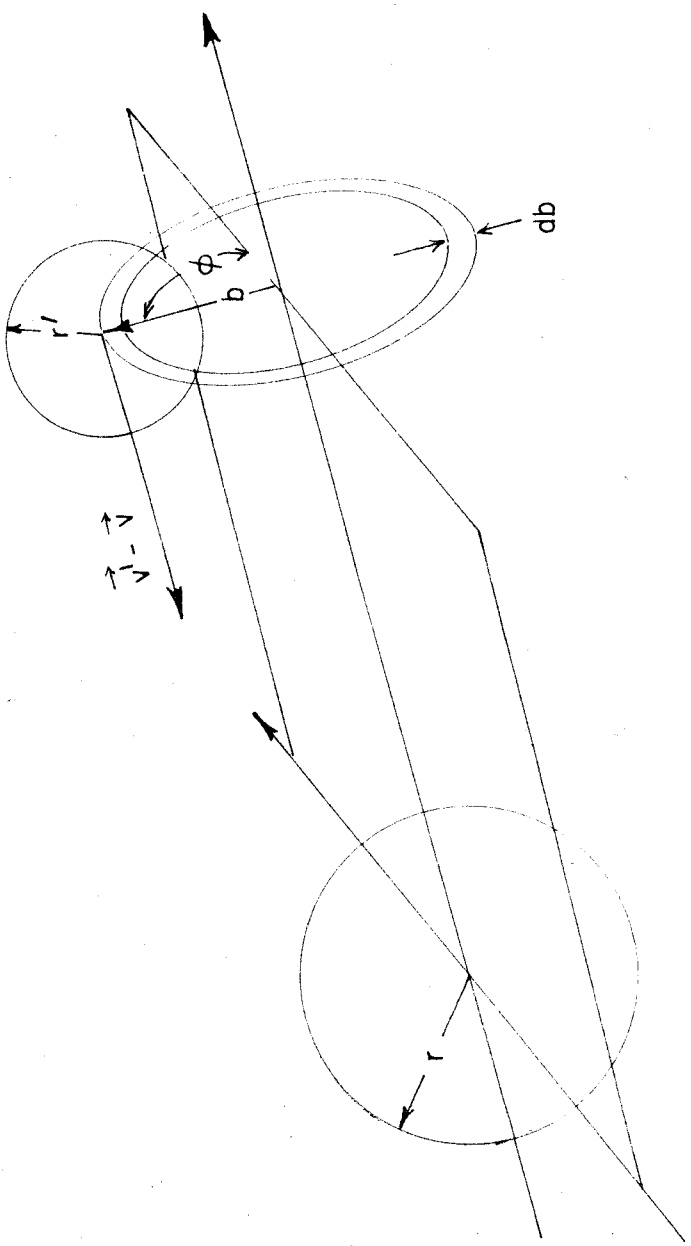

Fig 14. Geometry of a collision.

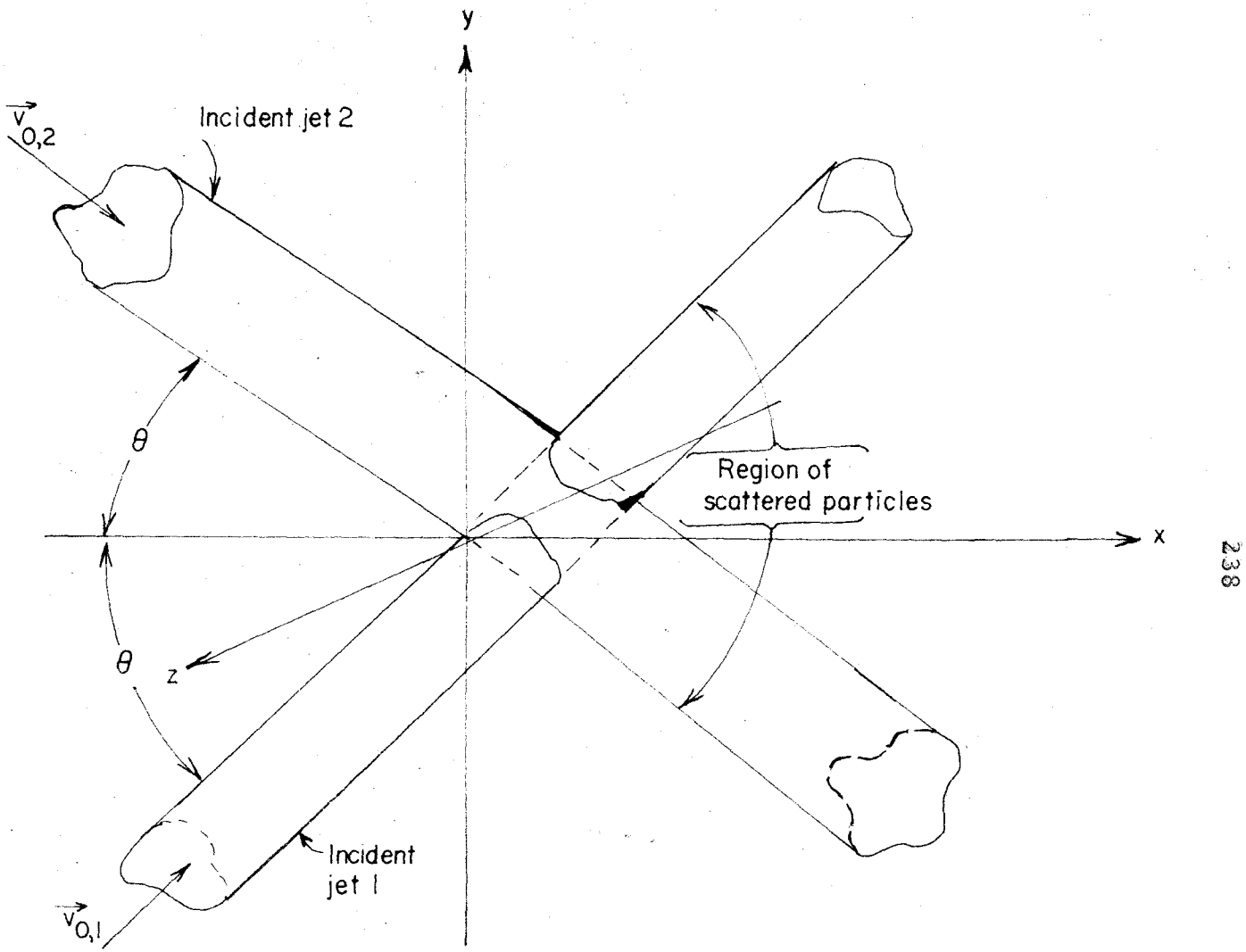

Fig 15. Geometry of impinging jet atomization.

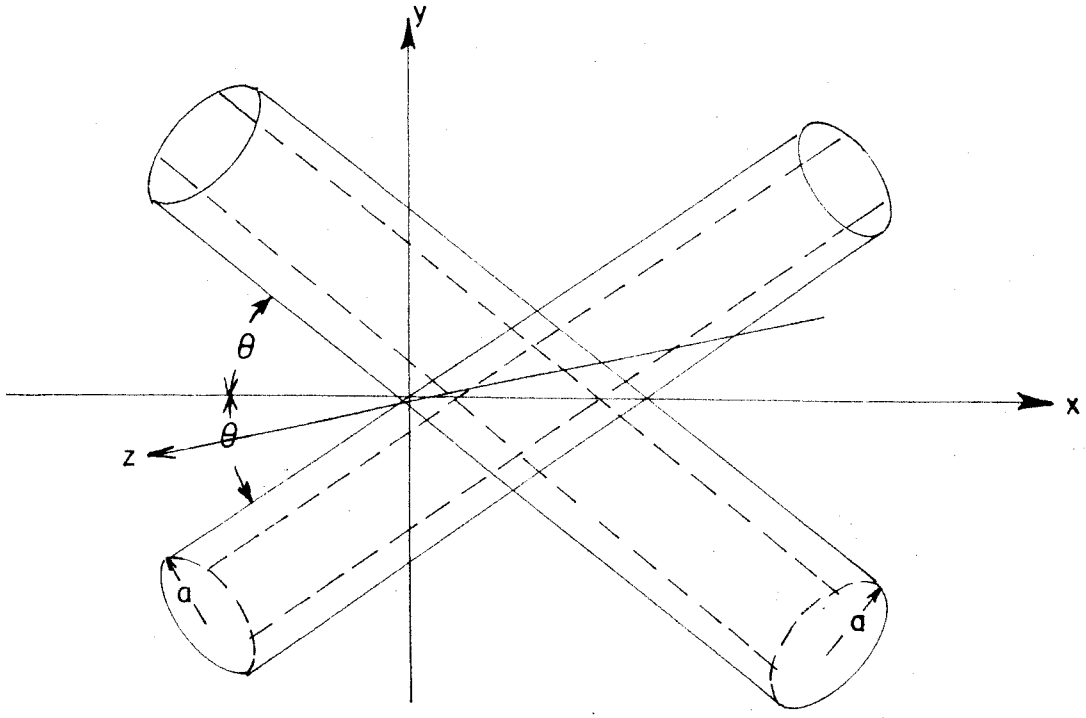

Fig 16a. Intersection of two cylindrical jets.

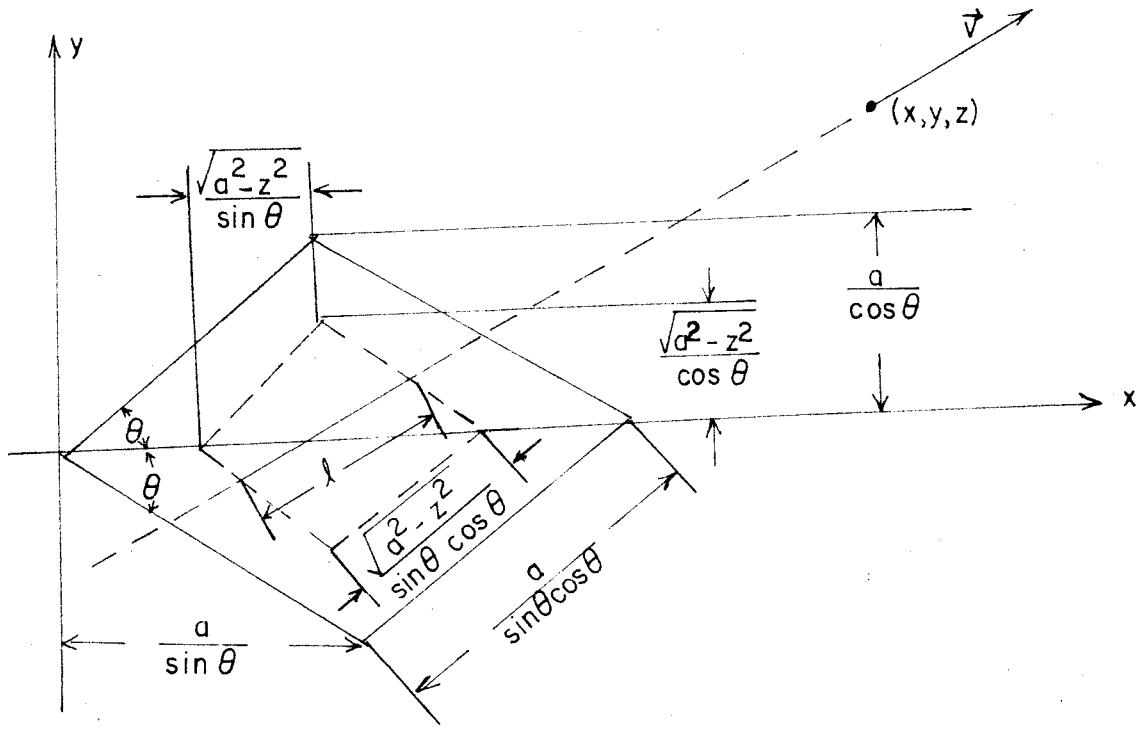

Fig 16b. The geometrical determination of the length ℓ for cylindrical jets.

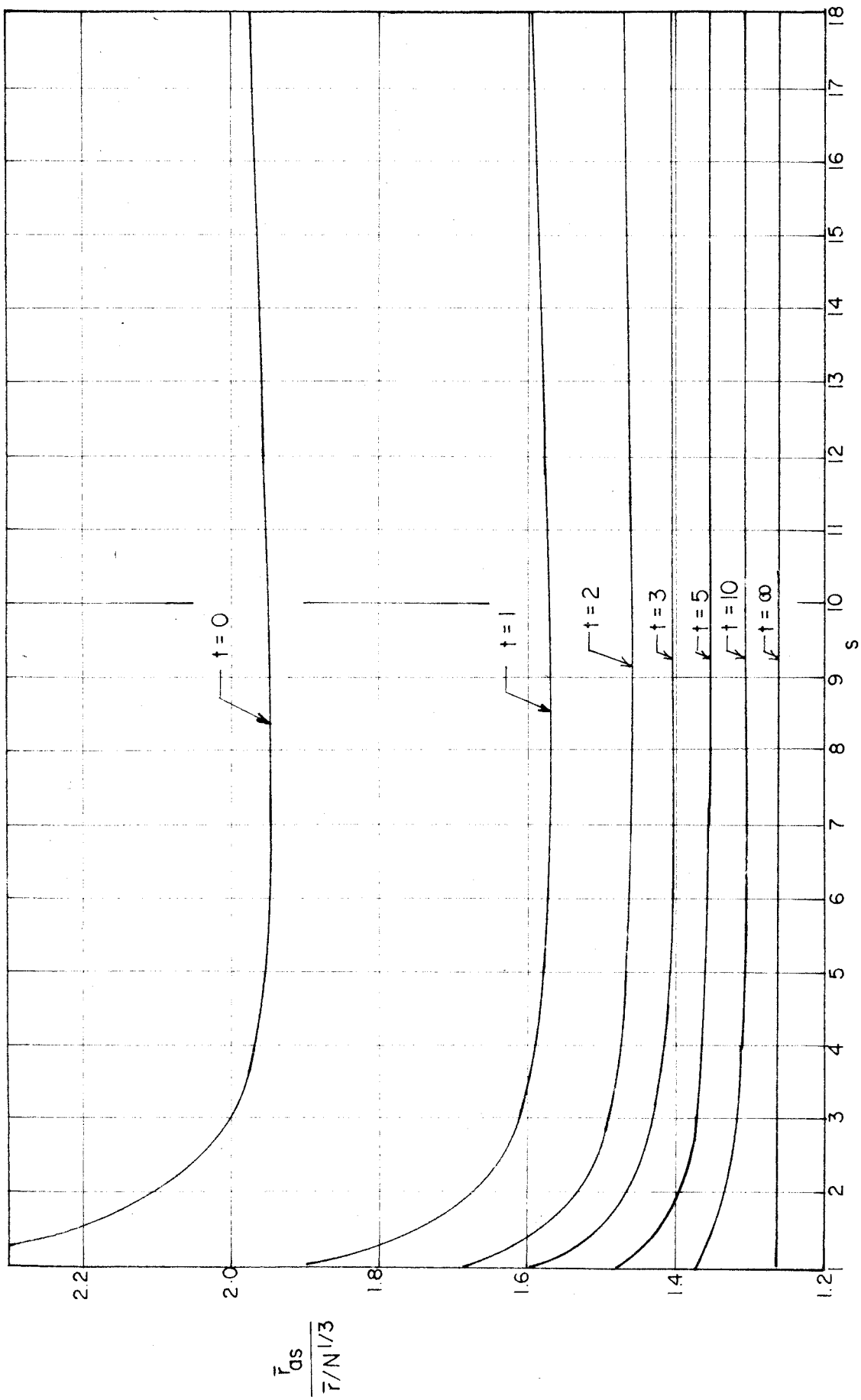

Fig 17. The number-weighted average asymptotic droplet radius on the axis of the scattered jet as a function of the size distribution parameters s and t of the incident jet.

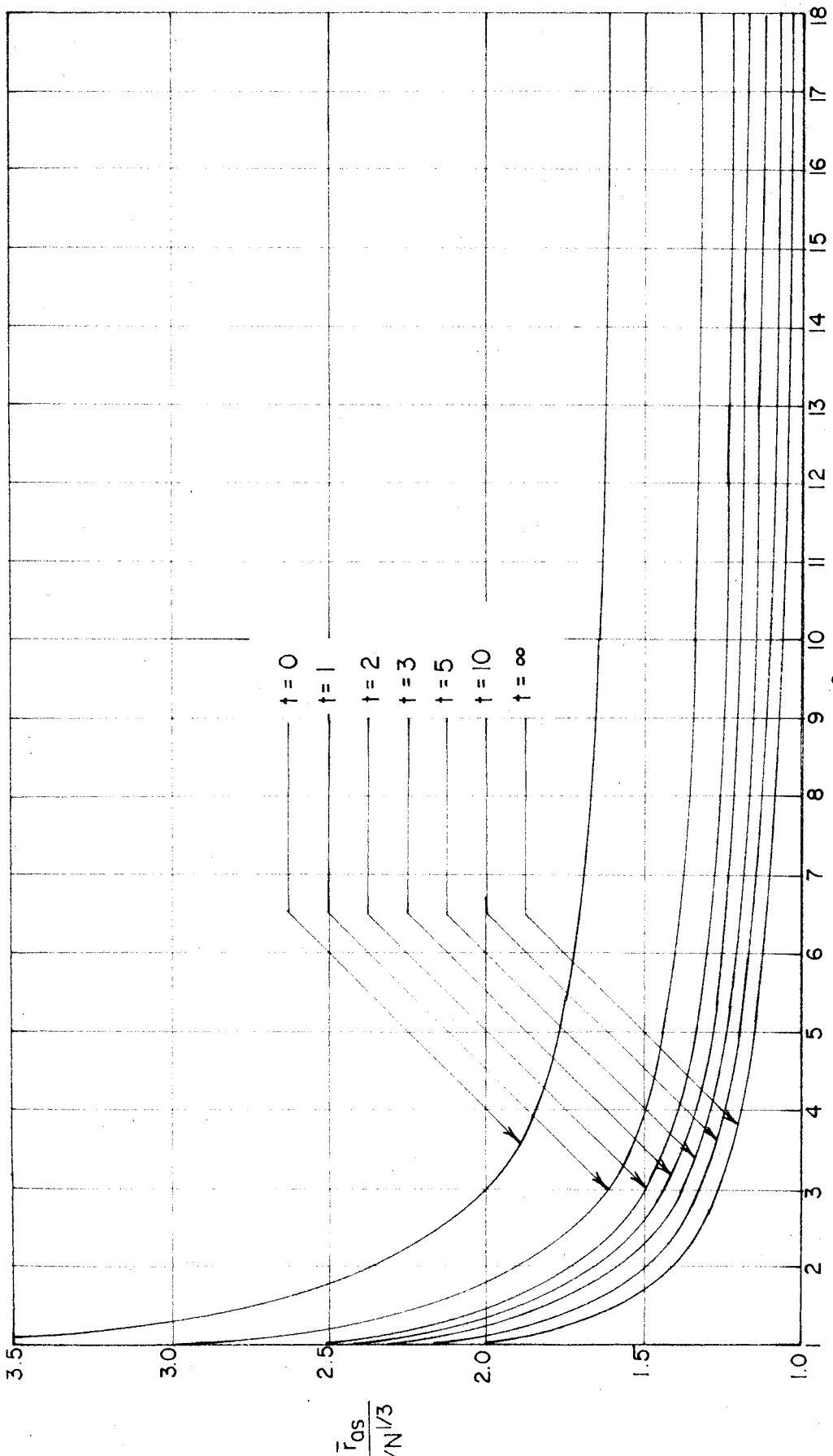

Fig 18. The number-weighted average asymptotic droplet radius on the edge of the scattered jet as a function of the size distribution parameters s and t of the incident jet.